

Fiscal Year 2016: Third Quarter

Progress Report
**Advanced Battery Materials
Research (BMR) Program**

Released September 2016
for the period of April – June 2016

Approved by

Tien Q. Duong, Advanced Battery Materials Research Program Manager
Vehicle Technologies Office, Energy Efficiency and Renewable Energy

TABLE OF CONTENTS

A Message from the Advanced Battery Materials Research Program Manager.....	1
Task 1 – Advanced Electrode Architectures	5
Task 1.1 – Higher Energy Density via Inactive Components and Processing Conditions (Vincent Battaglia, Lawrence Berkeley National Laboratory)	6
Task 1.2 – Electrode Architecture-Assembly of Battery Materials and Electrodes (Karim Zaghib, HydroQuebec).....	8
Task 1.3 – Design and Scalable Assembly of High-Density, Low-Tortuosity Electrodes (Yet-Ming Chiang, Massachusetts Institute of Technology)	11
Task 1.4 – Hierarchical Assembly of Inorganic/Organic Hybrid Silicon Negative Electrodes (Gao Liu, Lawrence Berkeley National Laboratory)	13
Task 2 – Silicon Anode Research.....	16
Task 2.0 – Novel Non-Carbonate Based Electrolytes for Silicon Anodes (Dee Strand, Wildcat Discovery Technologies).....	17
Task 2.1 – Development of Silicon-Based High-Capacity Anodes (Ji-Guang Zhang and Jun Liu, PNNL; Prashant Kumta, University of Pittsburgh)	24
Task 2.2 – Pre-Lithiation of Silicon Anode for High-Energy Lithium-Ion Batteries (Yi Cui, Stanford University) ...	27
Task 3 – High-Energy Density Cathodes for Advanced Lithium-Ion Batteries.....	30
Task 3.1 – Studies of High-Capacity Cathodes for Advanced Lithium-Ion Systems (Jagjit Nanda, Oak Ridge National Laboratory).....	31
Task 3.2 – High Energy Density Lithium Battery (Stanley Whittingham, SUNY Binghamton).....	34
Task 3.3 – Development of High-Energy Cathode Materials (Ji-Guang Zhang and Jianming Zheng, Pacific Northwest National Laboratory)	37
Task 3.4 – <i>In Situ</i> Solvothermal Synthesis of Novel High-Capacity Cathodes (Feng Wang and Jianming Bai, Brookhaven National Laboratory)	40
Task 3.5 – Novel Cathode Materials and Processing Methods (Michael M. Thackeray and Jason R. Croy, Argonne National Laboratory)	43
Task 3.6 – Lithium-Bearing Mixed Polyanion (LBMP) Glasses as Cathode Materials (Jim Kiggins and Andrew Kercher, Oak Ridge National Laboratory)	46
Task 3.7 – Advanced Cathode Materials for High-Energy Lithium-Ion Batteries (Marca Doeff, Lawrence Berkeley National Laboratory)	48
Task 3.8 – Lithium Batteries with Higher Capacity and Voltage (John B. Goodenough, UT Austin).....	51
Task 3.9 – Exploiting Cobalt and Nickel Spinels in Structurally Integrated Composite Electrodes (Michael M. Thackeray and Jason R. Croy, Argonne National Laboratory)	53
Task 3.10 – Discovery of High-Energy Lithium-Ion Battery Materials (Wei Tong, Lawrence Berkeley National Laboratory)	56

Task 4 – Electrolytes for High-Voltage, High-Energy Lithium-Ion Batteries.....58

Note: This task is closed. Projects awarded from a recent BMR call in this area will start in FY 2017.

Task 5 – Diagnostics59

Task 5.1 – Design and Synthesis of Advanced High-Energy Cathode Materials (Guoying Chen, Lawrence Berkeley National Laboratory) 60

Task 5.2 – Interfacial Processes – Diagnostics (Robert Kostecki, Lawrence Berkeley National Laboratory).....62

Task 5.3 – Advanced *In Situ* Diagnostic Techniques for Battery Materials (Xiao-Qing Yang and Xiqian Yu, Brookhaven National Laboratory) 65

Task 5.4 – NMR and Pulse Field Gradient Studies of SEI and Electrode Structure (Clare Grey, Cambridge University)68

Task 5.5 – Optimization of Ion Transport in High-Energy Composite Cathodes (Shirley Meng, UC San Diego).....71

Task 5.6 – Analysis of Film Formation Chemistry on Silicon Anodes by Advanced *In Situ* and *Operando* Vibrational Spectroscopy (Gabor Somorjai, UC Berkeley, and Phil Ross, Lawrence Berkeley National Laboratory)74

Task 5.7 – Microscopy Investigation on the Fading Mechanism of Electrode Materials (Chongmin Wang, Pacific Northwest National Laboratory).....76

Task 5.8 – Characterization and Computational Modeling of Structurally Integrated Electrodes (Michael M. Thackeray and Jason R. Croy, Argonne National Laboratory)79

Task 6 – Modeling Advanced Electrode Materials82

Task 6.1 – Electrode Materials Design and Failure Prediction (Venkat Srinivasan, Lawrence Berkeley National Laboratory)83

Task 6.2 – Predicting and Understanding Novel Electrode Materials from First Principles (Kristin Persson, Lawrence Berkeley National Laboratory).....85

Task 6.3 – First Principles Calculations of Existing and Novel Electrode Materials (Gerbrand Ceder, Massachusetts Institute of Technology).....88

Task 6.4 – First Principles Modeling of SEI Formation on Bare and Surface/Additive Modified Silicon Anode (Perla Balbuena, Texas A&M University)90

Task 6.5 – A Combined Experimental and Modeling Approach for the Design of High-Current Efficiency Silicon Electrodes (Xingcheng Xiao, General Motors, and Yue Qi, Michigan State University) 93

Task 6.6 – Predicting Microstructure and Performance for Optimal Cell Fabrication (Dean Wheeler and Brian Mazzeo, Brigham Young University)96

Task 7 – Metallic Lithium and Solid Electrolytes	98
Task 7.1 – Mechanical Properties at the Protected Lithium Interface (Nancy Dudney, ORNL; Erik Herbert, Michigan Technological University; and Jeff Sakamoto, University of Michigan).....	100
Task 7.2 – Solid Electrolytes for Solid-State and Lithium–Sulfur Batteries (Jeff Sakamoto, University of Michigan)	103
Task 7.3 – Composite Electrolytes to Stabilize Metallic Lithium Anodes (Nancy Dudney and Frank Delnick, Oak Ridge National Laboratory).....	105
Task 7.4 – Overcoming Interfacial Impedance in Solid-State Batteries (Eric Wachsman, Liangbing Hu, and Yifei Mo, University of Maryland, College Park)	108
Task 7.5 – Nanoscale Interfacial Engineering for Stable Lithium-Metal Anodes (Yi Cui, Stanford University)	111
Task 7.6 – Lithium Dendrite Suppression for Lithium-Ion Batteries (Wu Xu and Ji-Guang Zhang, Pacific Northwest National Laboratory)	114
Task 8 – Lithium–Sulfur Batteries	117
Task 8.1 – New Lamination and Doping Concepts for Enhanced Lithium–Sulfur Battery Performance (Prashant N. Kumta, University of Pittsburgh).....	119
Task 8.2 – Simulations and X-Ray Spectroscopy of Lithium–Sulfur Chemistry (Nitash Balsara, Lawrence Berkeley National Laboratory)	122
Task 8.3 – Novel Chemistry: Lithium Selenium and Selenium Sulfur Couple (Khalil Amine, Argonne National Laboratory)	125
Task 8.4 – Multi-Functional Cathode Additives (MFCA) for Lithium-Sulfur Battery Technology (Hong Gan, Brookhaven National Laboratory, and Co-PI Esther Takeuchi, Brookhaven National Laboratory and Stony Brook University).....	128
Task 8.5 – Development of High-Energy Lithium–Sulfur Batteries (Jie Xiao and Jun Liu, Pacific Northwest National Laboratory)	131
Task 8.6 – Nanostructured Design of Sulfur Cathodes for High-Energy Lithium-Sulfur Batteries (Yi Cui, Stanford University).....	134
Task 8.7 – Addressing Internal “Shuttle” Effect: Electrolyte Design and Cathode Morphology Evolution in Lithium–Sulfur Batteries (Perla Balbuena, Texas A&M University)	136
Task 8.8 – Mechanistic Investigation for the Rechargeable Lithium–Sulfur Batteries (Deyang Qu, U Wisconsin - Milwaukee; Xiao-Qing Yang, BNL)	139
Task 8.9 – Statically and Dynamically Stable Lithium–Sulfur Batteries (Arumugam Manthiram, U Texas Austin).....	142
Task 9 – Li-Air Batteries	145
Task 9.1 – Rechargeable Lithium–Air Batteries (Ji-Guang Zhang and Wu Xu, PNNL)	146
Task 9.2 – Efficient Rechargeable Li/O ₂ Batteries Utilizing Stable Inorganic Molten Salt Electrolytes (Vincent Giordani, Liox)	149
Task 9.3 – Lithium–Air Batteries (Khalil Amine, ANL)	152
Task 10 – Sodium-Ion Batteries	155
Task 10.1 – Exploratory Studies of Novel Sodium-Ion Battery Systems (Xiao-Qing Yang and Xiqian Yu, Brookhaven National Laboratory)	156

LIST OF FIGURES

Figure 1. Electrode performance data for uncalendered electrodes of two different molecular weight binders (red for low molecular weight, LMW; and blue for high molecular weight, HMW). Numbers indicate the area specific capacity (mAh/cm ²) of each electrode.	7
Figure 2. Scanning electron microscopy images of silicon powder obtained with different milling times (a) 0 hr, (b) 3 hrs, (c) 9 hrs and (d) 24 hrs of wet-milling with 1 mm diameter beads and 2200 rpm agitating speed in the 20 wt% solid contents of an IPA (isopropyl alcohol) solution.....	9
Figure 3. X-ray diffraction patterns of silicon powder milled with different time; (orange) 0 hr, (green) 3 hrs, (blue) 9 hrs, and (red) 24 hrs.	9
Figure 4. Formation voltage profile of silicon powder wet-milled with different times: (a) 0 hr, (b) 3 hrs, (c) 9 hrs, and (d) 24 hrs.....	10
Figure 5. Cycle life of nano-Si powder with different loading level; capacity controlled cycle test (depth of discharge 40%).....	10
Figure 6. Scanning electron microscopy images of low-tortuosity LiCoO ₂ cathode and mesocarbon microbeads (MCMB) graphite anode.....	12
Figure 7. (a) Dynamic stress test (DST) protocol. (b) Voltage-net capacity plots of LiCoO ₂ electrodes with or without aligned pore channels under DST tests. (c) Statistic results of areal capacity achieved under DST tests.....	12
Figure 8. Cycling performance of the SiO/PFM electrodes with or without NaCl. (a) Areal capacity versus cycle number. (b) Specific capacity versus cycle number. (c) First- and (d) thirtieth-cycle voltage curves of samples with and without NaCl.	14
Figure 9. Tomographically reconstructed cross-section and volume rendering of (a-c) the control SiO/PFM electrode and (d-f) the SiO/PFM electrode with porosity generation. The pores induced by NaCl are marked with arrows in the cross-section.	14
Figure 10. Room-temperature cycle life improved with Wildcat formulations.....	18
Figure 11. New formulations outperform control with 10% fluoroethylene carbonate (FEC).	19
Figure 12. Capacity after high-temperature storage experiment.....	20
Figure 13. Area specific impedance of formulations after 60°C storage for two weeks.	20
Figure 14. Wildcat noncarbonate formulation demonstrates feasibility at higher voltage.	21
Figure 15. Low-temperature performance of formulations.	21
Figure 16. Electrolyte component costs.	22
Figure 17. (a) Cycling stability of porous-Si-graphite electrode. (b) The cycling stability of porous-Si-graphite electrodes with and without Ge coating.	25
Figure 18. Specific discharge capacity versus cycle numbers for different active electrodes based <i>nc</i> -Si/MM'O composite. Inset table shows the summary of performance of the materials.	25
Figure 19. Characterizations and electrochemical performance of SiO ₂ NPs before and after thermal lithiation. (a, b) Transmission electron microscopy images of sol-gel synthesized SiO ₂ NPs (a) and lithiated SiO ₂ NPs (b). (c) X-ray diffraction pattern of lithiated SiO ₂ NPs. (d) First-cycle delithiation capacity of lithiated SiO ₂ NPs (red) and SiO NPs (blue). Galvanostatic lithiation/delithiation profile of SiO ₂ NPs in first cycle (orange). The capacity is based on the mass of SiO or SiO ₂ in the anode. (e) First-cycle voltage profiles of graphite/lithiated SiO ₂ composite (84:6 by weight, red) and graphite control cell (blue). (f) Cycling performance of graphite/lithiated SiO ₂ composite (84:6 by weight, red), graphite/lithiated SiO composite (84:6 by weight, blue) and graphite control cell (black) at C/20 for first three cycles, and C/5 for the following cycles (1C = 0.372 A/g C, the capacity is based on the mass of the active materials, including graphite, and SiO and SiO ₂ in Li _x Si/Li ₂ O composites). The purple line is the Coulombic efficiency of graphite/lithiated SiO ₂ composite.	28

Figure 20. (a) Average (bulk) Cu K-edge X-ray absorption near edge structure (XANES) from an uncycled cell and cell charged <i>ex situ</i> . (b) Phase maps from transmission X-ray microscopy XANES data collected <i>in situ</i> during charge at three different electrode positions. Phase maps were generated by linear combination fitting using the bulk XANES shown in panel a. Transmission images at 9115 eV are also shown.	32
Figure 21. (a) Average (bulk) Ni K-edge X-ray absorption near edge structure (XANES) from an uncycled cell and cell charged <i>ex situ</i> . (b) Phase maps from transmission X-ray microscopy XANES data collected <i>in situ</i> during charge. Phase maps were generated by linear combination fitting using the bulk XANES shown in panel a. Transmission images at 8465 eV are also shown.	32
Figure 22. The electrochemical behavior of the Sn_7Fe anode versus lithium metal: (top) capacity over 500+ cycles; and (bottom) capacity as a function of rate (the insert shows the voltage profile); charge and discharge with the same current rate. The weight of active material is given at the top right.	35
Figure 23. (a) Initial charge/discharge profiles, and (b) discharge capacity versus cycle number of different NMC cathode materials at C/10 in the voltage range of 2.7 ~ 4.8 V.	38
Figure 24. (a-c) Crystal structure of pristine NMC-333 cathode. (a) Aberration-corrected high angle annular dark field (HAADF) Z-contrast image. (b) Scanning transmission electron microscopy (STEM) image showing the layered structure viewed down the [100] zone axis. (c) Atomic model showing the atomic arrangement of R-3m phase in the [100] zone projection. (d-i) Crystal structure of NMC-333 particle after 100 cycles between 2.0~4.8 V at C/10. (d-e) HAADF Z-contrast image showing micro crack formation. (f-h) STEM images showing significant micro crack and lattice expansion in the cycled particle. (i) Intensity plot along the yellow dashed line shown in (h).	38
Figure 25. Setup for <i>in situ</i> hydrothermal/ solvothermal synthesis. (a) Illustration of a micro-reactor for <i>t</i> and <i>T</i> -resolved X-ray studies. (b) Photograph of an autoclave-based reactor system, equipped with multiple gauges/meters for monitoring <i>T</i> , <i>P</i> , and <i>PH</i> values online.	41
Figure 26. Solvothermal synthesis of Ni-rich layered cathode materials using the autoclave reactor (shown in Figure 25b). (a, b) Evolution of the temperature (<i>T</i> ; red) and pressure (<i>P</i> ; blue) in the water and ethylene glycol solvent. (c) Laboratory X-ray diffraction patterns (Cu source) of the intermediate (after hydrothermal treatment) and final $\text{LiNi}_{0.5}\text{Mn}_{0.5}\text{O}_2$ (after post-treatment).	41
Figure 27. (a) First-cycle voltage profiles of LiCoO_2 (black), $0.95\text{LiCoO}_2 \cdot 0.05\text{Li}_{1.1}\text{Mn}_{1.9}\text{O}_4$ (red), and $0.90\text{LiCoO}_2 \cdot 0.10\text{Li}_{1.1}\text{Mn}_{1.9}\text{O}_4$ (blue), (b) corresponding capacity versus cycle data (4.6-2.0V, 15mA/g), and (c) $0.95\text{LiCoO}_2 \cdot 0.05\text{Li}_{1.1}\text{Mn}_{1.9}\text{O}_4$ coated with ~0.5nm AlW_xF_y cycled between 4.5-3.0V. (All data versus Li/Li^+ at 30°C, 15 mA/g). Inset shows dQ/dV plots of cycles 1 (black) and 50 (red). Stars indicate phase transitions in LCO.	44
Figure 28: Discharge curves for sodium copper phosphate / vanadate glasses.	47
Figure 29. Discharge curves for potassium copper phosphate / vanadate glasses.	47
Figure 30. Soft X-ray absorption spectroscopy data in total electron yield mode for NMC-622 materials during the first cycle at various states-of-charge: valence state change of nickel (top), manganese (middle) and cobalt (bottom) during the first cycle.	49
Figure 31. Activation energy of a Na-glass as a function of time for different temperatures and experimental procedures.	52
Figure 32. (A) Calculated $(\text{Li}_4\text{O}_3)^{2-}$ dipole cluster for an A-glass. (b) A postulated $(\text{Li}_2\text{O}_2)^2\text{-Li}_{+2n}$ ferroelectric chain segment aligned by an electric field.	52
Figure 33. X-ray diffraction patterns of $\text{LiCo}_{1-x}\text{Ni}_x\text{O}_2$ samples prepared at (a) 700°C and (b) 800°C.	54
Figure 34. (a, c) Normalized discharge profiles, and (b, d) dQ/dV plots of $\text{LiCo}_{1-x}\text{Ni}_x\text{O}_2$ prepared at (a, b) 700°C and (c, d) 800°C.	54
Figure 35. X-ray diffraction of $(1-x) \text{Li}_2\text{NiO}_2 \cdot x \text{Li}_2\text{CuO}_2$ ($x = 0, 0.2, 0.4, 0.6$) solid solutions.	57
Figure 36. (a) The first-cycle voltage profiles, and (b) cycling performance of the as-synthesized $(1-x) \text{Li}_2\text{NiO}_2 \cdot x \text{Li}_2\text{CuO}_2$ ($x = 0, 0.2, 0.4, 0.6$) solid solutions. (12 mA/g, 4.6 ~ 1.5 V).	57

Figure 37. (a) Mn, (b) Co, and (c) Ni L-edge soft X-ray absorption spectroscopy (XAS) spectra collected on recovered separators and the pristine electrodes. (d) Co low/high L3 peak ratio determined from the soft XAS spectra (Auger electron yield, total electron yield, and fluorescence yield modes) of the crystals recovered after 45 cycles. (e) Transition metal concentration in the electrolytes recovered after 45 cycles. (f) Capacity retention of the various $\text{Li}_{1.2}\text{Ni}_{0.13}\text{Mn}_{0.54}\text{Co}_{0.13}\text{O}_2$ half-cells cycled between 2.5 and 4.6 V at 20 mA/g.	61
Figure 38. Electron energy loss spectroscopy spectra and scanning transmission electron microscopy image of binder- and carbon-free NMC electrodes cycled in Swagelok versus lithium up to 4.4-2.8V with 1 M LiPF_6 , ethylene carbonate (EC), diethyl carbonate (DEC), or EC/DEC (1/2 wt.).....	64
Figure 39. <i>In situ</i> X-ray diffraction of NMC during the first charge. Contour plot of the 003 diffraction peak of $\text{Li}_{1-x}\text{Ni}_{1/3}\text{Co}_{1/3}\text{Mn}_{1/3}\text{O}_2$ with increasing x between x = 0 and x = 0.7 during the first charge process at different C rates (0.1C, 1C, 10C, 30C, 60C). Data were collected at X14A at NSLS with a wavelength of 0.7747 Å.	66
Figure 40. Discharge capacity of silicon as a function of cycle number.	69
Figure 41. ^{13}C , ^7Li and ^{19}F nuclear magnetic resonance of electrode samples prepared with ^{13}C (a) ethylene carbonate (blue) and (b) dimethyl carbonate (purple) labeled electrolytes following cycling.....	69
Figure 42. Schematic showing microscale processes: electrode pore structure becomes denser with cycling, restricting Li^+ diffusion to surface regions near the separator and to surface regions of large pores. The focused ion beam scanning electron microscopy electrode cross sections show the increasing density of the electrode pore structure.....	69
Figure 43. (a) First-cycle voltage profile of NMC-442 and Li-rich, where the voltage range is 2.0 – 4.8V, at $\text{C}/20 = 12.5 \text{ mA g}^{-1}$. Soft X-ray absorption spectroscopy results (total electron yield mode) at various states of charge in the first cycle of O K-edge (b) NMC-442 and (c) Li-rich NMC. (c) Comparison of O 3d/4sp band intensity ratios between NMC-442 and Li-rich NMC.	72
Figure 44. (a) bright field transmission electron microscopy image of the partially lithiated silicon and color-code (insert), (b) corresponding orientation map, and (c) strain map from a partially lithiated grain.....	72
Figure 45. This image shows the sum frequency generation (ssp) signal at the C-H stretch at open current potential of 1 M LiClO_4 in ethylene carbonate (EC), and EC : FEC (fluoroethylene carbonate) (9:1, w/w) in contact with a-Si anode.	75
Figure 46. The sum frequency generation (ssp) signal for the carbonyl stretch ($\text{C}=\text{O}$) at open current potential of 1 M LiClO_4 in ethylene carbonate (EC), and EC : (fluoroethylene carbonate) FEC (9:1, w/w) in contact with a-Si anode.	75
Figure 47. Intergranular and intragranular cracks in 4.7 V 100 cycles NMC-333 cathode materials. Cross section scanning electron microscopy images of secondary particles from (a) pristine and (b) 100 cycles electrode. (c-d) Scanning transmission electron microscopy – high angle annular dark field images from 100 cycles NMC-333 showing intragranular cracks along (001) plane. Yellow arrows indicate real cracks and pink arrows indicate incubation cracks.	77
Figure 48. Atomic structure in computational unit cell for the layered spinel shortly before the onset of the voltage plateau (a, top) and toward the end of the plateau (a, bottom). (b) Density of O-O pairs with bond lengths less than 1.7Å as a function of simulation time for delithiated layered-layered (LL, red) and layered-spinel (LS, blue) structures.	80
Figure 49. (a) Concentration dependent conductivity of two different polysulfide solutions, expected to contain primarily Li_2S_6 or Li_2S_8 . (b) Concentration dependent conductivity of LiTFSI salt in 1:1 DOL/DME solvent. Comparison with experiment is also provided.	84
Figure 50. (a) Nyquist plot to estimate the impedance before and after potentiostatic polarization for two different concentrations of LiTFSI salt. (b) Current profile during potentiostatic polarization at 10mV for 0.2M and 1.0M LiTFSI salt concentrations. (c) Transference number of lithium ions extracted using the Bruce-Vincent method.....	84

Figure 51. Illustrations of the Li_2MnO_3 bulk as well as surface planes. The figures present (a) the conventional unit cell structure and (b) the schematics of an arbitrary facet (red plane). (c-e) The three possible surface groups with respect to the relation between their normal direction and the Li/Mn stacking direction (001).	86
Figure 52. Unlike in the layered structure, lithium sites in cation-disordered structures are not equivalent. The spread of lithium site energies manifests itself as additional slope in the voltage profile.	89
Figure 53. Calculated voltage range owing to non-equivalent lithium sites (red) and tetrahedral lithium (blue) for the lithium transition-metal oxides of the first-row transition metals. The dashed line indicates a voltage of 4.5 V as a guideline for the stability limit of conventional liquid electrolytes.	89
Figure 54. $\text{LiF}/\text{Li}_2\text{O}$ “grain boundary” model, with lithium (blue), F (purple), and O (red).	91
Figure 55. Structural snapshots at the final delithiation stage of (a) fast and (b) slow rates. (c) Lithium concentration change upon delithiation. (d) The concentration profile of a- Li_xSi core at the final delithiation stage.	94
Figure 56. Phase diagram of failure modes of silicon thin-film islands on cycling.	94
Figure 57. Micrograph of lithium surface showing part of the indentation array. This surface was not exposed to dose of CO_2 . Bar is 30 μm	101
Figure 58. Modulus of lithium film, showing the correction used to account for the stiff glass substrate.	101
Figure 59. Impedance for Li-LLZO-Li sample before and after passing current in one direction at $\sim 5 \mu\text{A}/\text{cm}^2$	101
Figure 60. X-ray diffraction patterns of LLZO as a function of densification time.	104
Figure 61. Ionic conductivity for improved spray coated composite electrolyte over Nylon.	106
Figure 62. Variation of current with time during dc polarization at different applied potential.	106
Figure 63. (a) Electrochemical window, (b) interface stability, and (c) Li-ion migration barrier of the proposed and previously demonstrated coating layer materials.	109
Figure 64. (a) EIS plot of Li/garnet/Li symmetric cell. (b) EIS plot and equivalent circuit of Li/gel/garnet/gel/Li symmetric cell.	109
Figure 65. Time-lapse images visualizing the detailed phenomenon of the spark reaction. The images of the reaction at different time of 0 ms (a), 20 ms (b), 40 ms (c), 60 ms (d), 80 ms (e), and 100 ms (f) were shown successively. The yellow arrow (image a) shows the initial contact point between GO and molten lithium, where the reaction initiated.	112
Figure 66. Deconvoluted X-ray photoelectron spectroscopy spectra of C 1s and O 1s before and after the spark reaction.	112
Figure 67. First-principles calculations on surface binding energy between lithium and bare graphene surface (a), carbonyl (C=O) groups (b), alkoxy groups (C-O) (c), and epoxyl (C-O-C) groups (d).	112
Figure 68. Electrochemical behaviors of different electrolytes in Li NMC cells. (a) Long-term cycling performance of the electrolytes with different salts in ethylene carbonate – ethylmethyl carbonate solvent mixture at the same charge and discharge current density of 1.75 mA cm^{-2} at 30°C . (b-d) Evolutions of charge/discharge voltage profiles of Li NMC cells using (b) conventional LiPF_6 electrolyte, (c) dual-salt (LiTFSI-LiBOB) electrolyte, and (d) additive-containing dual-salt electrolyte.	115
Figure 69. Cycling performance of Li NMC cells with 3.0 mAh cm^{-2} NMC loading and using an additive-containing dual-salt electrolyte at 30°C	115
Figure 70. X-ray diffraction pattern of synthesized doped sulfur.	120
Figure 71. (a) X-ray diffraction patterns showing the infiltration of sulfur into the Inorganic Framework Material (IFM) showing retention of IFM structure. (b) Cycling behavior of sulfur infiltrated IFM.	120
Figure 72. Radical concentration in Li_2S_x in TEGDME.	123
Figure 73. Fraction of sulfur in the form of S_3^{2-} in solution.	123
Figure 74. Li^+ coordinated by 6 oxygen atoms (left); and Li^+ coordinated by 2 sulfur and 2 oxygen atoms (right).	123

Figure 75. Scanning electron microscopy images and elemental mapping of a typical selenium-doped sulfur/carbon cathode material.	126
Figure 76. (a) First charge/discharge curve at 0.05C and (b) cycle performance at 0.2C, with (c) rate performance and (d) cycle performance at different rates of Selenium-doped S/C cathode materials.	126
Figure 77. Tape testing – adhesion.	129
Figure 78. Tape test – areal weight loss.	129
Figure 79. Cycled electrode delamination.	129
Figure 80. Hybrid electrode cycling at 1C.	129
Figure 81. (a) Li-S cell voltage evolution during 2 hours' rest and subsequent first discharging process at a 0.1C rate with sulfur cathode prepared with 5 wt% additive (sulfur loading is 4.5 mg cm ⁻²). (b) Dependence of areal capacity on sulfur loading for cathode with (brown) and without (black) additive.	132
Figure 82. Atomic conformations and binding energy for Li ₂ S ₆ species adsorption on (a) Ni ₃ S ₂ , (b) SnS ₂ , (c) FeS, (d) CoS ₂ , (e) VS ₂ , and (f) TiS ₂ . Here, green, yellow, grey, purple, brown, blue, red and cyan balls represent lithium, sulfur, nickel, tin, iron, cobalt, vanadium, and titanium atoms, respectively.	135
Figure 83. (a) Variation in microstructure porosity during discharge of a Li-S cell at C/4 rate. Three regimes with hydrostatic compression, relaxation, and tension are shown. Cell porosity with and without volume expansion is indicated with solid and dashed lines, respectively. (b) Cell performance at three different C-rates for a particular microstructure with and without mechanical expansion.	137
Figure 84. Cyclic voltammograms of different catholytes with 1M LiTFSi/DME on glassy carbon electrode. Scan rate of 30mV/s. Black line = S ₈ saturated electrolyte; red line = simulated electrolyte A; blue line = 20mM methyl triflate; green line = simulated electrolyte A after derivatization by methyl triflate; magenta line = S ₈ saturated electrolyte with 20mM methyl triflate.	140
Figure 85. HPLC/UV chromatogram for the derivatized electrolytes from Li-S batteries polarized at 2.3V (vs Li/Li ⁺). Black line = <i>ex-situ</i> derivatization method; red line = <i>in-situ</i> derivatization method.	140
Figure 86. Dynamic cycling performance of the cells employing (a) spherical-carbon/single wall carbon nanotube (SWCNT)-coated separators and (b) layer-by-layer (LBL) carbon nanofiber (CNF)-coated separators. Static self-discharge analysis of the cells with and without the LBL CNF-coated separator (c) LBL multiwall carbon nanotube (MWCNT)-coated separator.	143
Figure 87. Cycling performance of B ₄ C cell and TiC cell under 100 mAh g ⁻¹ at 0.1 mA cm ⁻² within the voltage range of 2.0~4.7 V. (a-b) Discharge and charge profiles of B ₄ C cell. (c) Discharge and charge profiles of TiC cell. (d) Capacity with cycles.	147
Figure 88. Cycling performance of Li-O ₂ cells with carbon nanotubes (CNTs)-based air electrodes before and after pretreatment under 1000 mAh g ⁻¹ at 0.1 mA cm ⁻² within the voltage range of 2.0~4.5 V. (a-b) Discharge and charge profiles of pristine CNTs electrode (a) and pretreated CNTs electrode C. (c) Capacity with cycling of pristine CNTs and four pretreated CNTs.	147
Figure 89. (a) First-cycle voltage and pressure profile for a Li-O ₂ cell using an IrO ₂ cathode. (b) Extended galvanostatic cycling (red) with O ₂ pressure analysis (blue) for the Li/LiNO ₃ -KNO ₃ /IrO ₂ , O ₂ cell. Green dashed line: E ₀ (2Li + O ₂ = Li ₂ O ₂). Current density: 0.05 mA/cm ²	150
Figure 90. Scanning electron microscopy images of (a) as-prepared IrO ₂ cathode prior to discharge and (b) IrO ₂ cathode discharged in LiNO ₃ -KNO ₃ molten salt electrolyte under O ₂ (Q = 2 mAh at j = 0.05 mA/cm ²).	150
Figure 91. Fourier transform infrared spectra of the charged Ir-rGO cathode cycled in the Li-O ₂ cell.	153
Figure 92. Nuclear magnetic resonance of the electrolyte on the cathode in the Li-O ₂ cell.	153
Figure 93. Structure evolution of O ₃ -NCFT during the electrochemical cycle. <i>Ex situ</i> X-ray diffraction (XRD) patterns collected during the first charge/discharge of the Na/O ₃ -NCFT cells under a current rate of C/10 at potential range between 2.0 V and 3.9 V. The corresponding charge-discharge profile is given on the right side of XRD patterns.	157

LIST OF TABLES

Table 1. Summary of final formulations for 18650 cells.	18
Table 2. Room-temperature and low-temperature ionic conductivities of formulations.....	22
Table 3. The calculated surface energies of all low Miller index facets denominated by their termination and Tasker type.	86
Table 4. Li ⁺ coordination environment in diglyme/Li ₂ S _x solution	123
Table 5. Data indicating that more S ₈ was consumed in the catholyte without the addition of methyl triflate.	140
Table 6. Molten nitrate Li-O ₂ cell characteristics: e ⁻ /O ₂ and OER/ORR ratios.	150

A MESSAGE FROM THE ADVANCED BATTERY MATERIALS RESEARCH PROGRAM MANAGER

The U.S. Department of Energy (DOE) Vehicle Technologies Office held its Annual Merit Review and Peer Evaluation (AMR) meeting on June 6-10, 2016, in Washington, D.C. During this time, the Advanced Battery Materials Research (BMR) Principal Investigators had the opportunity to review their past year's achievements. Forty-four research projects whose subject matters included electrode modeling, diagnostics, cell analysis, silicon anodes, cathodes, metallic lithium and solid electrolytes, sulfur electrodes, lithium-air and sodium-ion batteries were assessed. The proceedings are available online (<http://energy.gov/eere/vehicles/vehicle-technologies-office-annual-merit-review-presentations>). This report gives an update on those projects since the AMR meeting, summarizing the activities performed from April 1, 2016, through June 30, 2016.

In the upcoming months, 14 additional projects will be added to the BMR program. Their focus will be on development of high-voltage electrolytes and additives, conformable and self-healing solid state electrolytes, lithium-metal protection, advanced material characterization techniques, and advanced battery material modeling. These efforts will begin the first quarter of FY 2017, and an update of their progress is anticipated in the first quarter report. A list of the new tasks is provided below:

- **Engineering Approaches to Dendrite-Free Lithium Anodes**

PI: Prashant N. Kumta (University of Pittsburgh)

Co-PIs: Moni K. Datta, Oleg. I. Velikokhatnyi, Prashanth H. Jampani

Objective: Utilize a novel approach to mitigate lithium dendrite formation by designing a composite lithium anode / current collector. Investigate composite structures consisting of a porous foam (for example, copper) and an optimal isomorphous lithium alloy (for example, lithium and magnesium).

- **Self-Assembling, Rechargeable Lithium Batteries from Alkali and Alkaline-Earth Halides**

PI: Yet-Ming Chiang (Massachusetts Institute of Technology)

Co-PI: Venkat Viswanathan (Carnegie Mellon University)

Objective: Conduct fundamental studies of an alkali-halide-based solid electrolyte to demonstrate self-healing properties to overcome low cycle life and safety concerns associated with dendrite formation for Li-metal batteries.

- **Self-Forming Thin Interphases and Electrodes Enabling 3D Structured High Energy Density Batteries**

PI: Glenn G. Amatucci (Rutgers, The State University of New Jersey)

Objective: Design a 3D metal fluoride all solid-state battery that has the potential for extremely high specific and volumetric energy densities (600 Wh/Kg, 1,400 Wh/L).

- **Advanced Li-Ion Battery Technology: High-Voltage Electrolyte**

PI: Joe Sunstrom (Daikin America, Inc.)

Project Director: Ronald Hendershot

Objective: Develop electrolyte formulations, based on fluoro-chemistries, which will allow significantly improved operating voltage (> 4.5 V), increased durability, and increased energy density of Li-ion batteries at a reasonable cost.

- **Electrochemically Responsive Self-Formed Li-Ion Conductors for High-Performance Li-Metal Anodes**

PI: Donghai Wang (Pennsylvania State University)

Objective: Develop protective, self-healing layers for Li-metal anodes that will allow high cycling efficiency ($> 99.7\%$) and dendrite free cycling. The protective layers will be based on organic-inorganic (that is, organo- Li_xS_y and organo- $\text{Li}_x\text{P}_y\text{S}_z$).

- **Multifunctional, Self-Healing Polyelectrolyte Gels for Long-Cycle-Life, High-Capacity Sulfur Cathodes in Li-S Batteries**

PI: Alex K.-Y. Jen (University of Washington, Seattle)

Co-PI: Jihui Yang

Objective: Design a novel gel electrolyte that possesses a self-healing property to suppress dendrites at the Li-metal electrode and traps polysulfides that are detrimental to Li-S battery cycle life.

- **Solid-State Inorganic Nanofiber Network-Polymer Composite Electrolytes for Lithium Batteries**

PI: Nianqiang Wu (West Virginia University)

Co-PI: Xiangwu Zhang (North Carolina State University)

Objective: Develop solid-state electrolytes that integrate a highly conductive inorganic nanofibrous network with a conductive polymer matrix composite to suppress dendrites in Li-metal batteries.

- **Dual Function, Solid-State Battery with Self-Forming, Self-Healing Electrolyte and Separator**

PI: Esther S. Takeuchi (The Research Foundation for the SUNY Stony Brook University)

Co-PIs: Kenneth Takeuchi, Amy C. Marschilok

Objective: to investigate a Li/I_2 battery containing a solid state, self-healing electrolyte/separator. Emphasize improving electrolyte conductivity and cycling efficiency in order to assess if the couple can potentially meet automotive battery requirements.

- **High Conductivity and Flexible Hybrid Solid-State Electrolyte**

PI: Eric Wachsman (University of Maryland)

Co-PIs: Liangbing Hu and Yifei Mo (University of Maryland)

Objective: Design self-healing, 3D conformal solid-state electrolytes based on garnet nanofibers and Li-ion conducting polymers. The electrolyte should prevent lithium dendrite formation and provide high conductivity at room temperature, resulting in high battery cycle life and rate capability.

- **In situ Diagnostics of Coupled Electrochemical-Mechanical Properties of Solid Electrolyte Interphases on Li-Metal for Rechargeable Batteries**

PI: Xingcheng Xiao (General Motors LLC)

Co-PIs: Brian W. Sheldon (Brown University), Huajian Gao (Brown University), Yue Qi (Michigan State University), and Yang-Tse Cheng (University of Kentucky)

Objective: Develop a comprehensive set of diagnostic techniques that enables the understanding of the mechanical/chemical degradation of the solid electrolyte interphase layer to improve the performance and cycle life of current Li-ion batteries.

- **Advanced Microscopy and Spectroscopy for Probing and Optimizing Electrode-Electrolyte Interphases in High-Energy Lithium Batteries**

PI: Y. Shirley Meng (University of California- San Diego)

Objective: Develop advanced microscopy and spectroscopy tools to understand and optimize the oxygen evolution that impacts the performance of current Li-ion cathodes.

- **Understanding and Strategies for Controlled Interfacial Phenomena in Li-Ion Batteries and Beyond**

PI: Perla B. Balbuena (Texas A&M Engineering Experiment Station)

Co-PIs: Partha P. Mukherjee and Jorge M. Seminario

Objective: Develop a multiscale modeling approach to study the chemical structures of electrolytes and the solid electrolyte interphase layers.

- **First Principles Modeling and Design of Solid-State Interphases for the Protection and Use of Li-Metal Anodes**

PI: Gerbrand Ceder (University of California-Berkeley)

Objective: Develop a comprehensive model using a combination of First Principles Density Functional Theory and *ab initio* molecular dynamics to identify promising materials candidates for all solid-state lithium batteries.

▪ **Dendrite Growth Morphology Modeling in Liquid and Solid Electrolytes**

PI: Yue Qi (Michigan State University)

Co-PIs: Long-Qing Chen, (Penn State University), Xingcheng Xiao (General Motors R&D Center),

Peng Lu (General Motors R&D Center)

Objective: Develop a multi-scale model that connects micron-scale phase-field models and atomic-scale Density Functional Theory (DFT)-based simulations via parameter- and relationship-passing to predict Li-metal dendrite morphology evolution, in both liquid and solid electrolytes.

Sincerely,

Tien Q. Duong

Manager, Advanced Battery Materials Research (BMR) Program

Energy Storage R&D

Vehicle Technologies Office

Energy Efficiency and Renewable Energy

U.S. Department of Energy

TASK 1 – ADVANCED ELECTRODE ARCHITECTURES

Summary and Highlights

Energy density is a critical characterization parameter for batteries for electric vehicles as there is only so much room for the battery and the vehicle needs to travel over 200 miles. The DOE targets are 500 Wh/L on a system basis and 750 Wh/L on a cell basis. Not only do the batteries need to have high energy density, they must also still deliver 1000 Wh/L for 30 seconds at 80% depth of discharge. To meet these requirements not only entails finding new, high energy density electrochemical couples, but also highly efficient electrode structures that minimize inactive material content, allow for expansion and contraction from one to several thousand cycles, and allow full access to the active materials by the electrolyte during pulse discharges. Under that context, the DOE Vehicle Technology Office (VTO) supports four projects in the BMR Program under Advanced Electrode Architectures: (1) Higher Energy Density via Inactive Components and Processing Conditions, LBNL, (2) Assembly of Battery Materials and Electrodes, HydroQuebec (HQ), (3) Design and Scalable Assembly of High-Density, Low-Tortuosity Electrodes, Massachusetts Institute of Technology (MIT), and (4) Hierarchical Assembly of Inorganic/Organic Hybrid Si Negative Electrodes, LBNL.

The four subtasks take two general engineering approaches to improving the energy density. Subtasks 1 and 3 attempt to increase energy density by making thicker electrodes and reducing the overall amount of inactive components per cell. Subtasks 2 and 4 attempt to increase the energy density of Li-ion cells by replacing graphitic anodes with Si-based active materials. All four attempts are based on determining a suitable binder and a proper methodology for assembling the active material.

The problem being addressed with the first approach is that the salt in the electrolyte must travel a further distance to meet the current demand during charge or discharge. If the salt cannot reach the back of the electrode at the discharge rates required of batteries for automobiles, the back of the electrode is not used. If the diffusional path through the electrode is tortuous or the volume for electrolyte is too low, the limiting current is reduced. Another problem with thicker electrodes is that they tend to not cycle as well as thinner electrodes and thus reach the end-of-life condition sooner, delivering fewer cycles.

The problem addressed by the second approach is that silicon suffers from two major issues, both associated with the 300% volume change the material experiences as it goes from a fully delithiated state to a fully lithiated one: (1) the alloying with lithium results in freshly exposed surface area to electrolyte during cycling that reduces the electrolyte and results in a lithium imbalance between the two electrodes, and (2) the volume change causes the particles to become electrically disconnected, which is further enhanced if particle fracturing also occurs, during cycling.

Highlight. This quarter, Battaglia's group at LBNL has demonstrated electrodes of 5.7 mAh/cm² that still meet the EV 30-second pulse power requirement.

Task 1.1 – Higher Energy Density via Inactive Components and Processing Conditions (Vincent Battaglia, Lawrence Berkeley National Laboratory)

Project Objective. Thicker electrodes with small levels of inactive components that can still deliver most of their energy at C-rates of C/3 should result in batteries of higher energy density. Higher energy density should translate to more miles per charge or smaller, less expensive batteries. Unfortunately, the limit to making thicker electrodes is not based on power capability but on mechanical capability; for example, thicker electrodes delaminate from the current collector during calendaring and slicing. The objective of this research is to produce a high energy density electrode with typical Li-ion components that does not easily delaminate and still meets the electric vehicle (EV) power requirements through changes to the polymer binder and concomitant changes to the processing conditions.

Project Impact. Today's batteries cost too much on a per kWh basis and have too low of an energy density to allow cars to be driven over 300 miles on a single charge. This research targets both of these problems simultaneously. By developing thicker, higher energy-density electrodes, the fraction of cost relegated to inactive components is reduced, and the amount of energy that can be introduced to a small volume can be increased. Macroscopic modeling suggests that this could have as much as a 20% impact on both numbers.

Out-Year Goals. In the first year, the project will change its binder supplier to a U.S. supplier willing to provide binders of differing molecular weights. The project will then establish the workability of the new binders, establish a baseline binder and processing conditions, and determine how thick an electrode can be made from the project's standard processes for making moderately thick electrodes.

In the outgoing years, changes will be made to the binder molecular weight and electrode processing conditions to whatever degree is necessary to increase the energy density while maintaining power capability. Changes in the processing conditions can include the time of mixing, rate of casting, temperature of the slurry during casting, drying conditions, and hot calendaring. Chemical modifications may include multiple binder molecular weights and changes in the conductive additive.

Collaborations. This project has collaborations with Zaghib's Group (HQ) for materials and cell testing; Wheeler's Group (Brigham Young University, BYU) for modeling analysis; Liu's group on polymer properties; Arkema for binders; and a commercial cathode material supplier.

Milestones

1. Fabricate laminates of NCM cast to different thicknesses using standard materials and various processing conditions to determine how thick one can cast an electrode that does not display cracking or delamination. (Q1 – Complete)
2. Fabricate laminates of NCM cast to different thicknesses using higher molecular weight binders and various processing conditions to determine how thick one can cast an electrode that does not show cracking or delamination. (Q2 – Complete)
3. Fabricate laminates of NCM cast to different thicknesses using standard materials and various processing conditions on current collectors with a thin layer of binder and conductive additive pre-coated on the current collector to determine how thick one can cast an electrode that does not show cracking or delamination. (Q3)
4. *Go/No-Go.* Determine if a higher molecular weight binder is worth pursuing to achieve thicker electrodes based on ease of processing and level of performance. If no, pursue a path of polymer-coated current collectors. (Q4 – Go)

Progress Report

Go/No-Go Milestone: Go. Determine if a higher molecular weight binder is worth pursuing to achieve thicker electrodes based on ease of processing and level of performance. If no, pursue a path of polymer-coated current collectors.

Last quarter, it was shown that thick electrodes fabricated with binders of a typical molecular weight, ca. 400 k g/mol, resulted in a thin film (ca. 25 mm thick) of carbon additive and binder on the surface. In addition, the distribution of carbon and binder in the bulk of the electrodes was nonuniform. With the use of a high molecular weight binder, ca. 1 M, no film was present and the bulk composition of the electrode was much more uniform as measured with Energy Dispersive Spectroscopy (EDS). This quarter, the performance of electrodes made of different thicknesses, and different binders before calendaring, are reported.

Figure 1 shows the performance of electrodes made with a lower molecular weight binder (LMW) and a higher molecular weight binder (HMW). None of the electrodes were calendered. On the ordinate the pulse power capability is plotted based on the resistance measured at 80% depth-of-discharge. On the abscissa is plotted 80% of the energy of the cell measured at a C-rate of C/3. The capacity per cm² is listed next to each data point on the graph.

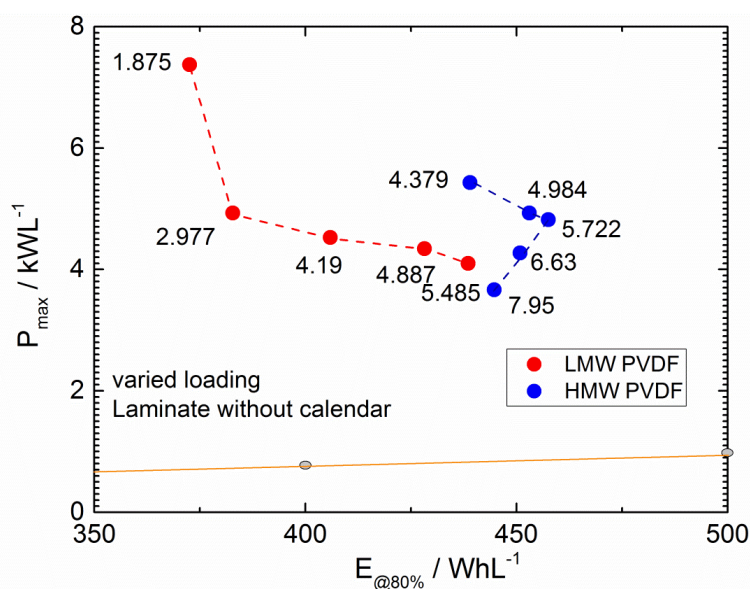


Figure 1. Electrode performance data for uncalendered electrodes of two different molecular weight binders (red for low molecular weight, LMW; and blue for high molecular weight, HMW). Numbers indicate the area specific capacity (mAh/cm²) of each electrode.

One sees that for the LMW electrode, the data stops at a loading of 5.485 mAh/cm². This is because electrodes of higher loading could not be produced as the laminate fell off of the current collector. One also sees that for electrodes of comparable loadings, the electrodes with the HMW provide both a higher energy density and a higher power density. This is different than had been expected. The electrode with a HMW binder was expected to show less energy and power, but would allow one to produce thicker electrodes which would surpass that of the LMW electrodes. Demonstrating better overall performance may be due to the fact that the carbon additive and binder migrate to the surface of LMW electrodes during drying, forming a film of carbon and binder. This film is probably affecting the performance at C/3 and resistance of the 30-second pulses.

Another point of interest is that electrodes with HMW do eventually show a maximum in energy density. Apparently, for electrodes produced at greater than 5.7 mAh/cm² loading with this binder, all of the material in the electrode is not accessible at discharge rates of C/3.

Task 1.2 – Electrode Architecture-Assembly of Battery Materials and Electrodes (Karim Zaghib, HydroQuebec)

Project Objective. The project goal is to develop an electrode architecture based on nano-silicon materials and design a full cell having high energy density and long cycle life. To achieve the objective, this project investigates the structure of nano-silicon materials that provide acceptable volume change to achieve long cycle life, while still maintaining the high-capacity performance of Si. The project scope includes the control of the particle size distribution of nano-Si materials, crystallinity, Si composition, and surface chemistry of the nano-Si materials. The focus is to develop electrode formulations and electrode architectures based on nano-Si materials that require optimized nano-Si/C composites and functional binders, as well as a controlled pore distribution in the electrode and the related process conditions to fabricate the electrode.

Project Impact. Silicon is a promising alternative anode material with a capacity of ~4200 mAh/g, which is about an order of magnitude higher than that of graphite. However, many challenges inhibiting the commercialization of Si remain unresolved. The primary culprit is viewed as the large volume variations of Si during charge/discharge cycles that result in pulverization of the particle and poor cycling stability. Success in developing highly reversible Si electrodes with acceptable cost will lead to higher energy density and lower cost batteries that are in high demand, especially for expanding the market penetration for EVs.

Out-Year Goals. This project investigates several steps to prepare an optimized composition and electrode structure of Si-based anode. HydroQuebec will use its advanced *in situ* analysis facilities to identify the limitations of the developed Si-based anode materials. *In situ* SEM will be used to monitor crack formations in the particles along with delamination at the binder/particle and current collector/particle interfaces to improve the electrode architecture and cycle life.

Previously, serious gas evolution was observed during the mixing and coating steps of Si-based electrodes. To overcome these technical issues, surface treatment of the nano-Si powder will be considered to utilize the water-based binders. A physical or chemical surface coating to protect the nano-Si powders will be explored. The project will also explore approaches to optimize the particle size distribution (PSD) to achieve better performance.

To achieve high gravimetric energy density (Wh/kg), the electrode loading (mg/cm^2) is a critical parameter in the electrode design. By increasing the anode loading to $2 \text{ mg}/\text{cm}^2$, a higher energy density of more than 300 Wh/kg can be achieved. Higher energy cells will be designed with high loading electrodes of $> 3 \text{ mAh}/\text{cm}^2$ by utilizing an improved electrode architecture. The energy density of these cells will be verified in the format of pouch-type full cells ($< 2 \text{ Ah}$); large format cells ($> 40 \text{ Ah}$) will be evaluated.

Collaborations. This project collaborates with BMR members: V. Battaglia and G. Liu from LBNL, C. Wong and Z. Jiguang from PNNL, and J. Goodenough from the University of Texas (UT).

Milestones

1. Failure mode analysis of large-format cells manufactured in 2015. (December 2015 – Complete)
2. Finalize the structure of nano-Si composite. (March 2016 – Complete)
3. Finalize the architecture of nano-Si composite electrode. *Go/No-Go*: > 300 cycles (80% retention) with loading level of $> 3 \text{ mAh}/\text{cm}^2$. (June 2016 – Complete)
4. Verification of performance in pouch-type full cell ($< 2 \text{ Ah}$). (September 2016 – Ongoing)

Progress Report

During this quarter, Hydro-Quebec focused on improving the electrochemical performance of wet-milled, nano-Si powder. Effort was focused on the evaluation of electrochemical performance and characterization of materials obtained with different milling times. In previous work, it was found that reducing the primary particle size obtained by the wet-milling process was limited to a range of ca. 100 nm, and the electrochemical performance of the final product, especially obtained by more severe conditions (high energy, small beads, less solid content) showed low Coulombic efficiency.

The metallurgical Si powder obtained by jet milling and sieved with 100-mesh (ca. 150 μm) was wet-milled in the circulation chamber filled with 1.0 mm diameter beads with IPA (isopropyl alcohol). The solid content was 20%, and the samples were collected at different milling times; 0, 3, 9, 24 hrs for physical characterization and electrochemical performance evaluation.

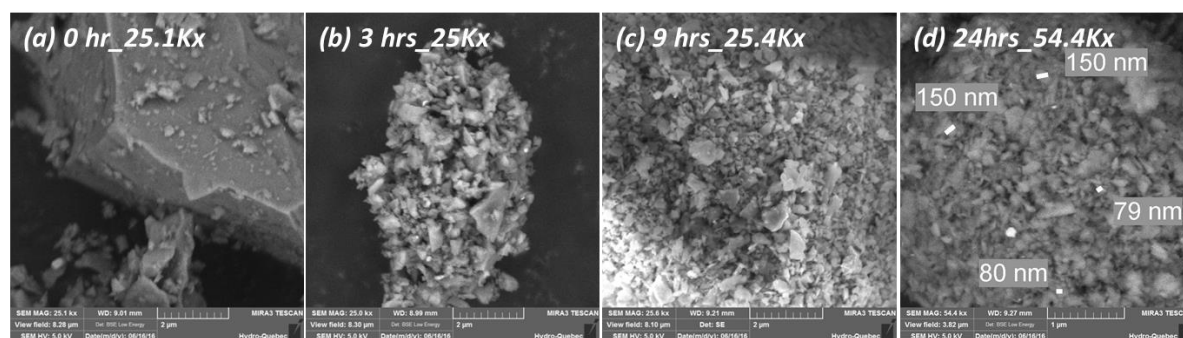


Figure 2. Scanning electron microscopy images of silicon powder obtained with different milling times (a) 0 hr, (b) 3 hrs, (c) 9 hrs and (d) 24 hrs of wet-milling with 1 mm diameter beads and 2200 rpm agitating speed in the 20 wt% solid contents of an IPA (isopropyl alcohol) solution.

The scanning electron microscopy (SEM) images (Figure 2) show that the edge of the particles turned blunt and the particle size was reduced with milling time. The particles appear flake shaped with longer milling times. These powders were analyzed by X-ray diffraction (XRD) (Figure 3) and the peak intensity of Si(111) and the crystalline size were both decreased with milling time. Accordingly, the FWHM of Si(111) and the peak intensity of Si-OH increased. The peak intensity ratio of Si-OH versus Si(111) increased up to 48% with longer milling times, indicating an increase of the surface area.

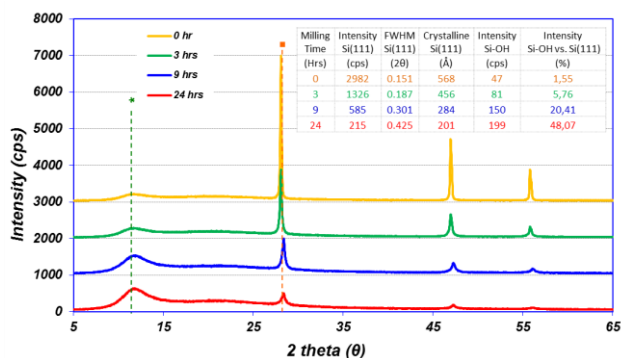


Figure 3. X-ray diffraction patterns of silicon powder milled with different time; (orange) 0 hr, (green) 3 hrs, (blue) 9 hrs, and (red) 24 hrs.

0.4 V. After 9 hrs of milling (Figure 4c-d), the plateau at 0.4 V disappeared, and the voltage profiles were nearly linear starting at around 0.1 V to around 0.6 V, which is similar to behavior previously observed with nano-Si powder produced by a plasma process.

Figure 4 shows the voltage profiles during formation cycle with 1st Coulombic efficiency and discharge capacity listed. The initial (0 hr) sample (Figure 4a) showed a typical discharge profile of micro-size Si powder that has a plateau at 0.4 V during delithiation; the 3-hr milled sample (Figure 4b) still had around 40% of the original plateau appearing at

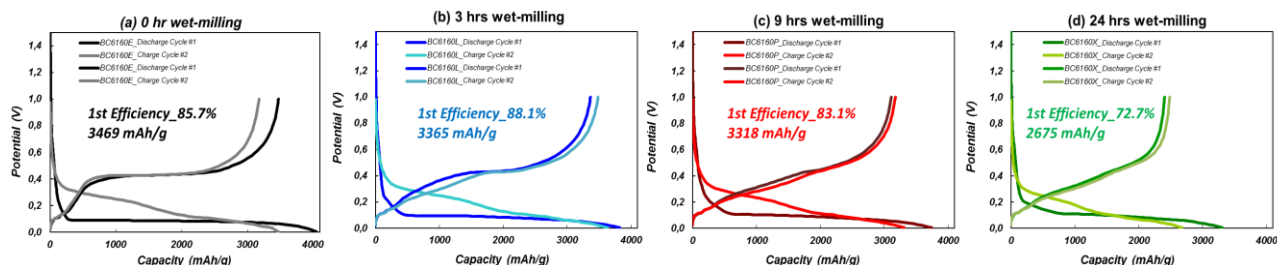


Figure 4. Formation voltage profile of silicon powder wet-milled with different times: (a) 0 hr, (b) 3 hrs, (c) 9 hrs, and (d) 24 hrs.

In addition, the first cycle Coulombic efficiency and discharge capacity decreased with milling time. This result confirms the capability of reproducing the expensive nano-Si produced with a plasma technique by optimizing the wet milling process.

It is worth noting that due to the volume expansion of Si material, the cycle life strongly depends on loading. Cycling at high loadings ($> 3 \text{ mAh/cm}^2$) leads to high volume variation, and the performance drops from

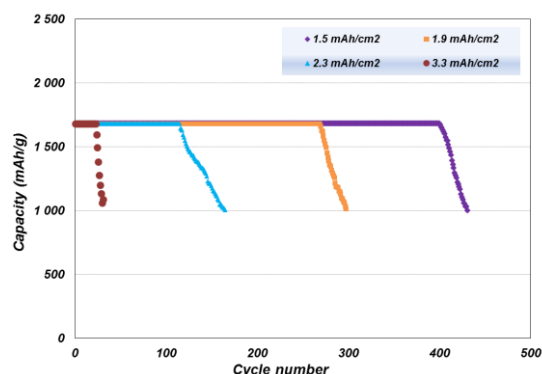


Figure 5. Cycle life of nano-Si powder with different loading level; capacity controlled cycle test (depth of discharge 40%).

contact losses and delamination. When cycling is done at lower percent depth of discharge (DOD), the cycle life improves since the anode will experience less deep stress (Figure 5). Technical challenges still remain, and more effort is required to improve the cyclability at high loadings to reach the high energy battery criteria. HQ is continuing the development effort by introducing other type of binders and electrolyte additives.

Deliverable: Two films of nano-Si/C electrodes were supplied as the second deliverable to LBNL for evaluation.

Task 1.3 – Design and Scalable Assembly of High-Density, Low-Tortuosity Electrodes (Yet-Ming Chiang, Massachusetts Institute of Technology)

Project Objective. The project objective is to develop scalable, high-density, low-tortuosity electrode designs and fabrication processes enabling increased cell-level energy density compared to conventional Li-ion technology, and to characterize and optimize the electronic and ionic transport properties of controlled porosity and tortuosity cathodes as well as densely sintered reference samples. Success is measured by the area capacity (mAh/cm^2) that is realized at defined C-rates or current densities.

Project Impact. The high cost ($\$/\text{kWh}$) and low energy density of current automotive Li-ion technology are in part due to the need for thin electrodes and associated high inactive materials content. If successful, this project will enable use of electrodes based on known families of cathode and anode active compositions, but with at least three times the areal capacity (mAh/cm^2) of current technology while satisfying the duty cycles of vehicle applications. This will be accomplished via new electrode architectures fabricated by scalable methods with higher active materials density and reduced inactive content; this will in turn enable higher energy density and lower-cost EV cells and packs.

Approach. Two techniques are used to fabricate thick, high-density electrodes with low tortuosity porosity oriented normal to the electrode plane: (1) directional freezing of aqueous suspensions; and (2) magnetic alignment. Characterization includes measurement of single-phase material electronic and ionic transport using blocking and non-blocking electrodes with ac and dc techniques, electrokinetic measurements, and drive-cycle tests of electrodes using appropriate battery scaling factors for EVs.

Out-Year Goals. The out-year goals are as follows:

- Identify anodes and fabrication approaches that enable full cells in which both electrodes have high area capacity under EV operating conditions. Anode approach will include identifying compounds amenable to the same fabrication approach as cathode, or use of very high-capacity anodes, such as stabilized lithium or Si-alloys that in conventional form can capacity-match the cathodes.
- Use data from best performing electrochemical couple in techno-economic modeling of EV cell and pack performance parameters.

Collaborations. Within BMR, this project collaborates with Antoni P. Tomsia (LBNL) in fabrication of low-tortuosity, high-density electrodes by directional freeze-casting, and with Gao Liu (LBNL) in evaluating Si anodes. Outside of BMR, the project collaborates with Randall Erb (Northeastern University) on magnetic alignment fabrication methods for low-tortuosity electrodes.

Milestones

1. Obtain 2-, 10- and 30- sec pulse discharge data for an electrode of at least $10 \text{ mAh}/\text{cm}^2$ area capacity. (December 2015 – Revised and complete)
2. Test at least one cathode and one anode, each having at least $10 \text{ mAh}/\text{cm}^2$ area capacity under an accepted EV drive cycle. (March 2016 – Complete)
3. *Go/No-Go:* Demonstrate a cathode or anode having at least $10 \text{ mAh}/\text{cm}^2$ area capacity that passes an accepted EV drive cycle. (June 2016 – Complete)
4. Construct and obtain test data for full cell in which area capacity of both electrodes is at least $10 \text{ mAh}/\text{cm}^2$. (September 2016)

Progress Report

Go/No-Go Milestone. Demonstrate a cathode or anode having at least 10 mAh/cm² area capacity that passes an accepted EV drive cycle.

This quarter, results are reported for dynamic stress tests (DST) of LiCoO₂ cathodes prepared through a recently developed room-temperature, emulsion-based magnetic alignment approach. An aqueous electrode formation was modified to form an oil-in-water emulsion as the solvent phase, in which is dispersed the electrode material (>95 wt%), carbon black, and the aqueous binder. The oil droplets that contain magnetite nanoparticles were then assembled and aligned normal to the electrode plane under a magnetic field, then removed by drying and rinsing to create aligned porosity. Except for addition of a small amount of the oil phase, the formulations of the slurry suspensions are similar to those for an aqueous electrode coating process for lithium ion. High-temperature sintering is no longer needed for this new magnetic alignment approach, compared to the previously reported process. Both LiCoO₂ cathodes and mesocarbon microbeads (MCMB) graphite anodes have been prepared.

Figure 6 shows the vertically aligned pore channels in the low-tortuosity LiCoO₂ cathode and MCMB graphite anode. These channels are 3-15 μm in diameter and hundreds of microns in length, extending through the electrode thickness. The tortuosity of these electrodes was measured through DC-depolarization experiments. The LiCoO₂ cathode (43% porosity) and graphite anode (51% porosity) were found to have tortuosity of 1.9 and 2.1, respectively.

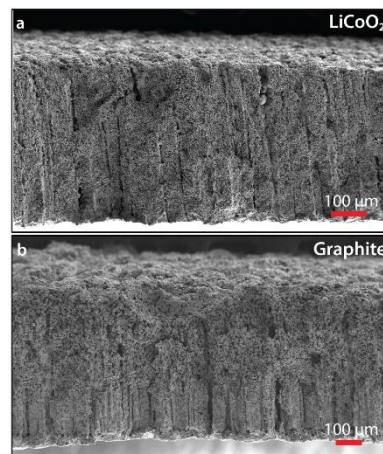


Figure 6. Scanning electron microscopy images of low-tortuosity LiCoO₂ cathode and mesocarbon microbeads (MCMB) graphite anode.

Half-cells were built using these LiCoO₂ electrodes and lithium metal as counter electrodes and tested using the DST protocol. This test protocol applies charge and discharge pulses of defined C-rate and duration, as shown in Figure 7a. The highest C-rate pulse discharge is 2C for 8 seconds. These LiCoO₂ electrodes are 430-440 μm in thickness and have 43% volume porosity. To test the effectiveness of the electrode fabrication technique, reference samples of similar thickness, without aligned porosity and thus high tortuosity ($\tau = 2.9$ based on DC-depolarization experiment), were prepared for testing via the same DST protocol. As shown in Figure 7b, the DST protocol was run repeatedly on each electrode, beginning with a fully charged cell, until a lower cut-off voltage of 2.5 V was reached during pulse discharge. The sample with aligned pore channels exhibits almost twice the discharge capacity of the sample without aligned pore channels, and reaches an area capacity of $10.95 \pm 0.61 \text{ mAh/cm}^2$. This performance meets the *Go/No-Go Milestone* of “Demonstrating a

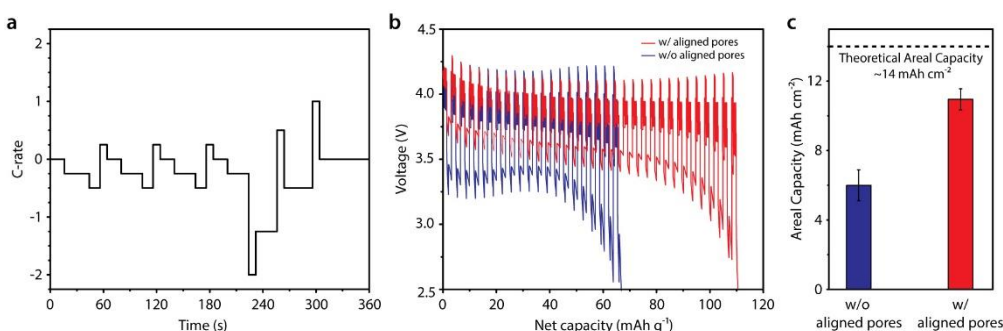


Figure 7. (a) Dynamic stress test (DST) protocol. (b) Voltage-net capacity plots of LiCoO₂ electrodes with or without aligned pore channels under DST tests. (c) Statistic results of areal capacity achieved under DST tests.

cathode or anode having at least 10 mAh/cm² area capacity that passes an accepted EV drive cycle.” The electrochemical measurements of low-tortuosity graphite anodes are ongoing.

Task 1.4 – Hierarchical Assembly of Inorganic/Organic Hybrid Silicon Negative Electrodes (Gao Liu, Lawrence Berkeley National Laboratory)

Project Objective. This work aims to enable silicon as a high-capacity and long cycle-life material for negative electrode to address two of the barriers of Li-ion chemistry for EV and plug-in hybrid electric vehicle (PHEV) application: insufficient energy density and poor cycle life performance. The proposed work will combine material synthesis and composite particle formation with electrode design and engineering to develop high-capacity, long-life, and low-cost hierarchical Si-based electrode. State of the art Li-ion negative electrodes employ graphitic active materials with theoretical capacities of 372 mAh/g. Silicon, a naturally abundant material, possesses the highest capacity of all Li-ion anode materials. It has a theoretical capacity of 4200 mAh/g for full lithiation to the $\text{Li}_{12}\text{Si}_5$ phase. However, Si volume change disrupts the integrity of electrode and induces excessive side reactions, leading to fast capacity fade.

Project Impact. This work addresses the adverse effects of Si volume change and minimizes the side reactions to significantly improve capacity and lifetime to develop negative electrode with Li-ion storage capacity over 2000 mAh/g (electrode level capacity) and significantly improve the Coulombic efficiency to over 99.9%. The research and development activity will provide an in-depth understanding of the challenges associated with assembling large volume change materials into electrodes and will develop a practical hierarchical assembly approach to enable Si materials as negative electrodes in Li-ion batteries.

Out-Year Goals. The three main aspects of this proposed work (that is, bulk assembly, surface stabilization, and lithium enrichment) are formulated into 10 tasks in a four-year period.

- Develop hierarchical electrode structure to maintain electrode mechanical stability and electrical conductivity. (bulk assembly)
- Form *in situ* compliant coating on Si and electrode surface to minimize Si surface reaction. (surface stabilization)
- Use prelithiation to compensate first-cycle loss of the Si electrode. (lithium enrichment)

The goal is to achieve a Si-based electrode at higher mass loading of Si that can be extensively cycled with minimum capacity loss at high Coulombic efficiency to qualify for vehicle application.

Collaborations. This project collaborates with the following: Vince Battaglia and Venkat Srinivasan of LBNL; Xingcheng Xiao of GM; Jason Zhang and Chongmin Wang of PNNL; and Phillip B. Messersmith of University of California at Berkeley (UC Berkeley).

Milestones

1. Investigate the impact of different side chain conducting moieties to the electric conductivity of the functional conductive binders. (December 2015 – Complete)
2. Quantify the adhesion group impact to the electrode materials and current collector. (March 2016 – Complete)
3. Fabricate higher loading electrode ($> 3 \text{ mAh/cm}^2$) based on the Si electrode materials and select binder; test cycling stability. (June 2016 – Complete)
4. Fabricate NMC/Si full cell and quantify the performance. (September 2016 – On schedule)

Progress Report

Control over porous electrode microstructures is critical for the continued improvement of Li-ion batteries. A convenient and economical method for controlling electrode porosity was developed, thereby enhancing material loading and stabilizing the cycling performance of Li-ion electrodes. Sacrificial NaCl is added to a Si-based electrode, which demonstrates an areal capacity of ca. 4 mAh/cm² at a C/8 rate (0.51 mA/cm²) and an areal capacity of 3 mAh/cm² at a C/2 rate (1.7 mA/cm²), one of the highest material loadings reported for a Si-based anode at such a high cycling rate. X-ray microtomography confirmed the improved porous architecture of the SiO electrode with NaCl. This versatile method was also successfully applied to nano-Si and lithium iron phosphate electrodes. The method developed here is expected to be compatible with the state-of-the-art Li-ion battery industrial fabrication processes, and therefore holds great promise as a practical technique for boosting the electrochemical performance of Li-ion batteries without changing material systems. (Please refer to Publication 1 for details).

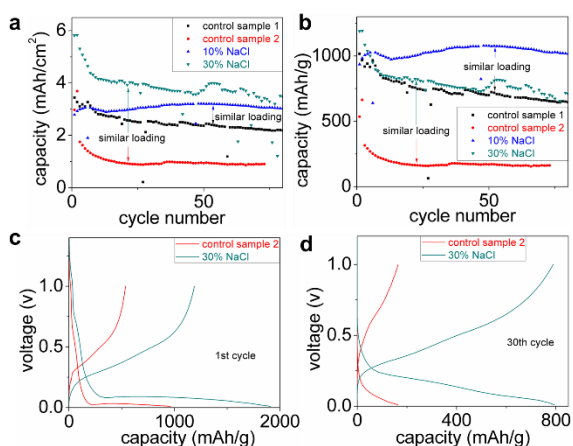


Figure 8. Cycling performance of the SiO/PFM electrodes with or without NaCl. (a) Areal capacity versus cycle number. (b) Specific capacity versus cycle number. (c) First- and (d) thirtieth-cycle voltage curves of samples with and without NaCl.

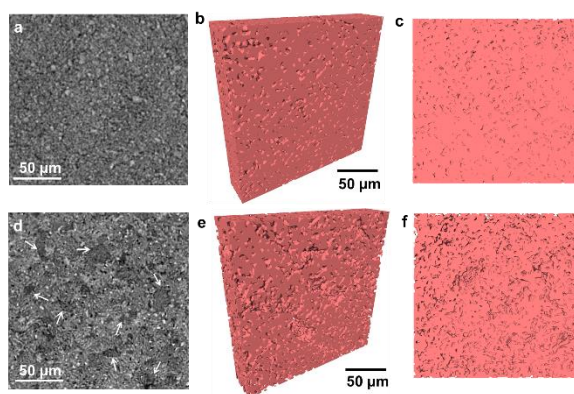


Figure 9. Tomographically reconstructed cross-section and volume rendering of (a-c) the control SiO/PFM electrode and (d-f) the SiO/PFM electrode with porosity generation. The pores induced by NaCl are marked with arrows in the cross-section.

Patents/Publications/Presentations

Publications

- Zhao, Hui, and Qing Yang, Neslihan Yuca, Min Ling, Kenneth Higa, Vincent S. Battaglia, Dilworth Y. Parkinson, Venkat Srinivasan, and Gao Liu. A Convenient and Versatile Method to Control the Electrode Microstructure toward High-Energy Lithium-Ion Batteries. *Nano Letters* 16 (2016): 4686.
- Zhao, Hui, and Allen Du (co-first author), Min Ling, Vincent Battaglia, and Gao Liu. Conductive Polymer Binder for Nano-silicon/Graphite Composite Electrode in Lithium-ion Batteries towards a Practical Application. *Electrochimica Acta* 209 (2016): 159-162.

Presentations

- South University of Science and Technology of China, Shenzhen, China (May 2016): “Development of High Area Loading and Stable Sulfur Electrode Through Interfaces Functionality Design for Lithium Sulfur Battery”; Gao Liu.
- BAK Battery Company, Shenzhen, China (May 2016): “Conductive Polymer Binder for Si Based Anode Materials”; Gao Liu.
- The 12th Biannual China International Battery Fair (CIBF), Shengzhen, China (May 2016): “Development of High Area Loading and Stable Sulfur Electrode Through Interfaces Functionality Design for Lithium Sulfur Battery”; Guo Ai, Zhihui Wang, Min Ling, and Gao Liu.

Task 2 – Silicon Anode Research

Summary and Highlights

Most Li-ion batteries used in state-of-the-art EVs contain graphite as their anode material. Limited capacity of graphite (LiC_6 , 372 mAh/g) is one barrier that prevents the long-range operation of EVs required by the EV Everywhere Grand Challenge proposed by the DOE Office of Energy Efficiency and Renewable Energy (EERE). In this regard, silicon is one of the most promising candidates as an alternative anode for Li-ion battery applications. Silicon is environmentally benign and ubiquitous. The theoretical specific capacity of silicon is 4212 mAh/g ($\text{Li}_{21}\text{Si}_5$), which is 10 times greater than the specific capacity of graphite. However, the high specific capacity of silicon is associated with large volume changes (more than 300 percent) when alloyed with lithium. These extreme volume changes can cause severe cracking and disintegration of the electrode and can lead to significant capacity loss.

Significant scientific research has been conducted to circumvent the deterioration of Si-based anode materials during cycling. Various strategies, such as reduction of particle size, generation of active/inactive composites, fabrication of Si-based thin films, use of alternative binders, and the synthesis of one-dimensional silicon nanostructures have been implemented by a number of research groups. Fundamental mechanistic research also has been performed to better understand the electrochemical lithiation and delithiation processes during cycling in terms of crystal structure, phase transitions, morphological changes, and reaction kinetics. Although significant progress has been made on developing Si-based anodes, many obstacles still prevent their practical application. Long-term cycling stability remains the foremost challenge for Si-based anode, especially for the high loading electrode ($> 3\text{mAh/cm}^2$) required for many practical applications. The cyclability of full cells using Si-based anodes is also complicated by multiple factors, such as diffusion-induced stress and fracture, loss of electrical contact among silicon particles and between silicon and current collector, and the breakdown of solid electrolyte interphase (SEI) layers during volume expansion/contraction processes. The design and engineering of a full cell with a Si-based anode still needs to be optimized. Critical research remaining in this area includes, but is not limited to, the following:

- Low-cost manufacturing processes have to be found to produce nano-structured silicon with the desired properties.
- The effects of SEI formation and stability on the cyclability of Si-based anodes need to be further investigated. Electrolytes and additives that can produce a stable SEI layer need to be developed.
- A better binder and a conductive matrix need to be developed. They should provide flexible but stable electrical contacts among silicon particles and between particles and the current collector under repeated volume changes during charge/discharge processes.
- The performances of full cells using silicon-based anode need to be investigated and optimized.

The main goal of this project is to have a fundamental understanding on the failure mechanism on Si based anode and improve its long-term stability, especially for thick electrode operated at full cell conditions. Success of this project will enable Li-ion batteries with a specific energy of $>350\text{ Wh/kg}$ (in cell level), 1000 deep-discharge cycles, 15-year calendar life, and less than 20% capacity fade over a 10-year period to meet the goal of the EV Everywhere Grand Challenge.

Highlight. The Stanford group developed lithiated SiO_2 nano particles as an anode with a capacity of 1543 mAh/g.

Task 2.0 – Novel Non-Carbonate Based Electrolytes for Silicon Anodes (Dee Strand, Wildcat Discovery Technologies)

Project Objective. The objective is to develop non-carbonate electrolytes that form a stable SEI on silicon alloy anodes, enabling substantial improvements in energy density and cost relative to current Li-ion batteries. These improvements are vital for mass market adoption of EVs. At present, commercial vehicle batteries employ cells based on LiMO_2 ($M = \text{Mn, Ni, Co}$), LiMn_2O_4 , and/or LiFePO_4 coupled with graphite anodes. Next generation cathode candidates include materials with higher specific capacity or higher operating voltage, with a goal of improving overall cell energy density. However, to achieve substantial increases in cell energy density, a higher energy density anode material is also required. Silicon anodes demonstrate very high specific capacities, with a theoretical limit of 4200 mAh/g and state-of-the-art electrodes exhibiting capacities greater than 1000 mAh/g. While these types of anodes can help achieve target energy densities, their current cycle life is inadequate for automotive applications. In graphite anodes, carbonate electrolyte formulations reductively decompose during the first-cycle lithiation, forming a passivation layer that allows lithium transport, yet is electrically insulating to prevent further reduction of bulk electrolyte. However, the volumetric changes in silicon upon cycling are substantially larger than graphite, requiring a much more mechanically robust SEI film.

Project Impact. Silicon alloy anodes enable substantial improvements in energy density and cost relative to current Li-ion batteries. These improvements are vital for mass market adoption of EVs, which would significantly reduce CO_2 emissions as well as eliminate the U.S. dependence on energy imports.

Out-Year Goals. Development of non-carbonate electrolyte formulations that:

- Form stable SEIs on 3M silicon alloy anode, enabling Coulombic efficiency > 99.9% and cycle life > 500 cycles (80% capacity) with NMC cathodes;
- Have comparable ionic conductivity to carbonate formulations, enabling high power at room temperature and low temperature;
- Are oxidatively stable to 4.6 V, enabling the use of high energy NMC cathodes in the future; and
- Do not increase cell costs over today's carbonate formulations.

Collaborations. Wildcat is working with 3M on this project. To date, 3M is supplying the silicon alloy anode films and NMC cathode films for use in Wildcat cells. Recently, ANL provided additional electrodes for testing.

Milestones

1. Assemble materials, establish baseline performance with 3M materials. (December 2013 – Complete)
2. Develop initial additive package using non-SEI forming solvent. (March 2014 – Complete)
3. Screen initial solvents with initial additive package. (June 2014 – Complete)
4. Design/build interim cells for the DOE. (September 2014 – Complete)
5. Improve performance with non-carbonate solvents and new SEI additives. (March 2015 – Complete)
6. Optimize formulations. (August 2015 – Complete)
7. Design/build final cells for the DOE. (March 2016 – Complete)

Progress Report

This quarter, the project completed the final tasks including: (1) optimization of the formulation, (2) measurement of performance across multiple metrics, (3) confirmation of ionic conductivity, and (4) cost analysis. In addition, the final 18650 cells were made by 3M and sent to ANL for testing.

The final optimization was completed, and these formulations were sent for large format (18650 cell testing). The optimization consisted of combinations of additives and co-solvents in both noncarbonate and carbonate solvents to give a good balance of performance across multiple metrics. Thus, the formulations with the absolute best cycle life were not necessarily those selected for 18650 cell testing, as they may have had a severe shortfall that could not be corrected with additional additives. A total of four final formulations (2-5) were identified for testing in 18650 cells compared to a baseline formulation containing ethylene carbonate / ethyl methyl carbonate (EC/EMC) (1:2 by volume) + 10 wt% fluoroethylene carbonate (FEC), as summarized in Table 1.

Table 1. Summary of final formulations for 18650 cells.

Formulation	Solvents	Additives
Control	EC/EMC (1:2 by volume)	10% FEC
2	EC/EMC (1:2 by volume)	2% LiBOB, 2% WDT-2317
3	EC/EMC (1:2 by volume)	2% WDT-2320
4	Noncarbonate combination	2% VC, 0.5% WDT-2094
5	Noncarbonate combination	2% WDT-2320, 2% WDT-2094
6	Noncarbonate combination	2% VC, 2% WDT-2093

Room-Temperature Cycle Life

Figure 10 shows the room-temperature cycle life of formulations 2-6 compared to the control electrolyte.

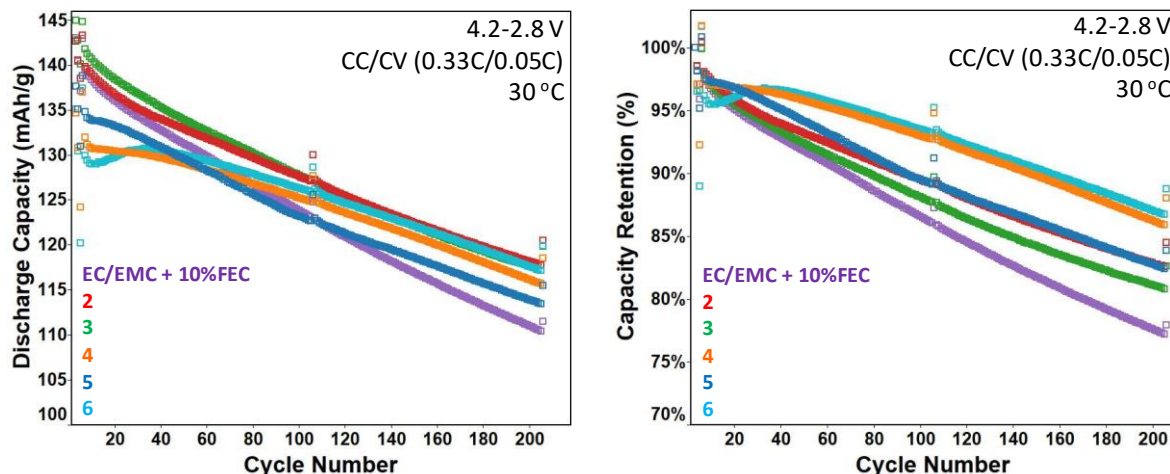


Figure 10. Room-temperature cycle life improved with Wildcat formulations.

All of the formulations identified by Wildcat improved capacity retention relative to the control. However, the two noncarbonate formulations (4, 5) had lower initial capacity. The best performing electrolyte in terms of capacity retention extrapolates to approximately double the cycle life of the control – 320 cycles. While the project goal was 500 cycles, post-mortem work suggests that electrode failure mechanisms occurred that were unrelated to true lithium loss due to SEI formation (reported last quarter). If active material utilization

decreases due to electrical isolation of particles or delamination from current collector, these problems cannot be affected by electrolyte improvements. Addressing these types of failure mechanisms was outside the scope of this project, but suggests that future efforts must address multiple failure mechanisms in parallel. Nevertheless, the new formulations show improved cycle life in full cells without the use of FEC.

Wildcat conducted a shelf life study of formulations 2-5, and found that formulation 4 was unstable over the course of weeks. Therefore, formulation 6 was substituted for formulation 4 in the 18650 cell testing. Formulation 6 showed similar room-temperature performance.

High-Temperature Cycle Life

The high-temperature cycle life of formulations 2-5 is shown in Figure 11.

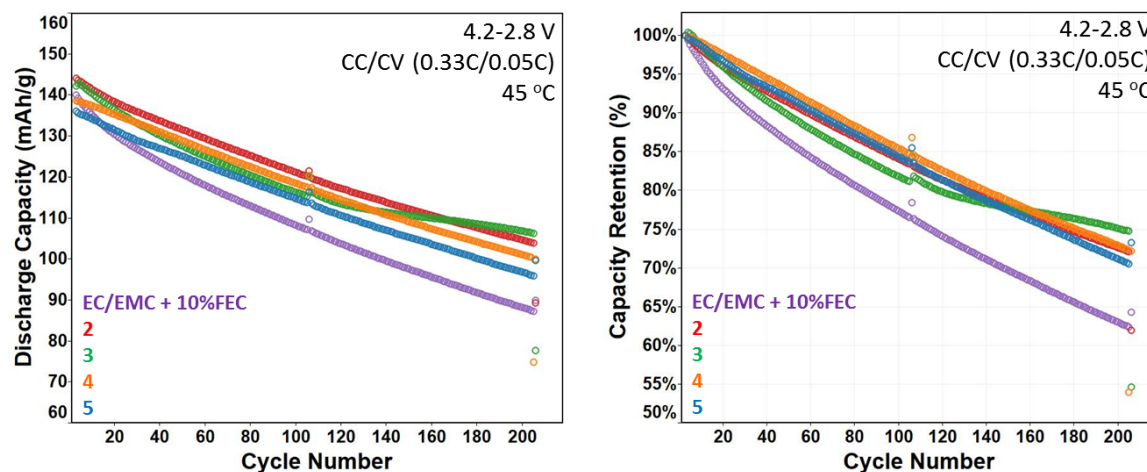


Figure 11. New formulations outperform control with 10% fluoroethylene carbonate (FEC).

All the final formulations outperform the control electrolyte containing 10% FEC. High-temperature performance of FEC is known to be problematic. Wildcat formulations offer significant value at high temperature due to replacement of FEC with other additives.

High-Temperature Storage

High-temperature storage (60°C) experiments for two weeks were performed. The capacities remaining after the high-temperature storage, as well as the recovered capacities, are shown in Figure 12. Both the remaining capacities and recovered capacities were measured at 30°C at C/10 discharge rate. Several of the new electrolytes (3, 4, and 5) showed lower capacities after high-temperature storage than the control. This self discharge could probably be minimized with further optimization of the formulations. All formulations showed similar or better recovered capacities to the control formulation containing 10% FEC.

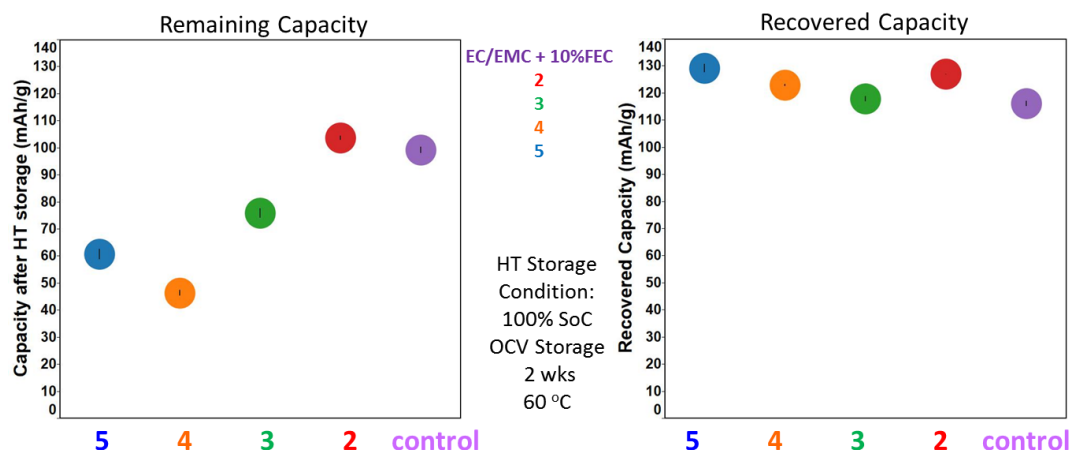


Figure 12. Capacity after high-temperature storage experiment.

The cell impedance growth after high temperature storage (60°C) for two weeks was also measured for these formulations. Figure 13 shows that the initial impedance of the four final (non-carbonate and carbonate-based) formulations is similar or lower to that of the control electrolyte with 10% FEC. After high-temperature storage, three of four formulations maintain similar area specific impedances.

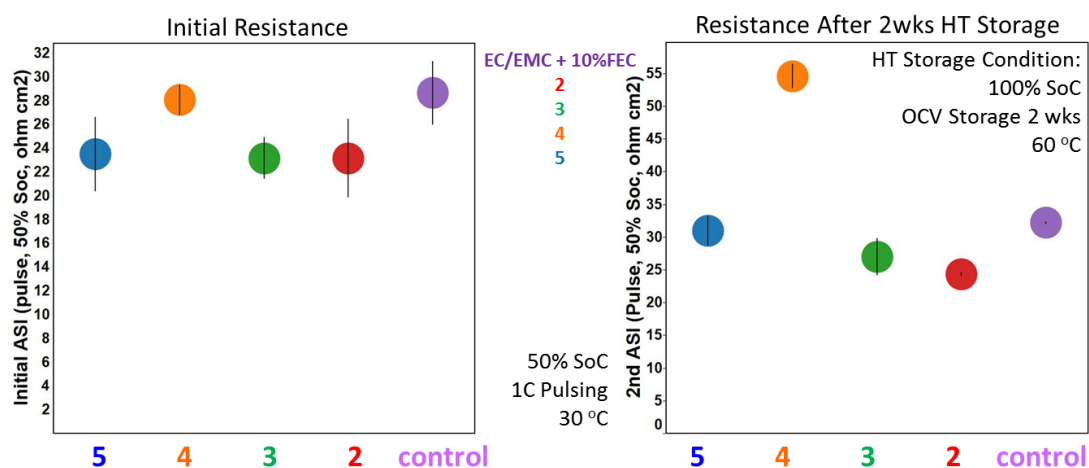


Figure 13. Area specific impedance of formulations after 60°C storage for two weeks.

High-Voltage Cycle Life

The new e formulations would be expected to have similar performance at high voltage as standard carbonate formulations, but benefit from elimination of the FEC. One of the new formulations was tested and optimized with high-voltage additives to demonstrate their feasibility at higher voltages, as shown in Figure 14. In this case, the FEC content in the control electrolyte was reduced to 2%, as it is known that this additive does not perform well at high voltage. The formulations could not be tested above 4.45 V, as the project did not have electrodes balanced for higher voltages. However, the results at 4.45 V show that with the addition of high-voltage additives, this new formulation can cycle better than the control.

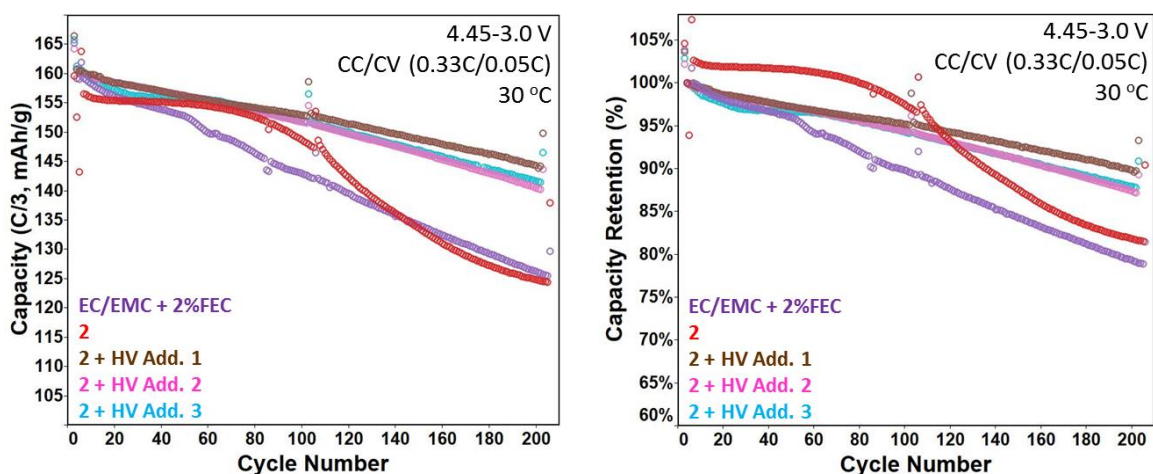


Figure 14. Wildcat noncarbonate formulation demonstrates feasibility at higher voltage.

Low-Temperature Performance

The low-temperature (-20°C) area specific impedance (ASI) and capacity retention on C/10 discharge were also measured for the formulations. As shown in Figure 15, the new formulations all showed similar or lower ASI and similar or higher discharge capacity (C/10) at -20°C compared to the 10% FEC control electrolyte.

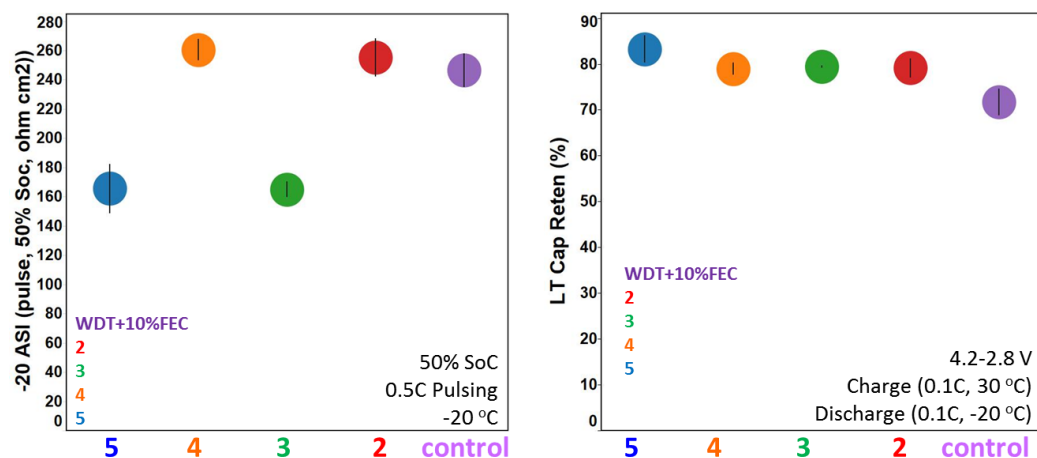


Figure 15. Low-temperature performance of formulations.

Ionic Conductivity

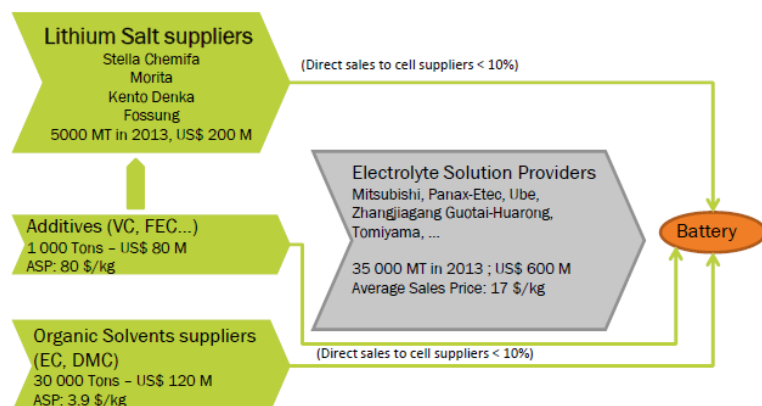
Ionic conductivity results for the formulations are summarized in Table 2. While the room-temperature ionic conductivities are less for the noncarbonate formulations (4-6), the low-temperature ionic conductivity is similar. In general, silicon anodes cannot be cycled at high rates, so room-temperature ionic conductivity can tolerate some decrease. However, to pass low-temperature cold crank tests, it is important not to significantly decrease the low-temperature ionic conductivity.

Table 2. Room-temperature and low-temperature ionic conductivities of formulations.

Formulation	25°C Ionic Conductivity (mS/cm)	-30°C Ionic Conductivity (mS/cm)
Control (10% FEC)	8.5	1.8
Control (2% FEC)	7.5	1.4
2	9.1	1.7
3	9.2	1.8
4	5.4	1.6
5	5.0	1.4
6	5.8	1.7

Cost Analysis

A cost comparison of the electrolytes was also performed. According to Avicenne Energy (4/2015, 24th Edition), carbonate solvents for battery use have an average selling price of \$3.9/kg (2013 data, Figure 16). Common additives such as FEC have an average selling price of \$80/kg. Most electrolytes used with silicon anodes today contain high concentrations (10 – 30 wt%) FEC, resulting in significant cost increases.

**Figure 16. Electrolyte component costs.**

Wildcat developed both carbonate and non-carbonate based formulations with improved performance over the course of this project. The carbonate-based formulations use typical carbonate solvents expected to match the average selling price of \$3.9/kg. Formulations 2 and 3 (carbonate) shown in preceding graphs contained no FEC, and contained much lower additive quantities. Formulation 2 contains 4 wt% total additive concentration, and formulation 3 contains 2 wt%. The specific additive packages used are combinations of common additives used today and newly discovered Wildcat additives. The common additives (used at 2 wt% or less) would compare in cost to those in the Avicenne report, so should not impart a cost increase in the new formulations relative to a standard carbonate formulation. Prices for the new additives can be found on line for small volumes on the order of \$5-10/kg, well under the average selling price of \$80/kg. The new additives are also used at typical concentrations of 2 wt% or less.

Similar additives are used in the noncarbonate formulations, so the cost comparison will depend on the relative costs of the solvents. Online prices for higher volume high purity anhydrous solvents used for the new formulations were on the order of \$3-5/kg (\$3000-\$5000/metric ton). Of course, the actual cost comparison will depend on many factors including purity of starting components and any required purification. Materials in this project were used as received and were not subjected to further purification.

In summary, the high level cost analysis of Wildcat new formulations does not show any obvious cost increases over today's state-of-the-art silicon electrolyte formulations, which contain high levels (10-30 wt%) of expensive FEC.

Patents/Publications/Presentations

Patents

- Four provisional patent applications have been filed. Several of these are being prepared as full utility patent applications.

Presentations

- DOE Annual Merit Review, Washington, D. C. (June 2014); D. A. Strand, Y. Zhu, G. Cheng, and M. Caldwell.
- The Battery Show, Novi, Michigan (September 2014); "Development of Novel Electrolytes for Silicon Anodes"; D. A. Strand, Y. Zhu, G. Cheng, and M. Caldwell.
- BMR Program Review Meeting, LBNL, Berkeley, California (January 2015): "Review: Development of Novel Electrolytes for Silicon Anodes"; D. A. Strand, Y. Zhu, G. Cheng, and M. Caldwell.
- 32nd International Battery Conference, Ft. Lauderdale, Florida (March 2015): "Novel Noncarbonate Electrolytes for Silicon Anodes"; D. A. Strand, Y. Zhu, G. Cheng, and M. Caldwell.
- 2nd International Forum on Cathode and Anode Materials for Advanced Batteries, Hangzhou, China (April 2015): "Novel Noncarbonate Electrolytes for Silicon Anodes"; B. Li, D. A. Strand, Y. Zhu, G. Cheng, and M. Caldwell.
- 227th ECS Meeting, Chicago (May 2015): "Development of Novel Lithium Ion Battery Electrolytes for Silicon Anodes"; Y. Zhu, D. A. Strand, and G. Cheng.
- DOE Annual Merit Review, Washington, D. C. (June 2015): "Novel Noncarbonate Electrolytes for Silicon Anodes"; D. A. Strand, Y. Zhu, G. Cheng, and M. Caldwell.
- 4th China Lithium Ion Battery Electrolytes Conference, Yangzhou, China (June 2015): "Development of Novel Electrolytes for Silicon Anodes"; G. Cheng, Y. Zhu, and D. A. Strand.
- AABC USA 2015, Troy, Michigan (June 2015): "Novel Noncarbonate Electrolytes for Silicon Anodes"; G. Cheng, Y. Zhu, and D. A. Strand.
- ABAA8, Bilbao, Spain (September 2015): "Development of Novel Electrolytes for Silicon Anodes"; D. A. Strand, Y. Zhu, and G. Cheng.
- Batteries 2015, Nice, France (October 2015): "Development of Novel Electrolytes for Silicon Anodes"; D. A. Strand, Y. Zhu, and G. Cheng.
- 12th China International Battery Fair (CIBF), Shenzhen, China (May 2016): "Development of Electrolytes for Silicon Anodes"; B. Li, Y. Zhu, D. Strand, and G. Cheng.
- 229th ECS Meeting, San Diego, California (June 2016): "Development of Electrolytes for Silicon Anodes"; Y. Zhu and D. Strand.
- International Meeting on Lithium Batteries (IMLB), Chicago, Illinois (June 2016): "Development of Electrolytes for Silicon Anodes"; Y. Zhu and D. Strand.

Task 2.1 – Development of Silicon-Based High-Capacity Anodes (Ji-Guang Zhang/Jun Liu, PNNL; Prashant Kumta, U Pittsburgh)

Project Objective. The project objective is to develop high-capacity and low-cost silicon-based anodes with good cycle stability and rate capability to replace graphite in Li-ion batteries. In one approach, the low-cost Si-graphite-carbon (SGC) composite will be developed to improve the long-term cycling performance while maintaining a reasonably high capacity. Si-based secondary particles with a nano-Si content of ~10 to 15 wt% will be embedded in the matrix of active graphite and inactive conductive carbon materials. Controlled void space will be pre-created to accommodate the volume change of silicon. A layer of highly graphitized carbon coating at the outside will be developed to minimize the contact between silicon and electrolyte, and hence minimize the electrolyte decomposition. New electrolyte additives will be investigated to improve the stability of the SEI layer. In another approach, nanoscale silicon and Li-ion conducting lithium oxide composites will be prepared by *in situ* chemical reduction methods. The stability of Si-based anode will be improved by generating the desired nanocomposites containing nanostructured amorphous or nanocrystalline Si as well as amorphous or crystalline lithium oxide (Si+Li₂O) by the direct chemical reduction of a mixture and variety of silicon sub oxides (SiO and SiO_x) and/or dioxides. Different synthesis approaches comprising direct chemical reduction using solution, solid-state, and liquid-vapor phase methods will be utilized to generate the Si+Li₂O nanocomposites. The electrode structures will be modified to enable high utilization of thick electrode.

Project Impact. Si-based anodes have much larger specific capacities compared with conventional graphite anodes. However, the cyclability of Si-based anodes is limited because of the large volume expansion characteristic of these anodes. This work will develop a low-cost approach to extend the cycle life of high-capacity, Si-based anodes. The success of this work will further increase the energy density of Li-ion batteries and accelerate market acceptance of EVs, especially for the PHEVs required by the EV Everywhere Grand Challenge proposed by the DOE/EERE.

Out-Year Goals. The main goal of the proposed work is to enable Li-ion batteries with a specific energy of > 200 Wh/kg (in cell level for PHEVs), 5000 deep-discharge cycles, 15-year calendar life, improved abuse tolerance, and less than 20% capacity fade over a 10-year period.

Milestones

1. Identify and synthesize the active-inactive Si-based nanocomposite with low-cost approach and a specific capacity ~800 mAh/g. (December 2015 – Complete)
2. Achieve 80% capacity retention over 200 cycles for graphite supported nano Si-carbon shell composite. (March 2016 – Complete)
3. Develop interface control agents and surface electron conducting additives to reduce the first-cycle irreversible loss and improve the Coulombic efficiency of Si-based anode. (June 2016 – Ongoing)
4. Optimize the cost-effective, scalable high-energy mechanical milling (HEMM) and solid state synthesis techniques for generation of active-inactive composite with capacities ~1000-1200 mAh/g. (June 2016 – Ongoing)
5. Achieve > 80% capacity retention over 300 cycles for thick electrodes (> 2 mAh cm⁻²) through optimization of the silicon electrode structure and binder. (September 2016 – Ongoing)
6. Synthesize the suitable active-inactive nanocomposite with Li₂O as matrix (Si+Li₂O) or intermetallic matrix (Si+ MnBm) of specific capacity ~1000-1200mAh/g. (September 2016 – Ongoing)

Progress Report

This quarter, the electrochemical performance of porous-Si-graphite composite was evaluated. Figure 17a shows the cycling stability of a typical electrode with the porous silicon and graphite ratio of 1:3. The specific capacity was calculated based on the active material (porous silicon and graphite). The electrode loading was $\sim 3 \text{ mAh cm}^{-2}$ at a low current density of $\sim 0.06 \text{ mA cm}^{-2}$. The areal capacity is $\sim 2.5 \text{ mAh cm}^{-2}$ at a charge-discharge current density of $\sim 0.4 \text{ mA cm}^{-2}$. The specific capacity is $\sim 610 \text{ mAh g}^{-1}$. The capacity retention is $\sim 88\%$ in 500 cycles.

In another effort, Ge coating on the porous-Si-graphite electrode was used to improve the cycling stability because it was reported that Ge has uniform volume change upon charge and discharge without cracking. Figure 17b shows typical cycling result of the electrode with and without Ge coating. The electrode without Ge coating shows stable cycling of ~ 170 cycles. The capacity retention is $\sim 97\%$. The electrode with 10 nm Ge coating, however, shows faster capacity fade. The capacity retention in 100 cycles is $\sim 89\%$. It is believed that the Ge layer sputtered on silicon electrode degraded the interface impedance of silicon electrode and led to faster capacity fade.

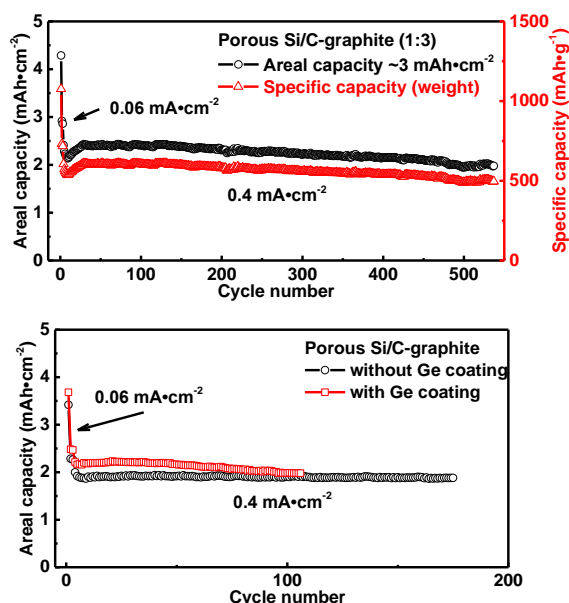


Figure 17. (a) Cycling stability of porous-Si-graphite electrode. (b) The cycling stability of porous-Si-graphite electrodes with and without Ge coating.

In previous quarters, formation of active-inactive nanocomposite comprising of nanocrystalline silicon (*nc*-Si) and metal oxide (MM')_nO_x [*nc*-Si+(MM')_nO_x] as matrix, obtained by high energy ball milling of SiO_x with a metal alloy (MM') reductant, has been reported. The nanocomposite shows a first- and second-cycle discharge capacity of $\sim 2130 \text{ mAh/g}$ and $\sim 1065 \text{ mAh/g}$, respectively, with a first-cycle irreversible loss (FIR) of 50% (Figure 2). However, it shows a rapid fade in capacity with a fade rate of 1.62% loss per cycle. Flexible nanofiber electrode was fabricated by impregnating (*nc*-Si+(MM')_nO_x) composite in the polymer derived CNF ($\sim 10\text{wt}\%$) by solution coating method followed by carbonization [(*nc*-Si+(MM')_nO_x)/CNF]. The electrochemical performance of (*nc*-Si+(MM')_nO_x)/CNF flexible fibre shows a first- and second-cycle discharge capacity of $\sim 1650 \text{ mAh/g}$ and $\sim 1325 \text{ mAh/g}$, respectively, with a FIR of $\sim 20\%$ (Figure 18). It is interesting to note that the second cycle discharge capacity of (*nc*-Si+(MM')_nO_x)/CNF is comparable to the nanocomposite (*nc*-Si+(MM')_nO_x) with a significant decrease in FIR. In addition, (*nc*-Si+(MM')_nO_x)/CNF shows a significant improvement in the cyclability up to 60 cycles in comparison to [*nc*-Si+(MM')_nO_x] with a fade in capacity $\sim 0.13\%$ loss per cycle (Figure 18). Extensive electrochemical characterization including electrochemical impedance, rate capability, degradation mechanism, etc. will be reported soon. Additionally, a new *nc*-Si/metal oxide composite has been synthesized by reducing SiO_x using metal hydrides. Two metal hydrides (M₁H and M₂H) were milled with SiO in argon atmosphere to obtain precursors that were further heat treated to form the *nc*-Si/MO nanocomposite. Electrochemical and materials evaluation results will be reported next quarter.

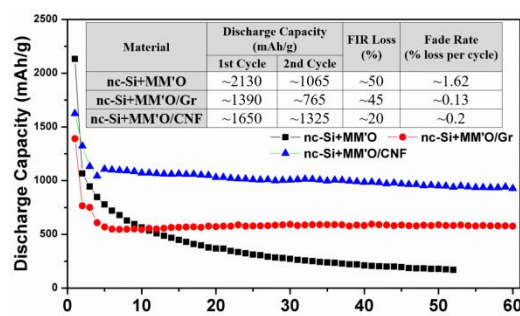


Figure 18. Specific discharge capacity versus cycle numbers for different active electrodes based *nc*-Si/MM'O composite. Inset table shows the summary of performance of the materials.

Patents/Publications/Presentations

Patent

- High-Capacity Conversion Reaction-based Cathode Additives for Lithium-Ion Batteries; WebDisclosure 197169.

Publications

- Epur, Rigved, and Madhumati Ramanathan, Moni K. Datta, Dae Ho Hong, Prashanth H. Jampani, Bharat Gattu, and Prashant N. Kumta. “Scribable Multi-Walled Carbon Nanotube-silicon Nanocomposites: A Viable Lithium-ion Battery System.” *Nanoscale* 7 (2015): 3504-3510.
- Epur, Rigved, and Prashanth H. Jampani, Moni K. Datta, Dae Ho Hong, Bharat Gattu, and Prashant N. Kumta. “A Simple and Scalable Approach to Hollow Silicon Nanotube (h-SiNT) Anode Architectures of Superior Electrochemical Stability and Reversible Capacity.” *J. Mater. Chem. A* 3 (2015): 11117-11129.

Presentations

- 18th International Meeting on Lithium Batteries, Chicago, Illinois (June 19-24, 2016): “Hard Carbon Coated Nano-Si/Graphite Composite as a High Performance Anode for Li-Ion Batteries”; Sookyung Jeong, Xiaolin Li, Jianming Zheng, Pengfei Yan, Ruiguo Cao, HeeJoon Jung, Chongmin Wang, Jun Liu, and Ji-Guang Zhang.
- 228th ECS Meeting, Phoenix, Arizona (October 2015): “Nano Silicon (Si_{NP}) Based Carbon Composite: Flexible Anode System in Lithium Ion Batteries”; B. Gattu, P. P. Patel, P. Jampani, M. K. Datta, and P. N. Kumta,
- 227th ECS Meeting, Chicago, Illinois (May 2015): “High Performing Hollow Silicon Nanotube Anodes for Lithium Ion Batteries”; B. Gattu, P. Jampani, P. P. Patel, M. K. Datta, and P. N. Kumta.

Task 2.2 – Pre-Lithiation of Silicon Anode for High-Energy Lithium-Ion Batteries (Yi Cui, Stanford University)

Project Objective. Prelithiation of high-capacity electrode materials such as silicon is an important means to enable those materials in high-energy batteries. This study pursues two main directions: (1) developing facile and practical methods to increase first-cycle Coulombic efficiency of silicon anodes, and (2) synthesizing fully lithiated silicon and other lithium compounds for pre-storing lithium.

Project Impact. The lithium loss for first cycle in existing Li-ion batteries will be compensated by using these cathode prelithiation materials. The cathode prelithiation materials have good compatibility with ambient air, regular solvent, binder, and the thermal processes used in current Li-ion battery manufacturing. This project's success will improve the energy density of existing Li-ion batteries and help to achieve high-energy-density Li-ion batteries for electric vehicles.

Out-Year Goals. Compounds containing a large quantity of lithium will be synthesized for pre-storing lithium ions inside batteries. First-cycle lithium loss will be compensated (for example, ~10%) by prelithiation with the synthesized conversion materials.

Collaborations. The project works with the following collaborators: (1) BMR principal investigators, (2) Stanford Linear Accelerator Center (SLAC): *in situ* X-ray, Dr. Michael Toney, and (3) Stanford: mechanics, Professor Nix.

Milestones

1. Synthesize artificial-SEI protected Li_xSi NPs with high capacity ($>2000\text{mAh/g Si}$) and improved stability in humid air (~10% relative humidity). (September 2015 – Complete)
2. Prelithiate conversion oxides by the reaction between molten lithium metal and oxide. (December 2015 – Complete)
3. Prelithiate SiO to form $\text{Li}_x\text{Si}/\text{Li}_2\text{O}$ composites with improved stability in ambient air with 40% relative humidity. (March 2016 – Complete)
4. Prelithiate SiO_2 to form $\text{Li}_x\text{Si}/\text{Li}_2\text{O}$ composites. (June 2016 – Complete)

Progress Report

Previously, SiO_2 was not considered to be electrochemically active for lithium storage, due to poor electrical and ionic conductivity. By using fine nanostructures, SiO_2 anodes have been recently demonstrated, but with limited capacity and quick capacity decay. Here, the project developed $\text{Li}_x\text{Si}/\text{Li}_2\text{O}$ composites via a one-pot metallurgical process using low-cost SiO_2 as the starting material to alloy thermally with molten lithium metal. Figure 19a shows SiO_2 NPs with a narrow size distribution around 90 nm. After metallurgical lithiation, the morphology of NPs remained, while the size changed to 200 nm due to volume expansion (Figure 19b). XRD pattern also confirms the formation of crystalline $\text{Li}_{21}\text{Si}_5$ and Li_2O during the alloying process (Figure 19c). To measure the real capacity and eliminate the possible capacity loss during the slurry coating process, lithiated SiO_2 NPs were dispersed in cyclohexane and then drop casted on copper foil. The extraction capacities of lithiated SiO_2 were 1543 mAh/g, based on the mass of SiO_2 (Figure 19d). The open circuit voltage (OCV) of lithiated SiO_2 NPs was below 0.1 V, confirming that the majority of SiO_2 has been successfully lithiated. Similar to lithiated SiO NPs, lithiated SiO_2 NPs can undergo slurry process with THF as slurry solvent and exhibit negligible capacity consumption. It is important to note that the galvanostatic discharge/charge profile of SiO_2 NPs (SiO_2 : Super P: PVDF=65:20:15 by weight, orange curve in Figure 19d) showed little delithiation capacity after the first lithiation cycle, indicating that the sol-gel synthesized SiO_2 NPs are electrochemically inactive. However, thanks to the thermal lithiation process, the inactive SiO_2 NPs can be successfully converted into high-capacity anode. As the final products of lithiated SiO and SiO_2 are the same, lithiated SiO_2 also serves as a prelithiation reagent. Similarly, lithiated SiO_2 NPs were mixed with graphite and PVDF in a weight ratio of 6:84:10 to achieve high 1st Coulombic efficiency of 99.7%. Due to the nanoscale dimension and the small amount, prelithiation reagents tend to be embedded in the interstices of graphite microparticles. Therefore, graphite prelithiated with lithiated SiO_2 NPs follow the trend of the graphite control cell and exhibit stable cycling performance at C/20 for the first three cycles and C/5 for the following cycles (1C=372 mAh/g, Figure 19f). The commercial graphite with $\text{Li}_x\text{Si}/\text{Li}_2\text{O}$ prelithiation reagents suppresses the undesired consumption of lithium from cathode materials, which in turn increases the energy density of the full cell.

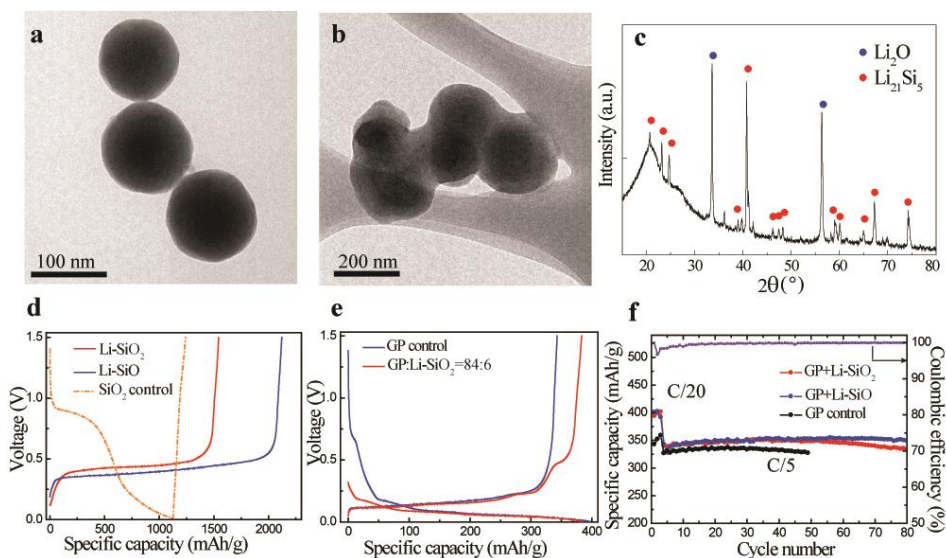


Figure 19. Characterizations and electrochemical performance of SiO_2 NPs before and after thermal lithiation. (a, b) Transmission electron microscopy images of sol-gel synthesized SiO_2 NPs (a) and lithiated SiO_2 NPs (b). (c) X-ray diffraction pattern of lithiated SiO_2 NPs. (d) First-cycle delithiation capacity of lithiated SiO_2 NPs (red) and SiO NPs (blue). Galvanostatic lithiation/delithiation profile of SiO_2 NPs in first cycle (orange). The capacity is based on the mass of SiO or SiO_2 in the anode. (e) First-cycle voltage profiles of graphite/lithiated SiO_2 composite (84:6 by weight, red) and graphite control cell (blue). (f) Cycling performance of graphite/lithiated SiO_2 composite (84:6 by weight, red), graphite/lithiated SiO composite (84:6 by weight, blue) and graphite control cell (black) at C/20 for first three cycles, and C/5 for the following cycles (1C = 0.372 A/g C, the capacity is based on the mass of the active materials, including graphite, and SiO and SiO_2 in $\text{Li}_x\text{Si}/\text{Li}_2\text{O}$ composites). The purple line is the Coulombic efficiency of graphite/lithiated SiO_2 composite.

Patents/Publications/Presentations

Patent

- High-capacity prelithiation reagents and lithium-rich anode materials, Patent Application No. 14/869,800.

Publication

- Zhao, J., and H. W. Lee, J. Sun, K. Yan, Y. Liu, W. Liu, Z. Lu, D. Lin, G. Zhou, and Y. Cui*. “Metallurgically Lithiated SiO_x Anode with High Capacity and Ambient Air Compatibility. *PNAS* 113 (2016): 7408.

TASK 3 – HIGH ENERGY DENSITY CATHODES FOR ADVANCED LITHIUM-ION BATTERIES

Summary and Highlights

Developing high energy density, low-cost, thermally stable, and environmentally safe electrode materials is a key enabler for advanced batteries for transportation. High energy density is synonymous with reducing cost per unit weight or volume. Currently, one major technical barrier toward developing high energy density Li-ion batteries is the lack of robust, high-capacity cathodes. As an example, the most commonly used anode material for Li-ion batteries is graphitic carbon, which has a specific capacity of 372 mAh/g, while even the most advanced cathodes like lithium nickel manganese cobalt oxide (NMC) have a maximum capacity of ~180 mAh/g. This indicates an immediate need to develop high-capacity (and voltage) intercalation type cathodes that have stable reversible capacities of 250 mAh/g and beyond. High volumetric density is also critical for transportation applications. Alternative high-capacity cathode chemistries such as those based on conversion mechanisms, Li-S, or metal air chemistries still have fundamental issues that must be addressed before integration into cells for automotive use. Successful demonstration of practical high energy cathodes will enable high energy cells that meet or exceed the DOE cell level targets of 400 Wh/kg and 600 Wh/L with a system level cost target of \$125/kWh.

During the last decade, many high-voltage cathode chemistries were developed under the BATT (now BMR) program, including Li-rich NMC and Ni-Mn spinels. Current efforts are directed toward new syntheses and modifications to improve their stability under high-voltage cycling condition (> 4.4 V) for Ni-rich NMC and Li-Mn-rich NMC (LMR-NMC) [Zhang/Jie, PNNL; Thackeray/Croy, ANL; Doeff and Tong, LBNL]. Three other subtasks are directed toward synthesis and structural stabilization of high-capacity polyanionic cathodes that can have > 1 lithium per transition metal (TM) and can be in crystalline or amorphous phases [Nanda, ORNL; Manthiram, UT Austin; Looney/Wang, BNL; Whittingham, State University of New York (SUNY) at Binghamton; and Kercher/Kiggans, ORNL]. Approaches also include aliovalent or isovalent doping to stabilize cathode structures during delithiation as well as stabilizing oxygen. John Goodenough's group at UT Austin is developing membranes to stabilize lithium metal anodes and eventually enable high-capacity cathodes in full cell configuration.

Highlights. The highlights for this quarter are as follows:

- **Task 3.1.** *In situ* transmission X-ray microscopy – X-ray absorption near edge structure (TXM – XANES) probes on the origin of irreversibility and capacity loss in $\text{Li}_2\text{-Cu-NiO}_2$ high-capacity cathodes.
- **Task 3.2.** Demonstrated the rate capability of the Sn-Fe anode over 500 cycles and at a volumetric capacity of at least 1.5 times that of graphite, 0.8 Ah/cc.
- **Task 3.3.** Investigated the structural/chemical evolution of different NMC cathodes during high-cutoff-voltage cycling (up to 4.8 V) and correlated with electrochemical activity.
- **Task 3.4.** Developed a new autoclave system for solvothermal synthesis of Ni-rich layered cathodes under controlled conditions (with well-defined T , P and pH).
- **Task 3.5.** Reported influence of a Li-rich spinel coating with a targeted composition, $\text{Li}_{1.1}\text{Mn}_{1.9}\text{O}_4$, on the electrochemical properties of LCO to address oxygen instability and evolution.
- **Task 3.6.** Investigated mixed alkali effect in glass cathodes: $\text{Na}_x\text{Cu}(\frac{1}{2}\text{PO}_3\frac{1}{2}\text{VO}_3)_{2+x}$ and $\text{K}_x\text{Cu}(\frac{1}{2}\text{PO}_3\frac{1}{2}\text{VO}_3)_{2+x}$.
- **Task 3.7.** Soft X-ray absorption spectroscopy (XAS) studies on Ni-rich NMC-622 shows irreversibility behavior in nickel redox activity during first cycle, unlike Mn and Co oxidation state.
- **Task 3.8.** Reported the activation energy of Na-glass electrolytes as function of temperature.
- **Task 3.9.** Structural and electrochemical evaluation of high-voltage $\text{LiCo}_{1-x}\text{Ni}_x\text{O}_2$ ($0 \leq x \leq 0.5$) cathode materials synthesized at 700°C and 800°C.
- **Task 3.10.** Synthesis and electrochemical characterization of Li_2NiO_2 and a series of $\text{Li}_2\text{Ni}_{1-x}\text{Cu}_x\text{O}_2$ ($0 < x < 1$) samples prepared by a solid state method.

Task 3.1 – Studies of High-Capacity Cathodes for Advanced Lithium-Ion Systems (Jagjit Nanda, Oak Ridge National Laboratory)

Project Objective. The overall project goal is to develop high energy density Li-ion electrodes for EV and PHEV applications that meet and/or exceed the DOE energy density and life cycle targets from the USDRIVE/USABC roadmap. Specifically, this project aims to mitigate the technical barriers associated with high-voltage cathode compositions such as LMR-NMC, and $\text{Li}_2\text{M}_x^{\text{I}}\text{M}_{1-x}^{\text{II}}\text{O}_2$, where M^{I} and M^{II} are transition metals that do not include Mn or Co. Major emphasis is placed on developing new materials modifications (including synthetic approaches) for high-voltage cathodes that will address issues such as: (i) voltage fade associated with LMR-NMC composition that leads to loss of energy over the cycle life; (ii) transition metal dissolution that leads to capacity and power fade; (iii) thermal and structural stability under the operating state-of-charge (SOC) range; and (iv) voltage hysteresis associated with multivalent transition metal compositions. Another enabling feature of the project is utilizing (and developing) various advanced characterization and diagnostic methods at the electrode and/or cell level for studying cell and/or electrode degradation under abuse conditions. The techniques include electrochemical impedance spectroscopy (EIS), micro-Raman spectroscopy; aberration corrected electron microscopy combined with electron energy loss spectroscopy (EELS), X-ray photoelectron spectroscopy (XPS), inductively coupled plasma – atomic emission spectroscopy (ICP-AES), fluorescence, and X-ray and neutron diffraction.

Project Impact. The project has short- and long- term deliverables directed toward VTO Energy Storage 2015 and 2022 goals. Specifically, work focuses on advanced electrode couples that have cell level energy density targets of 400 Wh/kg and 600 Wh/l for 5000 cycles. Increasing energy density per unit mass or volume reduces the cost of battery packs consistent with the DOE 2022 EV Everywhere goal of \$125/kWh.

Out-Year Goals. The project is directed toward developing high-capacity cathodes for advanced Li-ion batteries. The goal is to develop new cathode materials that have high capacity, use low cost materials, and meet the DOE road map in terms of safety and cycle life. Under this project two kinds of high energy cathode materials are studied. Over the last few years, the principal investigator (PI) has worked on improving cycle life and mitigating energy losses of high-voltage Li-rich composite cathodes (referred to as LMR-NMC) in collaboration with the voltage fade team at ANL. Efforts also include surface modification of LMR-NMC cathode materials to improve their electrochemical performance under high-voltage cycling ($> 4.5\text{V}$). The tasks also include working in collaboration with researchers at Stanford Synchrotron Research Laboratory (SSRL) and Advanced Light Source (ALS, LBNL) to understand local changes in morphology, microstructure, and chemical composition under *in situ* and *ex situ* conditions.

Collaborations. This project collaborates with Johanna Nelson, SSRL, SLAC: X-ray imaging and XANES; Guoying Chen, LBNL: *in situ* XAS and XRD; Feng Wang, BNL: X-ray synchrotron spectroscopy and microscopy; and Bryant Polzin, Argonne Research Laboratory: CAMP Facility for electrode fabrication.

Milestones

1. Synthesize three compositions of $\text{Li}_2\text{Cu}_x\text{Ni}_{1-x}\text{O}_2$ cathodes with x between 0.4-0.6 and improve their anionic stability by fluorination. *Subtask 1.1:* Fluorination of Li_2CuO_2 (Q1 – Complete). *Subtask 1.2:* Fluorination of $\text{Li}_2\text{Cu}_x\text{Ni}_{1-x}\text{O}_2$ with $x \sim 0.4\text{-}0.6$ (Q2 – Complete).
2. Identify roles of Ni and F in obtaining reversible redox capacity at higher voltage, and stabilize Ni-rich compositions. *Subtask 2.1:* XANES, microscopy, and X-ray photoelectron spectroscopy (XPS) studies (Q3 – Complete). *Subtask 2.2:* Gas evolution and electrochemistry (Q4 – Smart Milestone).

Progress Report

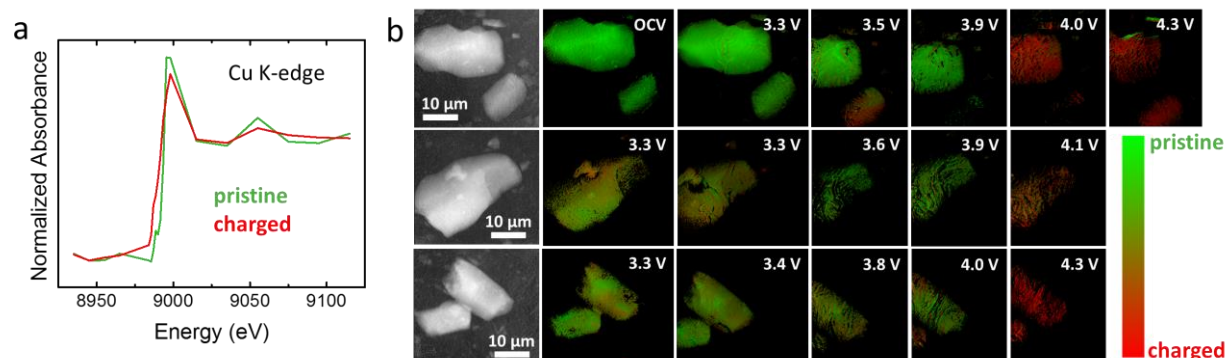


Figure 20. (a) Average (bulk) Cu K-edge X-ray absorption near edge structure (XANES) from an uncycled cell and cell charged *ex situ*. (b) Phase maps from transmission X-ray microscopy XANES data collected *in situ* during charge at three different electrode positions. Phase maps were generated by linear combination fitting using the bulk XANES shown in panel a. Transmission images at 9115 eV are also shown.

As part of the third milestone, the project focused on understanding the role of Ni (and Cu) redox activity and accompanying structural and compositional changes. These results will shed some light on the stability and phase evolution of Ni-rich Li-Ni-Cu-O composition. The experiments were carried out at the TXM-XANES beamline (BL 6-2c) at SSRL, Stanford. The team carried out *in situ* TXM as a function of voltage monitoring both the Cu and Ni K-edges. Figure 20a shows the changes in Cu K-edge when the $\text{Li}_2\text{Cu}_{0.5}\text{Ni}_{0.5}\text{O}_2$ is fully charged to 4.3 V. The direction of the shift is opposite what would be expected if Cu^{2+} were oxidized to Cu^{3+} . The shift likely reflects a change in coordination or structure, and not a change in the formal oxidation state of Cu. This is consistent with earlier work, which indicated that copper was not oxidized up to 4.3 V versus Li/Li⁺. The project compared the changes spatially at three different positions of the electrode, as shown in Figure 20b. The XANES maps were generated using linear combination fitting. At each of the three electrode positions, the phase maps show a significant change in the Cu chemistry above 4.0 V. The transformation is largely uniform across entire particles. Changes in the XANES spectra correlate with the voltage at which significant gas evolution occurs. TXM-XANES collected *in situ* at the Ni K-edge (Figure 21) closely follow the results from the Cu K-edge. Significant changes in the shape of the absorption

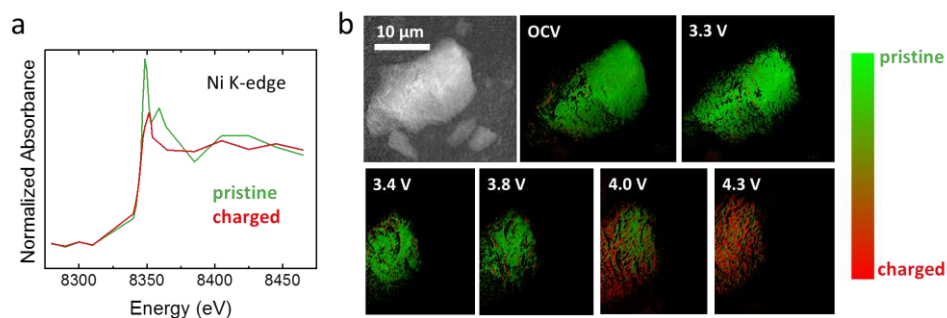


Figure 21. (a) Average (bulk) Ni K-edge X-ray absorption near edge structure (XANES) from an uncycled cell and cell charged *ex situ*. (b) Phase maps from transmission X-ray microscopy XANES data collected *in situ* during charge. Phase maps were generated by linear combination fitting using the bulk XANES shown in panel a. Transmission images at 8465 eV are also shown.

edge are evident after charging above 4.0 V. Figure 21b shows phase maps generated by linear combination fitting using the XANES in Figure 21a. A mixture of phases is present at 4.0 V, but at 4.3 V the particle is almost fully transformed. Further work will be needed to fully interpret the phases that form during the initial charge.

Patents/Publications/Presentations

Publication

- Allu, S., and S. Kalnaus, S. Simunovic, J. Nanda, J. A. Turner, and S. Pannala. “A Three-dimensional Memo-macroscopic Model for Li-ion Intercalation Batteries.” *J. Power Sources* 325 (2016): 42-50.

Presentations

- PNNL, Richland, Washington (May 27-29, 2016): “Beyond Lithium-ion 9, n, *In-situ* Neutron Imaging and Diffraction of Lithiation in Graphite Anodes”; H. Zhou, J. Nanda, et al. Poster.
- DOE Annual Merit Review, Washington D. C. (June 6-10, 2016): “Studies on High Capacity Lithium-ion Cathodes for Advance Lithium-ion”; Jagjit Nanda and Rose Ruther. Poster.

Task 3.2 – High Energy Density Lithium Battery (Stanley Whittingham, SUNY Binghamton)

Project Objective. The project objective is to develop the anode and cathode materials for high energy density cells for use in PHEVs and EVs that offer substantially enhanced performance over current batteries used in PHEVs and with reduced cost. Specifically, the primary objectives are to:

- Increase the volumetric capacity of the anode by a factor of 1.5 over today's carbons
 - Using a SnFeC composite conversion reaction anode
- Increase the capacity of the cathode
 - Using a high-capacity conversion reaction cathode, CuF_2 , and/or
 - Using a high-capacity 2 Li intercalation reaction cathode, VOPO_4
- Enable cells with an energy density exceeding 1 kWh/liter

Project Impact. The volumetric energy density of today's Li-ion batteries is limited primarily by the low volumetric capacity of the carbon anode. If the volume of the anode could be cut in half, and the capacity of the cathode to over 200 Ah/kg, then the cell energy density can be increased by over 50% to approach 1 kWh/liter (actual cell). This will increase the driving range of vehicles.

Moreover, smaller cells using lower cost manufacturing will lower the cost of tomorrow's batteries.

Out-Year Goals. The long-term goal is to enable cells with an energy density of 1 kWh/liter. This will be accomplished by replacing both the present carbon used in Li-ion batteries with anodes that approach double the volumetric capacity of carbon, and the present intercalation cathodes with materials that significantly exceed 200 Ah/kg. By the end of this project, it is anticipated that cells will be available that can exceed the volumetric energy density of today's Li-ion batteries by 50%.

Collaborations. The Advanced Photon Source (APS) at ANL and, when available, the National Synchrotron Light Source II at BNL will be used to determine the phases formed in both *ex situ* and *operando* electrochemical cells. University of Colorado, Boulder, will provide some of the electrolytes to be used.

Milestones

1. Determine the optimum composition Li_xVOPO_4 . (December 2015 – Complete)
2. Demonstrate VOPO_4 rate capability. (March 2016 – Complete)
3. Demonstrate Sn_2Fe rate capability. (June 2016 – Complete)
4. Demonstrate CuF_2 rate capability. (September 2016)
5. *Go/No-Go*: Demonstrate lithiation method. *Criteria*: A cycling cell containing lithium in one of the intercalation or conversion electrodes must be achieved. (September 2016)

Progress Report

The goal of this project is to synthesize tin-based anodes that have 1.5 times the volumetric capacity of the present carbons, and conversion and intercalation cathodes with capacities over 200 Ah/kg. The major effort in this third quarter of year two was to complete the cycling evaluation of the conversion anode material, Sn_yFeC , and determine its rate capability versus a lithium anode.

Milestone 3. The goal of this milestone is to demonstrate the rate capability of the tin-iron anode over 500 cycles and at a volumetric capacity of at least 1.5 times that of graphite, 0.8 Ah/cc. A chemically synthesized Sn_yFe anode was evaluated versus a lithium anode. The first 10 cycles were performed at a rate of C/10 on both lithium insertion and removal (discharge and charge); the next 10 were carried at C/5 on both charge and discharge; for the next 20 cycles the discharge rate was increased to C/2 and the remaining cycles were all at C discharge, while the charge rate was maintained at a C/5 rate. Figure 22 (top) shows the capacity over the first 550 cycles in the voltage window 0.01-1.5V. After 500 cycles the gravimetric capacity was 414 mAh/g. This translates into a final volumetric capacity of 1.2 Ah/cc, 1.5 times the 0.8 Ah/cc of graphite. The rate capability is also shown in Figure 22 (bottom). This data is comparable to that of the mechanochemically synthesized Sn_2FeC composite recently reported (see publications below) and shows the feasibility of these tin-based materials as anodes for advanced lithium batteries.

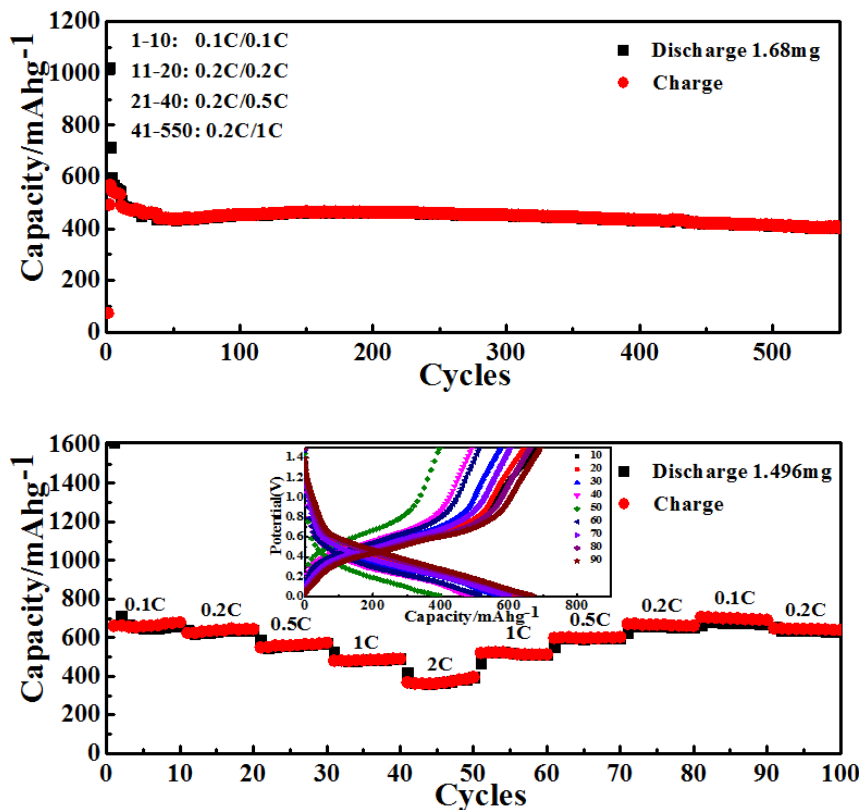


Figure 22. The electrochemical behavior of the Sn_yFe anode versus lithium metal: (top) capacity over 500+ cycles; and (bottom) capacity as a function of rate (the insert shows the voltage profile); charge and discharge with the same current rate. The weight of active material is given at the top right.

Patents/Publications/Presentations

Publication

- Dong, Zhixin, and R. Zhang, D. Ji, N. A. Chernova, K. Karki, S. Sallis, L. Piper, and M. S. Whittingham. “The Anode Challenge for Lithium-ion Batteries: A Mechanochemically Synthesized Sn-Fe-C Composite Anode Surpasses Graphitic Carbon.” *Advanced Science* 3 (2016): 1500229.

Presentation

- DOE Annual Merit Review, Washington, D. C. (June 9, 2016): “High Energy Density Lithium Battery.”

Task 3.3 – Development of High-Energy Cathode Materials (Ji-Guang Zhang and Jianming Zheng, Pacific Northwest National Laboratory)

Project Objective. The project objective is to develop high-energy-density, low-cost, cathode materials with long cycle life. The previous investigation demonstrates that synthesis condition, synthesis approach, and surface modification have significant effects on the performances of high-voltage spinel and LMR-NCM cathodes. These valuable understandings will be used to guide the development of high-energy-density, enhanced long-term cycling stability of Ni-rich $\text{LiNi}_x\text{Mn}_y\text{Co}_z\text{O}_2$ (NMC) cathode materials that can deliver a high discharge capacity with long-term cycling stability.

Project Impact. Although state-of-the-art layered structure cathode materials such as $\text{LiNi}_x\text{Mn}_y\text{Co}_z\text{O}_2$ (NMC) have relatively good cycling stability when charged to 4.3 V, their energy densities need to be further improved to meet the requirements of EVs. This work focuses on the two closely integrated parts: (1) Develop the high energy-density NMC layered cathode materials for Li-ion batteries; and (2) characterize the structural properties of the NMC materials by a variety of diagnostic techniques including scanning transmission electron microscopy (STEM)/EELS, energy dispersive X-ray (EDX) mapping, and secondary ion mass spectrometry (SIMS), and correlate with part 1. The success of this work will increase the energy density of Li-ion batteries and accelerate market acceptance of EVs, especially for PHEVs required by the EV Everywhere Grand Challenge proposed by DOE/EERE.

Out-Year Goals. The long-term goal of the proposed work is to enable Li-ion batteries with a specific energy of $> 96 \text{ Wh kg}^{-1}$ (for PHEVs), 5000 deep-discharge cycles, 15-year calendar life, improved abuse tolerance, and less than 20% capacity fade over a 10-year period.

Collaborations. This project engages with the following collaborators:

- Dr. Bryant Polzin (ANL) – NMC electrode supply
- Dr. X.Q. Yang (BNL) – *in situ* XRD characterization during cycling
- Dr. Kang Xu (U.S. Army Research Laboratory) – new electrolyte

Milestones

1. Identify NMC candidates that can deliver 190 mAh g^{-1} at high voltages. (December 2015 – Complete)
2. Complete multi-scale quantitative atomic level mapping to identify the behavior of Co, Ni, and Mn in NMC during battery charge/discharge, correlation with battery fading characteristics. (March 2016 – Complete)
3. Identify structural/chemical evolution of modified-composition NMC cathode during cycling. (June 2016 – Complete)
4. Optimize compositions of NMC materials to achieve improved electrochemical performance (90% capacity retention in 100 cycles). (September 2016 – Ongoing)

Progress Report

This quarter's milestone is complete. The structural/chemical evolution of different NMC cathodes during high-cutoff-voltage cycling was identified. The capacity degradation mechanism of NCM cathodes with different compositions (various Ni, Co, Mn contents) at a charge cutoff voltage up to 4.8 V was systematically investigated, utilizing advanced characterization techniques. The initial charge/discharge voltage profiles demonstrated that discharge capacities of higher than 200 mAh g⁻¹ could be achieved at a charge cutoff of 4.8 V (Figure 23a). The long-term cycling performance of different NMC cathodes was found to be very sensitive to detailed material compositions (Figure 23b). The high-voltage stability of the four NMCs follows the trend of NMC-442 > NMC-532 ~ NMC-622 > NMC-333 at charge cut-off of 4.8 V. Since the capacity degradation mechanism of NMC-532 charged to a high cut-off voltage of 4.8 V has already been reported by other groups, the detailed capacity fading mechanism of NMC-442 and NMC-333 during high-voltage cycling was studied in detail in this work.

NMC-442 showed the best cycling performance as compared to other NMCs, due to superior structural/interfacial stability at high charge cutoff voltage of 4.8 V, as evidenced by the limited evolution surface reconstruction layer (disordered rock-salt phase, 2~3 nm) and the limited accumulation of resistive SEI layer. However, NMC-333 exhibited the poorest cycling stability because of inferior structural/interfacial stability at charge to 4.8 V (Figure 24). This could be ascribed to the higher Co content in NMC-333 and the considerable overlap between the Co^{3+/4+} : 3d band with the top of the O²⁻ : 2p band, which induced the significant oxygen extraction when charged to a voltage ≥ 4.5 V. The continuous oxygen extraction at high voltage gave rise to formation of a significant quantity of oxygen vacancies inside the particle, largely weakening the electrical attraction between the transition metal (TM) ions and reduced oxygen coordinates. Furthermore, the build up of internal micro strain associated with the anisotropic volume variation at deep lithium de/intercalations resulted in micro crack formation inside the primary particles (Figure 24). Due to significant loss of oxygen coordinates, the micro crack region may not be capable of reversible Li-ion storage, resulting in fast capacity fade of NMC-333 when cycled under such a high charge cut-off voltage. The fundamental findings emphasize that the material composition (especially Co content) effect should be taken into account for developing next-generation NMC cathode materials for high-voltage battery systems.

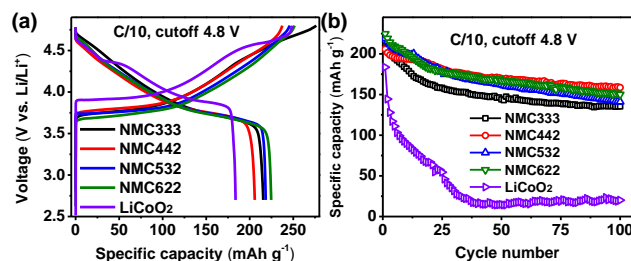


Figure 23. (a) Initial charge/discharge profiles, and (b) discharge capacity versus cycle number of different NMC cathode materials at C/10 in the voltage range of 2.7 ~ 4.8 V.

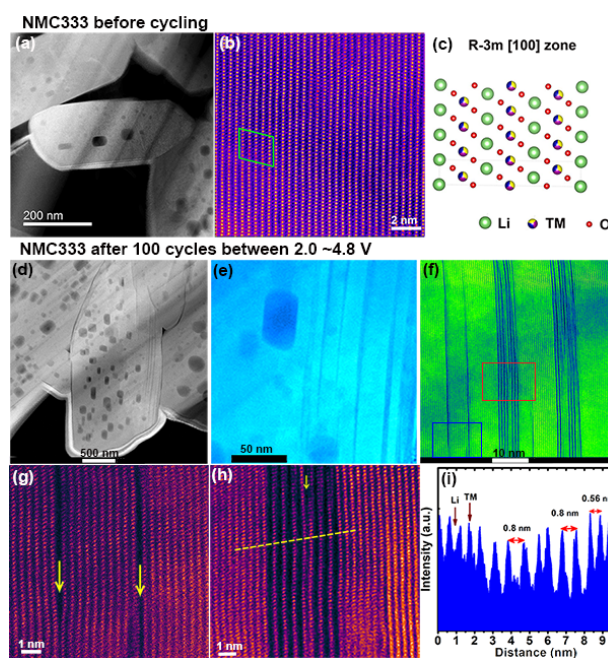


Figure 24. (a-c) Crystal structure of pristine NMC-333 cathode. (a) Aberration-corrected high angle annular dark field (HAADF) Z-contrast image. (b) Scanning transmission electron microscopy (STEM) image showing the layered structure viewed down the [100] zone axis. (c) Atomic model showing the atomic arrangement of R-3m phase in the [100] zone projection. (d-i) Crystal structure of NMC-333 particle after 100 cycles between 2.0~4.8 V at C/10. (d-e) HAADF Z-contrast image showing micro crack formation. (f-h) STEM images showing significant micro crack and lattice expansion in the cycled particle. (i) Intensity plot along the yellow dashed line

Patents/Publications/Presentations

Presentation

- 18th International Meeting on Lithium Batteries: IMLB 2016, Chicago, Illinois (June 19-24, 2016): “The Effects of Synthesis Conditions on the Performances of Ni-rich $\text{LiNi}_x\text{Mn}_y\text{Co}_z\text{O}_2$ Cathode Materials for Lithium-ion Batteries”; Jianming Zheng, Pengfei Yan, Jie Xiao, Chongmin Wang, and Ji-Guang Zhang.

Task 3.4 – *In Situ* Solvothermal Synthesis of Novel High-Capacity Cathodes (Feng Wang and Jianming Bai, Brookhaven National Laboratory)

Project Objective. The goal is to develop novel high-capacity cathodes with precise control of the phase, stoichiometry, and morphology. Despite considerable interest in developing low-cost, high-energy cathodes for Li-ion batteries, designing and synthesizing new cathode materials with the desired phases and properties has proven difficult, due to complexity of the reactions involved in chemical synthesis. Building on established *in situ* capabilities/techniques for synthesizing and characterizing electrode materials, this project will undertake *in situ* studies of synthesis reactions under real conditions to identify the intermediates and to quantify the thermodynamic and kinetic parameters governing the reaction pathways. The results of such studies will enable strategies to “dial in” desired phases and properties, opening up a new avenue for synthetic control of the phase, stoichiometry, and morphology during preparation of novel high-capacity cathodes.

Project Impact. Present-day Li-ion batteries are incapable of meeting the targeted miles of all-electric-range within the weight and volume constraints, as defined by the DOE in the EV Everywhere Grand Challenge. New cathodes with higher energy density are needed for Li-ion batteries so that they can be widely commercialized for plug-in electric vehicle (PEV) applications. The effort will focus on increasing energy density (while maintaining the other performance characteristics of current cathodes) using synthesis methods that have the potential to lower cost.

Out-Year Goals. This project is directed toward developing novel high-capacity cathodes, with a focus on Ni-rich layered oxides. Specifically, synthesis procedures will be developed for making LiNiO_2 and a series of Co/Mn substituted solid solutions, $\text{LiNi}_{1-x}\text{M}_x\text{O}_2$ ($\text{M}=\text{Co}, \text{Mn}$); through *in situ* studies, this project undertakes systematic investigations of the impact of synthesis conditions on the reaction pathways and cationic ordering processes toward the final layered phases. The structural and electrochemical properties of the synthesized materials will be characterized using s-XRD, neutron scattering, transmission electron microscopy (TEM), EELS, and various electrochemical techniques. The primary goal is to develop a reversible cathode with an energy density of 660 Wh/kg or higher.

Collaborations. This project engages with the following collaborators: Lijun Wu and Yimei Zhu at BNL; Khalil Amine, Zonghai Chen, and Yang Ren at ANL; Jagjit Nanda and Ashfia Huq at ORNL; Nitash Balsara, Wei Tong, and Gerbrand Ceder at LBNL; Arumugam Manthiram at UT Austin; Scott Misture at Alfred University; Peter Khalifha at SUNY; Kirsuk Kang at Seoul National University; Brett Lucht at University of Rhode Island; and Jason Graetz at HRL Laboratories.

Milestones

1. Develop synthesis procedures for preparing Ni-Mn-Co layered oxides. (December 2015 – Complete)
2. Identify the impact of synthesis conditions on the reaction kinetics and pathways toward forming layered Ni-Mn-Co oxides via *in situ* studies. (March 2016 – Complete)
3. Develop new capabilities for monitoring synthesis parameters (pressure, temperature, and *PH* values) in real time during solvothermal synthesis of cathode materials. (June 2016 – On schedule)
4. Identify synthetic approaches for stabilizing the layered structure of Ni-Mn-Co cathodes. (September 2016 – On schedule)

Progress Report

For *in-situ* X-ray studies of synthesis reactions, several types of micro-reactors have been developed under this project. Figure 25a shows one of them, specified for *in situ* solvothermal synthesis, wherein the temperature (T) of the solution is precisely controlled and measured, allowing studies of T dependence of the kinetics and thermodynamics of reactions. It is also desirable to track other synthesis parameters, particularly pressure (P), PH that usually evolves with time (t) and/or T , and impact reaction kinetics/pathway; however, they are neither measurable (limited by the current design of micro-reactors) nor predictable due to complexity of the synthesis reactions. To corroborate the results from *in situ* X-ray studies, an autoclave-based reactor system was developed (Figure 25b), with multiple meters/gauges to monitor P , T and PH online as synthesis reactions are progressing within the sealed reactor.

On one hand, large quantities of materials (in \sim grams) can be synthesized using an autoclave reactor (as opposed to micro-reactors) for further electrochemical/structural analysis and complement to the *in situ* X-ray studies; on the other hand, the measured parameters from the autoclave reactor, that is, P and PH and their correlation with T , can be used to estimate the P , PH values in the micron-sized *in situ* reactor when the two types of reactors are set for a same reaction (provided that the volumes of the reactors and solution can be measured). Thus, the structural evolution during synthesis and its dependence on the full set of parameters (T , P , and PH) can now be investigated for mechanistic understanding of the formation of intermediates (for example, tendency toward forming various polymorphs) and the associated kinetic reaction pathways. Such complementary *ex situ/in situ* measurements (using two types of reactors) provide new avenues for synthetic control of the structure and electrochemical properties of cathode materials.

The newly developed autoclave system has been applied to solvothermal synthesis of Ni-rich layered cathodes under controlled conditions (with well-defined T , P and PH). In Figure 26a-b, typical $T(t)$, $P(t)$ curves, both from hydrothermal and solvothermal synthesis of $\text{LiNi}_{0.5}\text{Mn}_{0.5}\text{O}_2$, are given to show how the auto-generated pressure evolved differently in water vs. ethylene glycol (EG) solvent. During the hydrothermal process, an initial PH value was ~ 9 , and then gradually decreased to ~ 7 by the end of the reaction; in contrast, the PH value remained constant, being around 7 during the solvothermal reaction. Figure 26c shows the XRD patterns of the intermediate phases, and the final $\text{LiNi}_{0.5}\text{Mn}_{0.5}\text{O}_2$ showing a phase-pure, well ordered layered structure. Results from systematic studies of the effect of t , T , P , and PH during synthesis of $\text{LiNi}_{0.5}\text{Mn}_{0.5}\text{O}_2$ and other Ni-rich layered cathodes will be reported in the future.

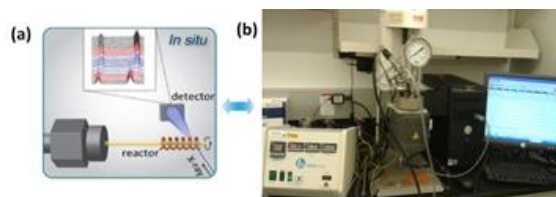


Figure 25. Setup for *in situ* hydrothermal/solvothermal synthesis. (a) Illustration of a micro-reactor for t and T -resolved X-ray studies. (b) Photograph of an autoclave-based reactor system, equipped with multiple gauges/meters for monitoring T , P , and PH values online.

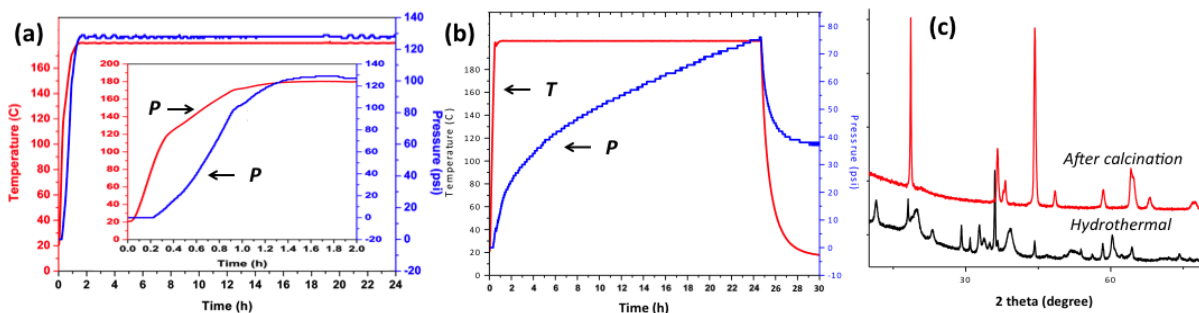


Figure 26. Solvothermal synthesis of Ni-rich layered cathode materials using the autoclave reactor (shown in Figure 25b). (a, b) Evolution of the temperature (T ; red) and pressure (P ; blue) in the water and ethylene glycol solvent. (c) Laboratory X-ray diffraction patterns (Cu source) of the intermediate (after hydrothermal treatment) and final $\text{LiNi}_{0.5}\text{Mn}_{0.5}\text{O}_2$ (after post-treatment).

Patents/Publications/Presentations

Publications

- Xu, J., and F. Lin, D. Nordlund, E. J. Crumlin, F. Wang, J. Bai, M. M. Doeff, and W. Tong. “Elucidation of the Surface Characteristics and Electrochemistry of High-performance LiNiO₂.” *Chem. Commun.* 52 (2016): 4239.
- Yoo, H. D., and Y. Li, Y. Liang, Y. Lan, F. Wang, and Y. Yao. “Intercalation Pseudocapacitance of Exfoliated Molybdenum Disulphide for Ultrafast Energy Storage.” *ChemNanoMat*. Accepted.

Presentation

- 33rd Annual International Battery Seminar and Exhibits, Fort Lauderdale, Florida (March 21-23, 2016): “Ternary Metal Fluorides as High-Energy Cathodes for Rechargeable Lithium Batteries”; F. Wang. Invited.
- Pacifichem 2015, Honolulu, Hawaii (December 15-20, 2015): “Rational Design and Synthesis of New Battery Materials via *In Situ* Studies”; F. Wang. Invited.

Task 3.5 – Novel Cathode Materials and Processing Methods (Michael M. Thackeray and Jason R. Croy, Argonne National Laboratory)

Project Objective. The project goal is to develop low-cost, high-energy, and high-power Mn-oxide-based cathodes for Li-ion batteries that will meet the performance requirements of PHEVs and EVs. Improving the design, composition, and performance of advanced electrodes with stable architectures and surfaces, facilitated by an atomic-scale understanding of electrochemical and degradation processes, is a key objective.

Project Impact. Standard Li-ion battery technologies are unable to meet the demands of the next-generation EVs and PHEVs. Battery developers and scientists will take advantage of both the applied and fundamental knowledge generated from this project to advance the field. In particular, this knowledge should enable progress toward meeting DOE goals for 40-mile, all-electric range PHEVs.

Approach. This project will exploit the concept and optimize the electrochemical properties of structurally integrated “composite” electrode structures with a prime focus on layered-layered-spinel (LLS) materials. Alternative processing routes will be investigated. ANL’s comprehensive characterization facilities will be used to explore novel surface and bulk structures by both *in situ* and *ex situ* techniques in pursuit of advancing the electrochemical performance of state-of-the-art cathode materials. A theoretical component will complement the experimental work of this project.

Out-Year Goals. The out-year goals are as follows:

- Identify high-capacity (‘layered-layered’ and ‘layered-spinel’) composite electrode structures and compositions that are stable to electrochemical cycling at high potentials (~4.5 V).
- Identify and characterize surface chemistries and architectures that allow fast Li-ion transport and mitigate or eliminate transition-metal dissolution.
- Use complementary theoretical approaches to further the understanding of electrode structures and electrochemical processes to accelerate the progress of materials development.
- Scale-up, evaluate, and verify promising cathode materials in conjunction with ANL’s scale-up and cell fabrication facilities.

Collaborators. This project engages with the following collaborators: Joong Sun Park, Bryan Yonemoto, Eunje Lee, and Roy Benedek (Chemical Sciences and Engineering, ANL).

Milestones

1. Optimize the composition, capacity, and cycling stability of structurally integrated cathode materials with a low (~10 – 20%) Li_2MnO_3 content. Target capacity = 200 mAh/g or higher (baseline electrode). (September 2016 – In progress)
2. Scale up the most promising materials to batch sizes required for evaluation by industry (10g-100g-1kg). (September 2016 – In progress)
3. Synthesize and determine the electrochemical properties of unique surface architectures that enable > 200 mAh/g at a > 1C rate. (September 2016 – In progress)

Progress Report

Layered and ‘layered-layered’ lithium TM oxides suffer from degradation mechanisms at high SOC. For example, oxygen loss, surface damage, and the migration of TMs into lithium layers conspire to reduce oxide performance through increased impedance, decreased cell voltage, and loss of cyclable lithium. Past reports have emphasized the strategy of incorporating spinel and/or spinel-type local structures and defects in an attempt to mitigate the above-mentioned degradation mechanisms. Of particular concern is oxygen loss at the surface of particles at high SOC. Large vacancy concentrations (for example, lithium) coupled with even small amounts of oxygen loss facilitate migration of the TMs, which alters the structure of near-surface layers. Because spinel structures are more stable against oxygen loss and TM migration, and can share a compatible oxygen lattice with their layered counterparts, incorporation of a spinel component at the surface of oxide particles may be an attractive strategy to create more robust cathode surfaces. LiCoO_2 (LCO) is a model system for studying surface-related degradation of cathode electrodes because of its well established electrochemical behavior. Here, the influence of a Li-rich spinel coating with a targeted composition, $\text{Li}_{1.1}\text{Mn}_{1.9}\text{O}_4$, on the electrochemical properties of LCO is reported.

Figure 27a shows the first charge/discharge cycles of a Li/LCO cell before and after wet-chemical treatments of the LCO electrode powder in acidic solutions of lithium and manganese nitrates, targeting LCO/spinel concentrations of .95/.05 and .90/.10, followed by firing in air at $\sim 500^\circ\text{C}$. Clearly observed in the first-cycle discharge is a plateau at $\sim 2.7\text{V}$ for the treated samples, consistent with the formation of a spinel-type component at the electrode surface. Figure 27b shows cycling data between 4.6-2.0V for the untreated and treated samples. A significant improvement in cell cycling stability was observed for the spinel-coated electrodes relative to the pure LCO electrode, with the 5% targeted spinel electrode delivering more than 200 mAh/g for 20 cycles. To stabilize the surface of the LCO electrode further, a $\sim 0.5\text{ nm}$ coating of AlW_xF_y was deposited directly on the electrode laminates by atomic layer deposition (ALD); this approach to use W- and F-based coatings has been discussed in earlier reports. Figure 27c shows the capacity vs. cycle plot of the $\text{Li}/0.95\text{LiCoO}_2 \cdot 0.05\text{Li}_{1.1}\text{Mn}_{1.9}\text{O}_4$ cell in which an AlW_xF_y coating had been applied to the cathode laminate. Cells were cycled between 4.5-3.0V at 15 mA/g and 30°C in lithium half-cells. Figure 27c shows that these electrodes delivered an extremely constant capacity ($\sim 185\text{ mAh/g}$) for 50 cycles. The dQ/dV plots (inset in Figure 27c) corresponding to cycles 1 and 50 show two distinct reversible redox peaks (starred), characteristic of a LCO electrode at high potentials; the data illustrate the excellent stability and reversibility of the coated LCO electrodes. Efforts to characterize and understand the surface structures of these electrode materials as well as NMC electrode systems are ongoing.

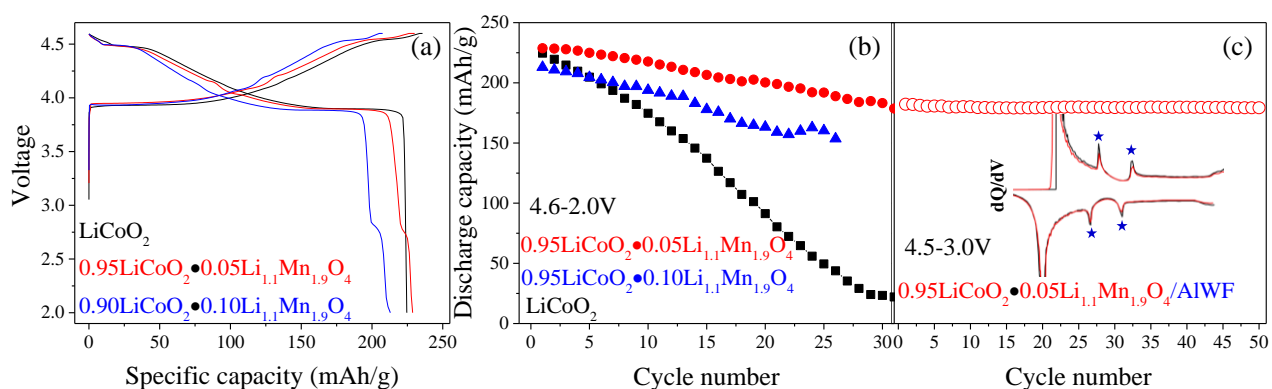


Figure 27. (a) First-cycle voltage profiles of LiCoO_2 (black), $0.95\text{LiCoO}_2 \cdot 0.05\text{Li}_{1.1}\text{Mn}_{1.9}\text{O}_4$ (red), and $0.90\text{LiCoO}_2 \cdot 0.10\text{Li}_{1.1}\text{Mn}_{1.9}\text{O}_4$ (blue), (b) corresponding capacity versus cycle data (4.6-2.0V, 15mA/g), and (c) $0.95\text{LiCoO}_2 \cdot 0.05\text{Li}_{1.1}\text{Mn}_{1.9}\text{O}_4$ coated with $\sim 0.5\text{ nm}$ AlW_xF_y cycled between 4.5-3.0V. (All data vs. Li/Li^+ at 30°C , 15 mA/g). Inset shows dQ/dV plots of cycles 1 (black) and 50 (red). Stars indicate phase transitions in LCO.

Patents/Publications/Presentations

Presentations

- Gordon Research Conference: Batteries, Ventura, California (February 2016): “Composite ‘Layered-Layered-Spinel’ Electrodes for High Energy Lithium-ion Batteries”; J. S. Park, J. R. Croy, E. Lee, and M. M. Thackeray.
- IMDEA Energy Institute, Madrid, Spain (March 7, 2016): “Energy Storage: Challenges and Opportunities in an Evolving Lithium Economy”; M. M. Thackeray. Invited.
- Metal Air Battery International Congress - MaBIC 16, Santander, Spain (March 9, 2016): “Tapping and Taming the Potential of Lithium-Oxygen Electrochemistry”; M. M. Thackeray. Invited.
- BMW Munich Battery Discussions, Garching, Germany (March 14-15, 2016): “Advances in the Structural Design of Cathodes for High Energy Li-ion Cells”; M. M. Thackeray. Invited.
- BMR Cathode Workshop, ORNL, Oak Ridge, Tennessee (March 15, 2016): “Challenges of High-Energy Cathode Materials”; J. R. Croy.

Task 3.6 – Lithium-Bearing Mixed Polyanion (LBMP) Glasses as Cathode Materials (Jim Kiggans and Andrew Kercher, Oak Ridge National Laboratory)

Project Objective. Develop mixed polyanion (MP) glasses as potential cathode materials for Li-ion batteries with superior performance to lithium iron phosphate for use in EV applications. Modify MP glass compositions to provide higher electrical conductivities, specific capacities, and specific energies than similar crystalline polyanionic materials. Test MP glasses in coin cells for electrochemical performance and cyclability. The final goal is to develop MP glass compositions for cathodes with specific energies up to near 1,000 Wh/kg.

Project Impact. The projected performance of MP glass cathode materials addresses the VTO Multi Year Program Plan goals of higher energy densities, excellent cycle life, and low cost. MP glasses offer the potential of exceptional cathode energy density up to 1000 Wh/kg, excellent cycle life from a rigid polyanionic framework, and low-cost, conventional glass processing.

Out-Year Goals. MP glass development will focus on compositions with expected multivalent intercalation reactions within a desirable voltage window and/or expected high-energy glass-state conversion reactions.

Polyanion substitution will be further adjusted to improve glass properties to potentially enable multi-valent intercalation reactions and to improve the discharge voltage and cyclability of glass-state conversion reactions. Cathode processing of the most promising mixed polyanion glasses will be refined to obtain desired cycling and rate performance. These optimized glasses will be disseminated to BMR collaborators for further electrochemical testing and validation.

Collaborations. The research work on alkali-bearing MP glass cathodes was performed at ORNL by a summer student researcher (A. Shay Chapel) from Pellissippi State Community College under the mentorship of program staff.

Milestones

1. Produce glass compositions for high-energy cathodes giving maximally oxidized transition metals upon first charge. (September 2016 – Milestone completion was delayed by equipment refurbishing.)
2. Produce unconventional glass cathodes using alternative glass formers or partial crystallinity. (June 2016 – Changed research plan to focus on mixed alkali effect.)

Progress Report

The mixed alkali effect is an orders-of-magnitude effect in glass physical properties (such as electrical conductivity, alkali diffusion, and chemical durability) that occurs when a mixture of alkali cations is present. The strength of the mixed alkali effect typically increases with the size difference between the alkali ions. While the mixed alkali effect has a strong effect on key cathode properties, the mixed alkali effect on cathode performance has not been explored. Therefore, a series of copper phosphate/vanadate glasses was produced with differing amounts of alkali cations to explore the possible mixed alkali effect on cathodes.

Because sodium cations are the closest alkali cation in size to lithium, sodium-bearing glasses were attempted first. While only one alkali was present in the as-made glass, a mixed Na-Li glass would form during discharge. Small sodium additions to copper phosphate/vanadate glass (0.05 Na per Cu) reduced the first-cycle irreversible loss, improved capacity retention during long-term cycling, and slightly improved higher power performance. Large sodium additions (1 Na per Cu) dramatically worsened cathode performance with higher irreversible loss in the first cycle, poor high-power performance, and a large capacity fade during long-term cycling.

Copper phosphate/vanadate glasses with a mixture of sodium and lithium were also tested. These glasses would demonstrate a mixed alkali effect as made. Similar to the Na-bearing glasses, the Na/Li-bearing glasses with a small sodium content (5% Na, 95% Li) showed the strongest reduction in first-cycle irreversible loss. Interestingly, the all-Na (100% Na) and all-Li (100% Li) glasses showed nearly identical irreversible loss, but the all-Na glass showed much greater capacity fade during long-term cycling.

Potassium cations are larger than sodium cations and would be expected to have a stronger mixed alkali effect when mixed with lithium. A small potassium addition (0.05 K per Cu) provided a small reduction in first-cycle irreversible loss, but further additions of K increased the first-cycle irreversible loss. A small potassium addition (0.05) improved higher power performance and capacity retention during long-term cycling better than a small sodium addition.

Comparing Na- and K-bearing glasses provided initial insights into the electrochemical impact of the mixed alkali effect. Keeping the non-Li alkali content low is necessary for good rate performance and low irreversible loss. A low non-alkali content (0.05 alkali per Cu) appears to improve capacity retention during long-term cycling.

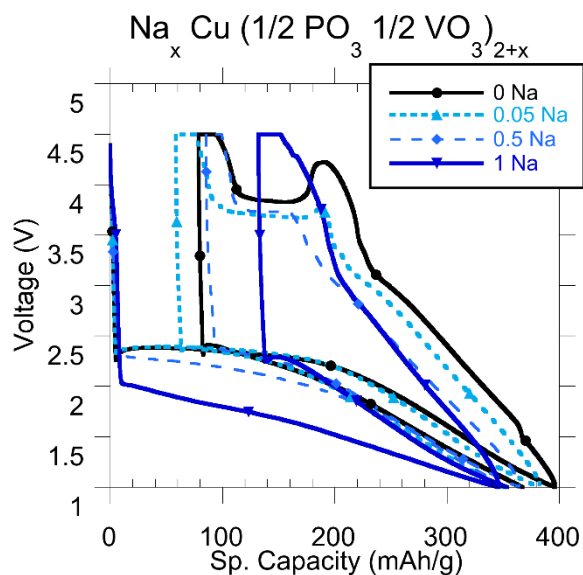


Figure 28: Discharge curves for sodium copper phosphate / vanadate glasses.

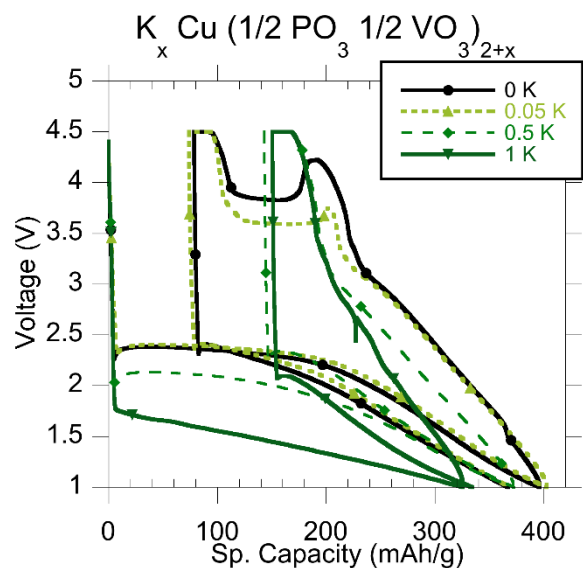


Figure 29. Discharge curves for potassium copper phosphate / vanadate glasses.

Task 3.7 – Advanced Cathode Materials for High-Energy Lithium-Ion Batteries (Marca Doeff, Lawrence Berkeley National Laboratory)

Project Objective. Microscopy and synchrotron X-ray absorption and photoemission techniques will be used to study the phenomenon of surface reconstruction to rock salt on NMC particle surfaces as a function of composition, synthesis method, surface chemistry, and electrochemical history. Because the surface reconstruction is implicated in capacity fading and impedance rise during high-voltage cycling, a thorough understanding of this phenomenon is expected to lead to principles that can be used to design robust, high-capacity NMC materials for Li-ion cells. The emphasis will be on stoichiometric NMCs with high Ni contents such as 622 and 523 compositions.

Project Impact. To increase the energy density of Li-ion batteries, cathode materials with higher voltages and/or higher capacities are required, but safety and cycle life cannot be compromised. Nickel rich NMCs can provide higher capacities and lower cost in comparison with low nickel content NMCs, but surface reactivity is an issue. A systematic evaluation of the effects of synthesis method, composition, and cell history on the surface reconstruction phenomenon will lead to higher capacity, robust and structurally stable positive electrode materials that result in higher energy density Li-ion cells than currently available.

Out-Year Goals. The information generated by the in-depth characterization will be used to design robust NMC materials that can withstand cycling to high potentials and deliver >200 mAh/g.

Collaborations. TXM was used this quarter to characterize NMC materials, with work done in collaboration with Yijin Liu (SSRL). Synchrotron and computational efforts continued in collaboration with Professor M. Asta (UC Berkeley); and Dr. Dennis Nordlund, Dr. Yijin Liu, and Dr. Dimosthenis Sokaras (SSRL). The TEM effort is in collaboration with Dr. Huolin Xin (BNL).

Milestones

1. Synthesize baseline NMC-523 and NMC-622 and Ti-substituted variants by spray pyrolysis and co-precipitation. (December 2015 – Completed)
2. Complete surface characterization of pristine materials by XAS and XPS. (March 2016 – Complete)
3. Complete soft XAS experiments on electrodes cycled to high potentials. (June 2016 – Complete)
4. *Go/No-Go*: Core-shell composites made by infiltration and re-firing of spray-pyrolyzed hollow spherical particles. (September 2016 – On track)

Progress Report

NMC-622 materials were successfully synthesized, and electrochemical performance was investigated last quarter. Last quarter, we also reported the crystal structure change during cycling through synchrotron *in situ* XRD. Besides the structural change, synchrotron-based soft XAS, atomic-scale STEM, and EELS were employed to investigate the changes of electronic structures in NMC materials during electrode preparation and under intense cycling (that is, 4.7 V and 50 cycles). All three TMs underwent reduction on electrode preparation. However, there is more significant change for Ni in comparison with Mn and Co. Moreover, the oxidation state of Ni exhibits depth-dependent characteristics, where the surface (Auger electron yield [AEY], total electron yield [TEY], and EELS data, not shown here) is more reduced than the bulk (fluorescence yield [FY] and EELS data, not shown here). Mn and Co did not show depth-dependent characteristics, although they were both slightly reduced upon electrode preparation.

As shown in Figure 30, nickel is oxidized during charge and then reduced to a lower oxidation state on discharge. However, the redox is not completely reversible. The trend of nickel oxidation state change is similar for the surface and the bulk (observed in AEY and FY modes, not shown here), although it is more oxidized in the bulk. After one complete cycle, nickel is more oxidized than in the pristine electrode, indicating that not all of the deintercalated lithium ions can be intercalated back into the structure. No obvious change was observed for Mn and Co oxidation states during the first charge and discharge, confirming that Ni is the primary metal providing redox activity.

All three TMs were reduced after intense cycling (50 cycles) at high-voltage cut-off (4.7 V), data not shown here. Mn and Co oxidation states remained the same during the first cycle. However, they were both reduced after long-time cycling at high voltage. The reduction for all three TMs could be the reason for the gradual fading of the capacity.

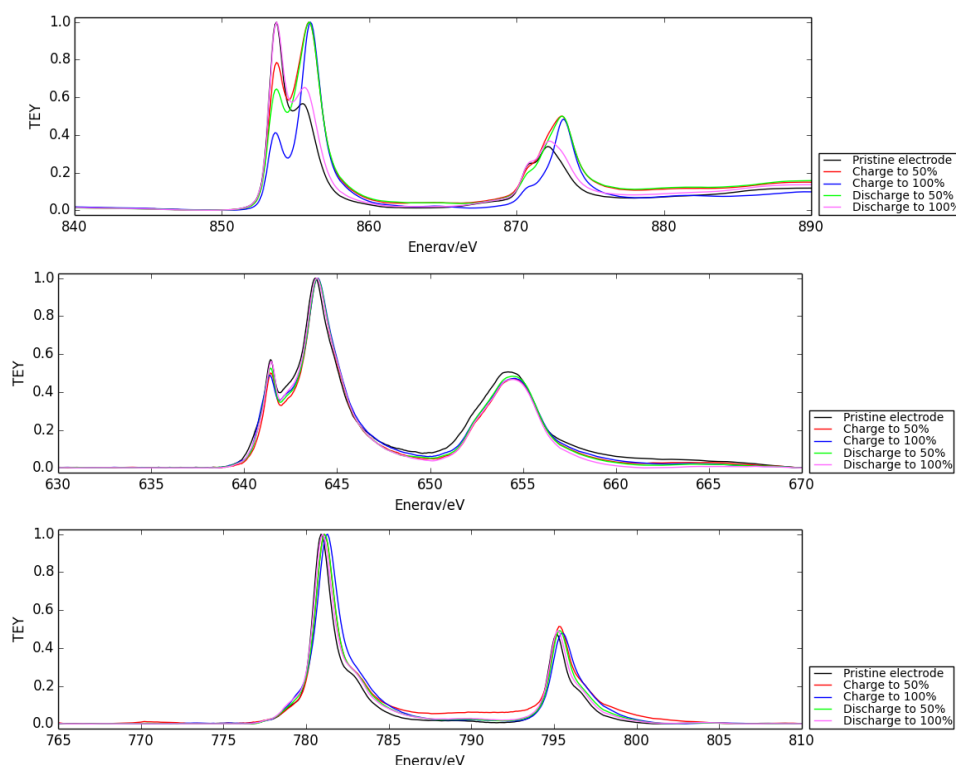


Figure 30. Soft X-ray absorption spectroscopy data in total electron yield mode for NMC-622 materials during the first cycle at various states-of-charge: valence state change of nickel (top), manganese (middle) and cobalt (bottom) during the first cycle.

Patents/Publications/Presentations

Publications

- Markus, Isaac, and Simon Engelke, Mona Shirpour, Mark Asta, and Marca Doeff. “Experimental and Computational Investigation of Lepidocrocite Anodes for Sodium-Ion Batteries.” *Chem. Mater.* (2016). doi: 10.1021/acs.chemmater.6b01074

Presentation

- 2016 CalCharge Industry Day, LBNL, Berkeley, California (May 19, 2016): “Structural Stability of Nickel-Rich Layered Cathode Materials”; Chixia Tian and Marca Doeff. Poster.
- 18th International Meeting on Lithium Batteries, Chicago, Illinois (June 19-24, 2016): “Understanding Interfacial Resistance of Al-Substituted $\text{Li}_7\text{La}_3\text{Zr}_2\text{O}_{12}$ Solid Electrolyte”; Wei Chen, Lei Cheng, and Marca Doeff.
- 18th International Meeting on Lithium Batteries, Chicago, Illinois (June 19-24, 2016): “Sodiation Kinetics of Metal Oxide Conversion Electrodes: A Comparative Study with Lithiation”; K. He, F. Lin, Y. Zhu, X. Yu, J. Li, R. Lin, D. Nordlund, T. C. Weng, R. M Richards, X. Q. Yang, M. Doeff, E. A. Stach, Y. Mo, H. Xin and D. Su.
- Materials Research Society Meeting, Phoenix, Arizona (March 28 - April 1, 2016): “Sodium Intercalation Mechanisms into Corrugated Titanate Structures for Na-ion Batteries”; Isaac Markus, Mona Shirpour, Simon Engelke, Siaufung Dang, Mark Asta, and Marca Doeff.
- Materials Research Society Meeting, Phoenix, Arizona (March 28 - April 1, 2016): “A Comparative Study on Cubic $\text{Li}_{6.4}\text{Al}_{0.2}\text{La}_3\text{Zr}_2\text{O}_{12}$: $\text{Li}_{6.4}\text{Ga}_{0.2}\text{La}_3\text{Zr}_2\text{O}_{12}$ Garnet Solid Solution”; D. Rettenwander, R. Wagner, L. Cheng, G. Amthauer, M. M. Doeff, G. J. Redhammer, and M. Wilkening.
- Recent Advances in Solid State Electrolytes for Energy Storage Tutorial, Advanced Automotive Battery Conference, Detroit, Michigan (June 13, 2016): “Preparation and Characterization of Garnet LLZO Solid Electrolytes for Lithium Batteries”; Marca M. Doeff. Invited.
- 229th meeting of the Electrochemical Society, San Diego, California (May 29 - June 3, 2016): “LLZO Ceramic Electrolytes: A Path Forward to Solid-State Batteries?”; Marca M. Doeff and Lei Cheng. Invited.
- Beyond Lithium Ion IX, Richland, Washington (May 24-26, 2016): “Recent Advances on Garnet LLZO Solid Electrolytes for Lithium Batteries”; Marca M. Doeff, Guoying Chen, and Lei Cheng. Invited.
- Materials Challenges in Alternative and Renewable Energy (MCARE2016), Clearwater, Florida (April 17-21, 2016): “Advances towards Solid State Batteries Using Garnet LLZO Electrolytes”; Marca M. Doeff and Lei Cheng. Invited.
- 2016 Battery Workshop, U. S. Department of Energy/Daimler A. G, Ulm, Germany (April 7, 2016): “Interfacial Behavior of NMC Cathodes and LLZO Garnet Solid Electrolytes”; Marca M. Doeff. Invited.
- Helmholtz Institute, Ulm, Germany (April 5, 2016): “Insights into the High Voltage Behavior of NMC Cathode Materials”; Marca M. Doeff. Invited.

Task 3.8 – Lithium Batteries with Higher Capacity and Voltage (John B. Goodenough, UT Austin)

Project Objective. The project objective is to develop an electrochemically stable alkali-metal anode that can avoid the SEI layer formation and the alkali-metal dendrites during charge/discharge. To achieve the goal, a thin and elastic solid electrolyte membrane with a Fermi energy above that of metallic lithium and an ionic conductivity $\sigma > 10^{-4} \text{ S cm}^{-1}$ will be tested in contact with alkali-metal surface. The interface between the alkali-metal and the electrolyte membrane should be free from liquid electrolyte, have a low impedance for alkali-metal transport and plating, and keep good mechanical contact during electrochemical reactions.

Project Impact. An alkali-metal anode (lithium or sodium) would increase the energy density for a given cathode by providing a higher cell voltage. However, lithium is not used as the anode in today's commercial Li-ion batteries because electrochemical dendrite formation can induce a cell short-circuit and critical safety hazards. This project aims to find a way to avoid the formation of alkali-metal dendrites and to develop an electrochemical cell with dendrite-free alkali-metal anode. Therefore, once realized, the project will have a significant impact by an energy-density increase and battery safety; it will enable a commercial Li-metal rechargeable battery of increased cycle life.

The key approach is to introduce a solid-solid contact between an alkali metal and a solid electrolyte membrane. Where SEI formation occurs, the creation of new anode surface at dendrites with each cycle causes capacity fade and a shortened cycle life. To avoid the SEI formation, a thin and elastic solid electrolyte membrane will be introduced, and liquid electrolyte will be eliminated from the anode surface.

Out-Year Goals. The out-year goals are to increase cell energy density for a given cathode and to allow low-cost, high-capacity rechargeable batteries with cathodes other than insertion compounds.

Collaborations. This project collaborates with A. Manthiram at UT Austin and with Karim Zaghib at HQ.

Milestones

1. Fabricate and test glass-fiber and cross-linked polymer membranes impregnated with Li^+ glass electrolytes. (December 2015 – Complete)
2. Test cycle life of plating/stripping lithium across Li^+ glass electrolyte. (March 2016 – Complete)
3. Optimize the heat treatment of the Li^+ and Na^+ glass electrolytes for achieving rapidly a $\sigma_i > 10^{-2} \text{ S cm}^{-1}$ at room temperature (June 2016 – Complete)
4. Test the cyclability of plating of metallic lithium and sodium anodes through the glass electrolyte. (September 2016 – Complete)

Progress Report

Low-cost glasses have been shown to be easily prepared as large-area, mechanically robust solid Li^+ or Na^+ electrolytes for safe rechargeable batteries. These glasses contain electric dipoles that can be oriented in an electric field, but it takes about 10 days at 25°C for them to age to where they have a cation conductivity $\sigma_i > 10^{-2} \text{ S cm}^{-1}$ with a motional enthalpy for cation transport of $\Delta H_m \sim 0.06 \text{ eV}$. These aged properties are comparable to those of the best flammable organic-liquid electrolytes used in today's Li-ion batteries. This quarter, the project has shown that the electric dipoles attract one another to coalesce over time into dipole clusters within which the same dipoles condense into negatively charged ferroelectric clusters that can be rotated and reversed in an ac electric field and that are charge-compensated by freed Li^+ or Na^+ cations. In addition, it was shown that the aging can be accomplished in minutes at 100°C in an ac electric field.

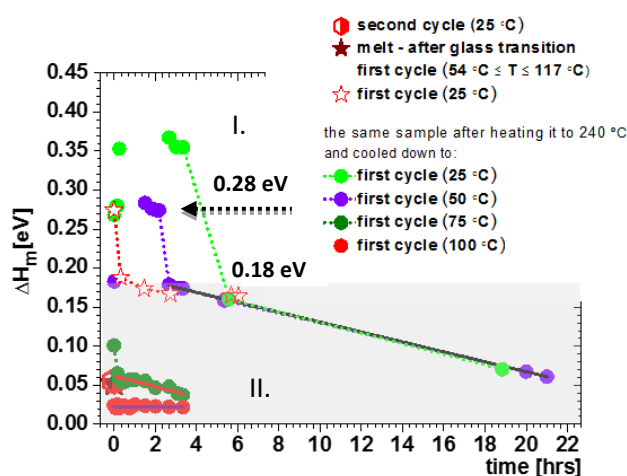


Figure 31. Activation energy of a Na-glass as a function of time for different temperatures and experimental procedures.

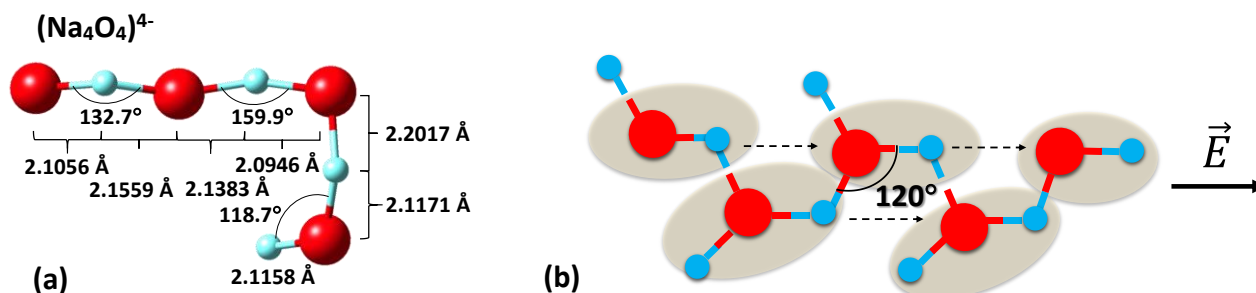


Figure 32. (A) Calculated $(\text{Li}_4\text{O}_3)^{2-}$ dipole cluster for an A-glass. (b) A postulated $(\text{Li}_2\text{O}_2)^2\text{-Li}^{+2n}$ ferroelectric chain segment aligned by an electric field.

Task 3.9 – Exploiting Cobalt and Nickel Spinel in Structurally Integrated Composite Electrodes (Michael M. Thackeray and Jason R. Croy, Argonne National Laboratory)

Project Objective. The project goal is to stabilize high-capacity, composite ‘layered-layered’ electrode structures with lithium-cobalt-oxide and lithium-nickel-oxide spinel components (referred to as LCO-S and LNO-S, respectively), or solid solutions thereof (LCNO-S), which can accommodate lithium at approximately 3.5 V versus metallic lithium. This approach and the motivation to use LCO-S and LNO-S spinel components, about which relatively little is known, is novel.

Project Impact. State-of-the-art Li-ion batteries are unable to satisfy the performance goals for PHEVs and all-electric EVs. If successful, this project will impact the advance of energy storage for electrified transportation as well as other applications, such as portable electronic devices and the electrical grid.

Approach. This work will focus on the design and synthesis of new spinel compositions and structures that operate above 3 V and below 4 V and to determine their structural and electrochemical properties through advanced characterization. This information will subsequently be used to select the most promising spinel materials for integration as stabilizers into high-capacity composite electrode structures.

Out-Year Goals. The electrochemical capacity of most high-potential Li-metal oxide insertion electrodes is generally severely compromised by their structural instability and surface reactivity with the electrolyte at low lithium loadings (that is, at highly charged states). Although some progress has been made by cation substitution and structural modification, the practical capacity of these electrodes is still restricted to approximately 160-170 mAh/g. This project proposes a new structural and compositional approach with the goal of producing electrode materials that can provide 200-220 mAh/g without significant structural or voltage decay for 500 cycles. If successful, the materials processing technology will be transferred to the ANL Materials Engineering and Research Facility (MERF) for scale up and further evaluation.

Collaborations. This project collaborates with Eungje Lee, Joong Sun Park, and Roy Benedek (Chemical Sciences and Engineering, ANL), Mali Balasubramanian (Advanced Photon Source, ANL), and V. Dravid and C. Wolverton (Northwestern University).

Milestones

1. Synthesize and optimize spinel compositions and structures with a focus on Co-based systems for use in structurally integrated layered-spinel electrodes. (Q4 – In progress; see text)
2. Determine electrochemical properties of Co-based spinel materials, and when structurally integrated in composite layered-spinel electrodes. (Q4 – In progress)
3. Evaluate the electrochemical migration of TM ions in Co-based layered-spinel electrodes. (Q4 – In progress)

Progress Report

Past reports have shown that lithium-cobalt-nickel-oxides ($\text{LiCo}_{1-x}\text{Ni}_x\text{O}_2$; $0 \leq x \leq 0.2$) prepared at ‘low-temperature’ (LT, $\sim 400^\circ\text{C}$) by solid-state synthesis have a lithiated spinel structure ($\text{Li}_2[\text{Co}_{1-2x}\text{Ni}_{2x}]_2\text{O}_4$, $Fd-3m$) that gradually transforms to a layered structure ($\text{Li}[\text{Co}_{1-x}\text{Ni}_x]\text{O}_2$, $R-3m$) on increasing the firing temperature. TEM and ^7Li magic angle spinning nuclear magnetic resonance (MAS NMR) data indicate that structurally integrated spinel, layered and intermediate layered/spinel configurations are formed most noticeably between 500°C and 800°C . These composite structures are of particular interest because they offer the possibility of tailoring the composition and amount of a lithiated spinel component, $\text{Li}_2[\text{Co}_{1-2x}\text{Ni}_{2x}]_2\text{O}_4$, needed to stabilize high-capacity ‘layered-layered’ $x\text{Li}_2\text{MnO}_3 \cdot (1-x)\text{LiMO}_2$ electrodes. Relatively little is known about these lithiated spinel materials, as previous studies have focused predominantly on the electrochemical properties of layered $\text{LiCo}_{1-x}\text{Ni}_x\text{O}_2$ structures that are of technological and commercial significance.^[1-3] In this respect, most attention has been placed on high-cobalt, that is, LiCoO_2 (LCO), and high-nickel, for example, $\text{LiNi}_{0.8}\text{Co}_{0.15}\text{Al}_{0.05}\text{O}_2$ (NCA) electrode materials. In this study, a series of $\text{LiCo}_{1-x}\text{Ni}_x\text{O}_2$ ($0 \leq x \leq 0.5$) materials, when synthesized at 700°C and 800°C , has been revisited; their electrochemical properties have been assessed in context of expected signatures of layered- and spinel-type structures.

The XRD patterns of $\text{LiCo}_{1-x}\text{Ni}_x\text{O}_2$ ($0 \leq x \leq 0.5$) samples, prepared at 700°C and 800°C are shown in Figure 33a-b. Although weak peaks of a $\text{Li}_8\text{Ni}_{16}\text{O}$ rock salt impurity phase were observed in several 700°C samples ($x \geq 0.3$), the solid solution behavior of Co and Ni in the structure was confirmed by a linearly increasing lattice volume as a function of Ni content, x (data not shown). The normalized discharge profiles and dQ/dV plots of the $\text{Li}/\text{LiCo}_{1-x}\text{Ni}_x\text{O}_2$ cells in Figure 34 clearly indicate the development of two electrochemical processes, one at ~ 3.9 V, attributed to a Co-rich layered structure and the other at ~ 3.5 V, attributed either to a Ni-rich layered structure or, alternatively, a lithiated-spinel structure, $\text{Li}_2[\text{Co}_{1-2x}\text{Ni}_{2x}]_2\text{O}_4$ (or both). What is particularly noteworthy about the data is that, for $x \geq 0.3$, the electrochemical profile adopts that of a Ni-rich electrode, while a lower nickel content $0 < x \leq 0.2$ appears to maintain some spinel-like character in the structure, and therefore some TM ions in the lithium layers, even when fired at 800°C . The data highlight the ability to tailor the spinel character of the structure by controlling composition and synthesis conditions. Work is in progress to determine the most effective lithiated spinel compositions that may stabilize high-capacity ‘layered-layered’ $x\text{Li}_2\text{MnO}_3 \cdot (1-x)\text{LiMO}_2$ electrode structures and mitigate voltage fade and impedance rise.

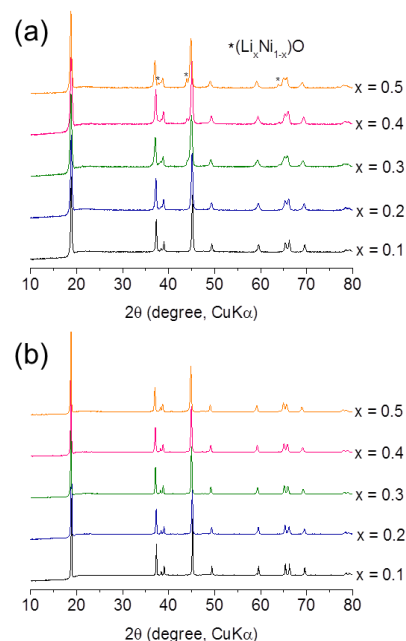
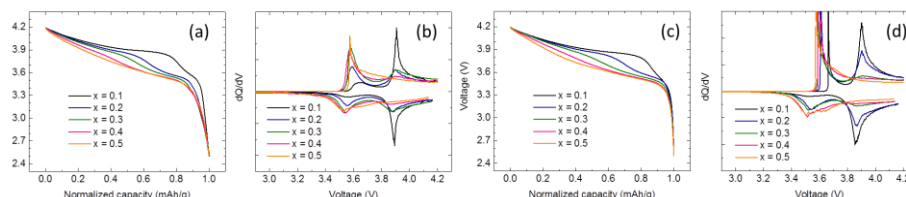


Figure 33. X-ray diffraction patterns of $\text{LiCo}_{1-x}\text{Ni}_x\text{O}_2$ samples prepared at (a) 700°C and (b) 800°C .

Figure 34. (a, c) Normalized discharge profiles, and (b, d) dQ/dV plots of $\text{LiCo}_{1-x}\text{Ni}_x\text{O}_2$ prepared at (a, b) 700°C and (c, d) 800°C .



[1] Delmas, C., and I. Saadoune. *Solid State Ionics* 53-56 (1992): 370.

[2] Ohzuku, T., and A. Ueda, M. Nagayama, Y. Iwakoshi, and H. Komori. *Electrochim. Acta* 38 (1993): 1159.

[3] Caurant, D., and N. Baffier, B. Garcia, and J. P. Pereira-Ramos. *Solid State Ionics* 91 (1996): 45.

Patents/Publications/Presentations

Publication

- Lee, E., and J. Blauwkamp, F. C. Castro, J. Wu, V. P. Dravid, P. Yan, C. Wang, S. Kim, C. Wolverton, R. Benedek, F. Dogan, J. S. Park, J. R. Croy, and M. M. Thackeray. “Exploring Lithium-Cobalt-Nickel-Oxide Spinel Electrodes for ≥ 3.5 V Li-ion Cells.” (2016 – Submitted)

Presentation

- 18th International Meeting on Lithium Batteries, Chicago, Illinois (June 19-24, 2016): “Structure and Electrochemistry of Lithium-Cobalt-Oxide Spinels and their Role in ‘Layered-Spinel’ Composite Cathode Materials and Processing Methods”; E. Lee, J. Blauwkamp, J. S. Park, J. Wu, F. Dogan, R. Benedek, J. R. Croy, V. Dravid, and M. M. Thackeray.

Task 3.10 – Discovery of High-Energy Lithium-Ion Battery Materials (Wei Tong, Lawrence Berkeley National Laboratory)

Project Objective. This project aims to develop a cathode that can cycle > 200 mAh/g while exhibiting minimal capacity and voltage fade. The emphasis will be on oxides with high nickel contents. This task focuses on the compositions in the Li-Ni-O phase space, which will be explored using a combinatorial materials approach to search for new high-capacity cathodes. The specific objectives of this project are to: (1) investigate and understand the correlation between the synthesis and electrochemical performance of Ni-based compounds, and (2) design, synthesize, and evaluate the potential new high-capacity cathodes within Li-Ni-O composition space using the percolation theory as a guideline.

Project Impact. In commercial Li-ion batteries, the well ordered, close-packed oxides, particularly, layered lithium transition metal oxides (LiTmO_2 , Tm is transition metal) are widely used. However, the energy density needs to be at least doubled to meet the performance requirements of EVs (300 to 400 miles). Although capacities approaching 300 mAh/g have been reported in Li-, Mn-rich layered oxide compounds, capacity decay and voltage fading in the long-term cycling are always observed. Therefore, new materials are urgently needed to make the breakthrough in Li-ion battery technology.

Approach. The recent discovery of high-capacity materials with lithium excess provides new insights into design principles for potential high-capacity cathode materials. According to the percolation theory, lithium excess is required to access 1 lithium exchange capacity in LiTmO_2 compounds. This seems to be independent of TM species; therefore, it could open up a composition space for the search of new materials with high capacity. The interesting $\text{Ni}^{2+}/\text{Ni}^{4+}$ redox is selected as the electrochemically active component, and combinatorial materials design concept will be used to discover the potential cathode material candidates in the Li-Ni-O phase space.

Out-Year Goals. The long-term goal is to search new high-energy cathodes that can potentially meet the performance requirements of EVs with a 300- to 400-mile range in terms of cost, energy density, and performance.

Collaborations. The PI closely collaborates with M. Doeff (LBNL) on soft XAS, C. Ban (NREL) on atomic layer deposition (ALD) coating, B. McCloskey (LBNL) for differential electrochemical mass spectrometry (DEMS), and R. Kostecki (LBNL) for Raman spectroscopy. Collaboration is also in progress with other BMR PIs (X.-Q. Yang and F. Wang, BNL; and K. Persson, LBNL) for crystal structure evolution on cycling and material computation.

Milestones

1. Determine synthetic approach and identify the key synthetic parameters for Ni^{3+} -containing compounds, for example, LiNiO_2 . (Q1 – Complete)
2. Complete the structural and electrochemical characterization of LiNiO_2 . (Q2 – Complete)
3. Determine synthetic approach and identify the key synthetic parameters for Ni^{2+} -containing compounds, for example, Li_2NiO_2 . (Q3 – Complete)
4. Complete the structural and electrochemical characterization of Li_2NiO_2 , and down select the synthetic approach for the phase screening within Li-Ni-O chemical space. (Q4 – Ongoing)

Progress Report

Li_2NiO_2 and a series of $\text{Li}_2\text{Ni}_{1-x}\text{Cu}_x\text{O}_2$ ($0 < x < 1$) samples were prepared by a solid state method. The three precursors, Li_2O , NiO , and CuO , were high-energy milled for 3 hours, and then annealed at 700°C for 12 hours under N_2 atmosphere. Figure 35 shows XRD patterns of the as-prepared $\text{Li}_2\text{Ni}_{1-x}\text{Cu}_x\text{O}_2$ ($0 < x < 1$) samples. All materials exhibited an orthorhombic *Immm*-type structure, indicating formation of a good solid solution between Li_2NiO_2 and Li_2CuO_2 . A small amount of NiO impurity was observed in the XRD pattern of Li_2NiO_2 , and it was removed by the Cu substitution. The shift of (002) and (200) diffraction peaks was due to substitution of larger Cu ions on the Ni sites.

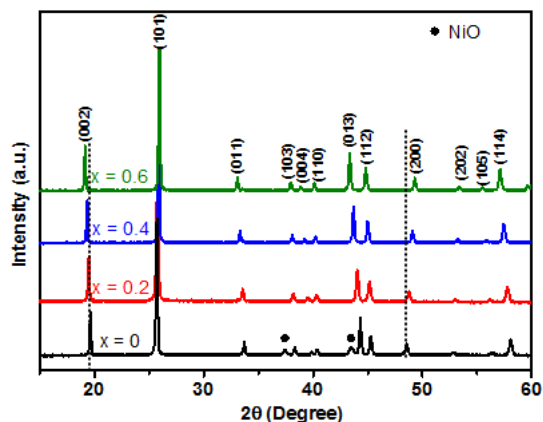


Figure 35. X-ray diffraction of $(1-x) \text{Li}_2\text{NiO}_2 \cdot x \text{Li}_2\text{CuO}_2$ ($x = 0, 0.2, 0.4, 0.6$) solid solutions.

The first-cycle voltage profiles are presented in Figure 36a. Electrodes were prepared by mixing 80 wt% active materials, 15 wt% carbon black conductive agent, and 5 wt% polyethylenetetrafluoride (PTFE) binder. The cells were cycled between 4.6 V and 1.5 V at a current density 12 mA/g. Li_2NiO_2 delivered a high charge capacity of 380 mAh/g and a discharge capacity of 330 mAh/g during the first cycle. With the Cu substitution, the charge capacity increased up to 440 mAh/g, likely due to removal of electrochemically inactive NiO . On the other hand, the discharge capacity increased with Cu content and reached 380 mAh/g at 0.6 Cu. Moreover, the Cu substitution led to a substantial change in voltage profiles: the charge profile was progressively decomposed into two small steps at 3.2 V and 3.6 V respectively; whereas, for the discharge profile, the 3.6 V step was reduced and the 2.1 V feature was observed in the Cu substituted samples. All these changes implied that Cu substitution had a direct effect on the phase transformation route and charge compensation mechanism. The cycling performance of these four samples is presented in Figure 36b. Although Cu substitution improved discharge capacity in the initial cycle, capacity retention was not effectively enhanced within the tested voltage window (4.6 – 1.5 V). Further studies are needed to elucidate the role of Cu substitution in the overall electrochemical reaction.

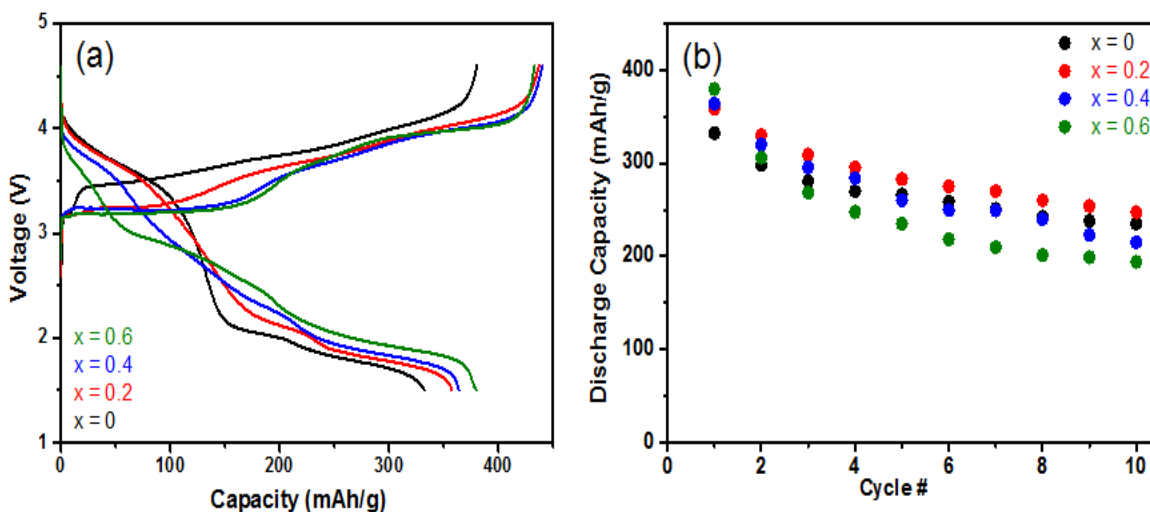


Figure 36. (a) The first-cycle voltage profiles, and (b) cycling performance of the as-synthesized $(1-x) \text{Li}_2\text{NiO}_2 \cdot x \text{Li}_2\text{CuO}_2$ ($x = 0, 0.2, 0.4, 0.6$) solid solutions. (12 mA/g, 4.6 ~ 1.5 V)

TASK 4 – ELECTROLYTES FOR HIGH-VOLTAGE, HIGH-ENERGY, LITHIUM-ION BATTERIES

NOTE: This task is now closed, with limited extension work being completed this fiscal year. The BMR has recently awarded new tasks in this area, which will begin next fiscal year.

Summary

The current Li-ion electrolyte technology is based on LiPF_6 solutions in organic carbonate mixtures with one or more functional additives. Li-ion battery chemistries with energy density of 175~250 Wh/Kg are the most promising choice. To further increase the energy density, the most efficient way is to raise either the voltage and/or the capacity of the positive materials. Several high-energy materials including high-capacity composite cathode $x\text{Li}_2\text{MnO}_3 \cdot (1-x)\text{LiMO}_2$ and high-voltage cathode materials such as $\text{LiNi}_{0.5}\text{Mn}_{1.5}\text{O}_4$ (4.8 V) and LiCoPO_4 (5.1 V) have been developed. However, their increased operating voltage during activation and charging poses great challenges to the conventional electrolytes, whose organic carbonate-based components tend to oxidatively decompose at the threshold beyond 4.5 V vs Li^+/Li .

Other candidate positive materials for PHEV application that have potential of providing high capacity are the layered Ni-rich NCM materials. When charged to a voltage higher than 4.5 V, they can deliver a much higher capacity. For example, $\text{LiNi}_{0.8}\text{Co}_{0.1}\text{Mn}_{0.1}\text{O}_2$ (NCM 811) only utilizes 50% of its theoretical capacity of 275 mAh/g when operating in a voltage window of 4.2 V – 3.0 V. Operating voltage higher than 4.4 V would significantly increase the capacity to 220 mAh/g; however, the cell cycle life becomes significantly shortened mainly due to the interfacial reactivity of the charged cathode with the conventional electrolyte. The oxidative voltage instability of the conventional electrolyte essentially prevents the practicality to access the extra capacities of these materials.

To address the above challenges, new electrolytes that have substantial high-voltage tolerance at high temperature with improved safety are needed urgently. Organic compounds with low HOMO (highest occupied molecular orbital) energy level are suitable candidates for high-voltage application. An alternative approach to address the electrolyte challenges is to mitigate the surface reactivity of high-voltage cathodes by developing cathode passivating additives. Like the indispensable role of SEI on the carbonaceous anodes, cathode electrolyte interphase (CEI) formation additives could kinetically suppress the thermodynamic reaction of the delithiated cathode and electrolyte, thus significantly improving the cycle life and calendar life of the high energy density Li-ion battery.

An ideal electrolyte for high-voltage, high-energy cathodes also requires high compatibility with anode materials (graphite or silicon). New anode SEI formation additives tailored for the new high-voltage electrolyte are equally critical for the high-energy Li-ion battery system. Such an electrolyte should have the following properties: high stability against 4.5 – 5.0 V charging state, particularly with cathodes exhibiting high surface oxygen activity; high compatibility with a strongly reducing anode under high-voltage charging; high lithium salt solubility ($> 1.0 \text{ M}$) and ionic conductivity ($> 6 \times 10^{-3} \text{ S/cm}$ @ room temperature); and non-flammability (no flash point) for improved safety and excellent low-temperature performance (-30°C).

TASK 5 – DIAGNOSTICS

Summary and Highlights

To meet the goals of VTO-Multi Year Program Plan and develop lower-cost, abuse-tolerant batteries with higher energy density, higher power, better low-temperature operation and longer lifetimes suitable for the next-generation of HEVs, PHEVs and EVs, there is a strong need to identify and understand structure-property-electrochemical performance relationships in materials, life-limiting and performance-limiting processes, and various failure modes to guide battery development activities and scale-up efforts. In the pursuit of batteries with high energy density, high cell operating voltages and demanding cycling requirements lead to unprecedented chemical and mechanical instabilities in cell components. Successful implementation of newer materials such as Si anode and high-voltage cathodes also requires better understanding of fundamental processes, especially those at the solid/electrolyte interface of both anode and cathode.

The BMR Task 5 takes on these challenges by combining model system, *ex situ*, *in situ*, and *operando* approaches with an array of the start-of-the-art analytical and computational tools. Four subtasks are tackling the chemical processes and reactions at the electrode/electrolyte interface. Researchers at LBNL use *in situ* and *ex situ* vibrational spectroscopy, far- and near-field scanning probe spectroscopy and laser-induced breakdown spectroscopy (LIBS) to understand the composition, structure, and formation/degradation mechanisms of the SEI at silicon anode and high-voltage cathodes. The University of California at San Diego (UCSD) subtask combines STEM/EELS, XPS, and *ab initio* computation for surface and interface characterization and identification of instability causes at both electrodes. At Cambridge, NMR is being used to identify major SEI components, their spatial proximity, and how they change with cycling. Subtasks at BNL and PNNL focus on the understanding of fading mechanisms in electrode materials, with the help of synchrotron based X-ray techniques (diffraction and hard/soft X-ray absorption) at BNL and high-resolution transmission electron microscopy (HRTEM) and spectroscopy techniques at PNNL. At LBNL, model systems of electrode materials with well defined physical attributes are being developed and used for advanced diagnostic and mechanistic studies at both bulk and single-crystal levels. These controlled studies remove the ambiguity in correlating material physical properties and reaction mechanisms to performance and stability, which is critical for further optimization. The final subtask takes advantage of the user facilities at ANL that bring together X-ray and neutron diffraction, X-ray absorption, emission and scattering, HRTEM, Raman spectroscopy, and theory to look into the structural, electrochemical, and chemical mechanisms in the complex electrode/electrolyte systems. The diagnostics team not only produces a wealth of knowledge that is key to developing next-generation batteries, it also advances analytical techniques and instrumentation that have a far-reaching effect on material and device development in a range of fields.

Highlights. The highlights this quarter are as follows:

- Cambridge University (Grey's Group) monitored the growth of the SEI on cycled Si/C/CMC electrodes and attributed the decreasing discharge capacity to primarily kinetics as the increased electrode tortuosity severely limits Li⁺ ion diffusion through the bulk of the electrode.
- LBNL (Chen's group) correlated the stability of Li- and Mn-rich layered oxide ($\text{Li}_{1.2}\text{Mn}_{0.13}\text{Mn}_{0.54}\text{Co}_{0.13}\text{O}_2$) cathodes to cycling-induced TM reduction and dissolution and reported the dominating effects of both particle morphology and surface area.
- PNNL (Wang's Group) reported that strain-induced intragranular cracks on layered oxide cathodes, which contribute to cell degradation at high voltages, initiate at grain interior rather than the surface.

Task 5.1 – Design and Synthesis of Advanced High-Energy Cathode Materials (Guoying Chen, Lawrence Berkeley National Laboratory)

Project Objective. The successful development of next-generation electrode materials requires particle-level knowledge of the relationships between materials' specific physical properties and reaction mechanisms to their performance and stability. This single-crystal-based project was developed specifically for this purpose, and it has the following objectives: (1) obtain new insights into electrode materials by utilizing state-of-the-art analytical techniques that are mostly inapplicable on conventional, aggregated secondary particles, (2) gain fundamental understanding on structural, chemical, and morphological instabilities during lithium extraction/insertion and prolonged cycling, (3) establish and control the interfacial chemistry between the cathode and electrolyte at high operating voltages, (4) determine transport limitations at both particle and electrode levels, and (5) develop next-generation electrode materials based on rational design as opposed to more conventional empirical approaches.

Project Impact. The project will reveal performance-limiting physical properties, phase-transition mechanisms, parasitic reactions, and transport processes based on the advanced diagnostic studies on well formed single crystals. The findings will establish rational, non-empirical design methods that will improve the commercial viability of next-generation $\text{Li}_{1+x}\text{M}_{1-x}\text{O}_2$ ($\text{M}=\text{Mn}$, Ni , and Co) and spinel $\text{LiNi}_x\text{Mn}_{2-x}\text{O}_4$ cathode materials.

Approach. This project scope will encompass the following: (1) Prepare crystal samples of Li-rich layered oxides and high-voltage Ni/Mn spinels with well defined physical attributes, (2) Perform advanced diagnostic and mechanistic studies at both bulk and single-crystal levels, and (3) Establish global properties and performance of the samples from the bulk analyses, while, for the single-crystal based studies, utilizing time- and spatial-resolved analytical techniques to probe material redox transformation and failure mechanisms.

Out-Year Goals. This project aims to determine performance and stability limiting fundamental properties and processes in high-energy cathode materials and to outline mitigating approaches. Improved electrode materials will be designed and synthesized.

Collaborations. This project collaborates with Drs. Y. Liu (SSRL), M. Doeff and P. Ross (LBNL), Simon Mun (GIST), J. Guo (ALS), C. Wang (PNNL), C. Grey (Cambridge), and A. Huq and J. Nanda (ORNL).

Milestones

1. Establish synthesis-structure-electrochemical property relationship in high-voltage Li-TM-oxides. (December 2015 – Complete)
2. *Go/No-Go*: Downselect alternative high-energy cathode materials for further investigation, if the material delivers > 200 mAh/g capacity in the voltage window of 2 – 4.5 V. (March 2016 – Complete with a Go/No-Go decision)
3. Determine lithium concentration and cycling dependent TM movement in and out of oxide particles. Examine the mechanism. (June 2016 – Complete)
4. Identify key surface properties and features hindering stable high-voltage cycling of Li-TM-oxides. (September 2016 – On schedule)

Progress Report

Studies were carried out to compare the changes in TM oxidation states, the dissolution and subsequent precipitation of TMs during half-cell cycling of $\text{Li}_{1.2}\text{Mn}_{0.13}\text{Mn}_{0.54}\text{Co}_{0.13}\text{O}_2$ crystal samples with six different morphologies (plate, needle, S-Poly, L-Poly, box and octahedron) that were previously synthesized in the lab. Coin cells with the composite electrodes consisting of 80 wt% oxide crystals, 10 wt% carbon additive and 10 wt% polyvinylidene fluoride (PVDF) binder, lithium foil counter and reference electrodes, Celgard 2400 polypropylene separator and 1 M LiPF_6 in EC-DEC (1:1) electrolyte were charged/discharged between 2.5 and 4.6 V at 20 mA/g and then disassembled to recover the separator, the electrolyte and the cathode crystals. Figure 37a-c shows the Mn, Co, and Ni soft XAS spectra (*L* edge, TEY mode) collected on the pristine electrodes as well as the separators recovered after either 30 or 45 cycles. All three TMs were detected on the separators, revealing the participation of a TM dissolution, migration, and deposition mechanism during cycling. While Mn, Co, and Ni were at 4+, 3+ and 2+ on the fresh electrodes, respectively, the oxidation state of the TMs on the separators was found to be at 2+ universally. The amount of deposited TMs increases with cycling, but it is morphology dependent, with the most deposits found in the cell containing the box sample and the least with the L-Poly sample. The separators also had a black appearance on the side facing the Li-metal anode. Significant reduction of Mn and Co was observed on cathode particles recovered after 45 cycles, evidenced by the soft XAS spectra collected on the electrodes. The low energy/high energy Co *L*3 peak ratios in three different detection modes of AEY, TEY and FY, with an approximate probing depth of 1-2, 2-5 and 50 nm, respectively, are shown in Figure 37d. The monotonous increase in oxidation state from AEY, TEY to FY suggests that Co reduction progressed from the surface to the bulk. The highest ratio, corresponding to most Co^{3+} reduction, was found on the box sample, whereas the lowest ratio was found on the L-Poly sample. TM concentration in the recovered electrolyte was analyzed by ICP and shown in Figure 37e. Compared to the plate, needle, and L-Poly samples, significantly more TM dissolution was observed on the S-Poly sample with the highest surface area and the box sample with the most reactive surface facets, suggesting effects of both particle morphology and surface area on the reactivity at particle surface. These results corroborate with the trend observed in cell capacity retention (Figure 37f) and provide clear evidence for the correlation between cycling stability and cycling-induced TM reduction and dissolution in electrolyte.

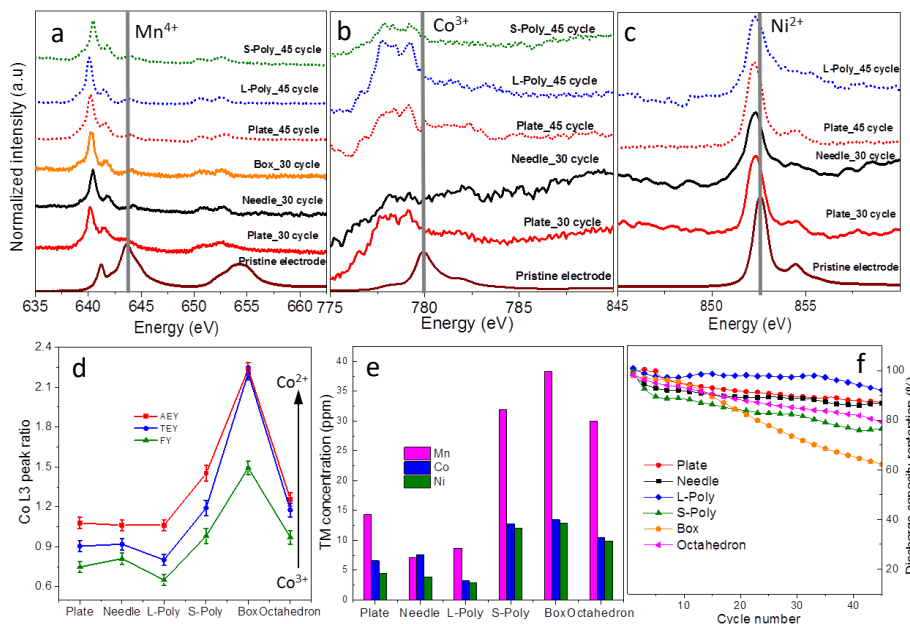


Figure 37. (a) Mn, (b) Co, and (c) Ni *L*-edge soft X-ray absorption spectroscopy (XAS) spectra collected on recovered separators and the pristine electrodes. (d) Co low/high *L*3 peak ratio determined from the soft XAS spectra (Auger electron yield, total electron yield, and fluorescence yield modes) of the crystals recovered after 45 cycles. (e) Transition metal concentration in the electrolytes recovered after 45 cycles. (f) Capacity retention of the various $\text{Li}_{1.2}\text{Ni}_{0.13}\text{Mn}_{0.54}\text{Co}_{0.13}\text{O}_2$ half-cells cycled between 2.5 and 4.6 V at 20 mA/g.

Task 5.2 – Interfacial Processes – Diagnostics (Robert Kostecki, Lawrence Berkeley National Laboratory)

Project Objective. The main task objective is to obtain detailed insight into the dynamic behavior of molecules, atoms, and electrons at electrode/electrolyte interfaces of high-voltage $\text{Li}[\text{Ni}_x\text{Mn}_y\text{Co}_z]\text{O}_2$ materials at a spatial resolution that corresponds to the size of basic chemical or structural and chemical building blocks. This project focuses on high Ni content NMC compositions such as 523 and 622, which are expected to achieve high discharge capacities even within conservative electrode potential limits. The aim of these studies is to unveil the structure and reactivity at hidden or buried interfaces and interphases that determine material, composite electrode and battery cell performance and failure modes. To accomplish these goals novel far- and near-field optical multifunctional probes must be developed and deployed *in situ*. This work constitutes an integral part of the concerted effort within the BMR Program, and it attempts to establish clear connections between diagnostics, theory/modelling, materials synthesis, and cell development efforts.

Project Impact. This project provides better understanding of the underlying principles that govern the function and operation of battery materials, interfaces, and interphases, which is inextricably linked with successful implementation of high-energy density materials such as $\text{Li}[\text{Ni}_x\text{Mn}_y\text{Co}_z]\text{O}_2$ compounds (NMCs) that can cycle stably to high potentials and deliver > 200 mAh/g at Coulombic efficiency close to 100%. This task also involves development and application of novel innovative experimental methodologies to study and understand the basic function and mechanism of operation of materials, composite electrodes, and high-energy Li-ion battery systems for PHEV and EV applications.

Approach. The *in situ/ex situ* investigations of surface reconstruction into rock salt on NMC samples of different morphology and composition will be linked with investigations of interfacial reactivity toward organic electrolytes. Pristine and cycled NMC powders and electrodes will be probed using surface- and bulk-sensitive techniques, including Fourier transform infrared (FTIR), attenuated total reflectance (ATR)-FTIR, near-field IR, and Raman spectroscopy and microscopy and scanning probe microscopy to identify and characterize changes in structure and composition. The effect of electrolyte composition, additives, and protective coatings will be explored to determine the mechanism and kinetics of surface phenomena and implications for long-term electrochemical performance of NMC cathodes in high-energy Li-ion systems.

Out-Year Goals. The requirements for long-term stability of Li-ion batteries are extremely stringent and necessitate control of the chemistry at a wide variety of temporal and structural length scales. Progress toward identifying the most efficient mechanisms for electrical energy storage and the ideal material depends on a fundamental understanding of how battery materials function and what structural/electronic properties limit their performance. This project provides better understanding of the underlying principles that govern the function and operation of battery materials, interfaces, and interphases, which is inextricably linked with successful implementation of high energy density materials in Li-ion cells for PHEVs and EVs.

Collaborations. This project collaborates with Marca Doeff, Vincent Battaglia, Chunmei Ban, Vassilia Zorba, and Bryan D. McCloskey.

Milestones

1. Build and test binder- and carbon-free model NMC electrodes. (December 2015 – Complete)
2. Complete preliminary characterization of interfacial activity of the baseline NMC material in organic carbonate electrolytes. (Q3 – Complete)
3. Determine relationship between surface reconstruction and surface layer formation during cycling in NMC electrodes. (Q4 – On schedule)
4. *Go/No-Go*: Demonstrate feasibility of *in situ* near-field FTIR microscopy and spectroscopy to study interfacial phenomena at Li-battery electrodes. *Criteria*: Stop development of near-field and LIBS techniques, if the experiments fail to deliver adequate sensitivity. (Q4 – On schedule)

Progress Report

This quarter, the project examined possible links between $\text{LiNi}_{0.33}\text{Mn}_{0.33}\text{Co}_{0.33}\text{O}_2$ surface reconstruction, metal dissolution, and surface film formation in organic carbonate electrolytes. The project focused on investigating the effect of various solvents in the electrolyte on the NMC interfacial behavior by EELS.

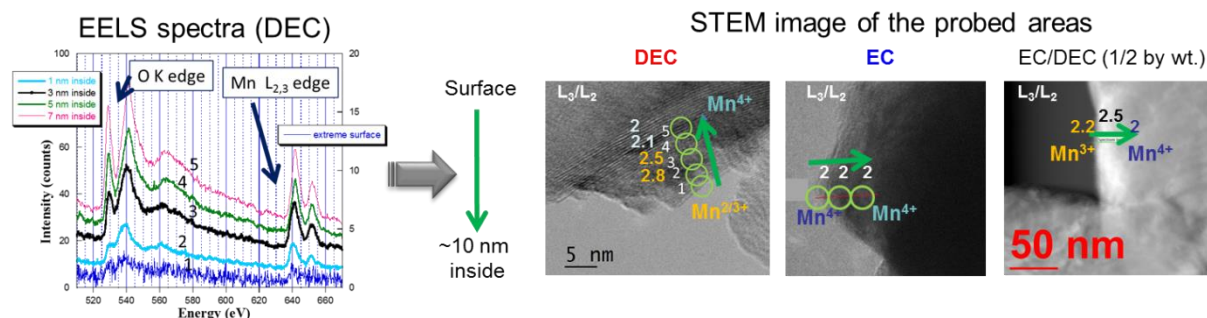


Figure 38. Electron energy loss spectroscopy spectra and scanning transmission electron microscopy image of binder- and carbon-free NMC electrodes cycled in Swagelok versus lithium up to 4.4-2.8V with 1 M LiPF_6 , ethylene carbonate (EC), diethyl carbonate (DEC), or EC/DEC (1/2 wt.).

It was previously shown that fluorescence intensity observed at the surface of TM oxide cathodes during cycling at high potentials varies strongly with the electrolyte solvent(s) composition. That is, fluorescence yield in the linear carbonate (diethyl carbonate, DEC)-based electrolyte is substantially higher than in EC or mixtures of EC/DEC, pointing at the major role of DEC oxidation on the origins of the fluorescence products. The project related the fluorescence with the surface film formation of insoluble fluorescent complexes from EC oxidation and soluble DEC oxidation products, which form at the cathode surface and diffuse away in the electrolyte. ICP measurements also revealed that the surface film formed with EC oxidation products inhibits Mn, Ni, and Co dissolution, which occurs at a rate twice as slow in EC-based electrolyte than in DEC.

To further understand the interfacial reactivity of NMC electrodes toward organic carbonate electrolytes, the project performed EELS experiments at low temperature, using a vacuum transfer sample holder, on non-washed binder- and carbon-free NMC electrodes cycled one time in a Swagelok cell versus Li-foil anode between 4.4 and 2.8 V in 1 M LiPF_6 , EC, DEC or EC/DEC (1/2 wt.) electrolytes. Surface reconstruction of NMC is usually associated with Mn, Ni, and/or Co reduction at the surface and the corresponding depletion of oxygen environment. Both phenomena can be probed using EELS by analyzing the Mn L₃/L₂ edge ratio to determine Mn oxidation state. As illustrated in Figure 38, the Mn oxidation state decreases at the surface of NMC during cycling and is associated with an electronic structure change evidenced at the O K edge. While these structural changes are easily identifiable in DEC electrolyte, with EC almost no variation of the transition metal oxidation state is observed at the surface.

These results are consistent with the literature data, and they support the general idea of Ni, Mn, and Co dissolution from $\text{LiNi}_{0.33}\text{Mn}_{0.33}\text{Co}_{0.33}\text{O}_2$ and surface TM reduction/surface reconstruction during cycling. Using the difference observed with EC or DEC, this result suggests a direct correlation between surface film formation, metal dissolution, and the corresponding fluorescence emission and surface reconstruction. The early formation of a surface film in the EC-based electrolyte during cycling limits the surface reconstruction by inhibiting EC oxidation and subsequent metal dissolution. As stronger fluorescence signal was associated with more surface reconstruction, the intensity of fluorescence from the electrolyte oxidation and metal dissolution products can be used to assess quantitatively the extent of surface structure transformation. Further investigations are ongoing to evaluate the role of rock salt surface layer formation on the battery performance and failure modes in NMC/graphite and NMC/Si battery systems.

Task 5.3 – Advanced *In Situ* Diagnostic Techniques for Battery Materials (Xiao-Qing Yang and Xiqian Yu, Brookhaven National Laboratory)

Project Objective. The primary project objective is to develop new advanced *in situ* material characterization techniques and to apply these techniques to support development of new cathode and anode materials for the next generation of Li-ion batteries for PHEVs. To meet the challenges of powering the PHEV, Li-ion batteries with high energy and power density, low cost, good abuse tolerance, and long calendar and cycle life must be developed.

Project Impact. The VTO Multi Year Program Plan describes the goals for battery: “Specifically, lower-cost, abuse-tolerant batteries with higher energy density, higher power, better low-temperature operation, and longer lifetimes are needed for the development of the next-generation of HEVs, PHEVs, and EVs.” The knowledge gained from diagnostic studies through this project will help U.S. industries develop new materials and processes for new generation Li-ion batteries in the effort to reach these VTO goals.

Approach. This project will use the combined synchrotron based *in situ* X-ray techniques (XRD, and hard and soft XAS) with other imaging and spectroscopic tools such as HRTEM and MS to study the mechanisms governing the performance of electrode materials and provide guidance for new material and new technology development regarding Li-ion battery systems.

Out-Year Goals. Complete the first-stage development of diagnostic technique to study kinetic property of advanced Li-ion electrode materials using time-resolved XRD and XAS (TR-XRD, TR-XAS) combined with STEM imaging and TXM. Apply this technique to study the structural changes of new cathode materials including various NCM and high-voltage spinel materials during high-rate cycling.

Collaborations. The BNL team will work closely with material synthesis groups at ANL (Drs. Thackeray and Amine) for the high-energy composite; and at PNNL for the Si-based anode materials. Such interaction between the diagnostic team at BNL and synthesis groups of these other BMR members will catalyze innovative design and synthesis of advanced cathode and anode materials. The project will also collaborate with industrial partners at General Motors and Johnson Controls, as well as with international collaborators.

Milestones

1. Complete the thermal stability studies of Fe substituted high-voltage spinel cathode materials $\text{LiNi}_{1/3}\text{Mn}_{4/3}\text{Fe}_{1/3}\text{O}_4$ in comparison with unsubstituted $\text{LiNi}_{0.5}\text{Mn}_{1.5}\text{O}_4$ using *in situ* TR-XRD and MS techniques. (December 2015 – Complete)
2. Complete the energy resolved TXM investigation on new concentration gradient NCM cathode sample particles in a noninvasive manner with 3D reconstructed by images through tomography scans to study the 3D Ni, Co, and Mn elemental distribution from surface to the bulk. (March 2016 – Complete)
3. Complete the *in situ* TR-XRD studies of the structural changes of $\text{Li}_{1-x}\text{Ni}_{1/3}\text{Co}_{1/3}\text{Mn}_{1/3}\text{O}_2$ from $x=0$ to $x=0.7$ during high-rate charge process at different C rates at 10C, 30C, and 60C. (June 2016 – Complete)
4. Complete the *in situ* TR-XAS of $\text{Li}_{1-x}\text{Ni}_{1/3}\text{Co}_{1/3}\text{Mn}_{1/3}\text{O}_2$ cathode material at Ni, Co, and Mn K-edge during 30C high-rate charge. (September 2016 – In progress)

Progress Report

The third milestones for FY2016 are completed.

This quarter, BNL focused on studies of formation of intermediate phases in a widely used $\text{LiNi}_{1/3}\text{Mn}_{1/3}\text{Co}_{1/3}\text{O}_2$ (NMC) cathode material during cycling at high-rate cycling (from 10C to 60C) by using ultrafast *in situ* TR-XRD.

Intermediate phases were observed when the current rates were increased to 10C, and became more pronounced at 30C and 60C. The results of these studies were presented in a paper recently accepted by *Advanced Energy Materials*

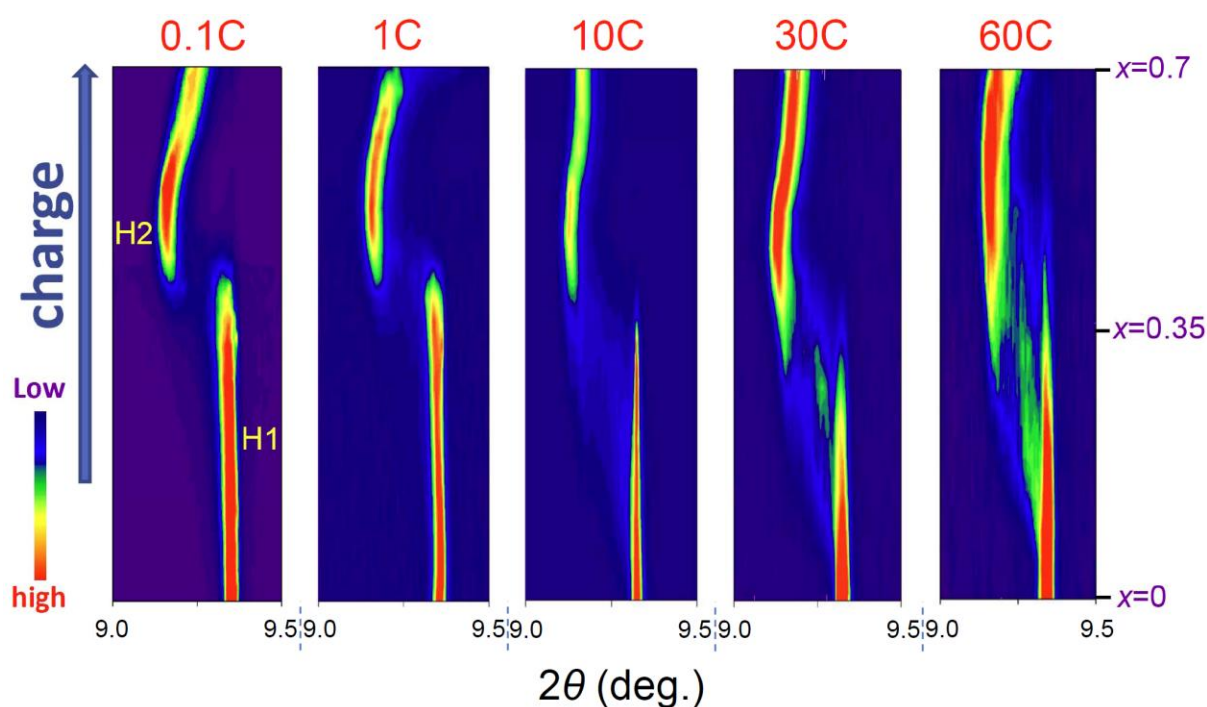


Figure 39. *In situ* X-ray diffraction of NMC during the first charge. Contour plot of the 003 diffraction peak of $\text{Li}_{1-x}\text{Ni}_{1/3}\text{Co}_{1/3}\text{Mn}_{1/3}\text{O}_2$ with increasing x between $x = 0$ and $x = 0.7$ during the first charge process at different C rates (0.1C, 1C, 10C, 30C, 60C). Data were collected at X14A at NSLS with a wavelength of 0.7747 Å.

Patents/Publications/Presentations

Publications

- Zhou, Yong-Ning, and Ji-Li Yue, Enyuan Hu, Hong Li, Lin Gu, Kyung-Wan Nam, Seong-Min Bak, Xiqian Yu, Jue Liu, Jianming Bai, Eric Dooryhee, Zheng-Wen Fu, and Xiao-Qing Yang.* “High-Rate Charging Induced Intermediate Phases and Structural Changes of Layer-Structured Cathode for Lithium-Ion Batteries.” Accepted by *Advanced Energy Materials* (aenm.201600597R2) on June 21, 2016.

Presentations

- International Conference on the Frontier of Advanced Batteries (CIBF 2016), Shenzhen, China (May 24, 2016): “Structural Characterization Studies of Advanced Electrode and Solid Electrolyte Materials for Li-ion and Sodium Batteries Using Synchrotron Based X-ray Techniques and TEM”; Xiqian Yu, Enyuan Hu, Jue Liu, Seongmin Bak, Hung Sui Lee, Xiao-Qing Yang*, Yong-Sheng Hu, Lin Gu, Hong Li, Xuejie Huang, and Liquan Chen. Invited.
- International Meeting of Lithium Batteries (IMLB 2016), Chicago, Illinois (June 20-24, 2016): “Explore the Effects of Microstructural Defects on Voltage Fade of Li- and Mn-Rich Cathodes”; Enyuan Hu, Yingchun Lyu, Huolin L. Xin, Jue Liu, Lili Han, Seong-Min Bak, Jianming Bai, Xiqian Yu*, Hong Li*, and Xiao-Qing Yang.* Poster presentation.
- International Meeting of Lithium Batteries (IMLB 2016), Chicago, Illinois (June 20-24, 2016): “Using New Quasi in-situ TEM Technique to Study Changes of Electrode Materials for Li-Ion and Na-Ion Batteries”; Ruoqian Lin, Enyuan Hu, Xiqian Yu, Xiao-Qing Yang, and Huolin Xin. Poster presentation.

Task 5.4 – NMR and Pulse Field Gradient Studies of SEI and Electrode Structure (Clare Grey, Cambridge University)

Project Objective. The formation of a stable SEI is critical to the long-term performance of a battery, since the continued growth of the SEI on cycling/aging results in capacity fade (due to lithium consumption) and reduced rate performance due to increased interfacial resistance. Although arguably a (largely) solved problem with graphitic anodes/lower voltage cathodes, this is not the case for newer, much higher capacity anodes such as silicon, which suffer from large volume expansions on lithiation, and for cathodes operating above 4.3 V. Thus it is essential to identify how to design a stable SEI. The objectives are to identify major SEI components, and their spatial proximity, and how they change with cycling. SEI formation on silicon versus graphite and high-voltage cathodes will be contrasted. Li⁺ diffusivity in particles and composite electrodes will be correlated with rate. The SEI study will be complemented by investigations of local structural changes of high-voltage/high-capacity electrodes on cycling.

Project Impact. The first impact of this project will be an improved, molecular based understanding of the surface passivation (SEI) layers that form on electrode materials, which are critical to the operation of the battery. Second, the project will provide direct evidence for how additives to the electrolyte modify the SEI. Third, it will provide insight to guide and optimize the design of more stable SEIs on electrodes beyond LiCoO₂/graphite.

Out-Year Goals. The project goals are to identify the major components of the SEI as a function of state of charge and cycle number on different forms of silicon. The project will determine how the surface oxide coating affects the SEI structure and will establish how the SEI on silicon differs from that on graphite and high-voltage cathodes. The project will determine how the additives that have been shown to improve SEI stability affect the SEI structure and will explore the effect of different additives that react directly with exposed fresh silicon surfaces on SEI structure. Via this program, the project will develop new NMR-based methods for identifying different components in the SEI and their spatial proximities within the SEI, which will be broadly applicable to the study of SEI formation on a much wider range of electrodes. These studies will be complemented by studies of electrode bulk and surface structure to develop a fuller model with which to describe how these electrodes function.

Collaborations. This project collaborates with B. Lucht (Rhode Island); J. Cabana, (UIC); G. Chen and K. Persson (LBNL); S. Whittingham (Binghamton); P. Bruce (St. Andrews); S. Hoffman and A. Morris (Cambridge); and P. Shearing (University College London).

Milestones

1. Identify the major carbon-containing break-down products that form on graphene platelets. (December 2015 – Complete; paper being written.)
2. *Go/No-Go:* Establish the difference between extrinsic and P-doped silicon nanowires. *Criteria:* If no difference in performance of P-doped wires established after the first cycle, terminate project. (March 2016 – Complete. No clear differences under conditions used to date. In process of terminating project and writing results.)
3. Complete SEI study of silicon nanoparticles by NMR spectroscopy. (June 2016 – Complete) Develop NMR methodology to examine cathode SEI. (Ongoing)
4. Produce first optimized coating for Si electrode. (September 2016 – Ongoing)

Progress Report

Following earlier work on binder-free Si/carbon electrodes, the project has performed extended cycling studies of Si/C/CMC electrodes (Figure 40), their capacity dropping steadily with cycling. The growth of the SEI was monitored by using ^7Li , ^{19}F , and ^{13}C , and enriched EC and dimethyl carbonate (DMC), the organics dominating the SEI. LiF formation was primarily seen in the first cycle, the solid organic phases growing noticeably in concentration between cycles 1 and 30 (Figure 41). Homonuclear ^{13}C NMR correlation experiments were used to identify the organic fragments in the sample extracted after 30 cycles, and in particular identify components involving more extensive radical reactions to form molecules such as lithium dicarbonate (LBDC) and lithium ethylene carbonate (LEC) (giving rise to peaks such as F in Figure 41a). There was no significant growth of solid organic SEI components between 30 and 60 cycles or SEI formation correlating with increasing electrode tortuosity, as observed by using focused-ion beam and SEM. A two-stage model for lithiation capacity loss is developed (Figure 42): initially, the lithiation capacity steadily decreases, and parasitic reactions and pronounced SEI growth are seen. Later, below 50% of the initial lithiation capacity, less silicon is (de)lithiated resulting in less volume expansion and contraction; the rate of parasitic reactions declines, and the Si SEI thickness stabilizes. The decreasing discharge capacity is primarily attributed to kinetics, the increased electrode tortuosity severely limiting Li^+ ion diffusion through the bulk of the electrode. The resulting restricted diffusion is consistent with the changes in the lithiation processes seen in the electrochemical capacity curves.

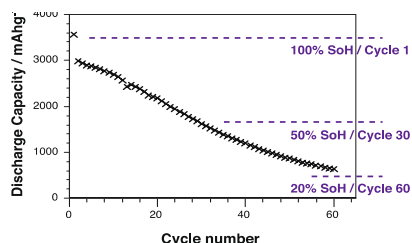


Figure 40. Discharge capacity of silicon as a function of cycle number.

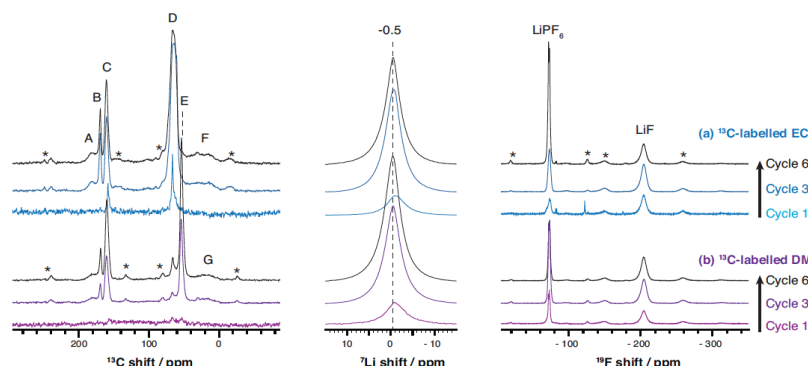


Figure 41. ^{13}C , ^7Li and ^{19}F nuclear magnetic resonance of electrode samples prepared with ^{13}C (a) ethylene carbonate (blue) and (b) dimethyl carbonate (purple) labeled electrolytes following cycling.

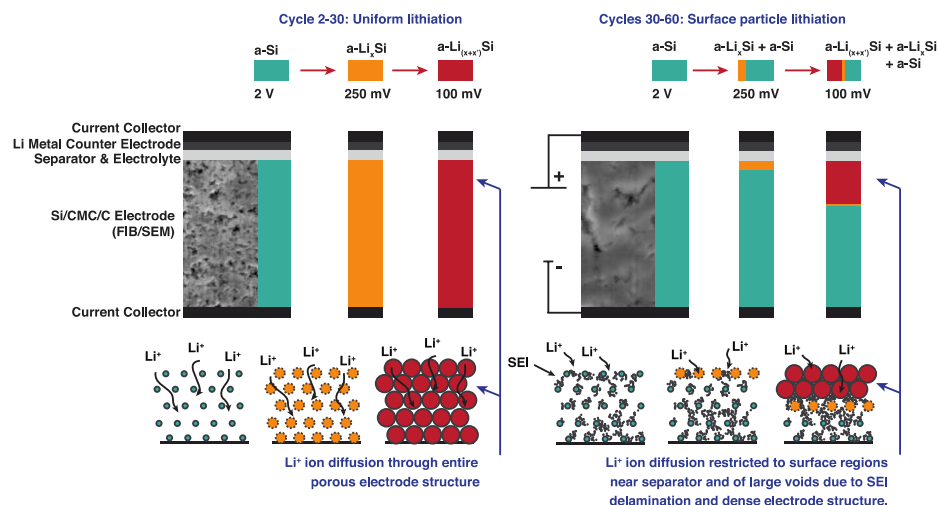


Figure 42. Schematic showing microscale processes: electrode pore structure becomes denser with cycling, restricting Li^+ diffusion to surface regions near the separator and to surface regions of large pores. The focused ion beam scanning electron microscopy electrode cross sections show the increasing density of the electrode pore structure.

Patents/Publications/Presentations**Publication**

- Michan, A. L., and G. Divitini, A. J. Pell, M. Leskes, C. Ducati, and C. P. Grey. “Solid Electrolyte Interphase Growth and Capacity Loss in Silicon Electrodes.” *J. Am. Chem. Soc.* 138 (2016): 7918. doi: 10.1021/jacs.6b02882
- Pecher, O., and P. M. Bayley, H. Liu, Z. Liu, N. M. Trease, and C. P. Grey. “Automatic Tuning Matching Cyclers (ATMC) *In situ* NMR Spectroscopy as a Novel Approach for Real-time Investigations of Li- and Na-ion batteries.” *J. Mag. Reson.* 265 (2016): 200. doi: 10.1016/j.jmr.2016.02.008

Presentations

- International Battery Association Meeting, Nantes, France (March 2016).
- 229th Electrochemical Society Meeting, San Diego, California (May 2016).
- NSF Ceramics Workshop, San Diego, California (May 2016).
- 18th International Meeting of Lithium Batteries (IMLB), Chicago, Illinois (June 2016).

Task 5.5 – Optimization of Ion Transport in High-Energy Composite Cathodes (Shirley Meng, UC San Diego)

Project Objective. This project aims to probe and control the atomic-level kinetic processes that govern the performance limitations (rate capability and voltage stability) in a class of high-energy composite electrodes. A systematic study with a powerful suite of analytical tools [including atomic resolution scanning transmission electron microscopy (a-STEM) and EELS, neutron, XPS and first principles (FP) computation] will elucidate approaches to optimize ion transport. Ultimately, this will hone in on the optimum bulk compositions and surface characteristics to improve the mechanistic rate and cycling performance of high-energy composite electrodes. Moreover, it aims to develop the large-scale synthesis efforts to produce materials with consistent performance. The surface-sensitive characterization tools will be extended to diagnose various silicon anode types.

Project Impact. If successful, this research will provide a major breakthrough in commercial applications of the class of high energy density cathode material for Li-ion batteries. Additionally, it will provide in-depth understanding of the role of surface modifications and bulk substitution in the high-voltage composite materials. The diagnostic tools developed here can also be leveraged to study a wide variety of cathode and anode materials for rechargeable batteries.

Approach. This unique approach combines STEM/EELS, XPS, and *ab initio* computation as diagnostic tools for surface and interface characterization. This allows for rapid identification of surface interphases that provide surface instability or stability in various types of electrode materials including both high-voltage cathodes and low-voltage anodes. Neutron enables the characterization of bulk material properties to enhance and further optimize high-energy electrode materials.

Out-Year Goals. The goal is to control and optimize Li-ion transport, TM migration, and oxygen activity in the high-energy composite cathodes and to optimize electrode/electrolyte interface in silicon anodes so that their power performance and cycle life can be significantly improved.

Collaborations. This work funds collaborations on EELS (Miaofang Chi, ORNL); molecular layer deposition (MLD, Chunmei Ban, NREL); neutron diffraction (Ken An, ORNL); soft XAS (Marca Doeff, LBNL); and XPS, time-of-flight SIMS (TOF-SIMS) characterization (Keith Stevenson, UT Austin). It supports collaborative work with Zhaoping Liu and Yonggao Xia at Ningbo Institute of Materials Technology and Engineering China.

Milestones

1. Quantify the SEI characteristics of MLD coated silicon anode on long cycling with a combination of STEM/EELS and XPS. (March 2016 – Complete)
2. Complete investigation of coating and morphology control for Li-rich, Mn-rich, layered oxides. (June 2016 – Complete)
3. Obtain the optimum nanoscale uniform crystalline lithium-lanthanum-titanium-oxide surface coating in Li-rich layered oxides when charged up to 4.8 V (or 5.0 V). (September 2016 – On schedule)
4. Apply the optimum surface modification and electrolyte additives for silicon/carbon anode with more than 87% first-cycle capacity retention and greater than 99.9% Coulombic efficiency. (On schedule)

Progress Report

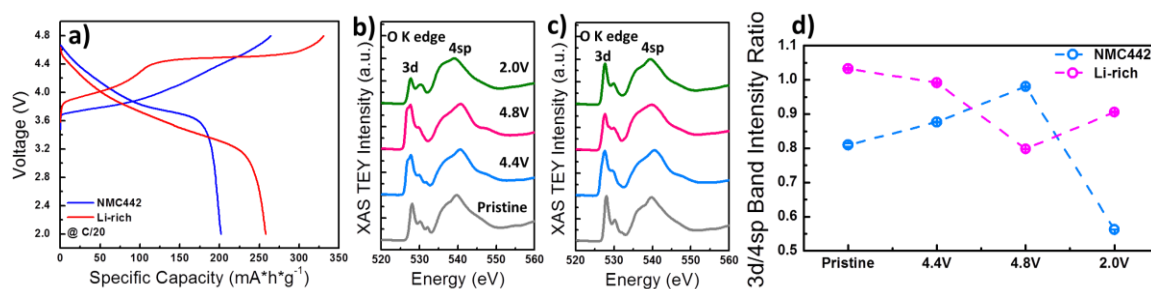


Figure 43. (a) First-cycle voltage profile of NMC-442 and Li-rich, where the voltage range is 2.0 – 4.8V, at C/20 = 12.5 mA g⁻¹. Soft X-ray absorption spectroscopy results (total electron yield mode) at various states of charge in the first cycle of O K-edge (b) NMC-442 and (c) Li-rich NMC. (d) Comparison of O 3d/4sp band intensity ratios between NMC-442 and Li-rich NMC.

Probing the Surface Oxygen Activities of Li-rich Layered Oxides Cathode via Soft XAS. Soft X-ray absorption spectroscopy (XAS) is a powerful characterization tool that can determine local atomic and electronic structures. TEY mode is applied to investigate the oxygen activities on the surface of $\text{LiNi}_{0.4}\text{Mn}_{0.4}\text{Co}_{0.2}\text{O}_2$ (NMC-442) and $\text{Li}_{1.2}\text{Ni}_{0.13}\text{Mn}_{0.53}\text{Co}_{0.13}\text{O}_2$ (Li-rich) at different states of charge. The broad structures above 534 eV correspond to the transition of O 1s to the hybridized states, consisting of metal 4sp and oxygen 2p orbitals. The pre-edge structure below 534 eV corresponds to the transition to the states of metal 3d and oxygen 2p orbitals. The intensity ratio of the 3d to 4sp band represents the amount of unoccupied 3d orbitals in the metal ions and a change in the local environment of oxygen, such as oxygen vacancies and peroxy/superoxy-like species. As shown in Figure 43, the 3d/4sp NMC-442 ratio increased during charge, indicating a larger amount of unoccupied 3d orbitals from the TM ion oxidation. The decrease of 3d/4sp ratio after one cycle suggests that the change of bond covalency between oxygen and the neighboring TMs are due to the formation of Co-O like rock-salt structure on the surface of NMC-442 material. While the decrease of 3d/4sp ratio of Li-rich during charge comes from the dramatic change in the local environment of oxygen, such as bond length and oxygen vacancies formation. More interestingly, this 3d/4sp ratio goes back to some extent after discharge, implying that the involved oxygen activities on the surface of Li-rich can be partially reversible.

Nano-scale Strain Mapping and Amorphization Evolution of Silicon Anodes on Lithiation Using TEM. Silicon anode undergoes large volume expansion on cycling, resulting in massive mechanical strain in the electrode. Therefore, it is important to measure quantitatively the strain evolution on cycling and correlate it with the electrochemical

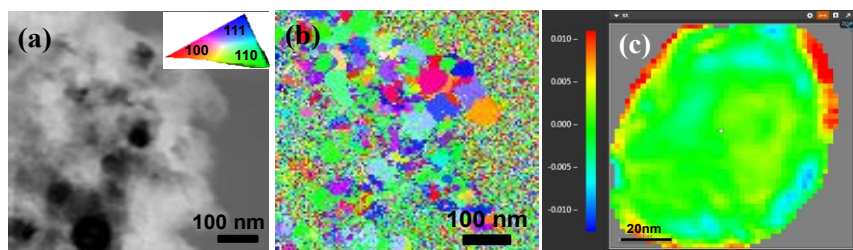


Figure 44. (a) bright field transmission electron microscopy image of the partially lithiated silicon and color-code (insert), (b) corresponding orientation map, and (c) strain map from a partially lithiated grain.

performance of the material. Herein, the crystallinity mapping and strain mapping of the partially lithiated silicon are presented using a novel method based on electron diffraction. The diffraction information can be generated by scanning a nano-size probe (NBED) across a sample. Figure 44 illustrates color-coded two-dimensional orientation and strain maps at 1 nm spatial resolution and 0.5° precessions. The amorphous regions can be distinguished by having small spots implying the formation of amorphous Li_xSi alloy upon the lithiation of silicon. In addition, the lithiation of crystalline silicon is accompanied by large strain formation shown in Figure 44c. The center of the grain was used as a reference and considerable strain variation from -1% to 2% (from the lower left to the upper right corner of the grain) was observed.

Patents/Publications/Presentations

Publications

- Qui, B., and M. Zhang, Li. Wu, J. Wang, Y. Xia, D. Qian, H. D. Liu, S. Hy, Y. Chen, K. An, Y. Zhu, Z. Liu, and Y. S. **Meng**. *Nature Comm.* (2016). doi: 10.1038/ncomms12108
- Sina, M., and J. Alvarado, H. Shobukawa, K. W. Schroder, K. Stevenson, and Y. S. Meng. “Direct Visualization of the Solid Electrolyte Interphase and Its Effects on Silicon Electrochemical Performance.” *Advanced Materials Interfaces* (2016). Accepted

Presentations

- 229th ECS Meeting, San Diego, California (2016): “Operando Lithium Dynamics in the Li-Rich Layered Oxide Cathode Material Via Neutron Diffraction”; H. Liu, Y. Chen, S. Hy, K. An, S. Venkatachalam, D. Qian, M. Zhang, and Y. S. Meng.
- 18th International Meeting on Lithium Batteries, Chicago, Illinois (2016): “Investigate the Lithium Dynamics in Li-Rich Layered Oxide Cathode Material Via Operando Neutron Diffraction”; H. Liu, Y. Chen, S. Hy, K. An, S. Venkatachalam, D. Qian, M. Zhang, and Y. S. Meng. Poster.
- 18th International Meeting on Lithium Batteries, Chicago, Illinois (2016): “Making the Invisible Visible - Advanced Diagnosis Methods for Lithium Ion Rechargeable Battery Materials”; Y. S. Meng. Invited.
- 229th ECS Meeting, San Diego, California (2016): “Visualizing the Solid Electrolyte Interphase Layer Evolution in Silicon Electrodes”; M. Sina, J. Alvarado, H. Shobukawa, and Y. S. Meng.
- 229th ECS Meeting, San Diego, California (2016): “Understanding the Factors that Improve the Cycling Performance of Silicon Anode for Li-Ion Batteries”; J. Alvarado, K. W. Schroder, T. A. Yersak, and Y. S. Meng.
- International Battery Association, Nantes, France (2016): “Interface Optimization Principles of Si Anode for Li-ion Batteries”; J. Alvarado, M. Sina, H. Shobukawa, and Y. S. Meng. Invited.

Task 5.6 – Analysis of Film Formation Chemistry on Silicon Anodes by Advanced *In Situ* and *Operando* Vibrational Spectroscopy

(Gabor Somorjai, UC Berkeley; Phil Ross, Lawrence Berkeley National Laboratory)

Project Objective. Understand the composition, structure, and formation/degradation mechanisms of the SEI on the surfaces of silicon anodes during charge/discharge cycles by applying advanced *in situ* vibrational spectroscopies. Determine how the properties of the SEI contribute to failure of silicon anodes in Li-ion batteries in vehicular applications. Use this understanding to develop electrolyte additives and/or surface modification methods to improve Si anode capacity loss and cycling behavior.

Project Impact. A high-capacity alternative to graphitic carbon anodes is silicon, which stores 3.75 lithium per silicon versus 1 lithium per 6 carbon, yielding a theoretical capacity of 4008 mAh/g versus 372 mAh/g for carbon. But silicon anodes suffer from large first-cycle irreversible capacity loss and continued parasitic capacity loss on cycling, leading to battery failure. Electrolyte additives and/or surface modification developed from new understanding of failure modes will be applied to reduce irreversible capacity loss, and to improve long-term stability and cyclability of silicon anodes for vehicular applications.

Approach. Model silicon anode materials including single crystals, e-beam deposited polycrystalline films, and nanostructures are studied using baseline electrolyte and promising electrolyte variations. A combination of *in situ* and *operando* FTIR, Sum Frequency Generation (SFG), and ultraviolet Raman vibrational spectroscopies are used to directly monitor the composition and structure of electrolyte reduction compounds formed on the silicon anodes. Pre-natal and post-mortem chemical composition is identified using XPS. The silicon films and nanostructures are imaged using SEM.

Out-Year Goals. Extend study of interfacial processes with advanced vibrational spectroscopies to high-voltage oxide cathode materials. The particular oxide to study will be chosen based on materials of interest and availability of the material in a form suitable for these studies (for example, sufficiently large crystals or sufficiently smooth/reflective thin films). The effect of electrolyte composition, electrolyte additives, and surface coatings will be determined, and new strategies for improving cycle life developed.

Milestones

1. Modifying the SFG apparatus to obtain high-resolution SFG spectra further allowing particles, thin film, and microstructures of silicon and the electrolyte interface research. (October 2015 – Complete)
2. Performing phase-specific SFG measurement under constant and dynamic potentials (-0.01 V, 0.5 V, and 1.0 V vs. Li/Li⁺) of 1 M LiPF₆ in EC without DEC to probe the SEI formed on amorphous silicon anodes. (January 2016 – Complete)
3. *Go/No-Go*: Can this task distinguish between the various SEI products in the C-H stretch mode (2800 – 3200 cm⁻¹)? If not, proceed to conventional C-O region (1700 – 1800 cm⁻¹). (June 2016 - Complete)
4. Performing fs-SFG measurement in tandem with cyclic voltammetry (CV, potential sweep) to find the ring opening kinetics of EC Preforming fs-SFG measurement in tandem with CV (potential sweep) to find the ring opening kinetics of EC. (September 2016)

Progress Report

The project has synthesized the following electrolyte solutions: 1.0 M LiClO_4 in EC, 1.0 M LiClO_4 in FEC and their mixture EC:FEC in a 9:1 w/w ratio to investigate the effect of fluorinated additives (FEC) on chemical composition of the SEI and surface ordering of electrolytes at electrolyte/amorphous silicon (a-Si) interface. The main conclusion this quarter is that FEC induces ordering of the adsorbed EC on a-Si anode. The results suggest that FEC induces a tighter packing of EC at the anode surface, consequently yielding a better SEI in Li-ion batteries. By tuning the SFG polarization configuration to *ssp* we have enhanced the SF signal sensitivity to adsorbates with a perpendicular dipole orientation in respect to the electrode surface. Figure 45 presents the a-Si / FEC based electrolyte interphase at open circuit potential (OCP) at the C-H stretch range. No prominent SFG features corresponding to FEC were detected from the interface. Presumably FEC molecules are either isotropic, well ordered in an up-down orientation, or flat in respect to the Si surface. With EC electrolyte, we observe two prominent peaks in SFG spectrum at OCP (black curve) in the frequency range of 2960 to 3075 cm^{-1} . The SFG of the EC : FEC carbonate mixture reveals that FEC induces better EC surface ordering (blue curve). The project has reached this conclusion by analyzing the origin of the new peaks at 2880 cm^{-1} and 2930 cm^{-1} . The findings suggest that the s-CH_2 at 2880 cm^{-1} is red shifted due to Van der Waals interactions with the a-Si surface. The peaks at 2930 cm^{-1} , 2990 cm^{-1} are associated with pure EC FTIR spectra. Figure 46 shows the SFG signal arising from EC and FEC mixtures in contact with a-Si anode at OCP in the carbonyl (C=O) stretch region. The main broad peak of EC (black curve) is $\sim 1820 \text{ cm}^{-1}$ (fundamental stretching) with a shoulder around 1780 cm^{-1} (Fermi resonance). Noticeably, on adding FEC (red curve), the Fermi resonance at 1780 cm^{-1} intensifies, which suggests a solid-like EC packing at the anode surface presumably due to better dipole-dipole stacking.

In conclusion, the project has observed that FEC on a-Si induces better ordering of the adsorbed EC on the silicon anode. The C-H and C=O stretch ranges yield that FEC induces the EC molecules to adsorb on the a-Si surface in a pure EC solid-like layer. On reduction, the shift of the C=O peak will enable the project to determine the SEI components. In both IR ranges, the project will conduct orientation analysis that will show whether the fluorinated SEI products are also orientated perpendicular to the a-Si surface.

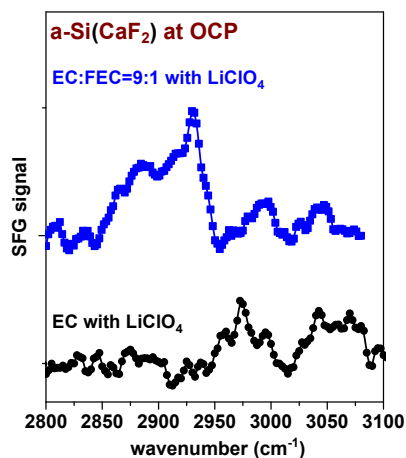


Figure 45. This image shows the sum frequency generation (ssp) signal at the C-H stretch at open current potential of 1 M LiClO_4 in ethylene carbonate (EC), and EC : FEC (fluoroethylene carbonate) (9:1, w/w) in contact with a-Si anode.

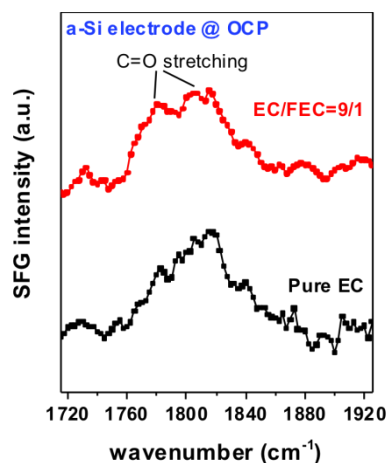


Figure 46. The sum frequency generation (ssp) signal for the carbonyl stretch (C=O) at open current potential of 1 M LiClO_4 in ethylene carbonate (EC), and EC : FEC (fluoroethylene carbonate) (9:1, w/w) in contact with a-Si anode.

Task 5.7 – Microscopy Investigation on the Fading Mechanism of Electrode Materials (Chongmin Wang, Pacific Northwest National Laboratory)

Project Objective. The overall objective is to develop low-cost, high-energy cathode materials with long cycle life. This part is focused on microscopy investigation on the fading mechanism of the electrode materials. The focus will be on using *ex situ*, *in situ*, and *operando* HR-TEM and spectroscopy to probe the structural evolution of electrodes and interfaces between the electrode and electrolyte and correlate this structural and chemical evolution with battery performance.

Project Impact. Both *ex situ* and *in situ* TEM have been demonstrated to be critical for probing the structure and chemistry of electrode and SEI layer. Recently, this task developed new *operando* characterization tools to characterize SEI formation and electrode/electrolyte interaction using a practical electrolyte, which is critical for making new breakthroughs in the battery field. The success of this work will increase the energy density of Li-ion batteries and accelerate market acceptance of EV, especially for PHEV required by the EV Everywhere Grand Challenge proposed by the DOE/EERE.

Approach. Extend and enhance the unique *ex situ* and *in situ* TEM methods for probing the structure of Li-ion batteries, especially for developing a biasing liquid electrochemical cell that uses a real electrolyte in a nano-battery configuration. Use various microscopic techniques, including *ex situ*, *in situ*, and especially the *operando* TEM system, to study the fading mechanism of electrode materials in batteries. This project will be closely integrated with other research and development efforts on high-capacity cathode and anode projects in the BMR Program to (1) discover the origins of voltage and capacity fading in high-capacity layered cathodes and (2) provide guidance for overcoming barriers to long cycle stability of electrode materials.

Out-Year Goals. The out-year goals are as follows:

- Multi-scale (ranging from atomic scale to meso-scale) *ex situ/in situ* and *operando* TEM investigation of failure mechanisms for energy-storage materials and devices. Atomic-level *in situ* TEM and STEM imaging to help develop a fundamental understanding of electrochemical energy storage processes and kinetics of electrodes.
- Extension of the *in situ* TEM capability for energy storage technology beyond lithium ions, such as Li-S, Li-air, Li-metal, sodium ions, and multi-valence ions.

Collaborations. The project is collaborating with the following PIs: Michael M. Thackeray and Khalil Amine (ANL); Chunmei Ban (NREL); Donghai Wang (Pennsylvania State University); Arumugam Manthiram (UT Austin); Guoying Chen, Wei Tong, and Gao Liu (LBNL); Yi Cui (Stanford University); Jason Zhang and Jun Liu (PNNL); and Xingcheng Xiao (GM).

Milestones

1. Complete multi-scale quantitative atomic level mapping to identify the behavior of Co, Ni, and Mn in NCM during battery charge/discharge. (March 2016 – Complete)
2. Complete quantitative measurement of structural/chemical evolution of modified-composition NCM cathode during cycling of battery. (June 2016 – Complete)
3. Complete the correlation between structure stability and charge voltage of NCM for optimized charge voltage. (September 2016)

Progress Report

In this work, strain induced degradation mechanism in cathode materials has been systematically studied. In macro level, strain can lead to mechanical integration failure. In micro level, formation of intragranular crack is one of the major degradation mechanisms, especially for high-voltage applications.

The detrimental effect of intragranular cracking is investigated for the commercialized $\text{LiNi}_{1/3}\text{Mn}_{1/3}\text{Co}_{1/3}\text{O}_2$ layered cathode (NMC-333). The comprehensive TEM observations unveiled previously unrecognized nature of intragranular cracks from four aspects:

- There are two kind intragranular cracks. One is the normally seen mechanical failure crack with two free surfaces; the other one is termed as premature crack with uniformly sub-nanometer crack width.
- The premature crack is not empty, but with loose materials inside.
- Many intragranular cracks were initiated from grain interior.
- Dislocations are acting as crack nucleation sites. This study pointed out future directions for mitigating intragranular cracking not only for layered cathode materials but also for other intercalation type cathodes.

For layered TM oxides, during charge process, lithium ions are extracted from the lattice, which usually causes lattice expansion along c direction and shrinkage along a and b directions, while this process reverses upon discharging (reversible insertion of lithium ions). For example, when NMC-333 is delithiated to $\text{Li}_{0.5}\text{Ni}_{1/3}\text{Mn}_{1/3}\text{Co}_{1/3}\text{O}_2$, the lattice could expand 2.0% along c direction and shrink 1.4% along a direction, which is a huge strain for oxides with ionic bonds. The project found that intragranular cracks in NMC-333 cathode can be easily created at high cutoff cycle voltage, which contributed to the cell's fast degradation. Besides real intragranular cracks that have two free surfaces, the project also identified tremendous premature intragranular crack whose surfaces are not completely free but with loose materials in between. Such premature cracks are generated by expanding the neighbored (003) planes (TM slabs) and exhibiting strip contrast while viewing them edge on in TEM. By examining many intragranular cracks, the project surprisingly found that many cracks were actually initiated from grain interior, which contradicts the proposed theoretical models as they predicted surface should be the favorite site for crack initiation. Through intensive TEM characterization, it was discovered that dislocations could act as nucleation sites of internal cracking. Based on experimental results, the project proposed a mechanism that can fully address the formation process of internal cracking in layered cathode.

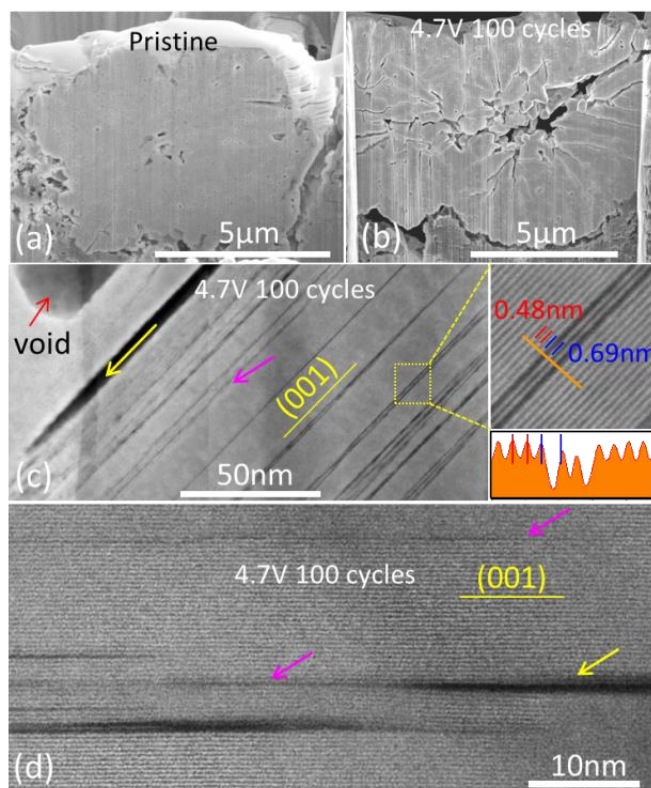


Figure 47. Intergranular and intragranular cracks in 4.7 V 100 cycles NMC-333 cathode materials. Cross section scanning electron microscopy images of secondary particles from (a) pristine and (b) 100 cycles electrode. (c-d) Scanning transmission electron microscopy – high angle annular dark field images from 100 cycles NMC-333 showing intragranular cracks along (001) plane. Yellow arrows indicate real cracks and pink arrows indicate incubation cracks.

Patents/Publications/Presentations

Publications

- Yan, Pengfei, and Jianming Zheng, Jiaxin Zheng, Zhiguo Wang, Gaofeng Teng, Saravanan Kuppan, Jie Xiao, Guoying Chen, Feng Pan, Ji-Guang Zhang, and Chong-Min Wang. “Ni and Co Segregations on Selective Surface Facets and Rational Design of Layered Lithium Transition-Metal Oxide Cathodes., *Adv. Energy Mater.* 6 (2016): 1502455.
- Gan, Zhaofeng, and Meng Gu, Jianshi Tang, Chiu-Yen Wang, Yang He, Kang L. Wang, Chongmin Wang, David J. Smith, and Martha R. McCartney. “Direct Mapping of Charge Distribution during Lithiation of Ge Nanowires Using Off-axis Electron Holography.” *Nano Lett.* 16 (2016): 3748–3753.

Task 5.8 – Characterization and Computational Modeling of Structurally Integrated Electrode (Michael M. Thackeray and Jason R. Croy, Argonne National Laboratory)

Project Objective. The primary project objective is to explore the fundamental, atomic-scale processes that are most relevant to the challenges of next-generation, energy-storage technologies, in particular, high-capacity, structurally integrated electrode materials. A deeper understanding of these materials relies on novel and challenging experiments that are only possible through unique facilities and resources. The goal is to capitalize on a broad range of facilities to advance the field through cutting-edge science, collaborations, and multi-disciplinary efforts to characterize and model structurally integrated electrode systems, notably those with both layered and spinel character.

Project Impact. This project capitalizes on and exploits DOE user facilities and other accessible national and international facilities (including skilled and trained personnel) to produce knowledge to advance Li-ion battery materials. Specifically, furthering the understanding of structure-electrochemical property relationships and degradation mechanisms will contribute significantly to meeting the near- to long-term goals of PHEV and EV battery technologies.

Approach. A wide array of characterization techniques including X-ray and neutron diffraction, X-ray absorption, emission and scattering, HR-TEM, Raman spectroscopy, and theory will be brought together to focus on challenging experimental problems. Combined, these resources promise an unparalleled look into the structural, electrochemical, and chemical mechanisms at play in novel, complex electrode/electrolyte systems being explored at ANL.

Out-Year Goals. The out-year goals are as follows:

- Gain new, fundamental insights into complex structures and degradation mechanisms of high-capacity composite cathode materials from novel, probing experiments carried out at user facilities and beyond.
- Investigate structure-property relationships that will provide insight into the design of improved cathode materials.
- Use knowledge and understanding gained from this project to develop and scale up advanced cathode materials in practical Li-ion prototype cells.

Collaborators. This project engages in collaboration with Eungje Lee, Joong Sun Park, Joel Blauwkamp, and Roy Benedek (Chemical Sciences and Engineering, ANL).

Milestones

1. Characterize bulk and surface properties of structurally integrated electrode materials using DOE user facilities at Argonne (APS, Electron Microscopy Center, and Argonne Leadership Computing Facility) and facilities elsewhere, for example, Spallation Neutron Source (ORNL) and the Northwestern University Atomic and Nanoscale Characterization Experimental Center (NUANCE). (September 2016 – In progress)
2. Use complementary theoretical approaches to further the understanding of the structural and electrochemical properties of layered-spinel electrodes and protective surface layers. (September 2016 – In progress)
3. Analyze, interpret, and disseminate collected data for publication and presentation. (September 2016 – In progress)

Progress Report

A key feature of $y[x\text{Li}_2\text{MnO}_3 \cdot (1-x)\text{LiMO}_2] \cdot (1-y)\text{LiM}_2\text{O}_4$ (M typically = Mn, Co, Ni) layered-layered-spinel (LLS), composite materials is the presence of TM ions in the lithium layer. Previous results have shown that Co content plays an important role in the overall performance of LLS materials when synthesized via “underlithiation” of parent, LL precursors. Simulations are being performed to elucidate the effect of Co in the lithium layer on structural stability during the first-charge voltage plateau. The simulations address two structures with composition $0.4\text{Li}_2\text{MnO}_3 \cdot 0.6\text{LiCoO}_2$; in one case, the LiCoO_2 component is set up with the lithiated spinel $\text{Li}_2\text{Co}_2\text{O}_4$ (rock salt) structure (that is, low temperature LiCoO_2) to form a LS composite (Figure 48a, top); the other case is a LL composite of layered LiCoO_2 and Li_2MnO_3 (not shown). First principles molecular dynamics simulations have been performed for a state of charge corresponding to the removal of all lithium from the lithium layer (in both LS and LL systems). The selected simulation temperature of 1000 K is higher than battery operating temperatures, but illustrates the trends at acceptable computational cost. The dynamical simulations (Figure 48a) illustrate the relative stability of the selected structures. Figure 48b shows the density of O-O “pairs” (defined as pairs of oxygen with bond lengths less than 1.7 Å) that are formed on complete delithiation of the lithium layer. The LS composite shows a higher density of O-O pairs toward the end of the first-charge voltage plateau than the LL composite. Moreover, the density of Mn ions (from the Li_2MnO_3 component) that have migrated to the lithium layer (not shown in the plot) is also higher in the LS composite than in the LL composite. Figure 48a (bottom) shows a snapshot of the delithiated LS structure at simulation times of several picoseconds.

The present simulations suggest that Co ions in the lithium layer, in $\text{Li}_2\text{Co}_2\text{O}_4$ -type domains, do not stabilize the structure during the first charge of the LS composite relative to the behavior of the LL composite. This finding, however, does not necessarily contradict experimental observations of the relatively low voltage fade in LLS systems. For example, LLS and their LL counterparts generally achieve very similar first-cycle charge capacities where the LLS electrodes generally achieve higher first-cycle discharge capacities (Coulombic efficiencies) and cycling stabilities. In addition, previous reports have shown that a small amount of nickel substitution in $\text{Li}_2\text{Co}_{2-x}\text{Ni}_x\text{O}_4$ enhances stability of the spinel phase. These observations may be related to local structures that form after the first charge and subsequent transformations that occur during cycling, rather than during the first charge. Thus, the presence of spinel may inhibit oxygen (or oxygen-vacancy) transport that occurs during cycling, and thereby slow down the transformations that enhance the low-voltage peak in dQ/dV , and thus reduce voltage fade. Alternatively, the pure $\text{Li}_2\text{Co}_2\text{O}_4$ - Li_2MnO_3 structures herein may behave quite differently than the complex nickel-containing compositions of practical LLS electrodes. Additional work is required to verify this interpretation.

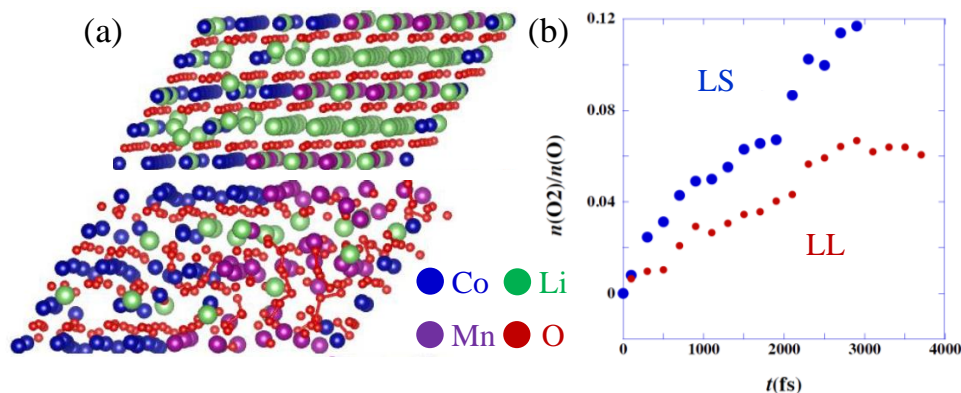


Figure 48. Atomic structure in computational unit cell for the layered spinel shortly before the onset of the voltage plateau (a, top) and toward the end of the plateau (a, bottom). (b) Density of O-O pairs with bond lengths less than 1.7 Å as a function of simulation time for delithiated layered-layered (LL, red) and layered-spinel (LS, blue) structures.

Patents/Publications/Presentations

Presentations

- DOE Annual Merit Review, Washington, D. C. (June 6-10, 2016): “Processing and Characterization of High Capacity Composite Electrode Structures (ES235)”; M. M. Thackeray and J. R. Croy.
- BASF, Argonne National laboratory, Lemont, Illinois (March 3, 2016): “Processing and Characterization of High Capacity Composite Electrode Structures”; M.M. Thackeray and J.R. Croy.

TASK 6 – MODELING ADVANCED ELECTRODE MATERIALS

Summary and Highlights

Achieving the performance, life, and cost targets outlined in the EV Everywhere Grand Challenge will require moving to next generation chemistries, such as higher capacity Li-ion intercalation cathodes, silicon and other alloy-based anodes, Li-metal anode, and sulfur cathodes. However, numerous problems plague the development of these systems, from material-level challenges in ensuring reversibility to electrode-level issues in accommodating volume changes, to cell-level challenges in preventing cross talk between the electrodes. In this task, a mathematical perspective is applied to these challenges to provide an understanding of the underlying phenomenon and to suggest solutions that can be implemented by the material synthesis and electrode architecture groups.

The effort spans multiple length scales from *ab initio* methods to continuum-scale techniques. Models are combined with experiments and extensive collaborations are established with experimental groups to ensure that the predictions match reality. Efforts are also focused on obtaining the parameters needed for the models, either from lower-length scale methods or from experiments. Projects also emphasize pushing the boundaries of the modeling techniques used to ensure that the task stays at the cutting edge.

In the area of intercalation cathodes, the effort is focused on understanding the working principles of the high Ni layered materials with an aim of understanding structural changes and the associated changes in transport properties. In addition, focus is paid to the assembling of porous electrodes with particles to predict the conduction behavior and developing tools to measure electronic conduction. This quarter, the lithium diffusion process in the excess-lithium material was studied. In the area of new disordered materials, the project is now making progress on predicting the voltage of the intercalation reaction. Finally, the use of micro probes to measure conductivity in a nondestructive technique continues.

In the area of silicon anodes, the effort is in trying to understand the interfacial instability and suggest ways to improve the cyclability of the system. In addition, effort is focused on designing artificial SEI layers that can accommodate the volume change, and in understanding the ideal properties for a binder to accommodate the volume change without delamination. Work on the SEI on these electrodes continues this quarter, with emphasis on understanding the effect of the type of electrolyte. This quarter, simulations of silicon anodes are focused on understanding lithium trapping.

In the area of sulfur cathodes, the focus is on developing better models for the chemistry with the aim of describing the precipitation reactions accurately. Efforts are focused on performing the necessary experiments to obtain a physical picture of the phase transformations in the system and in measuring the relevant thermodynamic, transport, and kinetic properties. In addition, changes in the morphology of the electrode are described and tested experimentally. This quarter, the transport properties, namely the conductivity, diffusion coefficient, and transference number were measured.

Task 6.1 – Electrode Materials Design and Failure Prediction (Venkat Srinivasan, Lawrence Berkeley National Laboratory)

Project Objective. The project goal is to use continuum-level mathematical models along with controlled experiments on model cells to (i) understand the performance and failure models associated with next-generation battery materials, and (ii) design battery materials and electrodes to alleviate these challenges. The research will focus on the Li-S battery chemistry and on microscale modeling of electrodes. Initial work on the Li-S system will develop a mathematical model for the chemistry along with obtaining the necessary experimental data, using a single ion conductor (SIC) as a protective layer to prevent polysulfide migration to the lithium anode. The initial work on microscale modeling will use the well understood $\text{Li}(\text{NiMnCo})_{1/3}\text{O}_2$ (NMC) electrode to establish a baseline for modeling next-generation electrodes.

Project Impact. Li-S cells promise to increase the energy density and decrease the cost of batteries compared to the state of the art. If the performance and cycling challenges can be alleviated, these systems hold the promise for meeting the EV Everywhere targets.

Out-Year Goals. At the end of this project, a mathematical model will be developed that can address the power and cycling performance of next-generation battery systems. The present focus is on microscale modeling of electrodes and Li-S cells, although the project will adapt to newer systems, if appropriate. The models will serve as a guide for better design of materials, such as in the kinetics and solubility needed to decrease the morphological changes in sulfur cells and increase the power performance.

Milestones

1. Replace parameters (porosity gradient and tortuosity) in macroscale NMC model with corresponding values or functions obtained from tomography data. (December 2015 – Complete)
2. Measure the relationship of film growth to electrochemical response and develop a model to interpret the relationship. (March 2016 – Complete)
3. Measure transport properties of polysulfide solutions using electrochemical methods. If unsuccessful at obtaining concentration-dependent diffusion coefficient, use fixed diffusion coefficient value in upcoming simulations. (June 2016 – No-go)
4. Incorporate measured properties into porous-electrode model of Li-S cell and compare to data. (September 2016 – In progress)

Progress Report

Measure Transport Properties of Polysulfide Solutions Using Electrochemical Methods. Sulfur (S_8) and lithium sulfide (Li_2S) were dissolved in stoichiometric amounts in a 1:1 DOL/DME solvent mixture. The resulting polysulfide solutions were expected to contain primarily Li_2S_6 or Li_2S_8 , depending on stoichiometry. Additionally, electrolyte solutions with a range of concentrations of LiTFSI in 1:1 DOL/DME solvent were prepared. Concentration-dependent conductivity values of the polysulfide solutions (Figure 49a) and electrolyte solutions (Figure 49b) were measured with a conductivity meter. Figure 49a indicates that with increasing concentration of sulfur within the polysulfide solution, conductivity increases and eventually saturates. Higher concentrations of sulfur were not obtained due to saturation and precipitation of polysulfides at room temperature. Figure 49b shows a decrease in conductivity of LiTFSI at higher concentrations, which may result from increased solution viscosity at high salt concentrations.

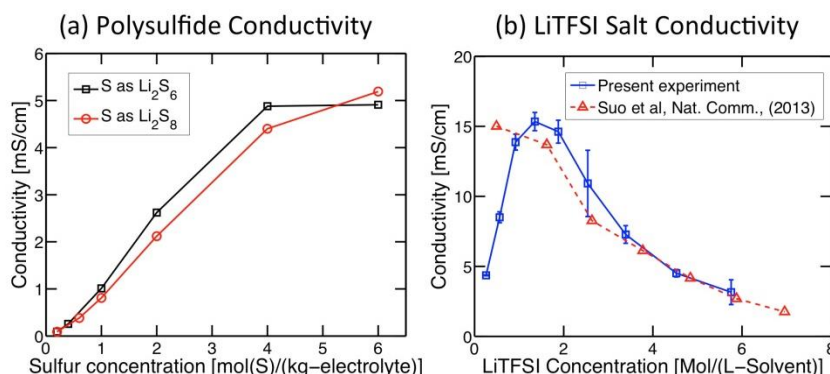


Figure 49. (a) Concentration dependent conductivity of two different polysulfide solutions, expected to contain primarily Li_2S_6 or Li_2S_8 . (b) Concentration dependent conductivity of LiTFSI salt in 1:1 DOL/DME solvent. Comparison with experiment is also provided.

Transference number values were obtained using the Bruce-Vincent method. Figure 50a shows the Nyquist plot used to estimate interfacial resistance. Evolution of current during potentiostatic polarization is shown in Figure 50b. Figure 50c indicates that the transference number of LiTFSI salt is around 0.45 and independent of lithium concentration.

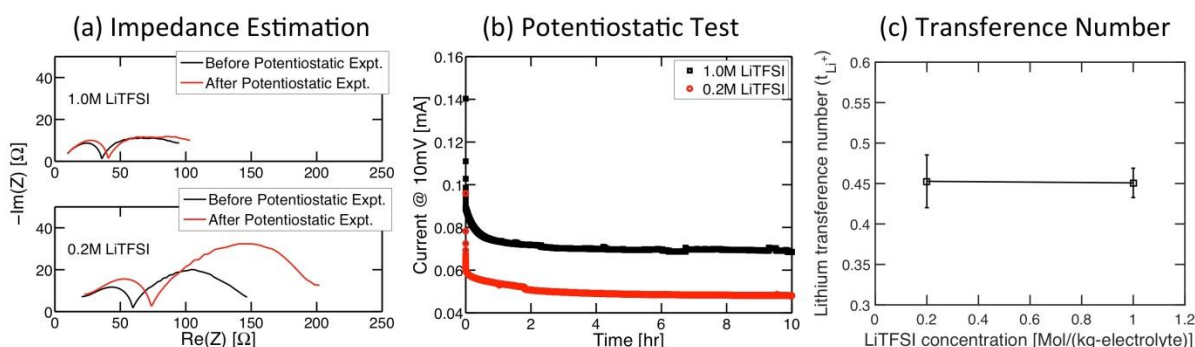


Figure 50. (a) Nyquist plot to estimate the impedance before and after potentiostatic polarization for two different concentrations of LiTFSI salt. (b) Current profile during potentiostatic polarization at 10mV for 0.2M and 1.0M LiTFSI salt concentrations. (c) Transference number of lithium ions extracted using the Bruce-Vincent method.

Finally, dilute solutions of the polysulfides were prepared, and fixed diffusion coefficients were measured using the chronoamperometry methodology. The Cottrell equation has been used to extract the value of diffusivity from the current decay under potentiostatic polarization. Plotting the current against the reciprocal of square root of time (not shown here) and measuring the slope yields the diffusivity values for Li_2S_6 and Li_2S_8 as $1.84 \times 10^{-10} \text{ m}^2/\text{s}$ and $2.68 \times 10^{-10} \text{ m}^2/\text{s}$. In summary, transport properties were obtained in electrolyte and polysulfide solutions through electrochemical methods. However, a reliable procedure for obtaining diffusivity values in concentrated solutions was not determined, hence the “no-go” decision on using concentration-dependent diffusion coefficient values in the simulations to be performed in the next quarter. Therefore, a constant value will be used in the simulations.

Task 6.2 – Predicting and Understanding Novel Electrode Materials from First Principles (Kristin Persson, Lawrence Berkeley National Laboratory)

Project Objective. The project aim is to model and predict novel electrode materials from first-principles focusing on (1) understanding the atomistic interactions behind the behavior and performance of the high-capacity lithium excess and related composite cathode materials, and (2) predicting new materials using the recently developed Materials Project high throughput computational capabilities at LBNL. More materials and new capabilities will be added to the Materials Project Lithium Battery Explorer App (www.materialsproject.org/apps/battery_explorer/).

Project Impact. The project will result in a profound understanding of the atomistic mechanisms underlying the behavior and performance of the lithium excess as well as related composite cathode materials. The models of the composite materials will result in prediction of voltage profiles and structural stability—the ultimate goal being to suggest improvements based on the fundamental understanding that will increase the life and safety of these materials. The Materials Project aspect of the work will result in improved data and electrode properties being calculated to aid predictions of new materials for target chemistries relevant for ongoing BMR experimental research.

Out-Year Goals. During years one and two, the bulk phase diagram will be established, including bulk defect phases in layered Li_2MnO_3 , layered LiMO_2 ($M = \text{Co}, \text{Ni}, \text{and Mn}$), and LiMn_2O_4 spinel to map out the stable defect intermediate phases as a function of possible TM rearrangements. Modeling of defect materials (mainly Li_2MnO_3) under stress/strain will be undertaken to simulate effect of composite nano-domains. The composite voltage profiles as function of structural change and lithium content will be obtained. In years two to four, the project will focus on obtaining lithium activation barriers for the most favorable TM migration paths as a function of lithium content, as well as electronic density of states (DOS) as a function of lithium content for the most stable defect structures identified in years one to two. Furthermore, stable crystal facets of the layered and spinel phases will be explored, as a function of O_2 release from surface and oxygen chemical potential. Within the project, hundreds of novel lithium intercalation materials will be calculated and made available.

Collaborations. This project engages in collaboration with Gerbrand Ceder (MIT), Clare Grey (Cambridge, UK), Mike Thackeray (ANL), and Guoying Chen (LBNL).

Milestones

1. Mn mobilities as a function of lithium content in layered Li_xMnO_3 and related defect spinel and layered phases. (March 2015 – Complete)
2. Surface facets calculated and validated for Li_2MnO_3 . (March 2016 – Complete)
3. Calculate stable crystal facets. Determine whether facet stabilization is possible through morphology tuning. (March 2016 – Complete)
4. *Go/No-Go*: Stop this approach if facet stabilization cannot be achieved. (May 2016 – Complete)
5. Lithium mobilities as a function of lithium content in layered Li_xMnO_3 and related defect spinel and layered phases. (September 2015 – Complete)

Progress Report

This project is focusing the final effort on the study of surface stability of the Li-excess layered materials using first-principles calculations. It systematically investigated all possible low Miller index surface facets of Li_2MnO_3 as a function of surface direction and termination. The Li_2MnO_3 surfaces can be organized into three surface groups with respect to the relation between their normal direction and the Li/Mn stacking direction. Using the slab-vacuum model, the calculated surface energies are summarized in Table 3.

In contrast with layered LiCoO_2 , the Li_2MnO_3 surfaces exhibit complicated cation mixing due to the excess lithium ion in the TM layers. Thus, the low Miller index surfaces of Li_2MnO_3 have 7 distinguishable facets that can be organized by means of the atomic configuration and crystal symmetry. All 7 surfaces are inevitably terminated with Li-cations (see Figure 51b). Specifically, the surface can be parallel (Figure 51c), perpendicular (Figure 51d), or at a slanted angle (Figure 51e) with respect to the Li/Mn stacking direction. The parallel group has one surface (001), the perpendicular group has three surfaces [(010), (100), and (110)], and finally the slanted angle group contains three surfaces [(011), (101), and (111)]. Additionally, all surfaces and their terminations can be classified according to the Tasker's criteria. Due to Tasker's classification, one surface exhibits Tasker type I (101), which is laminated with the single neutral layers. Two surfaces exhibit Tasker type II [(010) and (111)], which contains two different laminations with a periodicity of three. Finally, three surfaces exhibit Tasker type III [(001), (100), (110), and (011)], which has two lamination layers. The surface group, Tasker classifications, and surface energies are summarized in Table 3. The calculations show that the (001) and (010) surfaces are energetically favorable facets of Li_2MnO_3 , which is consistent with experimental observations. Due to its direction, the (011) surface is not favorable in the Wulff construction.

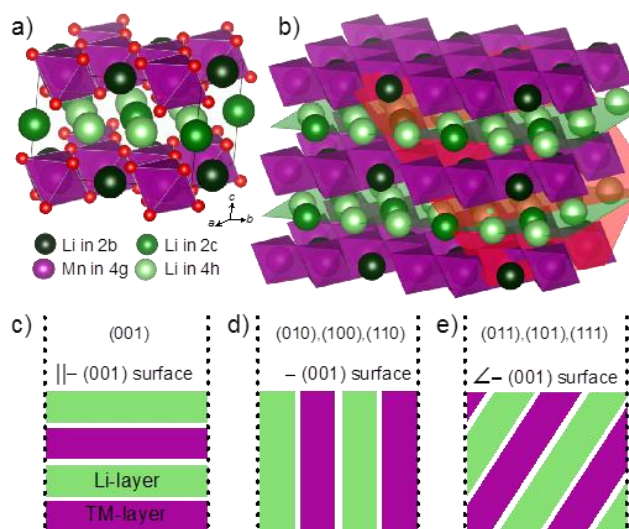


Figure 51. Illustrations of the Li_2MnO_3 bulk as well as surface planes. The figures present (a) the conventional unit cell structure and (b) the schematics of an arbitrary facet (red plane). (c-e) The three possible surface groups with respect to the relation between their normal direction and the Li/Mn stacking direction (001).

Table 3. The calculated surface energies of all low Miller index facets denominated by their termination and Tasker type.

Surface Group	Facet	Tasker	γ (J/m^2)
Parallel	001	III	0.98
Perpendicular	010	II	1.27
	100	III	1.30
	110	III	1.37
Slanted angle	011	III	1.17
	101	I	1.50
	111	II	1.23

Patents/Publications/Presentations

Publication

- Shin, Yongwoo, and Kristin A. Persson. “Surface Morphology and Surface Stability against Oxygen Loss of the Li-excess Li_2MnO_3 Cathode Material as a function of Li Concentration.” Submitted, 2016.

Task 6.3 – First Principles Calculations of Existing and Novel Electrode Materials (Gerbrand Ceder, MIT)

Project Objective. Identify the structure of layered cathodes that leads to high capacity. Clarify the role of the initial structure as well as structural changes upon first charge and discharge. Give insight into the role of lithium excess and develop methods to predict ion migration in layered cathodes upon cycling and during overcharge. Develop predictive modeling of oxygen charge transfer and oxygen loss. Give insight into the factors that control the capacity and rate of Na-intercalation electrodes, as well as Na-vacancy ordering. Develop very high-capacity layered cathodes with high structural stability (> 250 mAh/g).

Project Impact. The project will lead to insight in how lithium excess materials work and ultimately to higher capacity cathode materials for Li-ion batteries. The project will help in the design of high-capacity cathode materials that are tolerant to TM migration.

Out-Year Goals. The out-year goals are as follows:

- Higher capacity Li-ion cathode materials
- Novel chemistries for higher energy density storage devices
- Guidance for the field in search for higher energy density Li-ion materials

Collaborations. This project collaborates with K. Persson (LBNL) and C. Grey (Cambridge).

Milestones

1. Model to predict compositions that will disorder as synthesized. (December 2015 – Complete)
2. At least one Ti-based compound with high capacity. (March 2016 – Complete)
3. Predictive model for the voltage curve (slope) of cation-disordered materials. (June 2016 – Complete)
4. Modeling capability for materials with substantial oxygen redox capability. (September 2016)

Progress Report

Cathode materials based on cation-disordered lithium TM oxides have recently been demonstrated to deliver high capacities and sustain efficient lithium transport, provided an excess of at least 10% of lithium compared to the TM concentration. Since the energy density is the product of capacity and voltage, an understanding of the effect of cation disorder on the voltage is crucial for the design of novel high-energy-density cathodes. The project has previously investigated how cation disorder affects the average lithium intercalation voltage in LiTMO_2 , and the results show that Li-TM disorder can either increase or reduce the TM redox voltage depending on the TM species.^[1] However, cation disorder not only modulates the average voltage but also the slope of the voltage profiles. Large voltage slopes are generally undesirable, as they could lead to inaccessible capacity at the end of charge.

In the layered ($\alpha\text{-NaFeO}_2$) structure all lithium sites are equivalent, and the cations are arranged such that every lithium site is surrounded by exactly 6 TM sites and 6 lithium sites. In contrast, in cation-disordered structures a distribution of local environments around lithium sites exists, so that the energies of the lithium sites vary. This effect necessarily leads to an additional slope in the voltage profile. Figure 52 shows the distribution of Li-site environments in a disordered structure with ideal random cation arrangement. Apart from the slope due to non-equivalent lithium sites, cation disorder may also result in the stabilization of tetrahedral lithium sites at the top of charge, which gives rise to an additional step in the voltage profile. Tetrahedral sites that are not coordinated by TM ions (0-TM sites) become stable for lithium when 3 of the surrounding 4 lithium atoms are extracted. Such 0-TM sites are not present in the layered structure, but may be created by cation disorder. To investigate to which extent the voltage slope and the stabilization of tetrahedral lithium depends on the TM species, the project employed Monte-Carlo simulations using first-principles based lattice model Hamiltonians.

The results from the calculations are shown in Figure 53. As seen in the figure, the voltage slope owing to nonequivalent lithium sites leads to a voltage spread between 1 V (LiFeO_2) and 3.5 V (LiTiO_2) depending on the TM species (red bars in Figure 53). The voltage slope for the early TMs Ti, V, and Cr is significantly larger than the slope predicted for the later TMs, as the strong TM-O hybridization in the LiTMO_2 of the later TMs effectively shields the Li-TM interaction in these structures, so that the energy of the lithium sites becomes less sensitive with respect to their local TM environment. In comparison to the Li-site energy contribution, the voltage spread owing to tetrahedral lithium (blue bars) is with 0.2-0.4 V much smaller.

[1] Abdellahi, A., et al. *Chem. Mater.* 28 (2016): 3659-3665.

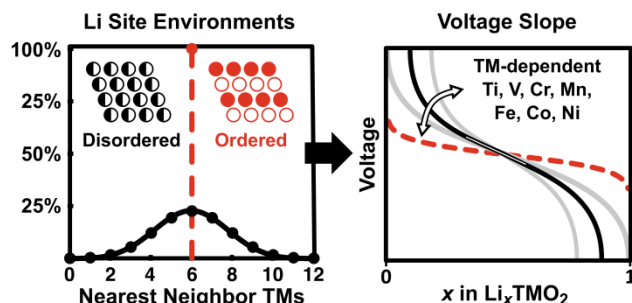


Figure 52. Unlike in the layered structure, lithium sites in cation-disordered structures are not equivalent. The spread of lithium site energies manifests itself as additional slope in the voltage profile.

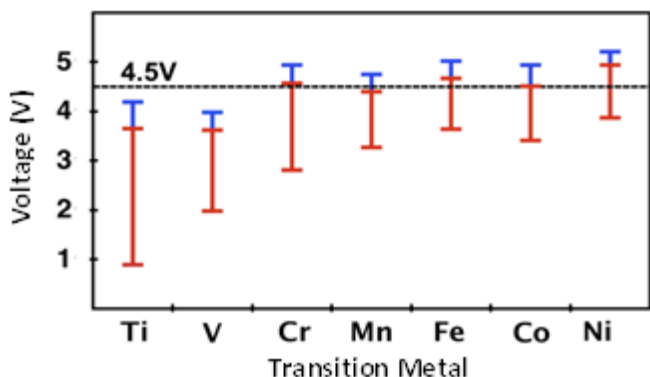


Figure 53. Calculated voltage range owing to non-equivalent lithium sites (red) and tetrahedral lithium (blue) for the lithium transition-metal oxides of the first-row transition metals. The dashed line indicates a voltage of 4.5 V as a guideline for the stability limit of conventional liquid electrolytes.

Task 6.4 – First Principles Modeling of SEI Formation on Bare and Surface/Additive Modified Silicon Anode (Perla Balbuena, Texas A&M University)

Project Objective. This project aims to develop fundamental understanding of the molecular processes that lead to the formation of a SEI layer due to electrolyte decomposition on Si anodes, and to use such new knowledge in a rational selection of additives and/or coatings. The focus is on SEI layer formation and evolution during cycling and subsequent effects on capacity fade through two concatenated problems: (1) SEI layers formed on lithiated silicon surfaces, and (2) SEI layers formed on coated surfaces. Key issues being addressed include the dynamic evolution of the system and electron transfer through solid-liquid interfaces.

Project Impact. Finding the correspondence between electrolyte molecular properties and SEI formation mechanism, structure, and properties will allow the identification of new/improved additives. Studies of SEI layer formation on modified surfaces will allow the identification of effective coatings able to overcome the intrinsic deficiencies of SEI layers on bare surfaces.

Approach. Investigating the SEI layer formed on modified silicon surfaces involves analysis of the interfacial structure and properties of specific coating(s) deposited over the silicon anode surface, characterization of the corresponding surface properties before and after lithiation, especially how such modified surfaces may interact with electrolyte systems (solvent/salt/additive), and what SEI layer structure, composition, and properties may result from such interaction. This study will allow identification of effective additives and coatings able to overcome the intrinsic deficiencies of SEI layers on bare surfaces. Once the SEI layer is formed on bare or modified surfaces, it is exposed to cycling effects that influence its overall structure (including the anode), chemical, and mechanical stability.

Out-Year Goals. Elucidating SEI nucleation and electron transfer mechanisms leading to growth processes using a molecular level approach will help establish their relationship with capacity fading, which will lead to revisiting additive and/or coating design.

Collaborations. Work with Chunmei Ban (NREL) consists in modeling the deposition-reaction of alucone coating on silicon surfaces and their reactivity. Reduction of solvents and additives on silicon surfaces were studied in collaboration with K. Leung and S. Rempe, from SNL. Collaborations with Professor Jorge Seminario (Texas A&M University, TAMU) on electron and ion transfer reactions, and Dr. Partha Mukherjee (TAMU) focusing on the development of a multi-scale model to describe the SEI growth on silicon anodes.

Milestones

1. Identify SEI nucleation and growth on silicon surfaces modified by deposition of alucone coatings as a function of degree of lithiation of the film. (December 2015 – Complete)
2. Quantify chemical and electrochemical stability of various SEI components: competition among polymerization, aggregation, and dissolution reactions. Evaluate voltage effects on SEI products stability. (March 2016 – Complete)
3. Identify alternative candidate electrolyte and coating formulations. (June 2016 – In progress)
4. *Go/No-Go*: Test potential candidate electrolyte and coating formulations using coarse-grained model and experimentally via collaborations. (September 2016)

Progress Report

Alternative Electrolytes. A systematic procedure has been implemented to determine potential solvent, salt, and additive candidates that may favor a stable SEI on lithiated silicon anodes. Based on the demonstrated good properties of FEC on silicon anodes, the work has been focused on the effect of fluorinated additives resulting from modifications of FEC, such as trifluoropropylene carbonate (TFPC) and trifluoroethyl ethyl carbonate (TFEEC). *Ab initio* molecular dynamics (AIMD) simulations were carried out on a lithiated silicon slab model surface in contact with an electrolyte phase containing the tested additive (solvent) + salt (LiPF_6). The following aspects were examined: (a) salt solvation by candidate additive, and its effect on salt dissociation/decomposition; (b) initial SEI reactions and subsequent SEI products; (c) effect of additive concentration on the previous issues; and (d) electrochemical stability of the SEI products. The main preliminary conclusions are:

- Solvation properties and steric constraints determine a very different pattern of SEI reactions for each molecule: TFPC results in intermediate products that lead to Li_2O and has a faster decomposition than the salt, whereas TFEEC favors salt anion decomposition first (leading to LiF) and later solvent decomposition yielding Li_2O .
- In both cases the formation of fluorinated polymers is expected since the CF_3 group remains intact in one of the radical anion products. Current efforts focus on refining these conclusions and examining the product stabilities. This systematic analysis is expected to lead to guidelines for electrolyte selection.

Electron Transfer through SEI Layer. Two different approaches are being pursued to investigate electron transfer through the SEI layer. (a) Seminario's group (TAMU) employing density functional theory (DFT) – Green's function theories determined electron leakage in selected finite models of materials formed at the

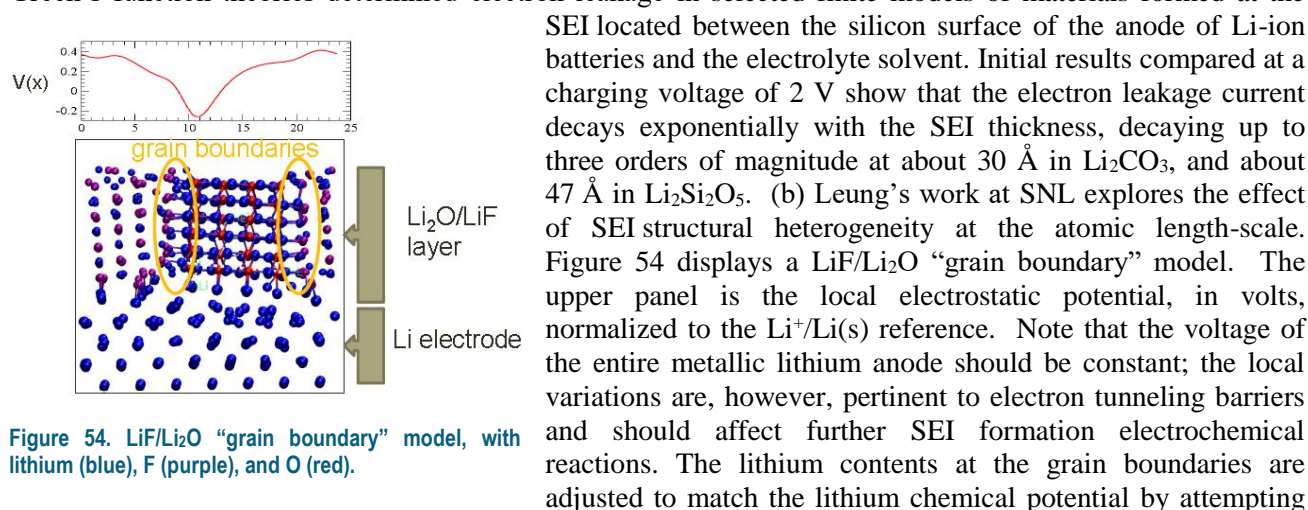


Figure 54. $\text{LiF/Li}_2\text{O}$ “grain boundary” model, with lithium (blue), F (purple), and O (red).

SEI located between the silicon surface of the anode of Li-ion batteries and the electrolyte solvent. Initial results compared at a charging voltage of 2 V show that the electron leakage current decays exponentially with the SEI thickness, decaying up to three orders of magnitude at about 30 Å in Li_2CO_3 , and about 47 Å in $\text{Li}_2\text{Si}_2\text{O}_5$. (b) Leung's work at SNL explores the effect of SEI structural heterogeneity at the atomic length-scale. Figure 54 displays a $\text{LiF/Li}_2\text{O}$ “grain boundary” model. The upper panel is the local electrostatic potential, in volts, normalized to the $\text{Li}^+/\text{Li(s)}$ reference. Note that the voltage of the entire metallic lithium anode should be constant; the local variations are, however, pertinent to electron tunneling barriers and should affect further SEI formation electrochemical reactions. The lithium contents at the grain boundaries are adjusted to match the lithium chemical potential by attempting

to introduce lithium vacancies and interstitials. The overall Fermi level of the $\text{Li}_2\text{O/LiF}$ -coated Li-metal anode model is roughly 0.1 V versus the $\text{Li}^+/\text{Li(s)}$ reference. However, the local electrostatic potential ($V(x)$) far from the coated lithium surface, averaged along the grain boundary direction and referenced to $\text{Li}^+/\text{Li(s)}$, reveals more interesting physics. $V(x)$ can be thought of as a “local voltage,” has a variation of ~0.6 V, with its lowest value at one of the two “grain boundaries.” Electrolyte and even SEI decomposition are expected to be enhanced at such low $V(x)$ regions where the electron tunneling barrier from the anode surface should be the lowest.

distribution. Based on these findings, the group is analyzing the energy wells in which Li^+ resides and characterizing them at different temperatures. Next quarter, the SEI and bulk electrolyte models will be coupled to investigate the influence of interfacial structure on Li^+ ion transfer.

Patents/Publications/Presentations

Publications

- Perez-Beltrán, S., and G. E. Ramirez-Caballero and P. B. Balbuena. “First Principles Calculations of Lithiation of a Hydroxylated Surface of Amorphous Silicon Dioxide.” *J. Phys. Chem. C* 119 (2015): 16424-16431.
- Ma, Y., and J. M. Martinez de la Hoz, I. Angarita, J. M. Berrio-Sanchez, L. Benitez, J. M. Seminario, S.-B. Son, S.-H. Lee, S. M. George, C. M. Ban, and P. B. Balbuena. “Structure and Reactivity of Alucone-Coated Films on Si and Li_xSi_y Surfaces.” *ACS Appl. Mater. Inter.* 7 (2015): 11948-11955.
- Martinez de la Hoz, J. M., and F. A. Soto and P. B. Balbuena. “Effect of the Electrolyte Composition on SEI Reactions at Si Anodes of Li-ion Batteries.” *J. Phys. Chem. C* 119 (2015): 7060-7068. doi: 10.1021/acs.jpcc.5b01228
- Soto, F. A., and Y. Ma, J. M. Martinez de la Hoz, J. M. Seminario, and P. B. Balbuena. “Formation and Growth Mechanisms of Solid-Electrolyte Interphase Layers in Rechargeable Batteries.” *Chem. Mater.* 27, no. 23 (2015): 7990-8000.
- You, X., and M. I. Chaudhari, S. B. Rempe, and L. R. Pratt. “Dielectric Relaxation of Ethylene Carbonate and Propylene Carbonate from Molecular Dynamics Simulations.” *J. Phys. Chem. B*. doi: 10.1021/acs.jpcb.5b09561
- Leung, K., and F. A. Soto, K. Hankins, P. B. Balbuena, and K. L. Harrison. “Stability of Solid Electrolyte Interphase Components on Reactive Anode Surfaces.” *J. Phys. Chem. C* 120 (2016): 6302-6313.
- Kumar, N., and J. M. Seminario. “Lithium-Ion Model Behavior in an Ethylene Carbonate Electrolyte Using Molecular Dynamics.” *J. Phys. Chem. C*, in press.

Task 6.5 – A Combined Experimental and Modeling Approach for the Design of High Current Efficiency Silicon Electrodes (Xingcheng Xiao, General Motors; Yue Qi, Michigan State University)

Project Objective. The use of high-capacity, Si-based electrode has been hampered by its mechanical degradation due to large volume expansion/contraction during cycling. Nanostructured silicon can effectively avoid silicon cracking/fracture. Unfortunately, the high surface to volume ratio in nanostructures leads to an amount of SEI formation and growth, and thereby low current/Coulombic efficiency and short life. Based on mechanics models, the project demonstrates that the artificial SEI coating can be mechanically stable despite the volume change in silicon, if the material properties, thickness of SEI, and the size/shape of silicon are optimized. Therefore, the project objective is to develop an integrated modeling and experimental approach to understand, design, and make coated silicon anode structures with high current efficiency and stability.

Project Impact. The validated model will ultimately be used to guide the synthesis of surface coatings and the optimization of silicon size/geometry that can mitigate SEI breakdown. The optimized structures will eventually enable a negative electrode with a 10x improvement in capacity (compared to graphite), while providing > 99.99% Coulombic efficiency; this could significantly improve the energy/power density of current Li-ion batteries.

Out-Year Goals. The out-year goal is to develop a well validated mechanics model that directly imports material properties either measured from experiments or computed from atomic simulations. The predicted SEI induced stress evolution and other critical phenomena will be validated against *in situ* experiments in a simplified thin-film system. This comparison will also allow fundamental understanding of the mechanical and chemical stability of artificial SEI in electrochemical environments and the correlation between the Coulombic efficiency and the dynamic process of SEI evolution. Thus, the size and geometry of coated silicon nanostructures can be optimized to mitigate SEI breakdown, providing high current efficiency.

Collaborations. This project engages in collaboration with LBNL, PNNL, and NREL.

Milestones

1. Identify critical mechanical and electrochemical properties of the SEI coating that can enable high current efficiency. (December 2015 – Complete)
2. Design a practically useful silicon electrode where degradation of the SEI layer is minimized during lithiation and delithiation. (March 2016 – Complete)
3. Construct an artificial SEI design map for silicon electrodes, based on critical mechanical and transport properties of desirable SEI for a given silicon architecture. (June 2016 – Complete)
4. Validated design guidance on how to combine the SEI coating with a variety of silicon nano/microstructures. *Go/No-Go*: Decision based on whether the modeling guided electrode design can lead to high Coulombic efficiency > 99.9%. (September 2016 – In progress)

Progress Report

Lithium Trapping on Delithiation Causing Irreversible Capacity Loss. A continuous delithiation algorithm using ReaxFF-based molecular dynamics (MD) simulations and implemented different delithiation rates to study the delithiation mechanism regarding the lithium trapping phenomena. On fast delithiation, insufficient time is allowed for lithium to diffuse from the $a\text{-Li}_x\text{Si}$ core to the oxide coating layer. Therefore, lithium near the surface are only allowed to diffuse out, whereas the movement of the lithium near the center of the $a\text{-Li}_x\text{Si}$ core is limited, generating a lithium concentration gradient that is characterized by low lithium concentration near the surface and high lithium concentration near the center, as shown in Figure 55d. Since lithium diffusivity in the silicon is concentration dependent, where increasing lithium concentration results in faster lithium diffusion, lithium diffusivity at the surface becomes slow, hindering the movement of the lithium near the surface; this results in significant amount of lithium trapped during the fast delithiation. In contrast, during slow delithiation, the lithium are allowed to diffuse out with nearly constant concentration throughout the delithiation process, which allows the lithium to continuously diffuse out until the final delithiation stage. Since the number of available lithium is directly related to the capacity, trapping of significant amount of lithium in the delithiated $a\text{-Li}_x\text{Si}$ on fast delithiation results in irreversible capacity loss.

A Phase Diagram for the Mechanical Stability of Silicon Islands on Cycling. The islands used in the experiments, with a thickness of 225 nm and a length of 15 μm , were predicted to be partially delaminated from the current collectors. This is consistent with the experimental observation that only the external Si/Cu interface debonded, while the internal interface remained adhered to the current collector. With the island thickness and length cautiously chosen, a partially delaminated, but stable, silicon island can be intentionally created, providing an ideal platform to probe the failure mechanisms with the layer on the top of the silicon island.

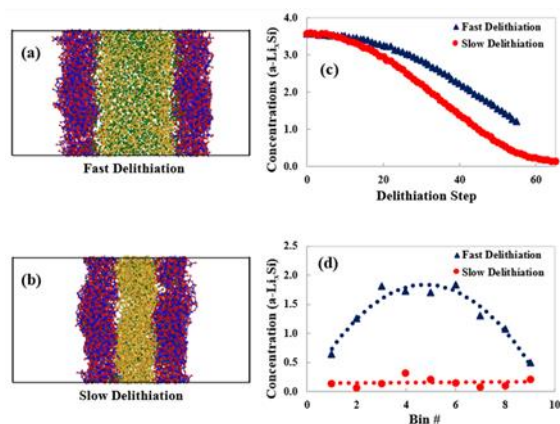


Figure 55. Structural snapshots at the final delithiation stage of (a) fast and (b) slow rates. (c) Lithium concentration change upon delithiation. (d) The concentration profile of $a\text{-Li}_x\text{Si}$ core at the final delithiation stage.

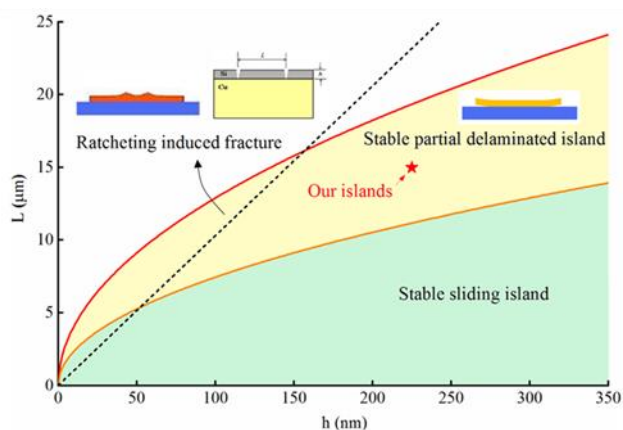


Figure 56. Phase diagram of failure modes of silicon thin-film islands on cycling.

Patents/Publications/Presentations**Presentations**

- Society of Vacuum Coaters 59th Annual Technical Conference, Indianapolis, Indiana (May 9-13, 2016): “Surface Engineering for Electrochemical Energy Storage – Challenges and Opportunities”; Yang-Tse Cheng.
- 229th ECS Meeting, San Diego, California (May 2016): “Computational Design of Coatings, Interfaces, and Nano-structures for Si-based Electrodes”; Yue Qi, Sung Yup Kim, and Kwang Jin Kim.
- International Meeting of Lithium Batteries (IMLB), Chicago, Illinois (June 23, 2016): “Synergetic Effects of Inorganic Components in Solid Electrolyte Interphase on High Cycle Efficiency of Lithium Ion Batteries”; Xingcheng Xiao.
- International Workshop on Cutting-edge Problems on Chemomechanics, Xi’an Jiaotong University, Xi’an, China (June 27, 2016): “Investigating Mechanical Degradation Mechanisms in Silicon Electrodes for Lithium Ion Batteries: A Thin Film Approach”; Huajian Gao. Invited.

Task 6.6 – Predicting Microstructure and Performance for Optimal Cell Fabrication (Dean Wheeler and Brian Mazzeo, Brigham Young University)

Project Objective. This work uses microstructural modeling coupled with extensive experimental validation and diagnostics to understand and optimize fabrication processes for composite particle-based electrodes. The first main outcome will be revolutionary methods to assess electronic and ionic conductivities of porous electrodes attached to current collectors, including heterogeneities and anisotropic effects. The second main outcome is a particle-dynamics model parameterized with fundamental physical properties that can predict electrode morphology and transport pathways resulting from particular fabrication steps. These two outcomes will enable the third, which is an understanding of the effects of processing conditions on microscopic and macroscopic properties of electrodes.

Project Impact. This work will result in new diagnostic tools for rapidly and conveniently interrogating electronic and ionic pathways in porous electrodes. A new mesoscale 3D microstructure prediction model, validated by experimental structures and electrode-performance metrics, will be developed. The model will enable virtual exploration of process improvements that currently can only be explored empirically.

Out-Year Goals. This project was initiated April 2013 and concludes March 2017. Goals by fiscal year are as follows.

- 2013: Fabricate first-generation micro-four-line probe, and complete associated computer model.
- 2014: Assess conductivity variability in electrodes; characterize microstructures of multiple electrodes.
- 2015: Fabricate first-gen ionic conductivity probe, N-line probe, and dynamic particle packing (DPP) model.
- 2016: Improve robustness of N-line probe and DPP model; assess structure correlation to conductivity.
- 2017: Using model and probe, evaluate effect of processing conditions.

Collaborations. Bryant Polzin (ANL) and Karim Zaghib (HQ) provided battery materials. Transfer of technology to A123 to improve their electrode production process took place in FY15. There are ongoing collaborations with Simon Thiele (IMTEK, University of Freiburg) and Mårten Behm (KTH, Sweden).

Milestones

1. Demonstrate that the DPP model can accurately imitate the mechanical calendering process for a representative electrode film. (December 2015 – Complete)
2. Develop a robust numerical routine for interpreting N-line conductivity measurements. (March 2016 – Complete)
3. *Go/No-Go:* Continue work on N-line probe and inversion routine if they can accurately determine anisotropic conductivity for test materials. (June 2016 – Partially complete)
4. *Go/No-Go:* Demonstrate correlations between DPP modeled conductivities and those determined by FIB/SEM and N-line probe. (September 2016 – Ongoing)

Progress Report

Milestone 3 Go/No-Go. A major accomplishment of this project is to show that the micro-N-line probe is a reliable and rapid means of measuring electronic conductivity of electrode materials in a nondestructive manner. It has also been shown to allow researchers to determine the amount of heterogeneity in conductivity across the electrode film, that is, to make a conductivity map. However, one final unmet goal of this work has been to assess the degree of anisotropy, meaning the difference in electronic conductivity in the in-plane and through-plane directions. It is believed that the through-plane conductivity is generally less than the in-plane conductivity by a factor of around 2, though this will depend on many factors including fabrication conditions and the shape of the active material particles. This anisotropy represents an inefficiency in the structure of typical electrodes, because higher through-plane conductivity is more desirable for battery performance.

The second milestone for FY 2016 was to generate an improved numerical inversion routine for inverting N-line conductivity measurements. That milestone, which was completed, was in preparation for the third milestone, which was to continue work on the N-line probe and inversion routine to verify that anisotropic conductivity can be measured for test materials. This third milestone is partially complete, and will be completed and reported by the end of the fourth quarter. At that point a Go/No-Go decision can be made on how suited the method is for determining anisotropic properties.

The current conductivity probe contains 6 parallel lines that contact the electrode sample. A suite of 12 unique experiments was developed that can be performed by passing current and measuring voltage differences through different combinations of lines. When the experiments are analyzed as a set, they should contain sufficient information to determine the anisotropic conductivity, in theory. Unfortunately, the interpreted results are quite sensitive to the degree of uncertainty in the electrical measurements. In other words, anisotropic measurements require a higher level of accuracy than previous measurements. Two strategies to solve this problem were begun and will conclude in the fourth quarter:

- Alter the method of analyzing the experiments so that that results are less sensitive to measurement variations that are caused by variable contact resistance between the probe and the sample surface.
- Alter the method of measuring electrical data to increase the reliability of results to refine the method to improve the performance.

Though unrelated to the present milestone, a significant breakthrough was achieved this quarter toward conveniently measuring ionic conductivity of electrodes. The method was used to measure a series of commercial electrodes provided by a major battery vendor. This improved method will likewise be further developed during the next few months and will be discussed in the final report for this project. The combination of electronic and ionic conductivity measurements made possible by this work provides a more complete picture of electrode performance.

TASK 7 – METALLIC LITHIUM AND SOLID ELECTROLYTES

Summary and Highlights

The use of a metallic lithium anode is required for advanced battery chemistries like Li-air and Li-S to realize dramatic improvements in energy density, vehicle range, cost economy, and safety. However, the use of metallic lithium with liquid and polymer electrolytes has been so far limited due to parasitic SEI reactions and dendrite formation. Adding excess lithium to compensate for such losses effectively negates the high energy density for lithium in the first place. For a long lifetime and safe anode, it is essential that no lithium capacity is lost to physical isolation from roughening, to dendrites or delamination processes, or to chemical isolation from side reactions. The key risk and current limitation for this technology is the gradual loss of lithium over the cycle life of the battery.

To date there are no examples of battery materials and architectures that realize such highly efficient cycling of metallic lithium anodes for a lifetime of 1000 cycles due to degradation of the Li-electrolyte interface. A much deeper analysis of the degradation processes is needed, so that materials can be engineered to fulfill the target level of performance for EV, namely 1000 cycles and a 15-year lifetime, with adequate pulse power. Projecting the performance required in terms of just the lithium anode, this requires a high rate of lithium deposition and stripping reactions, specifically about 40 μm Li per cycle, with pulse rates up to 10 and 20 nm/s (15 mA/cm²) charge and discharge, respectively. This is a conservative estimate, yet daunting in the total mass and rate of material transport. While such cycling has been achieved for state-of-the-art batteries using *molten* sodium in Na-S and zebra cells, solid sodium and lithium anodes are proving more difficult.

The efficient and safe use of metallic lithium for rechargeable batteries is then a great challenge, and one that has eluded research and development efforts for years. BMR Task 7 takes a broad look at this challenge for both solid state batteries and batteries continuing to use liquid electrolytes. Four of the projects are new endeavors; two are ongoing. For the liquid electrolyte batteries, PNNL researchers are examining the use of cesium salts and organic additives to the typical organic carbonate electrolytes to impede dendrite formation at both the lithium and graphite anodes. If successful, this is the simplest approach to implement. At Stanford, novel coatings of carbon and boron nitride with a 3D structure are applied to the lithium surface and appear to suppress roughening and lengthen cycle life. A relatively new family of solid electrolytes with a garnet crystal structure shows superionic conductivity and good electrochemical stability. Four programs chose this family of solid electrolytes for investigation. Aspects of the processing of this ceramic garnet electrolyte are addressed at the University of Maryland and at the University of Michigan (UM), with attention to effect of flaws and composition. Computational models will complement their experiments to better understand interfaces and reduce the electrode area specific resistance (ASR). At ORNL, composite electrolytes composed of ceramic and polymer phases are being investigated, anticipating that the mixed phase structures may provide additional means to adjust the mechanical and transport properties. The last project takes on the challenge to use nano-indentation methods to measure the mechanical properties of the solid electrolyte, the Li-metal anode, and the interface of an active electrode. Each of these projects involves a collaborative team of experts with the skills needed to address the challenging materials studies of this dynamic electrochemical system.

Highlights. The highlights for this quarter are as follows:

- Demonstrated a method to correct the apparent elastic modulus of lithium, measured by indentation, for the effect of a stiff substrate; this is applicable and necessary for lithium films on a ceramic solid electrolyte. (7.1)
- A self-supporting ceramic-polymer electrolyte membrane was spray formed and determined to be stable with lithium metal. (7.3)

- Modeling identified surface coatings likely to stabilize the LLZO garnet – LiCoO₂ interface. (7.4)
- The reaction of lithium with graphene oxide films was studied, including the spark reaction accompanying the formation of H₂ and reaction with trace oxygen. (7.5)
- A new, and as yet unidentified, electrolyte additive improved the cycling stability of Li|| NMC half cells to achieve > 200 cycles at 1mA cm⁻². (7.6)

Task 7.1 – Mechanical Properties at the Protected Lithium Interface (Nancy Dudney, ORNL; Erik Herbert, Michigan Technological U; Jeff Sakamoto UM)

Project Objective. This project will develop understanding of the Li-metal SEI through state-of-the-art mechanical nano-indentation methods coupled with solid electrolyte fabrication and electrochemical cycling. The goal is to provide the critical information that will enable transformative insights into the complex coupling between the microstructure, its defects, and the mechanical behavior of Li-metal anodes.

Project Impact. Instability and/or high resistance at the interface of lithium metal with various solid electrolytes limit the use of the metallic anode for batteries with high-energy density batteries, such as Li-air and Li-S. The critical impact of this endeavor will be a much deeper analysis of the degradation, so that materials can be engineered to fulfill the target level of performance for EV batteries, namely 1000 cycles and a 15-year lifetime, with adequate pulse power.

Approach. Mechanical properties studies through state-of-the-art nano-indentation techniques will be used to probe the surface properties of the solid electrolyte and the changes to the lithium that result from prolonged electrodeposition and dissolution at the interface. An understanding of the degradation processes will guide future electrolyte and anode designs for robust performance. In the first year, the team will address the two critical and poorly understood aspects of the protected Li-metal anode assembly: (1) the mechanical properties of the solid electrolyte and (2) the morphology of the cycled lithium metal.

Out-Year Goals. Work will progress toward study of the electrode assembly during electrochemical cycling of the anode. This project hopes to capture the formation and annealing of vacancies and other defects in the lithium and correlate this with the properties of the solid electrolyte and the interface.

Collaborations. This project funds work at ORNL, Michigan Technological University (MTU), and UM. Asma Sharafi (UM, Ph. D. student) and Dr. Robert Schmidt (UM) also contribute to the project. Steve Visco (PolyPlus) will serve as a technical advisor.

Milestones

1. Determine elastic properties of battery grade lithium from different sources and preparation, comparing to values from the reference literature. (September 2015 – Complete)
2. Compare lithium properties, uncycled versus cycled, using thin-film battery architecture. (June 2016 – Partially complete. This will use a ceramic electrolyte pellet rather than thin-film battery to address a larger and more relevant lithium transport per area.)
3. View annealing of defects following a single stripping and plating half cycle, using thin-film battery architecture. (September 2016 – On schedule. This will also use an electrolyte pellet rather than thin-film battery.)

Progress Report

The project continues to refine the approach for extracting relevant mechanical properties of vapor deposited lithium films by nanoindentation. Shown in Figure 57 is an array of indents into a clean lithium film, 5 μm thick, on a glass ($E_{\text{glass}} = 69 \text{ GPa}$) substrate. Grain size for lithium varies from about 5-30 μm , with a clear variation in the surface contrast from grain to grain. So far, different grains and grain boundary regions are not distinguishable. Because the film is thin relative to the grain size, it is likely to be only one grain thick, but this needs to be verified. The project is experimenting with means to passivate the film surface with a dose of CO_2 , but so far better results are obtained for the “cleaner” surfaces (as in Figure 57) without deliberate passivation. Unfortunately, a reliably clean surface is hard to reproduce and protect. Results from the initial indentation to a depth of $\sim 200 \text{ nm}$ will be disregarded in most cases because of surface contamination.

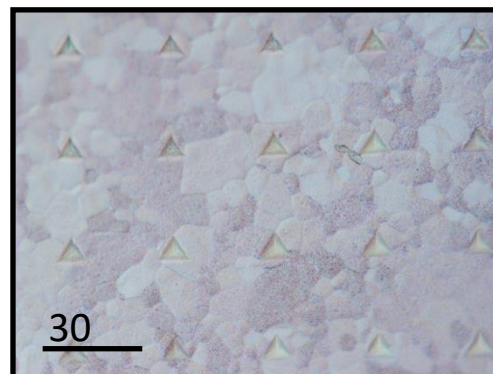


Figure 57. Micrograph of lithium surface showing part of the indentation array. This surface was not exposed to dose of CO_2 . Bar is 30 μm .

Figure 58 shows a dynamic indentation study where a very small harmonic oscillation is applied to the tip during an exceptionally slow constant strain rate loading and subsequent hold at 1000 nm. Following the model presented in Hay and Crawford, the apparent modulus of the film is nicely corrected for the case of a compliant film on a stiff substrate. This gives a nearly constant modulus independent of the displacement. This method, along with the constant load hold approach described last quarter, will provide the information needed to probe the active lithium near SEI.

Tests using lithium films deposited onto highly polished LLZO disks are underway (replacing the thin film architecture in the milestones). These were prepared with thin (2 μm) Li on one side and thick (8 μm) Li on the other. Prolonged current over 6 days yields 5 μm Li on each side, which is then probed by nanoindentation. The lithium is contacted along the edge to preserve the smooth surface of

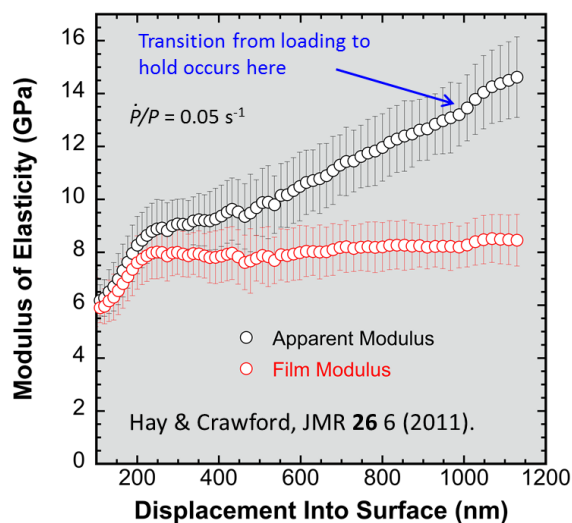


Figure 58. Modulus of lithium film, showing the correction used to account for the stiff glass substrate.

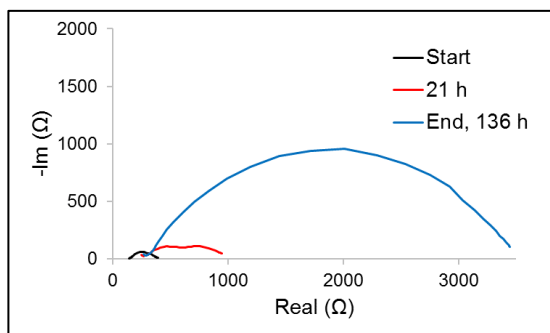


Figure 59. Impedance for Li-LLZO-Li sample before and after passing current in one direction at $\sim 5 \mu\text{A}/\text{cm}^2$.

the lithium, so no stack pressure was applied to the lithium. The indentation will be reported next quarter. Figure 59 shows an example of the change in the sample impedance from the start and after 1 and 6 days of ‘one-way’ lithium transport. Vapor-deposited lithium provides a low interface impedance compared to lithium physically pressed to the LLZO surface. Further tests will identify the particular interface that is becoming resistive, which may be at the LLZO interface or even at the stainless contact to the edge of the lithium film.

Patents/Publications/Presentations

Publication

- Schmidt, Robert D., and Jeffrey Sakamoto, “In-situ Non-destructive Acoustic Characterization of Solid State Electrolyte Cells.” *J. Power Sources* 324 (2016): 126-133.

Presentation

- DOE Annual Merit Review Meeting, Washington, D. C. (June 6-10, 2016): “Mechanical Properties at the Protected Lithium Interface”; Nancy Dudney, Erik Herbert, Jeff Sakamoto, P. S. Phani, R. Schmidt, A. Sharafi, and T. Thompson. Poster.

Task 7.2 – Solid Electrolytes for Solid-State and Lithium–Sulfur Batteries (Jeff Sakamoto, University of Michigan)

Project Objectives. *Enable advanced Li-ion solid-state and lithium-sulfur EV batteries using LLZO solid-electrolyte membrane technology.* Owing to its combination of fast ion conductivity, stability, and high elastic modulus, LLZO exhibits promise as an advanced solid-state electrolyte. To demonstrate relevance in EV battery technology, several objectives must be met. First, LLZO membranes must withstand current densities approaching $\sim 1 \text{ mA/cm}^2$ (commensurate with EV battery charging and discharging rates). Second, low ASR between lithium and LLZO must be achieved to achieve cell impedance comparable to conventional Li-ion technology ($\sim 10 \text{ Ohms/cm}^2$). Third, low ASR and stability between LLZO and sulfur cathodes must be demonstrated.

Project Impact. The expected outcomes will: (i) enable Li-metal protection, (ii) augment DOE access to fast ion conductors and/or hybrid electrolytes, (iii) mitigate Li-polysulfide dissolution and deleterious passivation of Li-metal anodes, and (iv) prevent dendrite formation. Demonstrating these aspects could enable Li-S batteries with unprecedented end-of-life, cell-level performance: $> 500 \text{ Wh/kg}$, $> 1080 \text{ Wh/l}$, > 1000 cycles, lasting > 15 years.

Approach. This effort will focus on the promising new electrolyte known as LLZO ($\text{Li}_7\text{La}_3\text{Zr}_2\text{O}_{12}$). LLZO is the first bulk-scale ceramic electrolyte to simultaneously exhibit the favorable combination of high conductivity ($\sim 1 \text{ mS/cm}$ at 298K), high shear modulus (61 GPa) to suppress Li-dendrite penetration, and apparent electrochemical stability ($0\text{--}6 \text{ V}$ vs Li/Li^+). While these attributes are encouraging, additional research and development is needed to demonstrate that LLZO can tolerate current densities in excess of 1 mA/cm^2 , thereby establishing its relevance for PHEV/EV applications. This project hypothesizes that defects and the polycrystalline nature of realistic LLZO membranes can limit the critical current density. However, the relative importance of the many possible defect types (porosity, grain boundaries, interfaces, surface and bulk impurities), and the mechanisms by which they impact current density, have not been identified. Using experience with the synthesis and processing of LLZO (Sakamoto and Wolfenstine), combined with sophisticated materials characterization (Nanda), this project will precisely control atomic and microstructural defects and correlate their concentration with the critical current density. These data will inform multi-scale computation models (Siegel and Monroe), which will isolate and quantify the role(s) that each defect plays in controlling the current density. By bridging the knowledge gap between composition, structure, and performance, this project will determine if LLZO can achieve the current densities required for vehicle applications.

Collaborations. This project collaborates with Don Siegel (UM atomistic modeling), Chuck Monroe (UM, continuum scale modeling), Jagjit Nanda (ORNL, sulfur chemical and electrochemical spectroscopy), and Jeff Wolfenstine (ARL, atomic force microscopy of Li-LLZO interfaces).

Milestones

1. Correlate the critical current density based on pore size, volume fraction porosity, and grain size. (Complete)

Progress Report

Correlate the Critical Current Density Based on Pore Size, Volume Fraction Porosity, and Grain Size. This project evaluated the effect of pore size, volume fraction porosity, and grain size on the critical current density (CCD) of LLZO. The LLZO was densified under various conditions, but all consisted of high-phase purity (Figure 60). To correlate the effect of pore size, volume fraction, and grain size on the CCD, dc cycling of Li-LLZO-Li symmetric cells was conducted. The correlation is complete. Based on the outcome of this study, it was determined that two types of defects may control the CCD, atomic and microstructural defects. Future work will focus on controlling these two defects to approach the goal of 1 mA/cm².

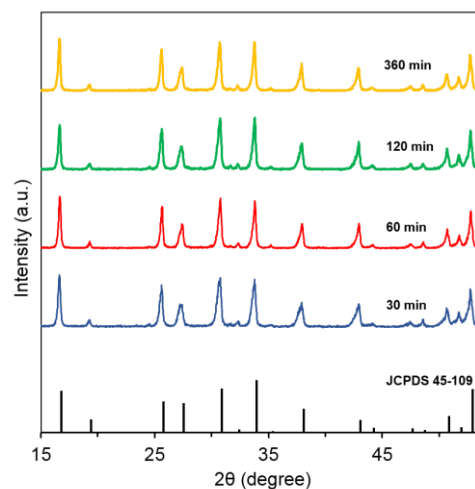


Figure 60. X-ray diffraction patterns of LLZO as a function of densification time.

Patents/Publications/Presentations

Publication

- Kim, Y., and A. Yoo, R. Schmidt, A. Sharafi, H. Lee, J. Wolfenstine, and J. Sakamoto. “Electrochemical stability of $\text{Li}_{6.5}\text{La}_3\text{Zr}_2\text{M}_{0.5}\text{O}_{12}$ ($\text{M} = \text{Nb}$ or Ta) against Metallic Lithium.” *Frontiers in Energy Research, section Energy Storage* (2016).

Presentations

- The Electrochemical Society, San Diego, California (May 29 – June 2, 2016): “Mechanical Stability of Solid Electrolyte Interfaces in Solid-State Batteries”; J. Sakamoto. Invited speaker.
- The Electrochemical Society, San Diego, California (May 29 – June 2, 2016): “Chemical Stability of Garnet Solid-state Electrolyte”; A. Sharafi.
- Beyond Lithium Ion IX, Richland, Washington (May 24-26, 2016): Solid-state Electrolytes Enabling Beyond Li-ion Cell Chemistries”; J. Sakamoto. Invited speaker.
- Beyond Lithium Ion IX, Richland, Washington (May 24-26, 2016): “Correlating the Effects of Air Exposure with Surface Chemistry and the Impedance of the $\text{Li-Li}_7\text{La}_3\text{Zr}_2\text{O}_{12}$ ”; A. Sharafi. Poster.
- Battery Congress, Troy, Michigan (May 16-18, 2016): “Can Solid-state Electrolytes Enable the Next Generation Energy Storage Technologies?”; J. Sakamoto. Invited speaker.
- Advanced Automotive Battery Conference, Detroit, Michigan (June 14-17, 2016): “Solid Electrolytes: An Enabling Technology for Vehicle Electrification”; J. Sakamoto. Invited speaker.

Task 7.3 – Composite Electrolytes to Stabilize Metallic Lithium Anodes (Nancy Dudney and Frank Delnick, Oak Ridge National Laboratory)

Project Objective. Prepare composites of representative polymer and ceramic electrolyte materials to achieve thin membranes that have the unique combination of electrochemical and mechanical properties required to stabilize the metallic lithium anode while providing for good power performance and long cycle life. Understand the Li-ion transport at the interface between polymer and ceramic solid electrolytes, which is critical to the effective conductivity of the composite membrane. Identify key features of the composite composition, architecture, and fabrication that optimize the performance. Fabricate thin electrolyte membranes to use with a thin metallic lithium anode to provide good power performance and long cycle life.

Project Impact. A stable lithium anode is critical to achieve high energy density with excellent safety, lifetime, and cycling efficiency. This study will identify the key design strategies that should be used to prepare composite electrolytes to meet the challenging combination of physical, chemical, and manufacturing requirements to protect and stabilize the Li-metal anode for advanced batteries. By utilizing well characterized and controlled component phases, the design rules developed for the composite structures will be generally applicable toward the substitution of alternative and improved solid electrolyte component phases as they become available. Success in this program will enable these specific DOE technical targets: 500-700 Wh/kg, 3000-5000 deep discharge cycles, and robust operation.

Approach. This project seeks to develop practical solid electrolytes that will provide stable and long-lived protection for the Li-metal anode. Current electrolytes all have serious challenges when used alone: oxide ceramics are brittle, sulfide ceramics are air sensitive, polymers are too resistive and soft, and many electrolytes react with lithium. Composites provide a clear route to address these issues. This project does not seek discovery of new electrolytes; rather, the goal is to study combinations of current well known electrolytes. The project emphasizes the investigation of polymer-ceramic interfaces formed as bilayers and as simple composite mixtures where the effects of the interface properties can be readily isolated. In general, the ceramic phase is several orders of magnitude more conductive than the polymer electrolyte, and interfaces can contribute an additional source of resistance. Using finite element simulations as a guide, composites with promising compositions and architectures are fabricated and evaluated for Li-transport properties using ac impedance and dc cycling with lithium in symmetric or half cells. General design rules will be determined that can be widely applied to other combinations of solid electrolytes.

Out-Year Goal. Use advanced manufacturing processes where the architecture of the composite membrane can be developed and tailored to maximize performance and cost-effective manufacturing.

Collaborations. Electrolytes under investigation include a garnet electrolyte from Jeff Sakamoto (UM) and ceramic powder from Ohara. Staff at Corning Corporation will serve as the industrial consultant. Student intern, Cara Herwig, from Virginia Technological University assisted this quarter.

Milestones

1. Measure the removal of solvent molecules introduced via solution synthesis or gas absorption from ceramic-polymer composite sheets under vacuum and heating conditions. (March 2016 – Complete)
2. Prepare ceramic-polymer electrolyte sheets with a coating, and map the uniformity with nano-indentation and by profiling the lithium plating. (September 2016 – On schedule)

Progress Report

This quarter, the project continued to improve the technique for spray coating aqueous suspensions of Ohara LATP powders in polyethylene oxide (PEO) with lithium triflate and additives. The aqueous suspension is coated using an airbrush onto copper foil and now also onto a nylon mesh. Nylon mesh with 47% opening acts as a support for holding the coating that is sprayed on both the sides of the mesh. This allows easy integration of the coating against electrodes in the battery. The coating filled the 100 μ m mesh openings in the nylon and thereby allowed smooth flow of lithium ions, although the nylon mesh itself is 78 μ meters thick.

Several composite membranes are compared in Figure 61. On copper foil, two electrolyte coated disks are pressed face to face for impedance measurement. In the case of nylon mesh, a single self-supporting electrolyte disk is pressed against blocking electrodes. The ionic conductivity of the coating over nylon is 5 μ S/cm and is twice that of the coating over copper foil. This proves the versatility of the spray coating onto various substrates, without significant change in ionic conduction. Likely the improvement in ionic conductivity for the nylon mesh supported electrolyte is attributed to the boundary-free, single continuous layer of electrolyte between the blocking electrodes. TEGDME additive mixed into the aqueous slurry suppressed the polymers from crystallizing at low temperatures as well as contributed to the uniformity of the coating.

A disk of composite electrolyte coating on nylon was also tested with symmetrical lithium electrodes for dc measurement under different applied potentials. The resultant equilibration current after several hours is noted. The equilibration current after each potential step is linearly proportional with the applied voltage and gives a dc conductivity of about 0.4 μ S/cm at 25°C. In addition, the impedance test carried out after dc measurement revealed ionic conductivity comparable to that measured with blocking electrodes. This presents evidence that the composite electrolyte is stable with the Li-metal electrodes. Further analysis is in progress to determine the lithium and electronic transference numbers.

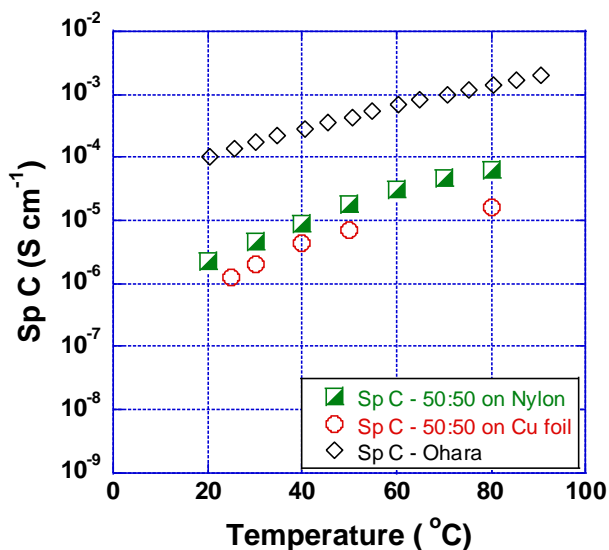


Figure 61. Ionic conductivity for improved spray coated composite electrolyte over Nylon.

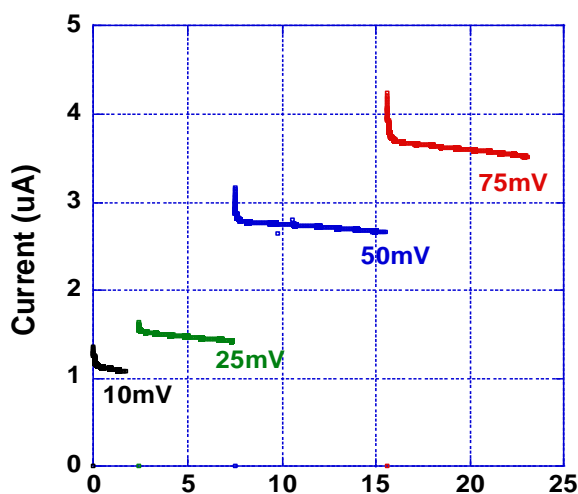


Figure 62. Variation of current with time during dc polarization at different applied potential.

Patents/Publications/Presentations/Presentations

Presentation

DOE Annual Merit Review Meeting, Washington, D. C (June 6-10, 2016): “Composite Electrolyte to Stabilize Metallic Lithium Anodes”; Nancy Dudney, Amaresh Samuthira Pandian, and Frank Delnick. Poster.

Task 7.4 – Overcoming Interfacial Impedance in Solid-State Batteries (Eric Wachsman, Liangbing Hu, and Yifei Mo, University of Maryland College Park)

Project Objective. Develop a multifaceted and integrated (experimental and computational) approach to solve the key issue in solid-state, Li-ion batteries (SSLIBs), interfacial impedance, with a focus on garnet-based solid-state electrolytes (SSEs), the knowledge of which can be applied to other SSE chemistries. The focus is to develop methods to decrease the impedance across interfaces with the solid electrolyte, and ultimately demonstrate a high power/energy density battery employing the best of these methods.

Project Impact. Garnet electrolytes have shown great promise for safer and high-energy density batteries. The success of the proposed research can lead to dramatic progress on the development of SSLIBs based on garnet electrolytes. With regard to the fundamental science, the project methodology by combining computations and experiments can lead to an understanding of the thermodynamics, kinetics and structural stability, and evolution of SSLIBs with the garnet electrolytes. Due to the ceramic nature of garnet electrolyte, being brittle and hard, garnet electrolyte particles intrinsically lead to poor contacts among themselves or with electrode materials. A fundamental understanding at the nanoscale and through computations, especially with interface layers, can guide design improvements and eventually lead to commercial use of such technologies.

Approach. SSLIB interfaces are typically planar, resulting in high impedance due to low specific surface area, and attempts to make 3D high surface area interfaces can also result in high impedance due to poor contact (for example, pores) at the electrode-electrolyte interface that hinder ion transport or degrade due to expansion/contraction with voltage cycling. This project will experimentally and computationally determine the interfacial structure-impedance relationship in SSLIBs to obtain fundamental insight into design parameters to overcome this issue. Furthermore, it will investigate interfacial modification (layers between SSE and electrode) to see if it can extend these structure-property relationships to higher performance.

Collaborations. This project is in collaboration with Dr. Venkataraman Thangadurai on garnet synthesis. It will collaborate with Dr. Leonid A. Bendersky (Leader, Materials for Energy Storage Program at NIST) and use neutron scattering to investigate the lithium profile across the bilayer interface with different charge-discharge rates. The project is in collaboration with Dr. Kang Xu in U.S. Army Research Laboratory (ARL) with preparation of perfluoropolyether (PFPE) electrolyte.

Milestones

1. Identify compositions of gel electrolyte to achieve $100 \Omega \cdot \text{cm}^2$. (Milestone 1 – Complete)
2. Determination of interfacial impedance in layered and 3D controlled solid state structures. (Milestone 2 – Complete)
3. Develop computation models to investigate interfacial ion transport with interlayers. (Milestone 3 – Complete)
4. Identify compositions out of 4 types of interlayers and processing with electrolyte/electrode interfacial impedance of $\sim 10 \Omega \cdot \text{cm}^2$. (Milestone 4 - Ongoing)

Patents/Publications/Presentations

Publications

- Fu, K., and Y. Gong, J. Dai, A. Gong, X. Han, Y. Yao, Y. Wang, C. Wang, Y. Chen, C. Yan, E. D. Wachsman, and L. Hu. “Flexible, Solid-State Lithium Ion-conducting Membrane with 3D Garnet Nanofiber Networks.” *Proceedings of the National Academy of Sciences* (2016). doi: 10.1073/pnas.1600422113

Presentations

- Stanford University, Stanford, California (June 28, 2016): “All-Solid-State Li-ion Batteries for Transformational Energy Storage”; Eric Wachsman.
- Nature Conference on Materials for Energy, Wuhan, China (June 11-14, 2016): “Ion Conducting Oxides for Electrochemical Energy Conversion and Storage”; Eric Wachsman. Keynote speaker.
- University of South Carolina, Columbia, South Carolina (March 18, 2016): “Ion Conducting Oxides for Electrochemical Energy Conversion and Storage”; Eric Wachsman.
- International Meeting on Lithium Batteries (IMLB), Chicago, Illinois (June 2016): “Computation-Guided Interface Engineering in All-Solid-State Li-Ion Batteries: Insights from First Principles Calculations”; Yifei Mo.
- 229th ECS meeting, San Diego, California (May 2016): “Critical Roles of Interface Engineering in All-Solid-State Li-Ion Batteries: Insights from First Principles Calculations”; Yifei Mo. Invited.
- TechConnect World Innovation Conference, Washington, D. C. (May 2016): “Accelerating Materials Design and Discovery Using Computational Approaches”; Yifei Mo. Invited.
- TechConnect World Innovation Conference, Washington, D. C. (May 2016): “Overcoming Materials Challenges in All-Solid-State Li-ion Batteries: Insights from Computational Modeling”; Yifei Mo.

Task 7.5 – Nanoscale Interfacial Engineering for Stable Lithium-Metal Anodes (Yi Cui, Stanford University)

Project Objective. This study aims to render Li-metal anode with high capacity and reliability by developing chemically and mechanically stable interfacial layers between lithium metal and electrolytes, which is essential to couple with sulfur cathode for high-energy, Li-S batteries. With the nanoscale interfacial engineering approach, various kinds of advanced thin films will be introduced to overcome issues related to dendritic growth, reactive surface, and virtually “infinite” volume expansion of Li-metal anode.

Project Impact. Cycling life and stability of Li-metal anode will be dramatically increased. The success of this project, together with breakthroughs of sulfur cathode, will significantly increase the specific capacity of lithium batteries and decrease cost as well, therefore stimulating the popularity of EVs.

Out-Year Goals. Along with suppressing dendrite growth, the cycle life, Coulombic efficiency, and current density of Li-metal anode will be greatly improved (that is no dendrite growth for current density up to 3.0 mA/cm², with Coulombic efficiency greater than 99.5%) by choosing the appropriate interfacial nanomaterial along with rational electrode material design.

Milestones

1. Detailed study on the Li-reduced graphene oxide (Li-rGO) composite anode. (June 2016 – Complete)

Progress Report

Previously, the project demonstrated synthesis of Li-rGO composite anode via thermal infusion of molten lithium into rGO membrane.¹ The rGO served as a stable host for lithium, which minimized the volume change at the whole electrode level during cycling and effectively suppressed lithium dendrite. This quarter, the project performed detailed studies on the composite electrode to understand the mechanism for molten lithium infusion.

Fabricating layered rGO films with uniform nanogaps and infusing lithium into the interlayer gaps are two key steps for electrode fabrication. To create uniform nanogaps, the project put densely stacked GO films into contact with molten lithium. Interestingly, a spark reaction can happen immediately across the whole film and expand the film into a more porous structure. The spark reaction process within 100 milliseconds is captured using digital camera and shown in Figure 65. The flame shown in the images illustrates the possible H_2 formation under the strong reduction condition in the presence of molten lithium and its combustion reaction with the trace amount of oxygen in the glove box. This can be one of the reasons for the interlayer expansion of GO. In addition, the sudden pressure release within the GO layers due to the removal of superheated residual water/surface functional groups is another cause of the spark reaction.

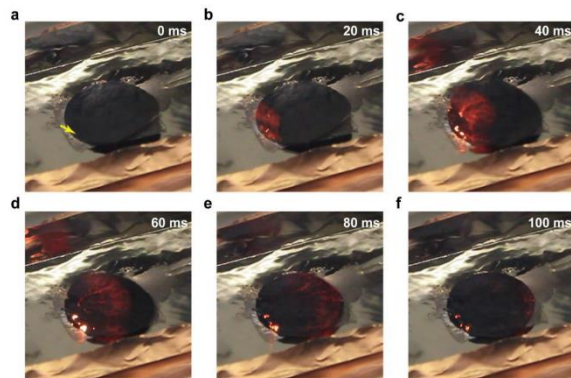


Figure 65. Time-lapse images visualizing the detailed phenomenon of the spark reaction. The images of the reaction at different time of 0 ms (a), 20 ms (b), 40 ms (c), 60 ms (d), 80 ms (e), and 100 ms (f) were shown successively. The yellow arrow (image a) shows the initial contact point between GO and molten lithium, where the reaction initiated.

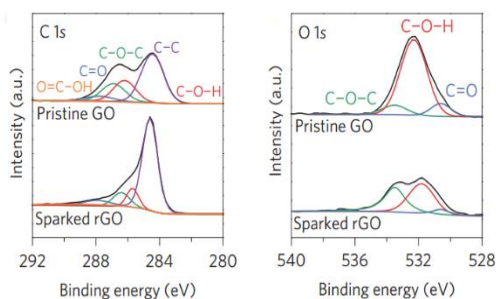


Figure 66. Deconvoluted X-ray photoelectron spectroscopy spectra of C 1s and O 1s before and after the spark reaction.

lithium and rGO surface groups (Figure 67). Functional groups such as carbonyl (3.080 eV) and alkoxy (2.974 eV) groups that remained after the spark reaction exhibit much stronger binding energy to lithium than the bare graphene counterpart (1.983 eV). Thus, the strong binding can greatly increase the surface lithiophilicity for efficient lithium intake into the porous rGO matrix.

XPS confirmed a significant reduction in oxygen after the spark reaction (Figure 66). As can be observed from the deconvoluted C 1s and O 1s spectra, the intensity corresponding to C–O–H dropped to ~50% of the original value, whereas the other surface functional groups exhibited limited decrease. This indicates that the spark reaction can selectively remove the relatively unstable functional groups on GO, which is beneficial to minimize the side reactions during battery cycling. On the other hand, the other more stable functional groups remained, which is crucial to maintain a strong interaction with molten lithium to facilitate infusion. The project subsequently carried out first-principles calculations on the binding energy between

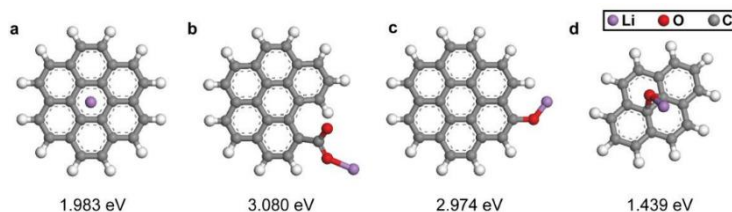


Figure 67. First-principles calculations on surface binding energy between lithium and bare graphene surface (a), carbonyl (C=O) groups (b), alkoxy groups (C–O) (c), and epoxy (C–O–C) groups (d).

Patents/Publications/Presentations

Publication

- Lin, D., et al. “Layered Reduced Graphene Oxide with Nanoscale Interlayer Gaps as a Stable Host for Lithium Metal Anodes.” *Nat. Nanotechnol.* (2016).

Task 7.6 – Lithium Dendrite Suppression for Lithium-Ion Batteries (Wu Xu and Ji-Guang Zhang, Pacific Northwest National Laboratory)

Project Objective. The project objective is to enable lithium metal to be used as an effective anode in rechargeable Li-metal batteries for long cycle life at a reasonably high current density. The investigation will focus on the effects of various lithium salts, additives, and carbonate-based electrolyte formulations on Li-anode morphology, lithium Coulombic efficiency, and battery performances in terms of long-term cycling stability at room temperature and elevated temperatures and at various current density conditions, rate capability, and low-temperature discharge behavior. The surface layers on lithium anode and cathode will be systematically analyzed. The properties of solvates of cation-solvent molecules will also be calculated to help explain the obtained battery performances.

Project Impact. Lithium metal is an ideal anode material for rechargeable batteries. Unfortunately, uncontrollable dendritic lithium growth and limited Coulombic efficiency during lithium deposition/stripping inherent in these batteries have prevented their practical applications. This work will explore the new electrolyte additives that can lead to dendrite-free lithium deposition with high Coulombic efficiency. The success of this work will increase energy density of lithium and Li-ion batteries and accelerate market acceptance of EVs, especially for PHEVs required by the EV Everywhere Grand Challenge proposed by the DOE/EERE.

Out-Year Goals. The long-term goal of the work is to enable lithium and Li-ion batteries with >120 Wh/kg (for PHEVs), 1000 deep-discharge cycles, a 10-year calendar life, improved abuse tolerance, and less than 20% capacity fade over a 10-year period.

Collaborations. This project engages in collaboration with the following:

- Bryant Polzin (ANL) – NCA, NMC, and graphite electrodes
- Vincent Battaglia (LBNL) – LFP electrode
- Chongmin Wang (PNNL) – Characterization by TEM/SEM

Milestones

1. Develop mixed salts electrolytes to protect aluminum substrate and Li-metal anode, and to maintain lithium Coulombic efficiency over 98%. (December 2015 – Complete)
2. Demonstrate over 500 cycles for Li|LFP cells with high LFP loading and at high current density cycling. (March 2016 – Complete)
3. Demonstrate over 200 cycles for 4-V Li-metal batteries with high cathode loading and at high current density cycling. (June 2016 – Complete)
4. Achieve over 500 cycles for 4-V Li-metal batteries with high cathode loading and at high current density cycling. (September 2016 – Ongoing)

Progress Report

This quarter, the effects of different electrolytes on battery performances of Li||NMC coin cells were tested at various charging/discharging current densities. The NMC cathode had a moderately high areal capacity of $\sim 1.75 \text{ mAh cm}^{-2}$ ($\sim 10.8 \text{ mg active material cm}^{-2}$). The electrolytes were 1.0 M LiTFSI-LiBOB dual-salt in ethylene carbonate – ethylmethyl carbonate (EC-EMC) solvent mixture without and with a small amount of additive X and 1.0 M LiPF₆ in EC-EMC as the control. As shown in Figure 68a, the cell using conventional LiPF₆ electrolyte shows an abrupt capacity drop after only ca. 60 cycles at the current density of 1.75 mA cm^{-2} for charging and discharging due to the quick formation of a highly resistive SEI layer entangled with lithium metal and a continuous growth toward the bulk of lithium metal, thus leading to the dramatic increase of cell impedance and the electrode over-potential (Figure 68b). In comparison, the cell using LiTFSI-LiBOB dual-salt electrolyte without additive shows greatly improved cycle life up to 450 cycles (with a capacity retention of 74.5%) prior to the sharp drop of discharge capacity (Figure 68a), and the cell experiences continuous capacity fade and increased cell over-potential during cycling (Figure 68c). The addition of additive X into the dual-salt electrolyte significantly improves the cycling performance of the Li||NMC cells. The capacity loss is only 2.9% in 500 cycles even at a charging current density of 1.75 mA cm^{-2} . More importantly, there is only very limited increase in cell over-potential after 500 cycles (Figure 68d), indicating that the interphase formed in the additive X-containing LiTFSI-LiBOB electrolyte is highly conductive for Li⁺ ion transportation as compared to those formed in the other two electrolytes. The project believes this fast charging capability and long cycling stability of X-added dual-salt electrolyte is the best performance ever reported for Li-metal batteries. More testing and analyses are under way.

The Li||NMC cells with high NMC loading (3.0 mAh cm^{-2}) were also tested with an additive-containing dual-salt electrolyte. After formation cycles at 0.3 mA cm^{-2} (that is, C/10 rate), the cells can be stably cycled for 200 times at 1.0 mA cm^{-2} (that is, C/3) charging and 3.0 mA cm^{-2} (that is, 1C) discharging (Figure 69), which achieves the Q3 milestone. As is known, increase in charging current density results in a shorter cycle life.

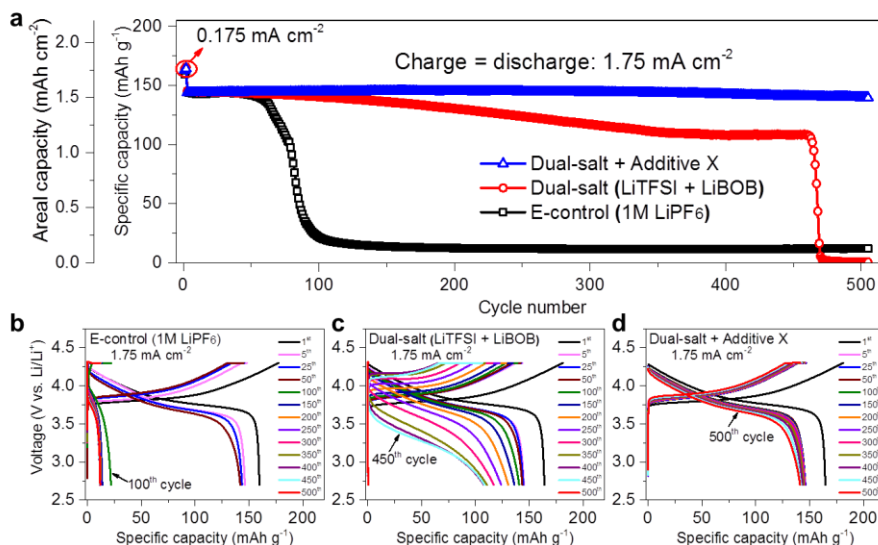


Figure 68. Electrochemical behaviors of different electrolytes in Li||NMC cells. (a) Long-term cycling performance of the electrolytes with different salts in ethylene carbonate – ethylmethyl carbonate solvent mixture at the same charge and discharge current density of 1.75 mA cm^{-2} at 30°C . (b-d) Evolutions of charge/discharge voltage profiles of Li||NMC cells using (b) conventional LiPF₆ electrolyte, (c) dual-salt (LiTFSI-LiBOB) electrolyte, and (d) additive-containing dual-salt electrolyte.

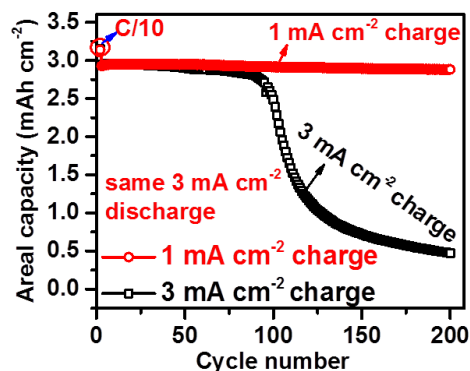


Figure 69. Cycling performance of Li||NMC cells with 3.0 mAh cm^{-2} NMC loading and using an additive-containing dual-salt electrolyte at 30°C .

Patents/Publications/Presentations

Publications

- Xiang, H., and P. Shi, P. Bhattacharya, X. Chen, D. Mei, M. E. Bowden, J. Zheng, J.-G. Zhang, and W. Xu.* “Enhanced Charging Capability of Lithium Metal Batteries Based on Lithium Bis(trifluoromethanesulfonyl)imide-Lithium Bis(oxalato)borate Dual-Salt Electrolytes.” *Journal of Power Sources* 318 (2016): 170-177.
- Xu, W.*, and H. Xiang, J. Zheng, D. Mei, P. Yan, R. Cao, M. H. Engelhard, M. E. Bowden, C. Wang, and J.-G. Zhang. “Synergistic Effects of CsPF₆ Additive and Propylene Carbonate Content on Enhancing Performances of Graphite Electrode in Lithium-Ion Batteries,” in *Electronic Proceedings of the 47th Power Sources Conference*, Orlando, Florida, Session 24.1 (June 13-16, 2016): 372-375.

Presentations

- 9th Symposium on Energy Storage Beyond Lithium-Ion, Richland, Washington (May 24-26, 2016): “LiTFSI-LiBOB Dual-Salt Electrolytes Enhancing the Charging Capacity of Rechargeable Lithium Metal Batteries”; H. Xiang, P. Shi, P. Bhattacharya, X. Chen, D. Mei, M. E. Bowden, J. Zheng, J.-G. Zhang, and W. Xu. Poster.
- 9th Symposium on Energy Storage Beyond Lithium-Ion, Richland, Washington (May 24-26, 2016): “Stable Operation of Lithium Metal Batteries by the Formation of a Transient High Concentration Electrolyte Layer during Fast Discharge”; J. Zheng, P. Yan, D. Mei, M. H. Engelhard, S. S. Cartmell, B. J. Polzin, C.-M. Wang, J.-G. Zhang, and W. Xu. Poster.
- DOE Annual Merit Review Meeting, Washington, D. C. (June 6-10, 2016): “Lithium Dendrite Prevention for Lithium-Ion Batteries”; W. Xu and J.-G. Zhang. Poster.
- 47th Power Sources Conference, Orlando, Florida (June 13-16, 2016): “Synergistic Effects of CsPF₆ Additive and Propylene Carbonate Content on Enhancing Performances of Graphite Electrode in Lithium-Ion Batteries”; W. Xu, H. Xiang, J. Zheng, D. Mei, P. Yan, R. Cao, M. H. Engelhard, M. E. Bowden, C. Wang, and J.-G. Zhang.
- 18th International Meeting on Lithium Batteries, Chicago, Illinois (June 19-24, 2016): “Stable Operation of Lithium Metal Batteries by the Formation of a Transient High Concentration Electrolyte Layer during Fast Discharge”; J. Zheng, P. Yan, D. Mei, M. H. Engelhard, S. S. Cartmell, B. J. Polzin, C. Wang, J.-G. Zhang, and W. Xu. Poster.

TASK 8 – LITHIUM–SULFUR BATTERIES

Summary and Highlights

Advances in Li-ion technology have been stymied by challenges involved in developing high reversible capacity cathodes and stable anodes. Hence, there is a critical need for development of alternate battery technologies with superior energy densities and cycling capabilities. In this regard, Li-S batteries have been identified as the next flagship technology, holding much promise due to the attractive theoretical specific energy densities of 2,567 Wh/kg. In addition, realization of the high theoretical specific capacity of 1,675 mAh/g corresponding to formation of Li_2S using earth-abundant sulfur renders the system highly promising compared to other available cathode systems. Thus, the research focus has shifted to developing Li–S batteries. This system, however, suffers from major drawbacks, as elucidated below.

- Limited inherent electronic conductivity of sulfur and sulfur compound based cathodes.
- Volumetric expansion and contraction of both the sulfur cathode and lithium anode.
- Soluble polysulfide formation/dissolution and sluggish kinetics of subsequent conversion of polysulfides to Li_2S resulting in poor cycling life.
- Particle fracture and delamination as a result of the repeated volumetric expansion and contraction.
- Irreversible loss of lithium at the sulfur cathode, resulting in poor Coulombic efficiency.
- High diffusivity of polysulfides in the electrolyte, resulting in plating at the anode and consequent loss of driving force (that is, drop in cell voltage).

These major issues cause sulfur loss from the cathode, leading to mechanical disintegration. Additionally, surface passivation of anode and cathode systems results in a decrease in the overall specific capacity and Coulombic efficiency upon cycling. As a result, the battery becomes inactive within the first few charge-discharge cycles. Achievement of stable high capacity in Li-S batteries requires execution of fundamental studies to understand the degradation mechanisms in conjunction with engineered solutions. BMR Task 8 addresses both aspects with execution of esoteric, fundamental *in situ* XAS and *in situ* electron paramagnetic resonance (EPR) studies juxtaposed with applied research comprising use of suitable additives, coatings, and exploration of composite morphologies. Both ANL and LBNL use X-ray based techniques to study phase evolution and loss of Coulombic efficiency in Se_8 during lithiation/delithiation, while understanding polysulfide formation in sulfur and polysulfides (PSL) in oligomeric PEO solvent, respectively. Work from PNNL, University of Pittsburgh (U Pitts), and Stanford University demonstrates high areal capacity electrodes in excess of 2 mAh/cm². Following loading studies reported in the first quarter, PNNL has performed *in situ* EPR to study reaction pathways mediated by sulfur radical formation. Coating/encapsulation approaches adopted by U Pitts and Stanford comprise flexible sulfur wire (FSW) electrodes coated with Li-ion conductors, and TiS_2 encapsulation of Li_2S in the latter, both ensuring polysulfide retention at sulfur cathodes. BNL work has focused on benchmarking of pouch cell testing by optimization of the voltage window and study of additives such as LiI and LiNO_3 . *Ab initio* studies at Stanford and U Pitts involving calculation of binding energies and reaction pathways, respectively, augment the experimental results. AIMD simulations performed at TAMU reveal multiple details regarding electrolyte decomposition reactions and the role of soluble polysulfides (PS) on such reactions. Using kinetic Monte Carlo (KMC) simulations, electrode morphology evolution and mesostructured transport interaction studies were also executed. Each of these projects has a collaborative team of experts with the required skill set needed to address the EV Everywhere Grand Challenge of 350 Wh/kg and 750 Wh/l, and cycle life of at least 1000 cycles.

Highlights. Studies at BNL and SUNY (Gan and Takeuchi) have identified cellulose polymer (CP) to be the most effective binder in minimizing delamination and ensuring sulfur particle adhesion to current collector both before and after cycling, while delamination is observed to occur in PVDF and severe cracking in the case of polyimide (PI) binder. Similarly, the use of additives has been shown (Xiao and Liu, PNNL) to be important in making high areal loading electrodes (>5 mg/cm² sulfur).

It was found (Qu and Yang, University Wisconsin Milwaukee and BNL) that the major polysulfide ions formed at the first reduction wave of elemental sulfur were the S_4^{2-} and S_5^{2-} species, while the widely accepted reduction products of S_8^{2-} and S_6^{2-} for the first reduction wave were in low abundance, that is, the immediate product of the electrochemical reduction of sulfur was not S_8^{2-} .

Task 8.1 – New Lamination and Doping Concepts for Enhanced Lithium–Sulfur Battery Performance (Prashant N. Kumta, University of Pittsburgh)

Project Objective. The project objective is to successfully demonstrate generation of novel sulfur cathodes for Li-S batteries meeting the targeted gravimetric energy densities ≥ 350 Wh/kg and ≥ 750 Wh/l with a cost target \$125/kWh and cycle life of at least 1000 cycles for meeting the EV Everywhere blueprint. The proposed approach will yield sulfur cathodes with specific capacity ≥ 1400 mAh/g, at ≥ 2.2 V, generating ~ 460 Wh/kg energy density higher than the target. Full cells meeting the required deliverables will also be made.

Project Impact. Identification of new laminated S-cathode-based systems displaying higher gravimetric and volumetric energy densities than conventional Li-ion batteries will likely result in new commercial battery systems that are more robust, capable of delivering better energy and power densities, and more lightweight than current Li-ion battery packs. Strategies and configurations based on new Li-ion conductor (LIC)-coated sulfur cathodes will also lead to more compact battery designs for the same energy and power density specifications as current Li-ion systems. Commercialization of these new S-cathode-based Li-ion battery packs will represent, fundamentally, a major hallmark contribution of the DOE VTO and the battery community.

Out-Year Goals. This is a multi-year project comprising of three major phases to be successfully completed in three years. Phase 1 (Year 1): Synthesis, Characterization, and Scale up of suitable LIC matrix materials and multilayer composite sulfur cathodes. This phase is completed. Phase 2 (Year 2): Development of LIC-coated sulfur nanoparticles, scale up of high-capacity engineered LIC-coated multilayer composite electrodes and doping strategies for improving electronic conductivity of sulfur. Phase 3 (Year 3): Advanced high energy density, high rate, extremely cyclable cell development.

Collaborations. The project collaborates with the following members with the corresponding expertise:

- Dr. Spandan Maiti (U Pitts): for mechanical stability and multi-scale modeling
- Dr. A. Manivannan (NETL): for XPS for surface characterization
- Dr. D. Krishnan Achary (U Pitts): for solid-state MAS-NMR characterization

Milestones

1. Develop novel LIC membrane systems using *ab initio* methods displaying impermeability to sulfur diffusion. (December 2014 – Complete)
2. Demonstrate capabilities for generation of novel sulfur 1D, 2D, and 3D morphologies exhibiting superior stability and capacity. (June 2015 – Complete)
3. Identification of suitable dopants and dopant compositions to improve electronic conductivity of sulfur. (October 2015 – Complete)
4. Fundamental electrochemical study to understand reaction kinetics, mechanism, and charge transfer kinetics. (October 2015 – Complete)
5. Preparing doped LIC with improved ionic conductivity. (January 2016 – Complete)
6. Doping sulfur with like-sized dopants with enhanced electronic properties. (April 2016 – Complete)
7. Developing organic and inorganic complex framework materials (CFM) as effective polysulfide traps. (July 2016 – Complete)
8. Synthesis of vertically aligned carbon nanotube (VACNT) and LIC coated nanosulfur based composite materials. (Ongoing)
9. Design and engineering of high-capacity LIC-coated sulfur nanoparticle. (Ongoing)

Progress Report

Phase 1 of the project concluded with successful demonstration of polysulfide shielding by LIC membranes that replaced the commercial separator – electrolyte complex. The principal aim of Phase 2 is to enhance the conductivity of the LIC materials identified in Phase 1 by doping with suitable dopants identified by DFT calculations followed by developing effective coating strategies of these materials to generate hetero structured composites of sulfur with CNT. The first and second quarters of Phase 2 included results demonstrating three-fold increase in ionic conductivity of LIC by doping and investigation of techniques to

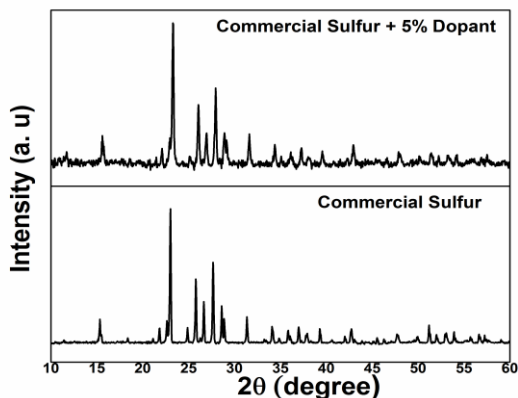


Figure 70. X-ray diffraction pattern of synthesized doped sulfur.

effectively coat LICs onto sulfur cathodes. CFMs developed last quarter demonstrated excellent polysulfide trapping ability. Work last quarter and this quarter identified chemical bonding of sulfur in CFMs to result in polysulfide trapping, albeit an initial capacity fade was identified to occur as a result of the CFM undergoing phase transformation. Work this quarter and next quarter is ongoing to address the same. The project also successfully doped commercially obtained sulfur (S_8) with like-sized dopants (Figure 70) to alter the electronic structure and enhance the electronic conductivity of sulfur. A comprehensive study of the effect of doping on sulfur is under way. As an additional subtask this quarter, an air-stable inorganic framework material

(IFM) was explored to trap polysulfides (Figure 71a). The IFMs exhibit very high (80%) sulfur infiltration and a low irreversible capacity loss of 15%. Further, the IFMs improved the first-cycle specific capacity of sulfur to ~1250 mAh/g, stabilizing at ~750 mAh/g (Figure 71b). The improved specific capacity of the sulfur electrode is attributed to the successful polysulfide trapping by IFMs, and work is in progress to improve performance further.

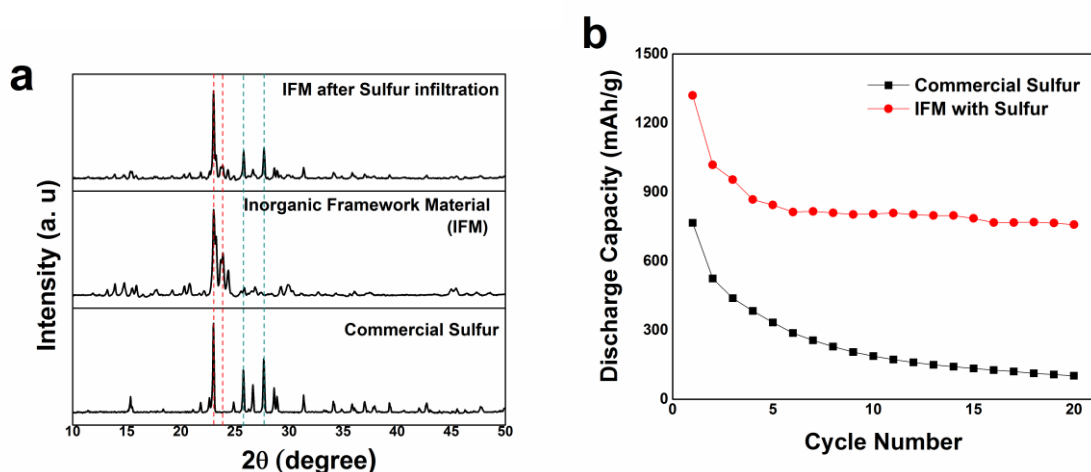


Figure 71. (a) X-ray diffraction patterns showing the infiltration of sulfur into the Inorganic Framework Material (IFM) showing retention of IFM structure. (b) Cycling behavior of sulfur infiltrated IFM.

Patents/Publications/Presentations

Publications

- Jampani, P. H., and B. Gattu, P. M. Shanthi, S. S. Damle, Z. Basson, R. Bandi, M. K. Datta, S. K. Park, and P. N. Kumta. “Flexible Sulfur Wires (Flex-SWs): A Versatile Platform for Lithium-sulfur Batteries.” *Electrochimica Acta* 212 (2016): 286-293.
- Shanthi, P. M., and P. H. Jampani, B. Gattu, M. Sweeney, M. K. Datta, and P. N. Kumta. “Nanoporous Non-carbonized Metal Organic Frameworks (MOFs): Effective Sulfur Hosts for High Performance Li-S Batteries.” *Journal of Physical Chemistry C* (2016), submitted.

Task 8.2 – Simulations and X-Ray Spectroscopy of Lithium–Sulfur Chemistry (Nitash Balsara, Lawrence Berkeley National Laboratory)

Project Objective. Li-S cells are attractive targets for energy storage applications as their theoretical specific energy of 2600 Wh/kg is much greater than the theoretical specific energy of current Li-ion batteries. Unfortunately, the cycle-life of Li-S cells is limited due to migration of species generated at the sulfur cathode. These species, collectively known as polysulfides, can transform spontaneously, depending on the environment, and it has thus proven difficult to determine the nature of redox reactions that occur at the sulfur electrode. The project objective is to use XAS to track species formation and consumption during charge-discharge reactions in a Li-S cell. Molecular simulations will be used to obtain X-ray spectroscopy signatures of different polysulfide species, and to determine reaction pathways and diffusion in the sulfur cathode. The long-term objective is to use mechanistic information to build high specific energy lithium-sulfur cells.

Project Impact. Enabling rechargeable Li-S cells has potential to change the landscape of rechargeable batteries for large-scale applications beyond personal electronics due to: (1) high specific energy, (2) simplicity and low cost of cathode (the most expensive component of Li-ion batteries), and (3) earth abundance of sulfur. The proposed diagnostic approach also has significant potential impact as it represents a new path for determining the species that form during charge-discharge reactions in a battery electrode.

Approach. Experimental XAS of charging/discharging lithium sulfur batteries will be used to examine battery reaction mechanisms *in situ*. Theoretical XAS calculations and MD simulations will be used to provide a molecular level understanding and conclusive interpretation of experimental observations.

Out-Year Goals. The out-year goals are as follows:

- Year 1: Simulations of sulfur and PSL in oligomeric PEO solvent. Prediction of X-ray spectroscopy signatures of PSL/PEO mixtures. Measurement of X-ray spectroscopy signatures of PSL/PEO mixtures.
- Year 2: Use comparisons between theory and experiment to refine simulation parameters. Determine speciation in PSL/PEO mixtures without resorting to ad hoc assumptions.
- Year 3: Build an all-solid lithium-sulfur cell that enables measurement of X-ray spectra *in situ*. Conduct simulations of reduction of sulfur cathode.
- Year 4: Use comparisons between theory and experiment to determine the mechanism of sulfur reduction and Li₂S oxidation in all-solid Li-S cell. Use this information to build Li-S cells with improved life-time.

Collaborations. This project collaborates with Tsu-Chien Weng, Dimosthenis Sokaras, and Dennis Nordlund at SSRL, SLAC National Accelerator Laboratory in Stanford, California.

Milestones

1. Establish disproportionation thermodynamics in solvents with high and low electron pair donor (EPD) numbers using theoretical calculations. (December 2015 – Complete)
2. Extend theoretical calculations of XAS to dimethylformamide, a model solvent for high EPD number solvents that stabilize radical polysulfide anions. (February 2016 – Complete)
3. Perform *in situ* XAS tests of Li-S charge/discharge. (May 2016 – Complete)
4. Vary charge/discharge rate for *in situ* XAS testing; compare reaction pathways. (August 2016 – On schedule)

Progress Report

UV visible (UV-Vis) spectroscopy and electron spin resonance (ESR) spectra of dimethylformamide (DMF) and TEGDME lithium polysulfide (Li_2S_x) solutions were obtained, which concluded that the trisulfur radical anions ($\text{S}_3^{\cdot-}$) are present in both systems. Quantitative analysis of the TEGDME solution spectra showed that the trisulfur radical concentration is a complex function of the sulfur concentration (C_S), and the lithium-to-sulfur ratio in the chemically mixed solution quantified by x_{mix} (if all the added sulfur resulted in formation of a single dianion species, it would be $\text{Li}_2\text{S}_{x_{\text{mix}}}$). Figure 72 below plots the $\text{S}_3^{\cdot-}$ concentration determined by applying Beer's Law to the UV-Vis spectra, C_R , against C_S and x_{mix} .

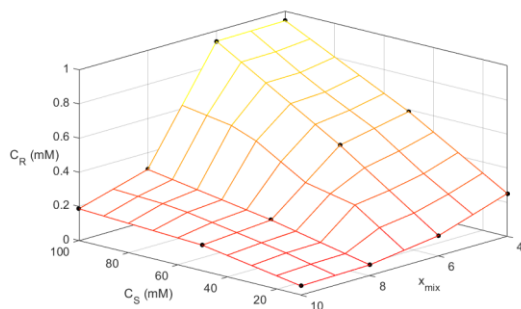


Figure 72. Radical concentration in Li_2S_x in TEGDME.

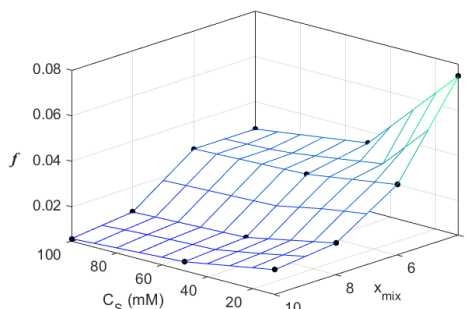


Figure 73. Fraction of sulfur in the form of $\text{S}_3^{\cdot-}$ in solution.

The radical concentration increases with C_S , but the increase is dramatic for low values of x_{mix} (that is, $x_{\text{mix}} = 4$). The fact that C_R increases with C_S is not surprising. To illustrate the effect of C_S and x_{mix} on the dianion:radical anion dissociation equilibrium, one can estimate the fraction of sulfur present in the form of $\text{S}_3^{\cdot-}$ in these solutions, f , using the equation $f = \frac{3C_R}{C_S}$. Figure 73 plots f against C_S and x_{mix} . The results showed that the $\text{S}_3^{\cdot-}$ fraction is the highest at low values of x_{mix} and low sulfur concentrations. The increase of f with decreasing C_S suggests that radical species are favored at low concentrations, while recombination of radicals to form dianion polysulfides is favored at higher sulfur concentrations.

The solvation environment of polysulfides in ether electrolytes theoretically is being studied. Figure 74 shows the solvation of a relatively free Li^+ solvated by six oxygens on two diglyme chains (left), and a Li^+ close to the sulfur chain solvated by two oxygens on one diglyme chain and two sulfur atoms on the tetra-sulfide chain (right). Table 4 shows the Li^+ ion coordination environment of Li_2S_x in diglyme solution.

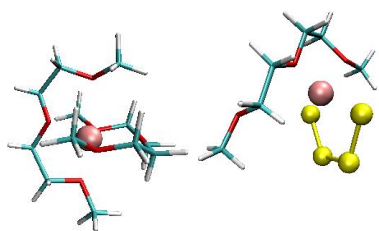


Figure 74. Li^+ coordinated by 6 oxygen atoms (left); and Li^+ coordinated by 2 sulfur and 2 oxygen atoms (right).

Table 4. Li^+ coordination environment in diglyme/ Li_2S_x solution.

	Inner Li^+ coordination			Outer Li^+ coordination		
	Oxygen	Sulfur	Total	Oxygen	Sulfur	Total
Li_2S_2	2	2	4	2	2	4
Li_2S_3	2	3	5	2	3	5
Li_2S_4	1	4	5	6	0	6
Li_2S_5	2	2	4	3	1	4
Li_2S_6	0	2	2	3	1	4
Li_2S_7	1	2	3	3	1	4
Li_2S_8	0.6	2	2.6	3	1	4

Patents/Publications/Presentations

Publications

- Wujcik, K., and D. Wang, A. Raghunathan, M. Drake, T. Pascal, J. Reimer, D. Prendergast, and N. P. Balsara. "Polysulfide Radical Anions in Ether-based Solvents." *J. Phys. Chem.*, under review.

Task 8.3 – Novel Chemistry: Lithium Selenium and Selenium Sulfur Couple (Khalil Amine, Argonne National Laboratory)

Project Objective. The project objective is to develop a novel S_xSe_y cathode material for rechargeable lithium batteries with high energy density and long life, as well as low cost and high safety.

Project Impact. Development of a new battery chemistry is promising to support the goal of PHEV and EV applications.

Approach. The dissolution of lithium polysulfides in nonaqueous electrolytes has been the major contribution to the low energy efficiency and short life of Li/S batteries. In addition, the insulating characteristics of both end members during charge/discharge (S and Li_2S) limit their rate capacity. To overcome this problem, S or Li_2S are generally impregnated in a carbon conducting matrix for better electronic conductivity. However, this makes it difficult to increase the loading density of practical electrodes. It is proposed here to solve the above barriers using the following approaches: (1) partially replace S with Se and (2) nano-confine the S_xSe_y in a nanoporous conductive matrix.

Out-Year Goals. When this new cathode is optimized, the following result can be achieved:

- A cell with nominal voltage of 2 V and energy density of 600 Wh/kg.
- A battery capable of operating for 500 cycles with low capacity fade.

Collaborations. This project engages in collaboration with the following:

- Professor Chunsheng Wang of University of Maryland
- Dr. Yang Ren and Dr. Chengjun Sun of APS at ANL

Milestones

1. Investigate the phase diagram of S_xSe_y system. (Q1 – Complete)
2. Encapsulating Se_2S_5 in nanoporous carbon. (Q1 – Complete)
3. Investigating the impact of fluorinated solvents on Se_2S_5 performance. (Ongoing)
4. Investigating Se doping of high S content for a higher energy density. (Ongoing)
5. Investigating the impact of the pore structure of carbon matrix on SeS system. (Ongoing)

Progress Report

Last quarter, the effect of a novel electrolyte on electrochemical performance and further reaction mechanism of selenium-sulfur based cathode materials was studied by using *in situ* NMR technique. Based on these findings, current work is focused on development of high-capacity selenium-doped sulfur cathode materials for long life rechargeable lithium batteries.

Figure 75 shows the SEM images and elemental mapping of a typical selenium-doped sulfur/carbon cathode material. As shown in Figure 75a-b, the Se-doped sulfur particles were assembled with carbon matrix to form secondary particles with a particle size of around 1-10 μm , which could enable a high tap density of the cathode material. Figure 75c-f clearly shows that carbon, selenium, and sulfur were distributed very uniformly throughout the whole sample, indicating a good dispersion of Se-doped sulfur in the carbon matrix.

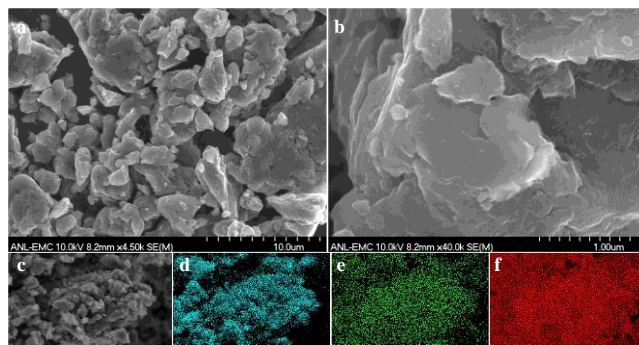


Figure 75. Scanning electron microscopy images and elemental mapping of a typical selenium-doped sulfur/carbon cathode material.

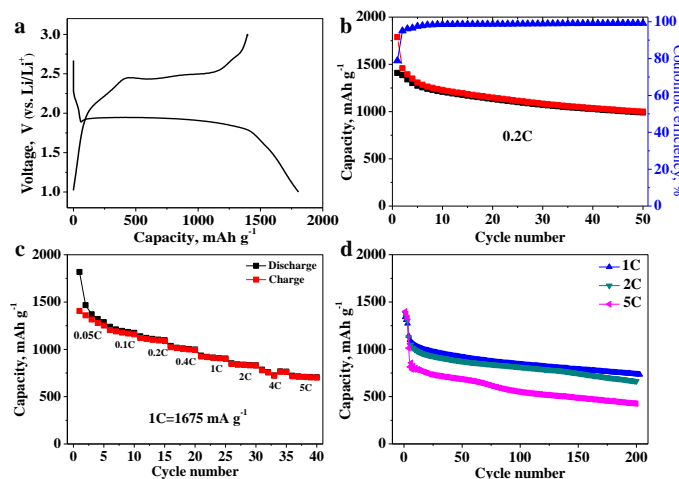


Figure 76. (a) First charge/discharge curve at 0.05C and (b) cycle performance at 0.2C, with (c) rate performance and (d) cycle performance at different rates of Selenium-doped S/C cathode materials.

Figure 76 shows the electrochemical performance of Se-doped S/C cathode materials using the novel electrolyte that was mentioned last quarter. Figure 76a shows a first discharge/charge curve at 0.05 C ($1C=1675 \text{ mAh g}^{-1}$), which presents a main discharge plateau at around 2.0 V and a charge plateau at 2.5 V. The initial reversible (charge) capacity is about $1409.0 \text{ mAh g}^{-1}$, leading to a high sulfur utilization of 84.1%. Figure 76b shows the cycling performance at 0.2 C. As can be seen, the Se-doped S/C cathode could still maintain a reversible capacity as high as 1000 mAh g^{-1} after 50 cycles of charge/discharge, and the Coulombic efficiency from second cycle was close to 100%, indicating a significant decrease in the shuttle effect. This should be attributed to the uniform dispersion of Se-doped sulfur in the conductive carbon matrix, which can be well maintained at the cathode side thus decreasing the dissolution of polyselenides and polysulfides and the reactions with the lithium anode. Figure 76c shows the rate performance of the Se-doped S/C cathode at different charge/discharge rates increasing successively from 0.05C, 0.1C, 0.2C, 0.4C, 1C, 2C, 4C to 5C. It can be clearly seen that Se-doped sulfur/carbon based cell demonstrate a superior rate capability with an average reversible capacity of 1321.9, 1179.2, 1102.1, 1006.2, 915.8, 835.6, 755.7 and 707.5 mAh g^{-1} , respectively. The cycle performance at high rates of charge/discharge was further evaluated and the results are shown in Figure 2d. At 1C and 2C cycling, the Se-doped S/C cathode could still deliver a reversible capacity of around 700 mAh g^{-1} after 200 cycles of charge/discharge, illustrating good cycle stability at high rate cycling. Even charged/discharged at an extreme high rate of 5 C, the cell still maintains a reversible capacity of over 400 mAh g^{-1} after 200 cycles. In conclusion, a high performance selenium-doped S/C cathode material for lithium batteries was demonstrated.

Patents/Publications/Presentations

Patent

- Guiliang Xu, Zonghai Chen, and Khalil Amine. Selenium-doped Sulfur Cathodes for Rechargeable Batteries. U. S. Patent, in process.

Task 8.4 – Multi-Functional Cathode Additives (MFCA) for Lithium–Sulfur Battery Technology (Hong Gan, Brookhaven National Laboratory; and Co-PI Esther Takeuchi, Brookhaven National Laboratory and Stony Brook University)

Project Objective. Develop a low-cost battery technology for PEV application utilizing Li-S electrochemical system by incorporating multifunctional cathode additives (MFCA), consistent with the long-term goals of the DOE EV Everywhere Grand Challenge.

Project Impact. The Li-S battery system has gained significant interest due to its low material cost potential (35% cathode cost reduction over Li-ion) and its attractive 2.8x (volumetric) to 6.4x (gravimetric) higher theoretical energy density compared to conventional Li-ion benchmark systems. Commercialization of this technology requires overcoming several technical challenges. This effort will focus on improving the cathode energy density, power capability, and cycling stability by introducing MFCA. The primary deliverable is to identify and characterize the best MFCA for Li-S cell technology development.

Approach. Transition metal sulfides are evaluated as cathode additives in sulfur cathode due to their high electronic conductivity and chemical compatibility to the sulfur cell system. Electrochemically active additives are also selected for this investigation to further improve energy density of the sulfur cell system. In the first year, the team has established the individual baseline sulfur and TM sulfide coin cell performances, and demonstrated the strong interactions between sulfur and various MFCA within the hybrid electrode. TiS_2 and FeS_2 were selected as the leading candidates for additional optimization studies with synthetic method developed. During the second year, leading candidates for the cathode optimization studies will be further narrowed down. More attention will be directed into electrode optimization and cell system optimization for improved electrode integrity, energy density, and electrochemical charge/discharge cycling performance. Examples for these efforts include electrode components (binder, carbon), electrode formulation optimization, and electrolyte optimization.

Out-Year Goals. This is a multi-year project comprised of two major phases to be successfully completed in three years. Phase 1 includes cathode and MFCA proof-of-concept investigations to be mostly completed during year 1 investigations. Phase 2 will include cell component interaction studies and full cell optimization. The work scope for year 2 will focus on the leading MFCA candidate selection, followed by hybrid electrode processing, material and formulation studies for optimized energy density, and cell electrochemical performance testing. The mechanistic studies of MFCA and sulfur interaction will continue throughout the year to advance fundamental understanding of the system.

Collaborations. This project collaborates with Dong Su, Xiao Tong, and Yu-chen Karen Chen-Wiegart at BNL and with Amy Marschilok and Kenneth Takeuchi at SBU.

Milestones

1. Synthesized MFCA evaluation and selection. (Q1 – Complete)
2. MFCA particle size effect study and best candidate selection. (Q2 – Complete)
3. Cathode process and material optimization. (Q3 – Ongoing)
4. Cathode formulation optimization. (Q4 – On schedule)

Progress Report

Last quarter, Phase 1 investigation was successfully completed with TiS_2 selected as the leading MFCA. Starting from this quarter, Phase 2 investigation will focus on the cathode mechanical integrity optimization by selecting and optimizing the binder materials and the conductive carbon additives. Cathode energy density optimization will be followed by cathode formulation and loading studies.

Binder Selection. PVDF has been used to process sulfur electrodes in all previous studies. Poor adhesion of the coated cathode was observed on the aluminum current collector, especially for the cycled electrodes. While the adhesion to the aluminum current collector may not be critical for coin cells due to the use of a spring to maintain the cell stack pressure, it will be critical to explore pouch cell designs in real applications where the stack pressure is typically not maintained via an external force. In the present study, five types of binder materials are tested for sulfur electrodes with a standard formulation of Sulfur:Carbon:Binder = 50:42:8 (weight ratio), including PVDF (baseline reference), PI, CP, polyvinylpyrrolidone (PVP), and polyacrylonitrile (PAN). Among these binders, PVP failed the slurry processing due to significant particles segregation. The sulfur electrodes with the other four binders were successfully coated with the total material loading $\sim 1.89 \text{ mg/cm}^2$. A Scotch™ tape test uncovered a significant effect of binder types on the electrode adhesion. The electrode with PAN exhibited total delamination from aluminum foil (Figure 77), while electrode with CP exhibited the lowest weight loss (Figure 78) and excellent adhesion to the aluminum current collector. Interestingly, after these electrodes being subjected to 100 discharge/charge cycles in coin cells, good adhesion is maintained for electrodes with CP and PAN binders, while a total delamination from aluminum current collector is observed for electrode with PVDF binder and severe cracking is observed for electrode with PI binder (Figure 79). At a C/10 discharge rate, the binder types do not show significant impact on Li-S coin cell cycle life, except that the electrode with PI binder exhibited lower Coulombic efficiency than that of the other three binders. Based on the above observation, CP is selected as the binder for the following confirmation study.

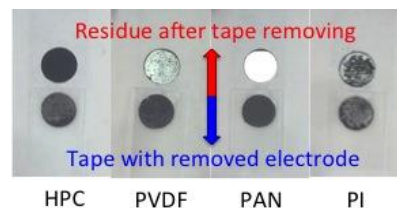


Figure 77. Tape testing – adhesion.

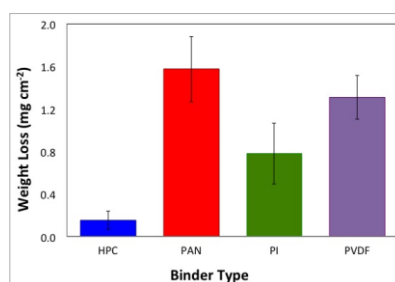


Figure 78. Tape test – areal weight loss.

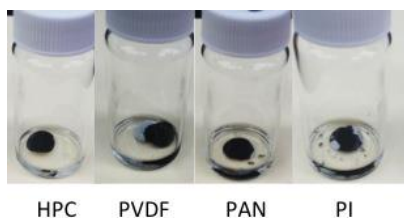


Figure 79. Cycled electrode delamination.

Confirmation Study with TiS_2 Additive. To confirm the effectiveness of CP binder for hybrid electrode with TiS_2 as cathode additive, the hybrid sulfur electrode with formulation of Sulfur: TiS_2 :Carbon:CP = 50:17:25:8 was prepared against the control of Sulfur:Carbon:CP = 50:42:8. Indeed, the Scotch™ tape testing confirmed good adhesion of both electrodes to the aluminum current collector. Good adhesion was also observed after cycling test. Cycling test under 1C discharge rate (with C/5 every 50 cycles) indicates the beneficial effect of TiS_2 additive on the cell capacity retention (Figure 80) that is still consistent with the group's previous observation when PVDF was used as binder material. Therefore, CP is selected for all future sulfur electrode optimization studies.

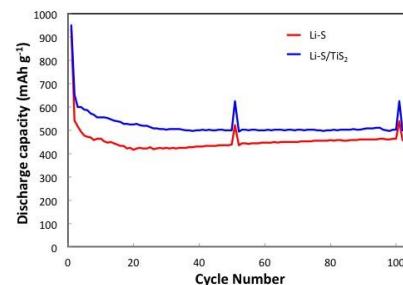


Figure 80. Hybrid electrode cycling at 1C.

Conductive Carbon Additive. Research on carbon additive optimization has begun.

Patents/Publications/Presentations

Patent

- Hong Gan and Ken Sun. “Hybrid Cathodes for Li-ion Battery Cells” – Patent Application S.N. 15/138,470 filed on 4/26/16.

Presentations

- JCESR/PNNL Li-S workshop (May 23, 2016): “Conductive CuS Cathode Additive for Li-S Battery”; K. Sun, D. Su, Q. Zhang, D. Bock, Y-C. K. Chen-Wiegart, A. C. Marschilok, K. J. Takeuchi, E. S. Takeuchi, and H. Gan. Poster.
- 229th ECS Spring Meeting, San Diego, California (May 29-June 2, 2016): “Transition Metal Sulfides as Conductive Additives for Sulfur Electrode in Li-S Battery” (# A02-0247); K. Sun, D. Su, Q. Zhang, D. Bock, A. C. Marschilok, K. J. Takeuchi, E. S. Takeuchi, and H. Gan.
- DOE Annual Merit Review, Washington, D. C. (June 6-10, 2016): “Multi-functional Cathode Additives for Li-S Battery Technology”; K. Sun, Q. Zhang, C. Cama, D. C. Bock, D. Su, Y-C. K. Chen-Wiegart, Xiao Tong, H. Liu, J. Jou, J. P. Huang, A. C. Marschilok, K. J. Takeuchi, E. S. Takeuchi, and H. Gan.
- 18th International Meeting on Lithium Batteries, Chicago, Illinois (June 19-24, 2016): “Capacity Contributing Conductive Cathode Additive for Sulfur Batteries” (#P1-1132); K. Sun, D. Su, X. Tong, D. C. Bock, C. Cama, R. A. DeMayo, J. P. Huang, Q. Zhang, A. C. Marschilok, K. J. Takeuchi, E. S. Takeuchi, and H. Gan. Poster.

Task 8.5 – Development of High-Energy Lithium–Sulfur Batteries (Jie Xiao and Jun Liu, Pacific Northwest National Laboratory)

Project Objective. The project objective is to develop high-energy, low-cost Li-S batteries with long lifespan. All proposed work will employ thick sulfur cathode (≥ 2 mAh/cm² of sulfur) at a relevant scale for practical applications. The diffusion process of soluble polysulfide out of thick cathode will be revisited to investigate cell failure mechanism at different cycling. Alternative anode will be explored to address the lithium anode issue. The fundamental reaction mechanism of polysulfide under the electrical field will be explored by applying advanced characterization techniques to accelerate development of Li-S battery technology.

Project Impact. The theoretical specific energy of Li-S batteries is ~ 2300 Wh/kg, which is almost three times higher than that of state-of-the-art Li-ion batteries. The major challenge for Li-S batteries is polysulfide shuttle reactions, which initiate a series of chain reactions that significantly shorten battery life. The proposed work will design novel approaches to enable Li-S battery technology and accelerate market acceptance of long-range EVs required by the EV Everywhere Grand Challenge.

Out-Year Goals. This project has the following out-year goals:

- Fabricate Li-S pouch cells with thick electrodes to understand sulfur chemistry/electrochemistry in the environments similar to the real application.
- Leverage the Li-metal protection project funded by the DOE and PNNL advanced characterization facilities to accelerate development of Li-S battery technology.
- Develop Li-S batteries with a specific energy of 400 Wh/kg at cell level, 1000 deep-discharge cycles, improved abuse tolerance, and less than 20% capacity fade over a 10-year period to accelerate commercialization of electrical vehicles.

Collaborations. This project engages in collaboration with the following:

- Dr. Xiao-Qing Yang (LBNL) – *In situ* characterization
- Dr. Bryant Polzin (ANL) – Electrode fabrication
- Dr. Xingcheng Xiao (GM) – Materials testing
- Dr. Jim De Yoreo (PNNL) – *In situ* characterization

Milestones

1. SEI study on graphite surface in the new EC-free electrolyte. (December 2015 – Complete)
2. Demonstrate prototype Li-ion sulfur cells with $> 95\%$ Coulombic efficiency (no additive) and $> 80\%$ capacity retention for 100 cycles. (March 2016 – Complete)
3. Identify effective approaches to facilitate electrolyte penetration within thick sulfur cathode (≥ 4 mg/cm²). (June 2016 – Complete)
4. Complete pouch cell assembly and testing by using optimized electrode and electrolyte. (September 2016 – In progress)

Progress Report

Sulfur cathode with high sulfur loading is the basis for developing high-energy Li-S batteries; however, previous study indicates significantly reduced sulfur utilization rate with an increase of sulfur loading above 4 mg cm^{-2} . This means electrode wetting becomes a key barrier for thick electrode, which is exacerbated when further squeezing electrode thickness or porosity to achieve high volumetric energy density for practical applications. Intrinsic reasons behind this problem may lie in (1) thick electrode accompanied by increased tortuosity, (2) poor affinity between sulfur/C cathode and electrolyte, and (3) reduced porosity and pore volume of calendered electrode. This leads to (1) significantly increased polarization resulting in decreased sulfur utilization rate and lower output voltage; and (2) poor cycling stability due to lack of electrolyte uptake. To address aforementioned electrode wetting issues, additives to both electrode and electrolyte have been

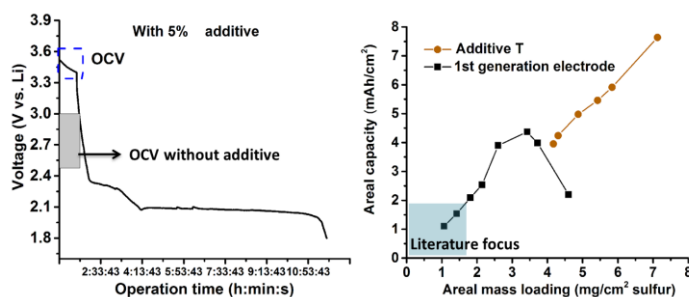


Figure 81. (a) Li-S cell voltage evolution during 2 hours' rest and subsequent first discharging process at a 0.1 C rate with sulfur cathode prepared with 5 wt% additive (sulfur loading is 4.5 mg cm^{-2}). (b) Dependence of areal capacity on sulfur loading for cathode with (brown) and without (black) additive.

proposed and demonstrate significant improvement for battery performance in terms of sulfur utilization, rate capability, and cycling stability. These findings enable utilization of high-loading sulfur cathode and advance development of high-energy Li-S batteries. Efforts this quarter were focused to address electrode wetting issues in high-loading sulfur electrode ($> 4 \text{ mg cm}^{-2}$). Industrial adaptable slurry coating method was used for electrode preparation. Multiple approaches have been employed, including additives for electrolyte, additives for electrode preparation, and synthesis of functionalized carbon materials. As a result, high sulfur utilization rate ($>1000 \text{ mAh g}^{-1}$) can be successfully achieved for cathode with sulfur loading up to 8 mg cm^{-2} . Figure 81 shows an example of improved electrochemical performance with high sulfur loading cathode by introducing only 5 wt% of electrode additive. It is interesting to find that with presence of additive the cell OCV is around 3.5 V versus Li/Li^+ , which is much higher than that of electrode without additive (below 3.0 V) and suggests smooth electrolyte penetration. The improved electrode wetting is expected to improve sulfur utilization rate for thick sulfur electrode. Figure 81b compares dependences of achievable areal capacity on sulfur loading with and without additive. Without additive, the electrode areal capacity exhibits a first growing and then declining trend with increasing of sulfur loading. Maximum areal capacity ($4\text{--}4.5 \text{ mAh cm}^{-2}$) can be obtained when sulfur loading is between 3 to 4 mg cm^{-2} . With additive, the areal capacity keeps on growing with increase of sulfur loading up to 8 mg cm^{-2} , showing almost linear increase trend with sulfur loading. Study on function mechanism of electrode and electrolyte additives is in progress.

Patents/Publications/Presentations

Publication

- Lu, D., and J. Tao, P. Yan, W. A. Henderson, Q. Li, Y. Shao, G. L. Graff, B. Polzin, C. Wang, J. Zhang, J. D. Yoreo, J. Liu, and J. Xiao. “Reversible Shielding of Electrodes.” Submitted for publication.

Presentations

- 9th Symposium on Energy Storage Beyond Li-ion (BLI-IX), Richland, Washington (May 24-26, 2016): “Non-lithium Metal Anode for Lithium-Sulfur Batteries”; D. Lu, et al.
- DOE Annual Merit Review, Washington, D. C. (June 6-10, 2016): “Development of High Energy Lithium Sulfur Battery”; J. Liu, et al.
- 18th International Meeting on Lithium Batteries (IMLB), Chicago, Illinois (June 19-24, 2016): “Lithium-Sulfur Batteries: High Loading Cathode, New Electrolyte and Non-Lithium Metal Anode”; D. Lu, et al.

Task 8.6 – Nanostructured Design of Sulfur Cathodes for High-Energy Lithium–Sulfur Batteries (Yi Cui, Stanford University)

Project Objective. The charge capacity limitations of conventional TM oxide cathodes are overcome by designing optimized nano-architected sulfur cathodes.

This study aims to enable sulfur cathodes with high capacity and long cycle life by developing sulfur cathodes from the perspective of nanostructured materials design, which will be used to combine with Li-metal anodes to generate high-energy Li-S batteries. Novel sulfur nanostructures as well as multifunctional coatings will be designed and fabricated to overcome issues related to volume expansion, polysulfide dissolution, and the insulating nature of sulfur.

Project Impact. The capacity and the cycling stability of sulfur cathode will be dramatically increased. This project's success will make Li-S batteries to power electric vehicles and decrease the high cost of batteries.

Out-Year Goals. The cycle life, capacity retention, and capacity loading of sulfur cathodes will be greatly improved (200 cycles with 80% capacity retention, $> 0.3 \text{ mAh/cm}^2$ capacity loading) by optimizing material design, synthesis, and electrode assembly.

Collaborations. This project engages in collaboration with the following:

- BMR PIs
- SLAC: *In situ* X-ray, Dr. Michael Toney
- Stanford: Professor Nix, mechanics; Professor Bao, materials

Milestones

1. Demonstrate synthesis to generate monodisperse sulfur nanoparticles with/without hollow space. (October 2013 – Complete)
2. Develop surface coating with one type of polymers and one type of inorganic materials. (January 2014 – Complete)
3. Develop surface coating with several types of polymers; Understand amphiphilic interaction of sulfur and sulfide species. (April 2014 – Complete)
4. Demonstrate sulfur cathodes with 200 cycles with 80% capacity retention and 0.3 mAh/cm^2 capacity loading. (July 2014 – Complete)
5. Demonstrate Li_2S cathodes capped by layered metal disulfides. (December 2014 – Complete)
6. Identify the interaction mechanism between sulfur species and different types of sulfides/oxides/metals, and find the optimal material to improve the capacity and cycling of sulfur cathode. (July 2015 – Complete)
7. Demonstrate the balance of surface adsorption and diffusion of Li_2S_x species on nonconductive metal oxides. (December 15 – Complete)
8. The selection criterion of metal oxide is proposed to guide the rational design of cathode materials for advanced Li-S batteries. (April-2016 – Complete)
9. Demonstrate lithium polysulfides adsorption and diffusion on the metal sulfides surface. (July 2016 – On schedule)

Progress Report

Last quarter's results indicate that an optimized balance between lithium polysulfides adsorption and surface diffusion is favorable for the lithium polysulfide species to deposit on the surface of oxide/carbon matrix, keeping active during the cycling and ensuring the final good cycling performance of batteries. The results are summarized, with the selection criterion of metal oxide to guide the rational design of cathode materials for advanced Li-S batteries. This report further explores the interaction mechanism between sulfur species and different types of metal sulfides, and identifying the optimal material to improve the capacity and cycling stability of sulfur cathode.

To study the interaction between lithium polysulfide and the metal sulfides, first-principle simulations were applied. Figure 82a-f shows the adsorption conformations for Li_2S_6 on various sulfides (VS_2 , CoS_2 , TiS_2 , FeS , SnS_2 and Ni_3S_2 are selected here). It can be clearly seen that the chemical interaction is dominantly contributed by the bond formed between lithium ion in Li_2S_6 and sulfur ion in sulfide. The binding energy, E_b , is computed to measure the binding strength between Li_2S_6 species and the anchoring materials (AM). It is defined as the energy difference between the Li_2S_6 -AM adsorbed system ($E_{\text{Li}_2\text{S}_6+\text{AM}}$) and the summation of pure Li_2S_6 ($E_{\text{Li}_2\text{S}_6}$) and pure AM (E_{AM}), which can be expressed as $E_b = E_{\text{Li}_2\text{S}_6} + E_{\text{AM}} - E_{\text{Li}_2\text{S}_6+\text{AM}}$ (the positive binding energy indicates that the binding interaction is favored, and the larger value the stronger anchoring effect). According to the simulation, the binding strengths between Li_2S_6 and Ni_3S_2 , SnS_2 , FeS , CoS_2 , VS_2 and TiS_2 are 0.72 eV, 0.80 eV, 0.87 eV, 1.01 eV, 1.04 eV and 1.02 eV, respectively. The magnitudes of E_b also indicate that the stronger interaction can induce better anchoring effect, which can improve the performance of Li-S battery. Furthermore, all the sulfide materials in the study can induce larger binding strength than that by graphene (0.67 eV), which exhibits very weak chemical binding to Li_2S_6 and adsorption dominated by physical Van der Waals (VdW) interaction. This is why these sulfides can mitigate polysulfide dissolution and suppress shuttle effect, leading to better performance in Li-S battery than that of commonly adopted sp^2 carbon materials.

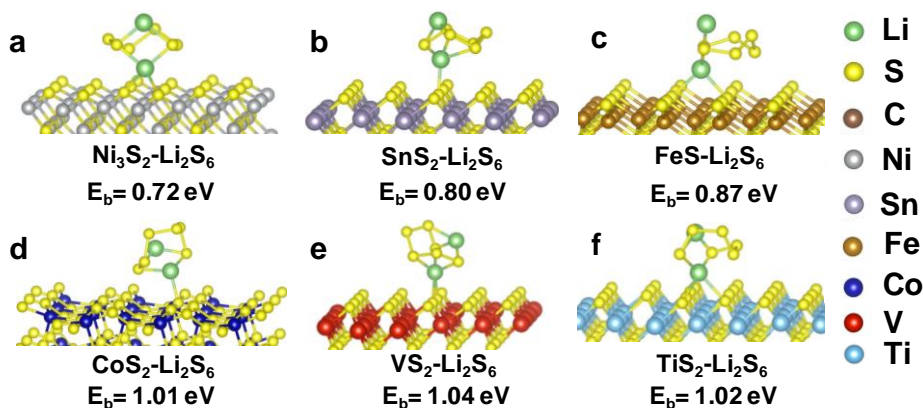


Figure 82. Atomic conformations and binding energy for Li_2S_6 species adsorption on (a) Ni_3S_2 , (b) SnS_2 , (c) FeS , (d) CoS_2 , (e) VS_2 , and (f) TiS_2 . Here, green, yellow, grey, purple, brown, blue, red and cyan balls represent lithium, sulfur, nickel, tin, iron, cobalt, vanadium, and titanium atoms, respectively.

Task 8.7 – Addressing Internal “Shuttle” Effect: Electrolyte Design and Cathode Morphology Evolution in Lithium–Sulfur Batteries (Perla Balbuena, Texas A&M University)

Project Objective. The project objective is to overcome the Li-metal anode deterioration issues through advanced Li-anode protection/stabilization strategies including (i) *in situ* chemical formation of a protective passivation layer and (ii) alleviation of the “aggressiveness” of the environment at the anode by minimizing the polysulfide shuttle with advanced cathode structure design.

Project Impact. Through formulation of alternative electrolyte chemistries as well as design, fabrication, and test of improved cathode architectures, it is expected that this project will deliver Li/S cells operating for 500 cycles at efficiency greater than 80%.

Approach. A mesoscale model including different realizations of electrode mesoporous structures generated based on a stochastic reconstruction method will allow virtual screening of the cathode microstructural features and the corresponding effects on electronic/ionic conductivity and morphological evolution. Interfacial reactions at the anode due to the presence of polysulfide species will be characterized with *ab initio* methods. For the cathode interfacial reactions, data and detailed structural and energetic information obtained from atomistic-level studies will be used in a mesoscopic-level analysis. A novel sonochemical fabrication method is expected to generate controlled cathode mesoporous structures that will be tested along with new electrolyte formulations based on the knowledge gained from the mesoscale and atomistic modeling efforts.

Out-Year Goals. By determining reasons for successes or failures of specific electrolyte chemistries, and assessing relative effects of composite cathode microstructure and internal shuttle chemistry versus that of electrolyte chemistry on cell performance, expected results are : (1) develop an improved understanding of the Li/S chemistry and ways to control it; (2) develop electrolyte formulations able to stabilize the Li anode; (3) develop new composite cathode microstructures with enhanced cathode performance; and (4) develop a Li/S cell operating for 500 cycles at an efficiency greater than 80%.

Collaborations. This is a collaborative work combining first-principles modeling (Perla Balbuena, TAMU), mesoscopic level modelling (Partha Mukherjee, TAMU), and synthesis, fabrication, and test of Li/S materials and cells (Vilas Pol, Purdue University).

Milestones

1. Complete coin cell testing of various C/S electrodes. (December 2015 – Complete)
2. Using electrochemical and transport modeling, gain an understanding of the mesoscopic interfacial reactions. (March 2016 – Complete)
3. Complete evaluation of deposition-induced stress and mechanical interplay. (June 2016 – Complete)
4. Determination of SEI nucleation and growth at the PS/Li anode interface. *Go/No-Go*: Determine reasons for electrolyte failure or success. (September 2016)

Progress Report

Dissolution/Deposition-induced Stress and Mechanical Interplay in the Li-S Cathode. A poromechanics-based computational methodology has been developed to evaluate the effect of mechanical interplay on electrode performance.

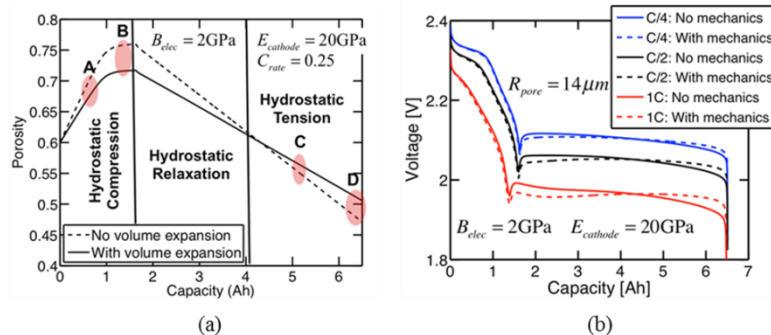


Figure 83. (a) Variation in microstructure porosity during discharge of a Li-S cell at C/4 rate. Three regimes with hydrostatic compression, relaxation, and tension are shown. Cell porosity with and without volume expansion is indicated with solid and dashed lines, respectively. (b) Cell performance at three different C-rates for a particular microstructure with and without mechanical expansion.

During the discharge process, the dissolution-precipitation induced change in volume results into three major regimes. “Hydrostatic compression” is due to dissolution of solid sulfur. “Hydrostatic relaxation” is due to precipitation of Li_2S , where the carbon substrate relaxes and comes back to the initial configuration. Toward the end of the discharge process, the volume occupied by the precipitated lithium sulfide exceeds the volume occupied by initially present solid sulfur. At this point, the electrolyte inside the cathode experiences higher internal pressure as compared to the electrolyte outside the cathode microstructure. Hence, the porous carbon substrate experiences a tensile hydrostatic stress to maintain equilibrium, and expands in size. This region is clearly denoted as the “hydrostatic tension” regime. Mechanical deformation (Figure 83b) decreases the extent of pore volume change experienced during dissolution of solid sulfur and precipitation of Li_2S . In the “hydrostatic relaxation” and “hydrostatic tension” regimes, the specific surface area is decreased and increased, respectively. Hence, in the second plateau, mechanical deformation initially decreases the cell voltage. Toward the end of the discharge process, cell voltage observed with volume expansion increases above that experienced without mechanical expansion.

Reactivity of the Lithium Anode. The effect of the oxidant LiNO_3 on the formation of protective layer on the Li-metal surface has been extensively examined with DFT and AIMD simulations. In the absence of soluble PS species, it is found that LiNO_3 rapidly reacts to form Li_2O and Li_3N that deposit on the surface. However, when long PS species are dissolved in the electrolyte, even faster reactions form Li_2S , which slows down the reduction of LiNO_3 . In an extended timeframe, results of DFT simulations suggest that LiNO_3 may react with Li_2S to form high-valence sulfur compounds. It is found that the formation of sulfates and sulfites is thermodynamically favorable. AIMD simulations determined the minimum thickness of the sulfate layer that would exert a protective role controlling further PS decomposition.

Interactions between Sulfur and Carbon in the Composite Cathode. DFT and AIMD simulations were conducted to determine the nature of the C-S interaction. It was concluded that in spite of the presence of vacancies or oxygenated surface groups, sulfur is very stable and only physical interactions are present. However, after lithiation, reduced sulfur interacts with the unsaturated carbon atoms, as shown previously.

Experimental Tests of Alternative Cathodes. Encapsulation of premade lithium sulfide particles with carbon to enhance conductivity via an *in situ* sonochemical synthesis approach. In this single step process, lithium sulfide is dispersed within an organic solvent of di(phenyl)methane via sonochemical energy. In the presence of argon gas, high-intensity sonochemical energy induces pyrolytic decomposition of phenyl groups into high purity carbon. The produced carbon deposits around the present lithium sulfide particles to create a secondary particle structure. The $\text{Li}_2\text{S}@\text{C}$ product is collected via centrifugation as the precipitate phase, and excess di(phenyl)methane is removed under low heat at temperature of ca. 100°C in an inert atmosphere. Current electrochemical data is being generated to elucidate the long-term cycling performance and rate performance of the $\text{Li}_2\text{S}@\text{C}$ material.

Patents/Publications/Presentations

Publications

- Liu, Z., and D. Hubble, P. B. Balbuena, and P. P. Mukherjee. “Adsorption of Insoluble Polysulfides Li_2S_x ($x = 1, 2$) on Li_2S Surfaces.” *Phys. Chem. Chem. Phys.* 17 (2015): 9032-9039.
- Camacho-Forero, Luis E., and Taylor W. Smith, Samuel Bertolini, and Perla B. Balbuena. “Reactivity at the Lithium-Metal Anode Surface of Lithium-Sulfur Batteries.” *J. Phys. Chem. C* 119, no. 48 (2015): 26828-26839.
- Tsai, C. S. J., and A. D. Dysart, J. H. Beltz, and V. G. Pol. “Identification and Mitigation of Generated Solid By-Products during Advanced Electrode Materials Processing.” *Environ. Sci. Technol.* 50, no. 5 (2016): 2627-2634.
- Dysart, Arthur A., and Juan C. Burgos, Aashutosh Mistry, Chien-Fan Chen, Zhixiao Liu, Perla B. Balbuena, Partha P. Mukherjee, and Vilas G. Pol. “Towards Next Generation Lithium-Sulfur Batteries: Non-Conventional Carbon Compartments/Sulfur Electrodes and Multi-Scale Analysis.” *J. Electrochem. Soc.* 163, no. 5 (2016): A730-741.
- Liu, Zhixiao, and Samuel Bertolini, Partha Mukherjee, and Perla B. Balbuena. “ Li_2S Film Formation on Lithium Anode Surface of Li-S batteries.” *ACS Appl. Mat. & Interfaces* 8, no. 7 (2016): 4700-4708.
- Kamphaus, Ethan, and Perla B. Balbuena. “Long-Chain Polysulfide Retention at the Cathode of Li-S Batteries.” *J. Phys. Chem. C* 120, no. 8 (2016): 4296-4305.
- Liu, Zhixiao, and Perla B. Balbuena and Partha P. Mukherjee. “Evaluating Silicene as a Potential Cathode Host to Immobilize Polysulfides in Lithium-Sulfur Batteries.” *J. Coord. Chem.* In press.
- Barai, P., and A. Mistry and P. P. Mukherjee. “Poromechanical Effect in the Lithium-Sulfur Battery Cathode.” *Extreme Mechanics Letters* (2016). doi: 10.1016/j.eml.2016.05.007

Presentation

- BMR Program Review Meeting, LBNL, Berkeley, California (January 22, 2016): “Addressing Internal ‘Shuttle’ Effect: Electrolyte Design and Cathode Morphology Evolution in Li-S Batteries DE-EE-0006832”; P. B. Balbuena.

Task 8.8 – Mechanistic Investigation for the Rechargeable Lithium–Sulfur Batteries (Deyang Qu, University of Wisconsin Milwaukee; Xiao-Qing Yang, BNL)

Project Objective. The primary objectives are to conduct focused fundamental research on the mechanism for Li-S batteries, investigate the kinetics of the sulfur redox reaction, develop electrolyte and additives to increase the solubility of Li_2S , and optimize the sulfur electrode design. In this objective, special attention will be paid to the investigation of highly soluble polysulfide species including both ions and radicals, and the potential chemical equilibrium among them. Through such investigation, the detail pathway for polysulfide shuttle will be better understood, and alleviation of the obstacle will be explored.

Project Impact. Rechargeable Li-S battery is a potential candidate to meet the demand of high-energy density for next generation rechargeable Li battery. Through the fundamental mechanistic investigation, the mechanism of Li-S batteries can be better understood, which will lead to the material design and battery engineering to materialize the potential of Li-S chemistry. Li-S batteries could enable competitive market entry of EVs by reducing the cost and extending the driving distance per charge.

One-Year Goals. The project has the following goals: (1) complete development of an analytical method for the quantitative and qualitative determination of all polysulfide ions in nonaqueous electrolytes, and (2) complete the initial design of an *in situ* electrochemical study for the sulfur reduction reaction.

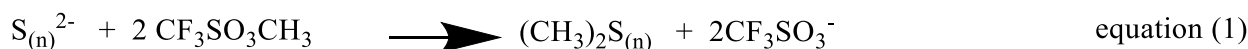
Collaborations. The principal investigator is the Johnson Control Endowed Chair Professor; the University of Wisconsin Milwaukee and BNL team has close collaboration with Johnson Controls' scientists and engineers. The collaboration enables the team to validate the outcomes of fundamental research in pilot-scale cells. This team has been working closely with top scientists on new material synthesis at ANL, LBNL, and PNNL, with U.S. industrial collaborators at General Motors, Duracell, and Johnson Control, as well as international collaborators in Japan and South Korea. These collaborations will be strengthened and expanded to give this project a vision both on today's state-of-the-art technology and on tomorrow's technology in development, with feedback from the material designer and synthesizers upstream as well as from the industrial end users downstream.

Milestones

1. Complete literature review and feasibility study of the methods for polysulfide determination. (December 2015 – Complete)
2. Complete development of the essay to determine all polysulfide ions. (March 2016 – Complete)
3. Complete design qualification for an *in situ* electrochemical high performance liquid chromatography MS (HPLC-MS) cell for Li-S investigation. (June 2016 – Complete)
4. Complete identification of polysulfide ions formed from elemental sulfur. (September 2016 – In progress)

Progress Report

This quarter, a reliable *in situ* electrochemical HPLC-MS method was developed for the investigation of Li-S batteries. The polysulfide ions formed during the first reduction wave of sulfur in Li-S battery were determined through both *in situ* derivatization, in which the derivatizer (shown in equation 1) was added in the electrolyte, and *ex situ* derivatization, where polysulfide ions were derivatized after taking the electrolyte out of the cell. As shown in Figure 84, the derivatized polysulfide ions were proven inert chemically and electrochemically in the potential window of interest. Therefore, by using *in situ* derivatization, the subsequent fast chemical reactions between the electrochemically formed polysulfides and sulfur during the timeframe of *ex situ* procedures can be avoided. It was found that the major polysulfide ions formed at the first reduction wave of elemental sulfur were the S_4^{2-} and S_5^{2-} species, while the widely accepted reduction products of S_8^{2-} and S_6^{2-} for the first reduction wave were in low abundance.



In Figure 85, Me_2S_8 (Me: $-CH_3$) was hardly present in the catholyte in which the derivatizer (methyl triflate) was added (*in situ*), and neither Me_2S_7 nor Me_2S_6 were the most abundant species in that catholyte. In other

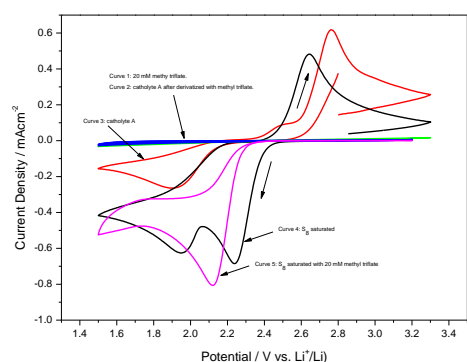


Figure 84. Cyclic voltammograms of different catholytes with 1M LiTFSi/DME on glassy carbon electrode. Scan rate of 30mV/s. Black line = S_8 saturated electrolyte; red line = simulated electrolyte A; blue line = 20mM methyl triflate; green line = simulated electrolyte A after derivatization by methyl triflate; magenta line = S_8 saturated electrolyte with 20mM methyl triflate.

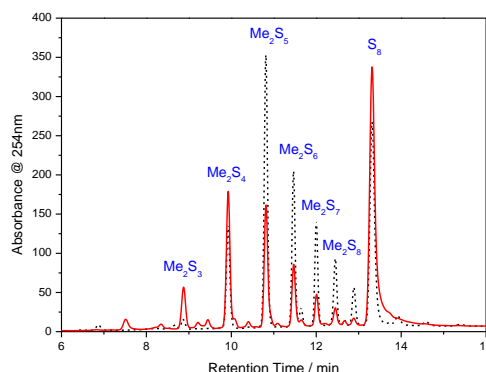


Figure 85. HPLC/UV chromatogram for the derivatized electrolytes from Li-S batteries polarized at 2.3V (vs Li/Li⁺). Black line = *ex situ* derivatization method; red line = *in situ* derivatization method.

words, the immediate product of the electrochemical reduction of sulfur was not S_8^{2-} . Significantly more long chain polysulfide ions were found in the *ex situ* derivatized catholyte. Although both cells were discharged to similar capacity, more S_8 was consumed in the catholyte without the addition of methyl triflate as

shown in Table 5. The consumption of sulfur which cannot be accounted electrochemically can be attributed to the chemical reactions between the polysulfide and sulfur.

Table 5. Data indicating that more S_8 was consumed in the catholyte without the addition of methyl triflate.

Derivatization method	Discharge capacity at 2.3V (mAh)	% sulfur remains based on 2-electron reduction	% elemental sulfur from HPLC/UV measurement
<i>In situ</i>	1.42	34.0%	37.9%
<i>Ex situ</i>	1.43	33.3%	24.9%

Patents/Publications/Presentations

Publication

- Zheng, Dong, and Xiaoqing Yang and Deyang Qu. “Stability of the Solid Electrolyte Interface on the Li Electrode in Li-S Batteries.” *ACS Appl. Mater. & Interface* 8 (2016): 10360-10366.

Presentations

- ECS Midwest chapter (April 5, 2016): “Rechargeable Lithium Sulfur Batteries – The Mechanism of Sulfur Redox Reaction.”
- China International Conference on the Frontier Technology of Advanced Batteries, CIBF2016, Shenzhen, China (May 24-26, 2016): “Quantitative and Qualitative Analysis of Dissolved Polysulfide Ions Formed during the Charge and Discharge of Li-S Batteries.”

Task 8.9 – Statically and Dynamically Stable Lithium–Sulfur Batteries (Arumugam Manthiram, U Texas Austin)

Project Objective. The project objective is to develop statically and dynamically stable Li-S batteries by integrating polysulfide-filter-coated separators with a protected Li-metal anode through additives or a modified Li_2S cathode with little or no charge barrier during first charge. The project includes demonstration of electrochemically stable cells with sulfur capacities of $> 1,000 \text{ mA h g}^{-1}$ and cycle life in excess of 500 cycles (dynamic stability) along with positive storage properties (static stability) at $> 70 \text{ wt\%}$ sulfur content and $\sim 5 \text{ mg cm}^{-2}$ loading that will make the Li-S technology superior to the present-day Li-ion technology in terms of cost and cell performance.

Project Impact. The combination of polysulfide-filter-coated separator, Li-metal-protection additives, and Li_2S cathode modifications offers a viable approach to overcome the persistent problems of Li-S batteries. This project is systematically integrating the basic science understanding gained in its laboratory of these three aspects to develop the Li-S technology as the next-generation power source for EVs. The project targets demonstrating cells with sulfur capacities of over $1,000 \text{ mA h g}^{-1}$ and cycle life in excess of 500 cycles along with good storage properties at high sulfur content and loading that will make the Li-S technology superior to the present-day Li-ion technology in terms of cost and cell performance.

Approach. Electrochemical stability of the Li-S cells is improved by three complementary approaches. (i) The first approach focuses on the establishment of an electrochemically stable cathode environment by employing PS-filter-coated separators. The PS-filter coatings aim to suppress the severe polysulfide diffusion and improve the redox capability of the Li-S cells with high-sulfur loadings. The study includes an understanding of the materials characteristics, fabrication parameters, electrochemical properties, and battery performance of the PS-filter-coated separators. (ii) The second approach focuses on electrode engineering from two aspects. First, the investigation of a Li-metal anode with coating- and additive-supporting approaches is aimed at improving the safety of Li-S cells. Second, the research on activated- Li_2S cathode with little or no charge-barrier will promote the performance and safety of the C- Li_2S cells. (iii) The integration of approaches (i) and (ii) would create statically and dynamically stable Li-S batteries for EVs.

Out-Year Goals. The overall goal is to develop statically and dynamically stable Li-S batteries with custom cathode and stabilized anode active materials. In addition to developing a high-performance battery system, a fundamental understanding of the structure-configuration-performance relationships will be established. Specifically, optimization of the electrochemical and engineering parameters of polysulfide-filter-coated separators aims at comprehensively investigating different coating materials and their corresponding coating techniques for realizing various high-performance custom separators. The developed polysulfide-filter-coated separators can be coupled with pure sulfur cathodes and allow pure sulfur cathodes to attain high sulfur loading and content. Multifunctional polysulfide-filter-coated separators, high-loading sulfur cathodes, stabilized-Li-metal anodes, activated- Li_2S cathodes, and novel approaches on the cell design and optimization are anticipated to provide an in-depth understanding of the full-cell battery chemistry and to realize statically and dynamically stable Li-S batteries for EVs.

Collaborations. This project collaborates with ORNL.

Milestones

1. Database of coating materials and polysulfide-filter coatings established. (December 2015 – Complete)
2. Database of fabrication parameters and S-filter-coated separators established. (March 16 – Complete)
3. Low-capacity fade rate and self-discharge testing completed. (June 2016 – Ongoing)
4. *Go/No-Go*: Lightweight design and electrochemical stability demonstrated. (September 2016 – Ongoing)

Progress Report

This quarter, the electrochemical analysis of Li-S batteries was launched employing various PS-filter-coated separators. The study focused on 12 carbon materials categorized into four groups: spherical, fibrous, tubular, and flaky carbon materials. Different PS-filter coatings were successfully used for reducing the fast capacity fade during dynamic cell cycling and suppressing the severe self-discharge during static cell resting. Preliminary battery performances show improved static and dynamic electrochemical stabilities. This quarter, therefore, work was concentrated on Milestone 3. By achieving higher performance values with the assembled cells as compared to the targeted values in the Milestone, the *Go/No-Go Milestone* was passed.

The dynamic electrochemical stability was examined with various PS-filter-coated separators. Figure 86a-b shows the cycle performances of the PS-filter-coated separators that were fabricated through two optimized fabrication processes. Figure 86a shows the electrochemical characteristics of the cell employing the first optimized fabrication method. Various spherical carbons were coated onto a Celgard separator with the support of single wall carbon nanotubes (SWCNTs). The spherical-carbon/SWCNT-coated separators that were prepared by vacuum-filtration method were optimized by using SWCNT as the conducting binder. The results demonstrate that the spherical-carbon/SWCNT-coated separators utilizing microporous spherical carbon (MPC) exhibit a high discharge capacity of 1,294 mAh g⁻¹. The corresponding areal capacity attains 4.9 mAh cm⁻². Both values exceed the targeted, milestone capacity values of 1,000 mAh g⁻¹ and 4.0 mAh cm⁻². The cells also have a promising reversible discharge capacity of above 600 mAh g⁻¹ with a low capacity fade rate of 0.26% cycle⁻¹ after 200 cycles.

Another case is the use of the layer-by-layer (LBL) vacuum-filtration technique for preparing optimized PS-filter-coated separators. The LBL carbon nanofiber (CNF)-coated separator is shown in Figure 86b. The fibrous carbon material has low surface area without microporous PS-trapping sites. It was demonstrated with these nonporous samples that an optimized LBL coating configuration provides the corresponding cells with high electrochemical utilization and stable cyclability. This new finding enables the simplification of fabrication and volume production. Besides attaining the targeted areal capacity value, specifically, the cells employing various CNF coatings show stable cycling performance with a high-capacity retention rate of 60% and a low capacity fade rate of 0.07 % per cycle for 400 cycles. In general, the excellent cycling performance is because the coating layer forms polysulfide traps and acts as an upper current collector to reutilize/reactivate the trapped active materials. The LBL CNF-coated separators also have good static electrochemical stability with limited self-discharge (Figure 86c). The project monitored the remaining capacity values after resting for 0, 15, 30, and 60 days. The preliminary results show that the cells retained a high fraction of the initial capacity values after resting for 60 days. The capacity retention rate and fade rate attain 75% and 0.003 day⁻¹ with the CNF#3 coating.

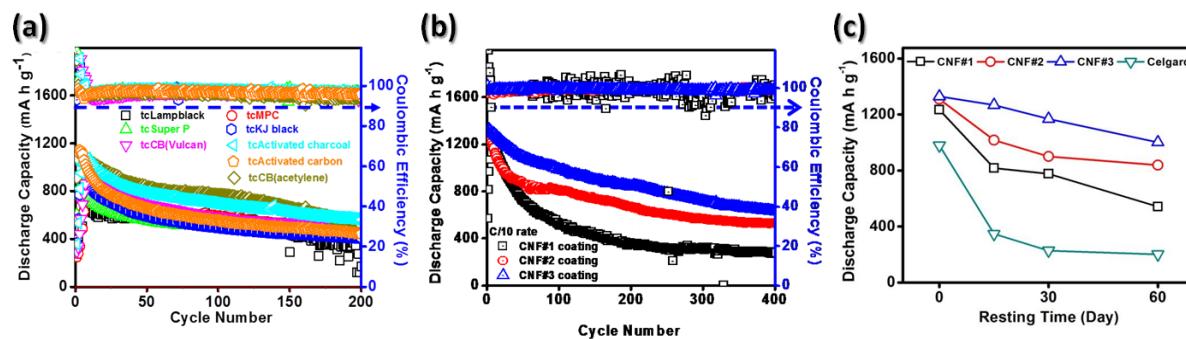


Figure 86. Dynamic cycling performance of the cells employing (a) spherical-carbon/single wall carbon nanotube (SWCNT)-coated separators and (b) layer-by-layer (LBL) carbon nanofiber (CNF)-coated separators. Static self-discharge analysis of the cells with and without the LBL CNF-coated separator (c) LBL multiwall carbon nanotube (MWCNT)-coated separator.

Patents/Publications/Presentations

Presentations

- Materials Challenges in Alternative and Renewable Energy (MCARE) Meeting, Clearwater, Florida (April 17-21, 2016): “Next Generation Battery Chemistries: Materials Challenges and Prospects”; A. Manthiram. Invited plenary talk.
- 229th Electrochemical Society Meeting, San Diego, California (May 29 – June 3, 2016): “High-energy-density, Long-life Lithium-sulfur Batteries”; A. Manthiram. Invited.
- DOE Annual Merit Review Meeting, Washington, D. C. (June 6-10, 2016): “Statically and Dynamically Stable Lithium-sulfur Batteries”; A. Manthiram.
- China Conference on Energy Materials and Energy Chemistry 2016, Hunan University, Changsha, China, (June 15-16, 2016): “Conversion-reaction Cathodes for Electrical Energy Storage: Challenges and Prospects”; A. Manthiram. Invited plenary talk.
- 18th International Meeting on Lithium Batteries, Chicago, Illinois (June 18-24, 2016): “Tandem Sulfur Cathodes with High Areal Capacity for Li-S Batteries”; C.-H. Chang, S.-H. Chung, and A. Manthiram.
- 18th International Meeting on Lithium Batteries, Chicago, Illinois (June 18-24, 2016): “Development of High-performance, High-loading Sulfur Cathodes”; S.-H. Chung, C.-H. Chang, and A. Manthiram.
- 18th International Meeting on Lithium Batteries, Chicago, Illinois (June 18-24, 2016): “Metal-Sulfur Batteries with High Sulfur Loading”; A. Manthiram. Invited.

TASK 9 – LITHIUM–AIR BATTERIES

Summary and Highlights

High-density energy storage systems are critical for EVs required by the EV Everywhere Grand Challenge. Conventional Li-ion batteries still cannot fully satisfy the ever-increasing needs because of their limited energy density, high cost, and safety concerns. As an alternative, the rechargeable Li-O₂ battery has the potential to be used for long-range EVs. The practical energy density of a Li-O₂ battery is expected to be ~ 800 Wh kg⁻¹. The advantages of Li-O₂ batteries come from their open structure; that is, they can absorb the active cathode material (oxygen) from the surrounding environment instead of carrying it within the batteries. However, the open structure of Li-O₂ batteries also leads to several disadvantages. The energy density of Li-O₂ batteries will be much lower if oxygen has to be provided by an onboard container. Although significant progress has been made in recent years on the fundamental properties of Li-O₂ batteries, the research in this field is still in an early stage, and many barriers must be overcome before practical applications. The main barriers include:

- Instability of electrolytes. Superoxide species generated during discharge or O₂ reduction process is highly reactive with electrolyte and other components in the battery. Electrolyte decomposition during charge or O₂ evolution process is also significant due to high over-potentials.
- Instability of air electrode (dominated by carbonaceous materials) and other battery components (such as separators and binders) during charge/discharge processes in an O-rich environment.
- Limited cyclability of the battery associated with instability of the electrolyte and other components of the batteries.
- Low energy efficiency associated with large over-potential and poor cyclability of Li-O₂ batteries.
- Low power rate capability due to electrode blocking by the reaction products.
- Absence of a low-cost, high-efficiency oxygen supply system (such as oxygen selective membrane).

The main goal of the PNNL Task is to provide a better understanding on the fundamental reaction mechanisms of Li-O₂ batteries and identify the required components (especially electrolytes and electrodes) for stable operation of Li-O₂ batteries. The PNNL researchers will investigate stable electrolytes and oxygen evolution reaction (OER) catalysts to reduce the charging overvoltage of Li-O₂ batteries and improve their cycling stability. New electrolytes will be combined with stable air electrodes to ensure their stability during Li-O₂ reaction. Considering the difficulties in maintaining the stability of conventional liquid electrolyte, the Liox team will explore the use of a nonvolatile, inorganic molten salt comprising nitrate anions and operating Li-O₂ cells at elevated temperature (> 80°C). It is expected that these Li-O₂ cells will have a long cycle life, low over potential, and improved robustness under ambient air compared to current Li-air batteries. At ANL, new cathode materials and electrolytes for Li-air batteries will be developed for Li-O₂ batteries with long cycle life, high capacity, and high efficiency. The state-of-the-art characterization techniques and computational methodologies will be used to understand the charge and discharge chemistries. The University of Massachusetts/BNL team will investigate the root causes of the major obstacles of the air cathode in the Li-air batteries. Special attention will be paid to optimizing high surface carbon material used in the gas diffusion electrode, catalysts, electrolyte, and additives stable in Li-air system and with capability to dissolve Li oxide and peroxide. Success of this project will establish a solid foundation for further development of Li-O₂ batteries toward practical applications for long-range EVs. The fundamental understanding and breakthrough in Li-O₂ batteries may also provide insight on improving the performance of Li-S batteries and other energy storage systems based on chemical conversion processes.

Highlight. The PNNL group demonstrated a non-carbon based air electrode based on boron carbide (B₄C), which exhibits a much better cycling stability than those of TiC electrode reported before.

Task 9.1 – Rechargeable Lithium–Air Batteries (Ji-Guang Zhang and Wu Xu, PNNL)

Project Objective. The project objective is to develop stable electrolyte and air electrode to reduce the charging overvoltage and improve the cycling stability of rechargeable lithium-oxygen (Li-O₂) batteries. New air electrode will be synthesized to improve the capacity and cycling stability of Li-O₂ batteries. New electrolytes will be investigated to ensure their stability during Li-O₂ reaction.

Project Impact. Li-air batteries have a theoretical specific energy that is more than five times that of state-of-the-art Li-ion batteries and are potential candidates for use in next-generation, long-range EVs. Unfortunately, the poor cycling stability and low Coulombic efficiency of Li-air batteries have prevented practical application to date. This work will explore a new electrolyte and electrode that could lead to long cyclability and high Coulombic efficiency in Li-air batteries that can be used in the next generation EVs required by the EV Everywhere Grand Challenge.

Out-Year Goals. The long-term goal of the proposed work is to enable rechargeable Li-air batteries with a specific energy of 800 Wh/kg at cell level, 1000 deep-discharge cycles, improved abuse tolerance, and less than 20% capacity fade over a 10-year period to accelerate commercialization of long-range EVs.

Collaborations. This project engages in collaboration with the following:

- Chunmei Ben (NREL) – Metal oxide coated glassy carbon electrode
- Chongmin Wang (PNNL) – Characterization of cycled air electrodes by TEM/SEM

Milestones

1. Synthesize and characterize the modified solvent and the TM oxide catalyst coated carbon material. (December 2015 – Complete)
2. Identify a modified carbon air electrode that is stable in a Li-O₂ battery by using conventional glyme solvent. (June 2016 – Complete)
3. Demonstrate stable operation of Li-O₂ battery by employing the new electrolyte and modified air electrode. (September 2016 – Ongoing)

Progress Report

This quarter, the electrochemical activity and chemical stability of boron carbide (B_4C) were systematically investigated as a non-carbon based oxygen electrode material for aprotic $Li-O_2$ batteries. XRD results demonstrate that B_4C nanoparticles are stable against Li_2O_2 and KO_2 . Due to the relatively low electronic conductivity ($\sim 1 \text{ S cm}^{-1}$) and specific surface area ($\sim 12.5 \text{ m}^2 \text{ g}^{-1}$) of B_4C powders, the content of non-conductive PTFE binder has been found to play an important role in the electrode performance, and the optimal PTFE content is 7 wt% in the B_4C /PTFE air electrode. $Li-O_2$ cells using the optimized B_4C -based air electrodes exhibit much better cycling stability than those using TiC-based air electrodes in 1 M LiTf-Tetraglyme electrolyte (Figure 87). The performance degradation of B_4C -based electrode is mainly due to the loss of active sites on B_4C electrode during cycles as identified by the structure and composition characterizations. These results clearly demonstrate that B_4C is a very promising alternative oxygen electrode material for aprotic $Li-O_2$ batteries. It can also be used as a standard electrode to investigate the stability of electrolytes.

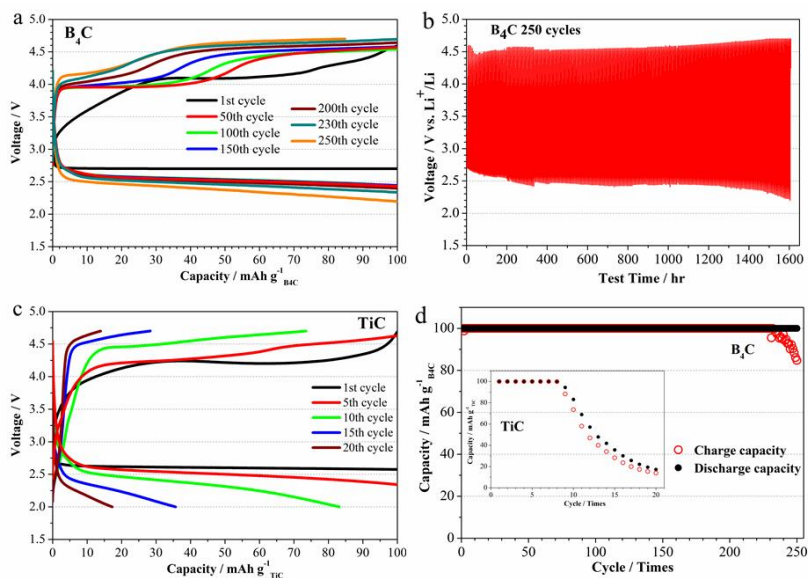


Figure 87. Cycling performance of B_4C cell and TiC cell under 100 mAh g^{-1} at 0.1 mA cm^{-2} within the voltage range of 2.0–4.7 V. (a-b) Discharge and charge profiles of B_4C cell. (c) Discharge and charge profiles of TiC cell. (d) Capacity with cycles.

A facial method was developed to pre-treat the CNTs-based air electrodes to generate an ultrathin artificial layer on the air electrode surface. The pre-treated CNTs air electrodes (Samples A, B, C and D) show improved cycle life in $Li-O_2$ cells with the conventional 1.0 M LiTf-Tetraglyme electrolyte under the 1000 mAh/g capacity limited test protocol (Figure 88). The optimized pre-treatment (Sample C) can enable the cycle life to 110 cycles from the 40 cycles for pristine CNTs electrode. The cycled samples will be further analyzed by microscopic characterization and XPS spectra next quarter.

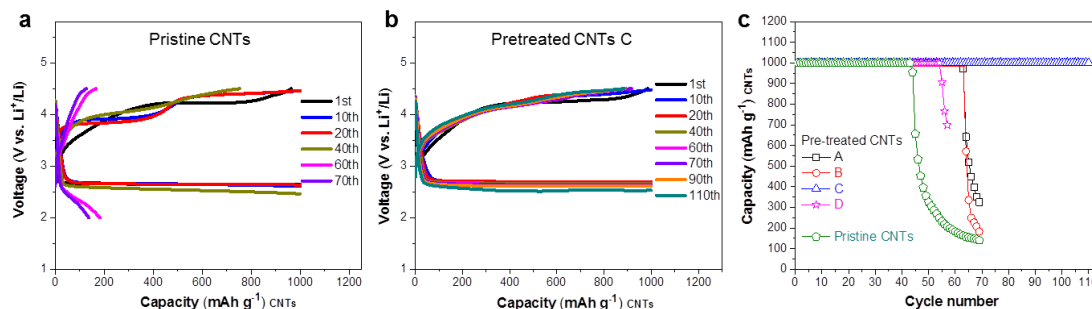


Figure 88. Cycling performance of $Li-O_2$ cells with carbon nanotubes (CNTs)-based air electrodes before and after pretreatment under 1000 mAh g^{-1} at 0.1 mA cm^{-2} within the voltage range of 2.0–4.5 V. (a-b) Discharge and charge profiles of pristine CNTs electrode (a) and pretreated CNTs electrode C. (c) Capacity with cycling of pristine CNTs and four pretreated CNTs.

Patents/Publications/Presentations

Publications

- Liu, B., and P. Yan, W. Xu,* J. Zheng, Y. He, L. Luo, M. E. Bowden, C.-M. Wang,* and J.-G. Zhang.* “Electrochemically Formed Ultrafine Metal Oxide Nanocatalysts for High-performance Lithium-oxygen Batteries.” *Nano Lett.* (2016), in press. doi: 10.1021/acs.nanolett.6b01556
- Song, S., and W. Xu,* R. Cao, L. Luo, M. H. Engelhard, M. E. Bowden, B. Liu, L. Estevez, C.-M. Wang, and J.-G. Zhang.* “B₄C as a Stable Non-Carbon Based Oxygen Electrode Material for Lithium-oxygen Batteries.” Submitted for publication.

Presentations

- 9th Symposium on Energy Storage Beyond Lithium-Ion, Richland, Washington (May 24-26, 2016): “Optimization of Concentrated DMSO-based Electrolytes for Stable Cycling of Li-O₂ Batteries”; B. Liu, W. Xu, P. Yan, M. H. Engelhard, X. Sun, D. Mei, S. T. Kim, J. Cho, C.-M. Wang, and J.-G. Zhang. Poster.
- 9th Symposium on Energy Storage Beyond Lithium-Ion, Richland, Washington (May 24-26, 2016): “B₄C as a Stable and Non-Carbon Based Oxygen Electrode Material for Aprotic Lithium-oxygen Batteries”; S. Song, W. Xu, R. Cao, L. Luo, M. H. Engelhard, M. E. Bowden, B. Liu, L. Estevez, C.-M. Wang, and J.-G. Zhang.* Poster.
- 18th International Meeting on Lithium Batteries, Chicago, Illinois (June 19-24, 2016): “B₄C as a Stable and Non-Carbon Based Oxygen Electrode Material for Aprotic Lithium-oxygen Batteries”; S. Song, W. Xu, R. Cao, L. Luo, M. H. Engelhard, M. E. Bowden, B. Liu, L. Estevez, C.-M. Wang, and J.-G. Zhang.* Poster.

Task 9.2 – Efficient Rechargeable Li/O₂ Batteries Utilizing Stable Inorganic Molten Salt Electrolytes (Vincent Giordani, Liox)

Project Objective. The project objective is to develop high specific energy, rechargeable Li-air batteries having lower overpotential and improved robustness under ambient air compared to current Li-air batteries. The technical approach involves replacing traditional organic and aqueous electrolytes with a nonvolatile, inorganic molten salt comprising nitrate anions and operating the cell at elevated temperature (> 80°C). The research methodology includes powerful *in situ* spectroscopic techniques coupled to electrochemical measurements (for example, electrochemical MS) designed to provide quantitative information about the nature of chemical and electrochemical reactions occurring in the air electrode.

Project Impact. If successful, this project will solve particularly intractable problems relating to air electrode efficiency, stability, and tolerance to the ambient environment. Furthermore, these solutions may translate into reduced complexity in the design of a Li-air stack and system, which in turn may improve prospects for use of Li-air batteries in EVs. Additionally, the project will provide materials and technical concepts relevant for developing other medium temperature molten salt Li battery systems of high specific energy, which may also have attractive features for EVs.

Out-Year Goals. The long-term goal is to develop Li-air batteries comprising inorganic molten salt electrolytes and protected lithium anodes that demonstrate high (> 500 Wh/kg) specific energy and efficient cyclability in ambient air. By the end of the project, it is anticipated that problems hindering use of both the Li anode and air electrode will be overcome due to materials advances and strategies enabled within the intermediate (> 80°C) operating temperature range of the system under development.

Collaborations. This project engages in collaboration with the following:

- Bryan McCloskey (LBNL): Analysis of air electrode and electrolyte
- Julia Greer (Caltech): Design of air electrode materials and structures

Milestones

1. Quantify e⁻/O₂ and oxygen evolution reaction / oxygen reduction reaction (OER/ORR) ratio for metals and metal alloys in half cells under pure O₂. (December 2015 – Complete)
2. Determine the kinetics and mechanisms of electrochemical nitrate reduction in the presence of O₂, H₂O, and CO₂. (March 2016 – Complete)
3. Synthesize electronically conductive ceramics and cermets. (March 2016 – Complete)
4. Quantify e⁻/O₂ and OER/ORR ratio for electronically conductive ceramics and cermets in half cells under pure O₂. (June 2016 – Complete)
5. *Go-No Go*: Demonstrate e⁻/O₂=2 and OER/ORR ratio=1, +/- 5% and correcting for the effect of Li₂O₂ crossover. (June 2016 – Complete)
6. Demonstrate Li₂O yield=1, e⁻/O₂=4 and OER/ORR ratio=1, +/- 5%. (September 2016 – Ongoing)
7. Demonstrate discharge specific power and power density ≥ 800 W/kg and ≥ 1600 W/L, respectively, based on air electrode mass and volume. (September 2016 – Ongoing)
8. Demonstrate solid electrolytes that are stable to molten nitrate electrolytes over a temperature range of 100°C to 150°C for 6 months or greater. (September 2016 – Ongoing)

Progress Report

This quarter, the project quantified e^-/O_2 and OER/ORR molar ratios for electronically conductive ceramics and cermets-based cathode in Li/O_2 cells. Table 6 lists data obtained for IrO_2 , RuO_2 , LSM-Ni and TiC, alongside carbon and precious metal cathode materials. Additional materials such as NbC, C_3N_4 , SiN, TiN, LSM-YSZ, YSZ, and SiB were also investigated, as the O_2 cathode material. Figures of Merit for this chemistry are $e^-/O_2 = 2.0$ both on discharge and on charge, and OER/ORR = 1 (overall cell cycling efficiency). Most reported materials showed $e^-/O_2 \neq 2.0$ and OER/ORR < 1, indicating existence of parasitic reactions during electrochemical cycling (for example, cathode material chemical oxidation). Interesting results were obtained with IrO_2 nanopowders. The noble metal oxide material was dry pressed on a stainless steel 316 mesh without binder or carbon additives and at a $\sim 10 \text{ mg/cm}^2$ loading. Electrochemical performance is depicted in Figure 89. Typical voltage profile for molten nitrate Li/O_2 cell is observed (very small overpotentials, that is, < 100 mV) with pressure analysis showing O_2 consumption during discharge and O_2 release during charge. The *Go/No-Go* decision point consisted in demonstrating $e^-/O_2 = 2$ and OER/ORR ratio = 1, $\pm 5\%$ and correcting for the effect of Li_2O_2 crossover. Precise O_2 quantification on the first cycle using pressure data and MS revealed e^-/O_2 ratios of 2.2 for both the discharge and the charge half-cycle, and OER/ORR ratio equals 0.95. Attempts to characterize the discharge product by XRD showed no crystalline Li_2O_2 on the surface of IrO_2 , while SEM images recorded before (at OCV) and after a 2 mAh discharge under O_2 (to 2.6 V cutoff) showed formation of a nano-textured material referred to as “platelets” on the IrO_2 particle surface (Figure 90). Further characterization is needed to confirm whether amorphous Li_2O_2 or a mixed-valence oxide/peroxide (Li_xO_2) material is formed during ORR. Extended cycling data (Figure 90b) show stable peak-to-peak O_2 pressure, which cannot be achieved when Super P carbon is used as the air cathode. *In situ* MS study during electrochemical cycling is ongoing to confirm O_2 is the only evolved gas during cell charging.

Table 6. Molten nitrate $Li-O_2$ cell characteristics: e^-/O_2 and OER/ORR ratios.

O_2 electrode	$(e^-/O_2)_{\text{discharge}}$	$(e^-/O_2)_{\text{charge}}$	OER/ORR
(Desired)	2.0	2.0	1.00
Super P Carbon	2.0	2.1	0.73
Boron-doped Carbon Nanotubes	2.0	2.3	0.49
Reduced Graphene Oxide	1.8	8.8	0.07
Nickel	2.2	8.0	0.28
Gold	3.8	5.7	0.77
Palladium	2.5	No OER	N/A
IrO_2	2.2	2.2	0.95
RuO_2	3.0	10.0	0.30
LSM-Ni	1.2	No OER	N/A
TiC	No ORR	No OER	N/A

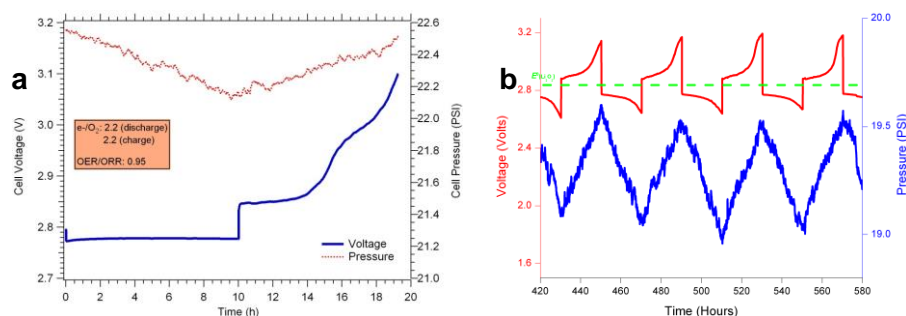


Figure 89. (a) First-cycle voltage and pressure profile for a $Li-O_2$ cell using an IrO_2 cathode. (b) Extended galvanostatic cycling (red) with O_2 pressure analysis (blue) for the $Li/LiNO_3-KNO_3-IrO_2, O_2$ cell. Green dashed line: $E_0 (2Li + O_2 = Li_2O_2)$. Current density: 0.05 mA/cm^2 .

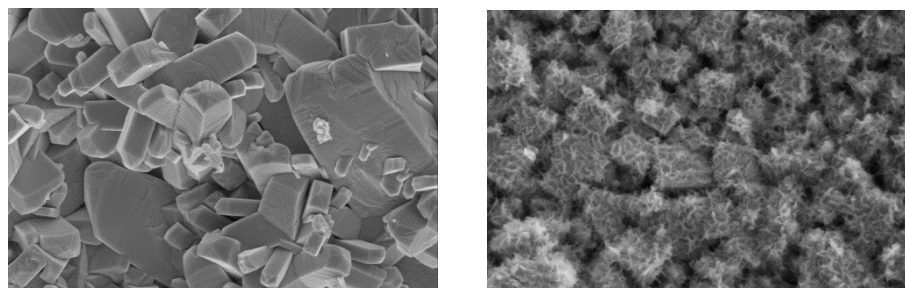


Figure 90. Scanning electron microscopy images of (a) as-prepared IrO_2 cathode prior to discharge and (b) IrO_2 cathode discharged in $LiNO_3-KNO_3$ molten salt electrolyte under O_2 ($Q = 2 \text{ mAh}$ at $j = 0.05 \text{ mA/cm}^2$).

Patents/Publications/Presentations

Presentation

- 18th International Meeting on Lithium Batteries, Chicago, Illinois (June 2016): “Intermediate Temperature Molten Salt Lithium Batteries, New Chemistries and Beyond”; V. Giordani.

Task 9.3 – Lithium–Air Batteries (Khalil Amine, ANL)

Project Objective. This project will develop new cathode materials and electrolytes for Li-air batteries for long cycle life, high capacity, and high efficiency. The goal is to obtain critical insight that will provide information on the charge and discharge processes in Li-air batteries to enable new advances to be made in their performance. This will be done using state-of-the-art characterization techniques combined with state-of-the-art computational methodologies to understand and design new materials and electrolytes for Li-air batteries.

Project Impact. The instability of current nonaqueous electrolytes and degradation of cathode materials limits the performance of Li-air batteries. The project impact will be to develop new electrolytes and cathode materials that are stable and can increase cycle life and improve efficiency of Li-air batteries.

Approach. The project is using a joint theoretical/experimental approach for design and discovery of new cathode and electrolyte materials that act synergistically to reduce charge overpotentials and increase cycle life. Synthesis methods, in combination with design principles developed from computations, are used to make new cathode architectures. Computational studies are used to help understand decomposition mechanisms of electrolytes and how to design electrolytes with improved stability. The new cathodes and electrolytes are tested in Li-O₂ cells. Characterization along with theory is used to understand the performance of the materials used in the cell and make improved materials.

Out-Year Goals. The out-year goals are to find catalysts that promote discharge product morphologies that reduce charge potentials and find electrolytes for long cycle life through testing and design.

Collaborations. This project engages in collaboration with Professor Amin Salehi (University of Illinois-Chicago), Professor Yang-Kook Sun (Hanyang University), Professor Yiyang Wu (Ohio State University), and Dr. Dengyun Zhai (China).

Milestones

1. Development of new cathode materials based on Pd nanoparticles and ZnO coated carbon that can improve efficiency of Li-O₂ batteries through control of morphology and oxygen evolution catalysis. (December 2015 – Complete)
2. Investigations of mixed K/Li salts and salt concentration on the performance of Li-O₂ batteries with goal of increasing cycle life. (March 2016 – Complete)
3. Computational studies of electrolyte stability with respect to superoxide species and salt concentrations for understanding and guiding experiment. (June 2016 – Complete)
4. Investigation of use of electrolytes to control the lithium superoxide content of discharge products of Li-O₂ batteries to help improve efficiency and cycling. (September 2016 – In progress)

Progress Report

Electrolyte decomposition was investigated for the Li-O₂ battery this project developed based on rGO with added Ir nanoparticles. This Li-O₂ cell resulted in the formation and stabilization of lithium superoxide as a discharge product. Evidence for the presence of lithium superoxide came from numerous experimental techniques. Theoretical calculations carried out indicated that the electrolyte used in this cell, tetraglyme (TEGDME), should be stable with respect to decomposition by the lithium superoxide as well as the superoxide anion for a reasonable amount of time. This is based on density functional calculations of many possible decomposition pathways from attack of the superoxide on C-H and C-O bonds. All pathways have significant lifetimes of days. This stability of the TEGDME in the presence of superoxide has been confirmed by experimental investigations of the electrolyte performance in this cell. In this work we used various techniques to detect potential decomposition products after various amounts of cycling. The Li-O₂ cell based on Ir-rGO cathode material can cycle for 40 or more cycles before failure, similar to what has been found for Li₂O₂ based Li-O₂ cells, indicating that the lithium superoxide is not any more reactive toward the electrolyte than lithium peroxide. In addition, the low charge potential will lead to fewer side reactions. The failure of the cell could be due to oxygen crossover to the anode resulting in the anode being converted to LiOH as evidenced by the corrosion of the anode and, possibly, the poisoning of Ir metal catalyst with cycling. When the cycled lithium anode is replaced by a new anode, the cell cycles for another 30 cycles.

There is little evidence of any side reactions in the Raman data for the first discharge cycle, from Raman and FTIR data after charging for up to 30 cycles, or from NMR data up to 20 cycles, although there could be a decomposition product not detected. The FTIR and Raman results also confirm that the discharge product is gone after charging. Issues with electrolyte stability and decomposition most likely still remain, similar to the electrolytes used for other Li-O₂ systems, but they do not seem any worse. The FTIR spectra of the charged Ir-rGO cathode and separators from a cathode discharged to 1000 mAh/g at a current density of 100 mAh/g after 2, 8, 30 cycles are shown in Figure 91. They show that no new peaks appear in the FTIR spectra with cycling in comparison with the pristine materials except in the separator that shows an increasing OH peak with cycling, which probably comes from the LiOH formed by the reactions occurring at the anode. The FTIR data also shows no evidence for decomposition products coming from the PVDF binder.

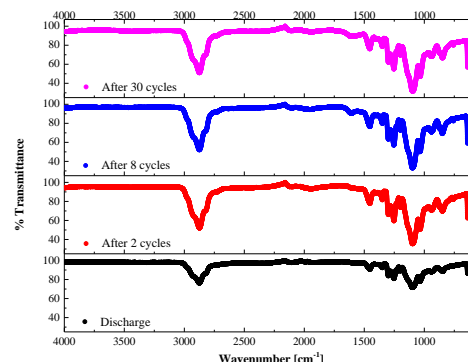


Figure 91. Fourier transform infrared spectra of the charged Ir-rGO cathode cycled in the Li-O₂ cell.

The residual electrolyte from the cathode and separator after one cycle (discharge and charge) for Ir-rGO was also extracted and subjected to NMR spectroscopy with DCCl₃ as solvent. The ¹H and ¹³C NMR results show peaks assigned to TEGDME and DCCl₃ only, and no peaks for decomposition products were detected as shown in Figure 92. Similar NMR results were also found for the second cycle and twentieth cycle. The NMR of THF-d₈ washings from the pristine electrolyte, the first cycle, and the twentieth cycle of the cathode and separator for Ir-rGO also showed no evidence of decomposition products.

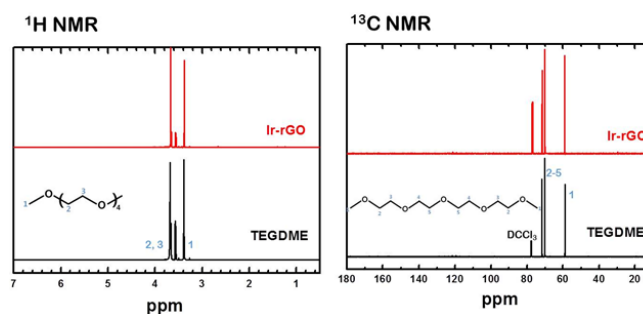


Figure 92. Nuclear magnetic resonance of the electrolyte on the cathode in the Li-O₂ cell.

Patents/Publications/Presentations

Publication

- Ma, L., and X. Luo, A. J. Kropf, J. Wen, X. Wang, S. Lee, D. J. Myers, Dean Miller, T. Wu, J. Lu, and K. Amine. “Insight into the Catalytic Mechanism of Bimetallic Platinum–Copper Core–Shell Nanostructures for Nonaqueous Oxygen Evolution Reactions.” *Nano Lett.* 16, no. 1 (2016): 781–785.

Presentation

- International Meeting on Lithium Batteries, Chicago, Illinois (June 19-24, 2016): “The Role of Lithium Superoxide in Li-O₂ Batteries”; L. A. Curtiss.

TASK 10 – SODIUM-ION BATTERIES

Summary and Highlights

To meet the challenges of powering the PHEV, the next generation of rechargeable battery systems with higher energy and power density, lower cost, better safety characteristics, and longer calendar and cycle life (beyond Li-ion batteries, which represent today's state-of-the-art technology) must be developed. Recently, Na-ion battery systems have attracted increasing attention due to the more abundant and less expensive nature of the sodium resource. The issue is not insufficient lithium on a global scale, but what fraction can be used in an economically effective manner. Most untapped lithium reserves occur in remote or politically sensitive areas. Scale-up will require a long lead time, involve heavy capital investment in mining, and may require the extraction and processing of lower quality resources, which could drive extraction costs higher. Currently, high costs remain a critical barrier to the widespread scale-up of battery energy storage. Recent computational studies on voltage, stability, and diffusion barriers of Na-ion and Li-ion materials indicate that Na-ion systems can be competitive with Li-ion systems.

The primary barriers and limitations of current state-of-the-art of Na-ion systems are as follows:

- Building a sodium battery requires redesigning battery technology to accommodate the chemical reactivity and larger size of sodium ions.
- Lithium batteries pack more energy than sodium batteries per unit mass. Therefore, for sodium batteries to reach energy densities similar to lithium batteries, the positive electrodes in the sodium battery need to hold more ions.
- Since Na-ion batteries are an emerging technology, new materials to enable sodium electrochemistry and the discovery of new redox couples along with the diagnostic studies of these new materials and redox couples are quite important.
- In sodium electrochemical systems, the greatest technical hurdles to overcome are the lack of high-performance electrode and electrolyte materials that are easy to synthesize, safe, and non-toxic, with long calendar and cycling life and low cost.
- Furthermore, fundamental scientific questions need to be elucidated, including (1) the difference in transport and kinetic behaviors between sodium and lithium in analogous electrodes; (2) sodium insertion/extraction mechanism; (3) SEI layer on the electrodes from different electrolyte systems; and (4) charge transfer in the electrolyte–electrode interface and Na⁺ ion transport through the SEI layer.

This task will use the synchrotron based *in situ* X-ray techniques and other diagnostic tools to evaluate new materials and redox couples, to explore fundamental understanding of the mechanisms governing the performance of these materials, and provide guidance for new material developments. This task will also be focused on developing advanced diagnostic characterization techniques to investigate these issues, providing solutions and guidance for the problems. The synchrotron based *in situ* X-ray techniques (XRD and hard and soft XAS) will be combined with other imaging and spectroscopic tools such as HR-TEM, MS, and TXM.

Task 10.1 – Exploratory Studies of Novel Sodium–Ion Battery Systems (Xiao-Qing Yang and Xiqian Yu, Brookhaven National Laboratory)

Project Objective. The primary objective is to develop new advanced *in situ* material characterization techniques and to apply these techniques to explore the potentials, challenges, and feasibility of new rechargeable battery systems beyond the Li-ion batteries, namely the Na-ion battery systems for PHEVs. To meet the challenges of powering the PHEV, new rechargeable battery systems with high energy and power density, low cost, good abuse tolerance, and long calendar and cycle life must be developed. This project will use the synchrotron based *in situ* X-ray diagnostic tools developed at BNL to evaluate the new materials and redox couples, exploring the fundamental understanding of the mechanisms governing the performance of these materials.

Project Impact. The VTO Multi Year Program Plan describes the goals for battery: “Specifically, lower-cost, abuse-tolerant batteries with higher energy density, higher power, better low-temperature operation, and longer lifetimes are needed for the development of the next-generation of HEVs, PHEVs, and EVs.” If this project succeeds, the knowledge gained from diagnostic studies and collaborations with U.S. industries and international research institutions will help U.S. industries develop new materials and processes for a new generation of rechargeable battery systems beyond Li-ion batteries, such as Na-ion battery systems in their efforts to reach these VTO goals.

Approach. This project will use the synchrotron based *in situ* X-ray diagnostic tools developed at BNL to evaluate the new materials and redox couples to enable a fundamental understanding of the mechanisms governing the performance of these materials and to provide guidance for new material and new technology development regarding Na-ion battery systems.

Out-Year Goals. Complete the *in situ* XRD and absorption studies of tunnel structured $\text{Na}_{0.66}[\text{Mn}_{0.66}\text{Ti}_{0.34}]\text{O}_2$ with high capacity and $\text{Na}(\text{NiCoFeTi})_{1/4}\text{O}_2$ with high rate and long cycle life capability as cathode materials for Na-ion batteries during charge-discharge cycling.

Collaborations. The BNL team has been working closely with top scientists on new material synthesis at ANL, LBNL, and PNNL, with U.S. industrial collaborators at General Motors, Duracell, and Johnson Control, and with international collaborators.

Milestones

1. Complete the synchrotron-based *in situ* XRD studies of tunnel structured $\text{Na}_{0.44}[\text{Mn}_{0.44}\text{Ti}_{0.56}]\text{O}_2$ as cathode material for Na-ion batteries during charge-discharge **cycling**. (December 2015 – Complete)
2. Complete *in situ* XRD of the $\text{Na}_{0.66}[\text{Mn}_{0.66}\text{Ti}_{0.34}]\text{O}_2$ high-capacity cathode material for Na-ion half-cell during discharge/charge cycling in a voltage range between 1.5 V and 3.9 V. (March 2016 – Complete)
3. Complete the synchrotron based XANES studies of $\text{Na}(\text{NiCoFeTi})_{1/4}\text{O}_2$ at Ni, Co, Fe, and Ti K-edge as cathode material for Na-ion batteries during charge-discharge cycling. (June 2016 – Complete)
4. Complete the synchrotron based *in situ* XRD studies of $\text{Na}(\text{NiCoFeTi})_{1/4}\text{O}_2$ as cathode material for Na-ion batteries during charge-discharge cycling. (December 2016 – In Progress)

Progress Report

This quarter, the 3rd milestones for FY 2016 were completed. BNL has been focused on studies of a novel single-phase quaternary O3-type layer-structured TM oxide $\text{Na}(\text{NiCoFeTi})_{1/4}\text{O}_2$ (O3-NCFT) synthesized by a simple solid-state reaction as a new cathode material for Na-ion batteries. It can deliver a reversible capacity of 90.6 mAh g^{-1} at a rate as high as 20 C. At 5 C, 75% of the initial specific capacity can be maintained after 400 cycles with a capacity-decay rate of 0.07% per cycle, demonstrating a superior long-term cyclability at high current density. Synchrotron based XRD characterizations revealed reversible phase transformations during the Na^+ deintercalation/intercalation process. XRD patterns were collected at a series of depths of charge and discharge states, as shown in Figure 93. The (003) and (006) peaks reflect the change of lattice parameter c , while (101) and (012) peaks mainly depend on the change of lattice parameter a and b . At the beginning of the charge, the (003) peak continuously shifted to the lower two-theta angles, indicating that a solid solution reaction was involved with c -axis expansion. As the sodium ions were extracted, when $x=0.85$, a new (003) peak emerges, as known, the (003) peak is a single-fold peak. Thus, every new (003) peak is a fingerprint for the formation of a new phase. Combining with other diffraction peaks, the new formed phase is resolved as a P3 stacking ordering. In the range of $0.85 > x > 0.75$, two-phase coexistence could be observed. During the discharge process $0.5 < x < 1$, the phase transition behavior follows an inversed way of the charge process. This reversible phase transition behavior in the range of $0.5 < x < 1$ is responsible for the excellent capacity retention.

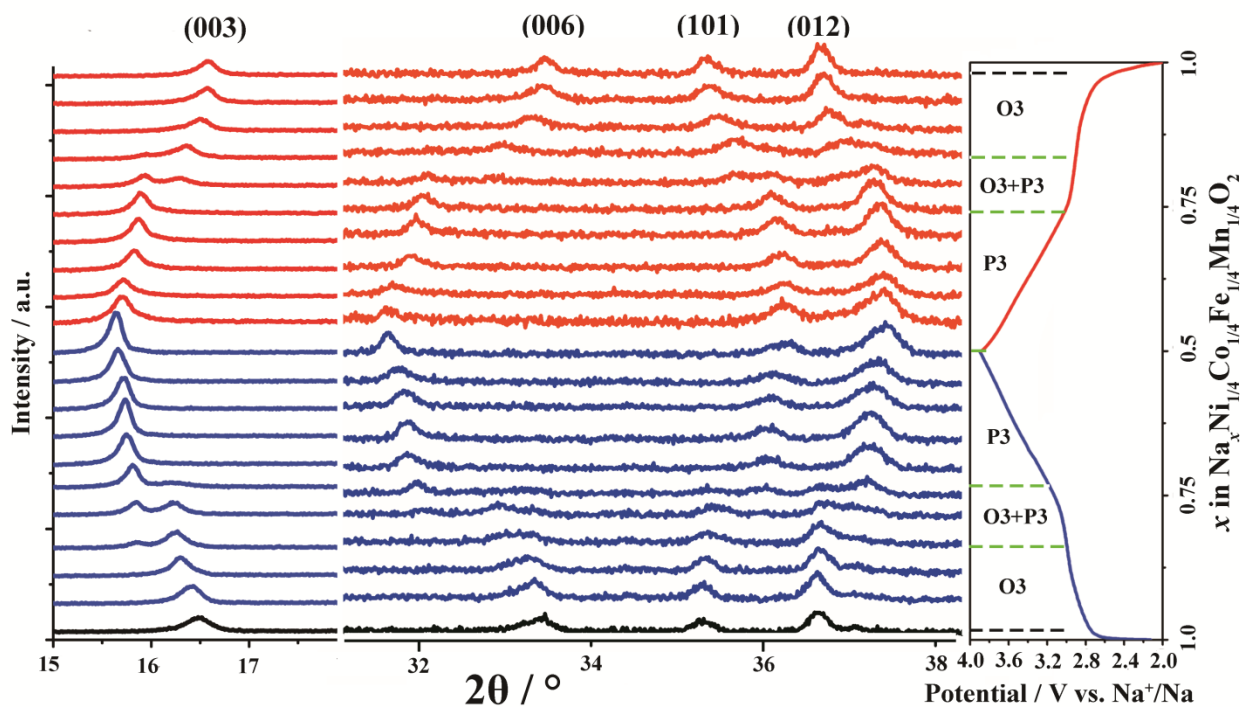


Figure 93. Structure evolution of O₃-NCFT during the electrochemical cycle. *Ex situ* X-ray diffraction (XRD) patterns collected during the first charge/discharge of the Na/O₃-NCFT cells under a current rate of C/10 at potential range between 2.0 V and 3.9 V. The corresponding charge-discharge profile is given on the right side of XRD patterns.

Patents/Publications/Presentations

Presentation

International Meeting of Lithium Batteries 2016 (IMLB2016), Chicago, Illinois (June 20-24, 2016):
“Investigation of the Charge Storage Mechanism of MXenes as Anode Materials for Na-Ion Batteries”;
Seong-Min Bak, Xiqian Yu, Ruimin Qiao, Wanli Yang, Babak Anasory, Yury Gogotsi, and Xiao-Qing
Yang. Poster.